



EFEECTO DE NANOTUBOS DE CARBONO EN LA GERMINACIÓN DE PLANTAS

EFFECT OF CARBON NANOTUBES IN THE GERMINATION OF PLANTS

TESIS

*Que para obtener el grado de Doctor en Ciencias en el
Área de Física. [Ph.D. Thesis]*

Presenta:

Dhirendra Kumar Tiwari

ASESOR

Dr. Luis Manuel Villaseñor Cendejas

MIEMBROS DEL COMITÉ

Dr. Hector Javier Villegas Moreno

CO-ASESOR

Dra. Nabanita Dasgupta-Schubert

Dr. Javier Lara Romero

Dr. Salomón Eduardo Borjas Garcia

Morelia, Michoacán, August 2013.

Universidad Michoacana de San Nicolás de Hidalgo
Instituto de Física y Matemáticas

**EFEECTO DE NANOTUBOS DE CARBONO EN LA
GERMINACIÓN DE PLANTAS**

**EFFECT OF CARBON NANOTUBES IN THE
GERMINATION OF PLANTS**

TESIS *Que para obtener el grado de **Doctor en
Ciencias en el Área de Física***
[DOCTOR OF PHILOSOPHY]

PRESENTA

*Maestría en Tecnología con especialidad en Tecnología
de Estados Sólidos*

DHIRENDRA KUMAR TIWARI

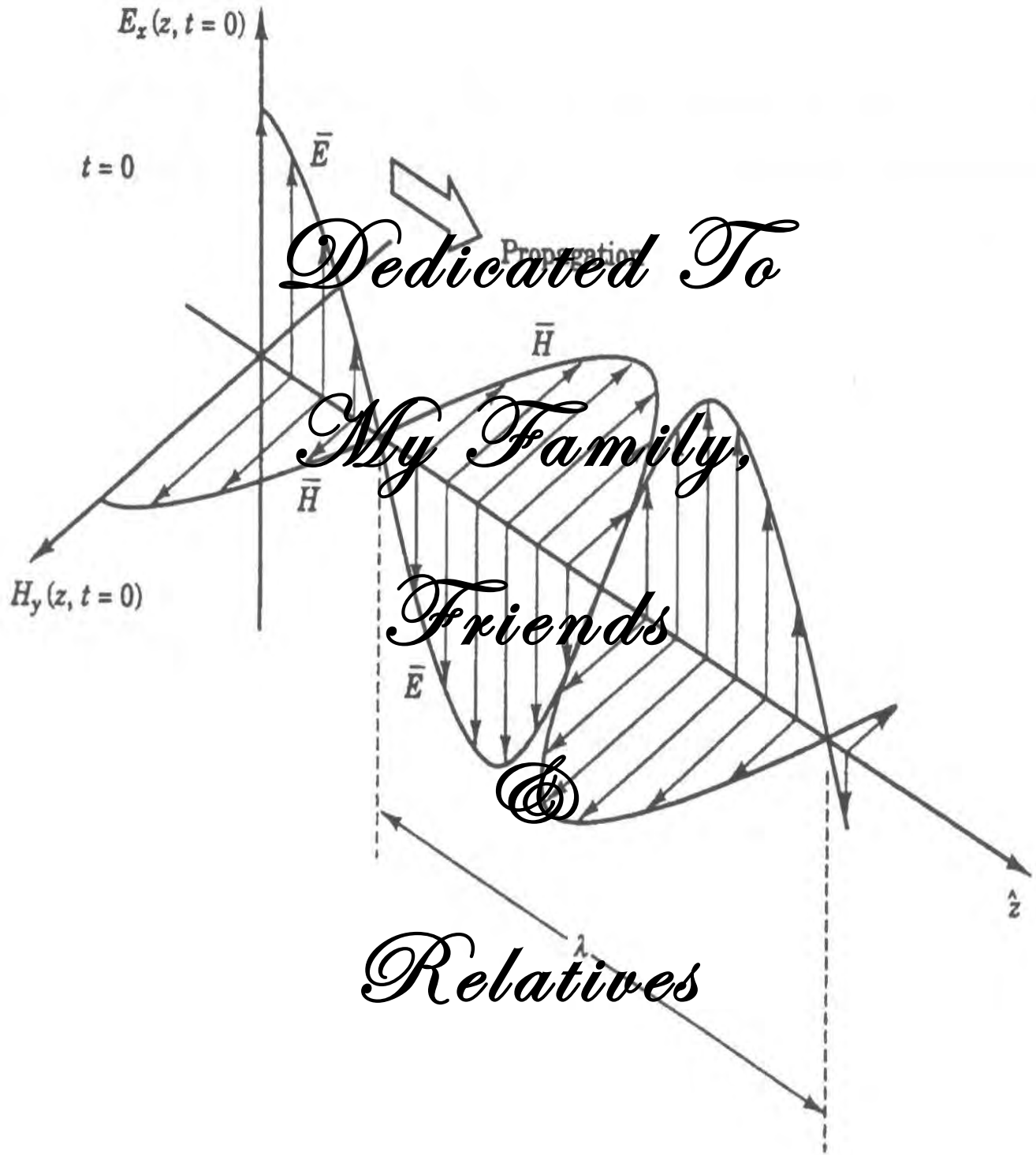
ASESOR

Dr. Luis Manuel Villaseñor Cendejas

CO-ASESOR

Dra. Nabanita Dasgupta-Schubert

Morelia, Michoacán, Agosto 2013.



Electric (E) and Magnetic (H) Fields

ACKNOWLEDGEMENT

The submission of this thesis conveys to an end a wonderful period of my "Doctoral Research" in Institute of Physics, University of Michoacan, Mexico. During the completion of this thesis I have experienced many joyous moments, as well as hurdles. I would like to thank those who gave me the strength and courage to continue and motivation to go ahead.

First and foremost, I would like to thank my thesis director, co-director and committee members, Prof. Dr. Luis Manuel Villaseñor Cendejas, Dr. Nabanita Dasgupta-Schubert, Dr. Javier Villegas, Dr. Javier Lara and Dr. Salomon E. Borjas Garcia for their support, understanding, leading skills, quality of my work, and patience during my research stay. It has been a great pleasure to work with them as a research scholar, I appreciate their contributions of time, thoughtfulness ideas, guide and advices to make my doctoral experience productive and stimulating, without their support this work would not have been possible. I would like to express my gratitude to Dr. Christian Schubert, program coordinators Dr. Ulises, Maria Elena Cervantes and other Professors & Students of IFM for their time, guidance, encouragement and helps during my stay.

The help and support of Lorena, Santos, Erika and other students of biological chemistry are unpayable. I would like to thank to the Institute of Metallurgical Research staffs, M.C. Maria Remedios Cisneros Magaña, Dr. Ariosto and others Profs for their kind support and providing an easy environment of lab facilities. I would like to acknowledge honorably to my friends and peoples surrounding for their helps, supports and makes my social life easier, during my stay in Morelia.

This research would not have been possible without the financial support of the National Council of Science and Technology (CONACYT), PIFI, IFM-UMSNH and CIC.

My warmest thanks go to my parents; without the love, support and encouragement of my family, this would have been a very hard journey. I thank my parents for teaching me good values such as hard work and appreciation for the gift of life. This journey was impossible without the support of my elder brother and sister; Dharmendra Tiwari & Kusum, who are my ideal and my great mentor during all my life and provide me a great technical educative

environment except all the complexity and mysterious moments of life. Also the encouragement of Dhananjay, Sarika, Suman and Kumud are highly appreciable. To Dr. Lexlie Ileri Rangel Vazquez; who always helps, guide, support and encourage me with her great creative mind and administrative skill during my Ph.D in Mexico. Any thank could not be sufficient for her, thank you.

Last, but not least, I would like to thank you, the reader. Any written work is a waste of time and effort without you, and as such I thank you for taking this important role upon your shoulders. I thank you, and hope you have as much fun reading this work as I had writing it.

INDEX

INDICE

LIST OF TABLES	xii
LIST OF FIGURES	xiv
ABSTRACT	1
RESUMEN	2
GENERAL INTRODUCTION	3
INTRODUCCIÓN GENERAL	5
JUSTIFICATION	7
JUSTIFICACIÓN	8
HYPOTHESIS	9
HIPÓTESIS	11
OBJECTIVE	14
OBJECTIVOS	15
CHAPTER 1 / CAPÍTULO 1	16 - 49
CHAPTER 1. NANOMATERIALS, ENVIRONMENT AND PLANTS	17
1.1 INTRODUCTION	17
1.2 NANOMATERIALS AND NANOTECHNOLOGY	18
1.3 POTENTIAL APPLICATIONS AND ENVIRONMENTAL EXPOSURE	19
1.4 CARBON NANOTUBES	22
1.5 APPLICATIONS OF CARBON NANOTUBE	23
1.6 ROLE OF CARBON NANOTUBE IN ENVIRONMENT	24
1.7 PLANTS AND ENVIRONMENT	25
1.8 WATER AND PLANT CELLS	27
1.9 SEED GERMINATION AND DORMANCY	28
1.10 FACTORS THAT AFFECT GERMINATION	33
1.11 PATTERN OF SEED GERMINATION	34

1.12	METABOLISM OF GERMINATION	37
1.13	GENOMICS AND PROTEOMICS IN SEED RESEARCH	43
1.14	REFERENCES	45
CHAPTER 2 / CAPÍTULO 2		50 - 80
CHAPTER 2. MATERIALS AND CHARACTERIZATION TECHNIQUES		51
2.1	EXPERIMENTAL PROCEDURE	51
2.1.1	Materials Description	51
2.1.2	Medium Preparation using Autoclave and Seed Germination	52
2.1.3	Medium Preparation using Magnetic Hot-Plate and Dark Germination of Seeds	52
2.1.4	Nutrient Concentration and Dispersion of MWCNT	53
2.1.5	Harvesting Germinated Seedling	54
2.1.6	Powder Preparations	54
2.2	CHARACTERIZATION TECHNIQUES	55
2.2.1	X-RAY FLUORESCENCE (XRF) SPECTROSCOPY	55
2.2.1.1	Fundamentals of XRF	55
2.2.1.2	Function of XRF	57
2.2.2	SCANNING ELECTRON MICROSCOPE (SEM)	58
2.2.2.1	Fundamental Principle	58
2.2.2.2	Working Method	59
2.2.2.3	Applications	59
2.2.2.4	Limitations	60
2.2.3	PROTON INDUCED X-RAY EMISSION (PIXE) SPECTROSCOPY	60
2.2.3.1	Basics of PIXE	60
2.2.3.2	Advantages of PIXE	60
2.2.3.3	The Benefit of X-ray Filters	62
2.2.3.4	System Description	63
2.2.4	INFRARED SPECTROSCOPY	64
2.2.4.1	Fundamentals of IR Spectroscopy	64
2.2.4.2	IR Frequency Range and Spectrum Presentation	66
2.2.5	UV-VISIBLE ABSORPTION SPECTROSCOPY	67

2.2.5.1	Background	67
2.2.5.2	Absorption Laws	68
2.2.5.3	Function of Spectrometer	69
2.2.6	ELECTROCHEMICAL IMPEDANCE SPECTROSCOPY (EIS)	71
2.2.6.1	Basic Theory of EIS	71
2.2.6.2	Impedance Response and its Complex Behavior	72
2.2.6.3	Nyquist Plot with Impedance Vector	73
2.2.6.4	The Bode Plot	74
2.2.6.5	Cole-Cole Plot	75
2.2.6.6	Examples of Nyquist and Bode Plot	76
2.2.6.7	Charge Transfer Reaction	76
2.2.7	RAMAN SPECTROSCOPY	78
2.3	REFERENCES	79
CHAPTER 3 / CAPÍTULO 3		81 - 113
ABSTRACT CHAPTER 3		82
RESUMEN CAPÍTULO 3		83
CHAPTER 3. INTERFACING CARBON NANOTUBES (CNT) WITH PLANTS: ENHANCEMENT OF GROWTH, WATER AND IONIC NUTRIENT UPTAKE IN MAIZE (ZEA MAYS) AND IMPLICATIONS FOR NANOAGRICULTURE		
		84
3.1	INTRODUCTION	84
3.2	EXPERIMENTAL SECTION	87
3.2.1	Materials	87
3.2.2	Substrate Preparation and Seedling Growth	87
3.2.3	Morphological Measurements and Microscopy	89
3.2.4	Elemental Analysis of the Seedling Tissue by Polarized Energy Dispersive X-Ray Fluorescence Analysis (PEDXRF)	90
3.2.5	Data Analysis	90
3.3	RESULTS	91
3.4	DISCUSSION	99
3.4.1	Water Content and Growth Indices (EXP-1)	99

3.4.2	Time Series Analysis (EXP-2) of Water Absorption and Growth Indices	101
3.4.3	Elemental Concentrations in Seedling Tissue (EXP-1 And EXP-3)	104
3.4.4	Water Contents, DWs and Surface Topography of Seedlings in EXP-3	107
3.5	SUMMARY AND CONCLUSION	108
3.6	REFERENCES	109
CHAPTER 4 / CAPÍTULO 4		114 - 135
ABSTRACT CHAPTER 4		115
RESUMEN CAPÍTULO 4		116
CHAPTER 4. STUDY OF CULTURE MEDIUM AND PURITY OF CARBON		
NANOTUBES IN PLANT GROWTH		117
4.1	INTRODUCTION	117
4.2	EXPERIMENTAL	118
4.2.1	Materials	118
4.2.2	Medium Composition and Germination	118
4.2.3	Analysis of Relative Element Concentration using Polarised Energy Dispersive X-Ray Fluorescence (pEDXRF) Technique	120
4.2.4	Morphological Measurements and Microscopy	121
4.2.5	Data Analysis	121
4.3	RESULTS	121
4.3.1	Role of Medium with The Presence of MWCNT	121
4.3.2	Relative Element Concentration	122
4.3.3	Comparative Study with Purity of MWCNT	124
4.3.4	Morphology of MWCNT Assisted Germination	125
4.3.5	Raman Analysis of Powder Samples of Plants	126
4.4	DISCUSSION	127
4.4.1	Weight, Length, and Water Content Statistics	127
4.4.2	Relative Element Concentration	129
4.4.3	Surface Topography	132
4.4.4	Raman Analysis	132
4.5	CONCLUSION	133
4.6	REFERENCES	134

CHAPTER 5 / CAPÍTULO 5	136 - 146
ABSTRACT CHAPTER 5	137
RESUMEN CAPÍTULO 5	138
CHAPTER 5. MATHEMATICAL MODELING OF WATER ABSORPTION	
KINETICS	139
5.1 INTRODUCTION	139
5.2 PELEG EQUATION	140
5.3 STATISTICAL ANALYSIS	140
5.4 RESULTS AND DISCUSSION	141
5.4.1 Kinetics of Water Supply: Peleg's Equation for Seedling	141
5.4.2 Peleg's Equation in Root and Shoot Water Absorption	142
5.4.3 Water Absorption Modeling of Seed Body (SB)	144
5.5 CONCLUSION	144
5.6 REFERENCES	145
CHAPTER 6 / CAPÍTULO 6	147- 163
ABSTRACT CHAPTER 6	148
RESUMEN CAPÍTULO 6	149
CHAPTER 6. INTERACTION OF CARBON NANOTUBES WITH MINERAL	
NUTRIENTS FOR THE PROMOTION OF TOMATO SEEDLINGS	150
6.1 INTRODUCTION	150
6.2 EXPERIMENTAL	151
6.2.1 Materials	151
6.2.2 Medium Preparation and Plant Growth	151
6.2.3 Elemental analysis using pEDXRF Spectrometry	153
6.2.4 Fourier Transform Infra Red (FT-IR) Spectroscopy	153
6.2.5 Data Analysis	154
6.3 RESULTS AND DISCUSSION	154
6.3.1 Without Nutrient Medium and Undispersed MWCNT	154
6.3.2 Nutrient-rich and dMWCNT Growth Medium Affects Better Germination	155
6.3.3 % Elemental Concentration Analysis	158
6.3.4 FTIR Analysis	161

6.4	CONCLUSION	162
6.5	REFERENCES	162
CHAPTER 7 / CAPÍTULO 7		164 - 175
ABSTRACT CHAPTER 7		165
RESUMEN CAPÍTULO 7		165
CHAPTER 7. SPECTROSCOPIC ANALYSIS OF IONIC AND METAL TRANSPORT ON PLANT SAMPLES GERMINATED WITH MULTI-WALLED CARBON NANOTUBES		
		166
7.1	INTRODUCTION	166
7.2	MATERIALS AND METHOD	166
7.3	RESULTS AND DISCUSSION	169
7.3.1	Plant Germination with MWCNT Assisted Nutrients Medium	169
7.3.2	XRF Analysis	170
7.3.3	FTIR Measurements	171
7.3.4	Raman Analysis	173
7.3.5	UV-Visible Analysis	174
7.4	CONCLUSION	175
FINAL CONCLUSIONS		176
CONCLUSIONES FINALES		179
APPENDIX I / ANEXO I		182 - 188
APPENDIX I: PLANT GERMINATION USING ACTIVATED CARBON (AC)		183
AI.1	INTRODUCTION	183
AI.2	MATERIALS AND METHOD	183
AI.3	RESULTS & DISCUSSION	184
AI.3.1	Activated Carbon Promots the Seed Germination	184
AI.3.2	XRF Measurement	186
AI.3.3	FTIR Analysis	187
AI.4	CONCLUSION	188
APPENDIX II / ANEXO II		189 - 195
APPENDIX II: CHARGE STATE SPECIATION IN IRON AND POTASSIUM CHLORIDE SOLUTIONS USING		

ELECTROCHEMICAL IMPEDANCE SPECTROSCOPY		190
AII.1	INTRODUCTION	190
AII.2	METHODOLOGY	191
AII.3	RESULTS & DISCUSSION	192
AII.3.1	Electrochemical Analysis of Iron Chloride Solutions	192
AII.3.2	Electrochemical Analysis of known Concentration of Potassium Chloride and unknown Biomatrix Solutions	194
AII.4	CONCLUSION	195
AII.5	REFERENCES	195
APPENDIX III / ANEXO III		196 - 203
APPENDIX III: DYNAMIC MATRIX ANALYSIS OF BIOLOGICAL SAMPLES USING PARTICLE INDUCED X-RAY EMISSION (PIXE) IMAGING		
		197
AIII.1	INTRODUCTION	197
AIII.2	SAMPLE PREPARATION	198
AIII.3	RESULTS AND DISCUSSION	199

LIST OF TABLES

LISTA DE TABLAS

CHAPTER 2

Table 2.1: Admittance and Impedance value calculation of different Circuit Arrangements. 78

CHAPTER 3

Table 3.1: Concentrations of the MWCNT ([MWCNT]) prepared in the bacteriological-agar (BA) medium. 88

Table 3.2: Concentrations of Fe(II) and Fe(III) introduced as their chlorides and the concentration of the MWCNT in the agarose medium. 89

CHAPTER 4

Table 4.1: Sample description of MWCNT assisted plant germination in agarose and BA culture medium. 119

Table 4.2: Sample description of MWCNT concentration of 20 mg/l with purity of 95 and 99 %. 120

CHAPTER 5

Table 5.1: Peleg coefficient values of water sorption on total seedling of maize plants germinated in control and MWCNT mediums during 7 days. 141

Table 5.2: Peleg coefficient values of water sorption on 7 days control and MWCNT germinated roots and shoots of maize plants. 143

Table 5.3: Peleg coefficient values of water sorption on 7 days control and MWCNT germinated seed body of maize plants. 144

Table 5.4: Coefficient of variation on water sorption of maize seedlings germinated during 7 days on control and MWCNT growth medium. 145

CHAPTER 6

Table 6.1: Sample description of germinated tomato plants in BA medium assisted with and without mwcnt. 152

Table 6.2: Sample description of germinated tomato plants in nutrient added and dmwcnt introduced BA growth medium. 153

CHAPTER 7

Table 7.1: Sample description of maize and tomato plants tretments used for germination. 167

Tabl 7.2: Description of powder samples of root, shoot and seed body of germinated plants of maize and tomato. 168

APPENDIX I

Table AI.1: Sample description of experiment performed. 184

APPENDIX II

TableAII.1: Concentration used and conductivity at that concentration of Iron Chloride solutions. 193

APPENDIX III

TableAIII.1: Detail of the PIXE analysed Samples. 198

LIST OF FIGURES

LISTA DE FIGURAS

CHAPTER 1

- Figure 1.1:** The schematic of a nanoparticle in aqueous solution illustrates some of the complexity at environmental interfaces. A close-up view of a highly simplified model of the electrical double layer at the nanoparticle-aqueous solution interface is also shown. 18
- Figure 1.2:** Seedling growth process. 27
- Figure 1.3:** Plant cell structure. 28
- Figure 1.4:** An overview of the major events that have been associated with the breaking of seed dormancy. 30
- Figure 1.5:** Time course of major events associated with germination and subsequent post germination growth. 31
- Figure 1.6:** Metabolic process in maize seed germination, a, b and c represents the changes in dry weight, water uptake and soluble protein during time respectively 38
- Figure 1.7:** Nuclie Acid and Lipd changes during metabolism of 120 hours in Maize seed germination. 39

CHAPTER 2

- Figure 2.1:** Milling machine to prepare the powder samples. 54
- Figure 2.2:** XRF device used to characterize the powder samples. 57
- Figure 2.3:** Schematic diagram of SEM. 58
- Figure 2.4:** PIXE device used for analysis. 63
- Figure 2.5:** Spectrum. 64
- Figure 2.6:** The wavelength λ of electromagnetic radiation. 68
- Figure 2.7:** Function of ultraviolet/visible spectrometer. 70
- Figure 2.8:** waveform of dI and dE. 72
- Figure. 2.9:** Lissajous figure. 73

Figure 2.10: Nyquist Plot.	74
Figure 2.11: Bode Plot.	75
Figure 2.12: Cole-Cole Plot.	75
Figure 2.13: Nyquist & Bode Plot Presentation.	76
Figure 2.14: Energy level diagram of states in Raman signal.	79

CHAPTER 3

Figure 3.1: Effect of multi-walled carbon nanotubes (MWCNT) on the 7-day germination and growth of maize in the BA medium (see table 3.1). (n=18). (a) % Water content of the whole seedling, the root and the shoot versus the [MWCNT]. (b) Root (RL) and shoot lengths (SL) with respect to their % water contents (c) dry weights (DW) and (d) fresh weights (FW) of the different morphological parts versus the [MWCNT]. The root and shoot DWs have been multiplied by 10 to accommodate them in the same graph. The dashed lines in (a), (c) and (d) are splined connectors only. The dotted lines in (b) are the linear regression fits to approximately quantify the trends. 92

Figure 3.2: Variation of growth indices with duration of germination of maize seedlings grown in BA with/without(≡Control) 20 mg/l MWCNT. (a) FW and DW. The dotted lines are the linear regression fits with the slopes (m) and correlation coefficient (R^2) values as shown. (b) % Water intake. The dotted lines are the logarithmic fits. (c) RL and SL with respect to % water intake by the seedling. The dotted and the dot-dashed lines are the logarithmic fits to the RL, the solid and dashed lines are the power-law fits of the SL, for the MWCNT and Control. The R^2 values respectively are 0.96, 0.88, 0.98, 0.98. (d) Test of universal allometric power law scaling of biology. The y-axis is the net water content of the shoots and roots, SW and RW respectively. The dotted, dot-dashed, solid and dashed lines are the power-law fits to the RW and SW with and without the MWCNT respectively. The R^2 values in sequence are, 0.986, 0.998, 0.998, 0.999. 93

Figure 3.3: Seedlings grown in agarose media (see table 3.2). (n=40 or 41). (a) Variation of % water of the seedling (b) Root and shoot DWs. 94

Figure 3.4: Elemental concentrations of the seedling samples corresponding to table 3.1 obtained using polarised energy dispersive x-ray fluorescence spectrometry (pEDXRF). 95

Figure 3.5: Elemental concentrations of the seedling samples corresponding to table 3.2 obtained using pEDXRF. The small errors bars are not visible, however the coefficients of variation averaged over all [MWCNT] are 0.1% to 3.2% for the different elements. 96

Figure 3.6: SEM images of the topography of the black-layer region of the seed-coat of the 7 day germinated maize seedling grown in agarose gel with some of the additives of table 3.2. (a) The analysed area near the black-layer (b) Control medium (c) MWCNT (20 mg/l) medium; the white arrows indicate the pores (d) Fe(III) (3×10^{-4} M) medium (A4) (e) Fe(II) (3×10^{-4} M) + MWCNT(20 mg/l) medium (A3). 98

CHAPTER 4

Figure 4.1: MWCNT concentration to plant germination in agarose and BA medium. (a) Length variation with respect to % water content. (b) Fresh and dry weight measurement for BA and Agarose germinated medium in presence of MWCNT. (c) Water availability in roots and shoots of 2 different germinated media system. 122

Figure 4.2: Relative concentration of present elements and incremental transport of selected elements with and without MWCNT. 123

Figure 4.3: comparative study of elemental transport with MWCNT purity in agarose medium germinated plants. 124

Figure 4.4: SEM image of MWCNT treated seed bodies. (a) Analyzed area. (b) Presence of MWCNT 10 mg/l concentration. (c) Presence of MWCNT 60 mg/l concentration. 125

Figure 4.5: Raman analysis of pure MWCNT (95 %) and powder sample of plant, germinated in agarose culture medium containing 60mg/l concentration of MWCNT. Raman measurement has been taken using 514.5 nm (green) laser of counts for 30 and 0.1 second respectively. 126

Figure 4.6: Luminescence analysis of MWCNT 95 % pure (Black line), powder sample of control medium germinated plants (Red line) [Table 1, A-0] and powder sample of MWCNT, 20 mg/l concentration assisted plants (Blue line) [Table 1, A-20]. 127

CHAPTER 5

Figure 5.1: Water absorption on maize seedling during 7 days germination in control and MWCNT assisted growth media system. 142

Figure 5.2: Water absorption on 7 days germinated root and shoots of maize seedling in control and MWCNT assisted growth media system. 143

Figure 5.3: Water absorption on 7 days germinated seed body of maize seedling in control and MWCNT growth mediums. 144

CHAPTER 6

Figure 6.1: Effect of pristine MWCNT on 7 days tomato seedlings (Table 1). a) Length of root and shoot growth on a medium with and without MWCNT. b) Total fresh and dry x 10 weight measurement with respect to MWCNT concentration. 155

Figure 6.2: Tomato seedling growth in the presence of dMWCNT of 14 and 27 days (Table 2). a) Root and shoot length measurement. b) Root and shoot length variation with respect to % water content. Results are shown average \pm SE of 10 plants per each treatment. 156

Figure 6.3: Effect of dMWCNT on growth and development of tomato plants of 14 & 27 days (Table 2) seedlings. a) Total fresh weight. b) Total dry weight. Results are shown average \pm SE of 10 plants per each treatment. 157

Figure 6.4: Percentage concentration of nutrient elements present in germinated tomato plants. C0-60 shows the samples germinated for 7 days with varying MWCNT concentration from 0 to 60 $\mu\text{g/ml}$ and without using any additional nutrient in the growth medium (Table 1). T0-10 are the samples germinated for 14 days in presence of 1-MS nutrient in growth medium and dMWCNT concentration 0-10 $\mu\text{g/ml}$ (Table 2). T'0-10 are the samples of 27 days germinated plants in presence of 1-MS nutrient and dMWCNT 0-10 $\mu\text{g/ml}$ Concentration in the growth medium (Table 2). 159

Figure 6.5: Detection of mwcnt in 14 and 27 days (Table 2) tomato seedlings using infrared spectrometer. 161

CHAPTER 7

Figure 7.1: Fresh and dry x10 weights of 9 days germinated maize plants as mentioned in Table 7.1. The results are shown average \pm SE of 10 plants. 169

Figure 7.2: Root and shoot lengths of 9 days germinated tomato plants of Table 7.1. 169

Figure 7.3: XRF measurement of plant samples of Maize (Table 2). Figures, a, b c and d explains the presence of different elements of plants samples of Table 1. 170

Figure 7.4: IR analysis of parts of maize plants (root, shoot and seed body) (Table 7.1).	171
Figure 7.5: IR analysis of parts of tomato plants. a) Root+Seed Body (R). b) Shoots (S).	172
Figure 7.6: Raman analysis of powder samples of shoot part of maize plants germinated with and without MWCNT (Table 2), pure MWCNT (black line) is used as a reference.	173
Figure 7.7: Raman analysis of powder samples of root part of maize plants germinated with and without MWCNT (Table 2), pure MWCNT (black line) is used as a reference.	173
Figure 7.8: Raman analysis of powder samples of seed body after 9 days of germination with and without MWCNT (Table 2), pure MWCNT (black line) is used as a reference.	174
Figure 7.9: Absorbance and transmission measurement of the samples listed in Table 7.2 using UV-Visible analysis.	174

APPENDIX I

Figure AI.1: Germination analysis of 9 days germinated Maize plants in activated carbon (AC) assisted culture medium. a) Total fresh weight measurement. b) Fresh root weight measurement. c) Measure of fresh shoot weight. d) Weight of fresh seed body. Results are shown average \pm SE of 7 plants per each treatment.	184
Figure AI.2: Growth of 9 days germinated Maize plants in (AC) assisted culture medium. a) Measure of root length. b) Measure of shoot length. Results are shown average \pm SE of 7 plants to each treatment.	185
Figure AI.3: Germination analysis of 9 days germinated tomato plants in activated carbon (AC) assisted culture medium. a) Total fresh weight measurement. b) Total dry weight measurement. c) Measure of root length. d) Measure of shoot length. Results are shown average \pm SE of 10 plants to each treatment.	185
Figure AI.4: XRF results of powder samples of maize plant. a) % Concentration of elements presence in root samples. b) % Concentration of elements in shoot samples. Y-axis plotted on log scale.	186
Figure AI.5: FTIR analysis of powder samples of germinated maize plants. a) Root samples. b) Shoot samples.	187
Figure AI.6: FTIR analysis of powder samples of germinated tomato plants. a) Root samples. b) Shoot samples.	187

APPENDIX II

Figure AII.1: Experimental setup of EIS measurement.	191
Figure AII.2: EIS measurements (Impedance plots) of chloride solutions of Fe ²⁺ , Fe ³⁺ and their mixed compositions, left figure shows the variation of real and imaginary impedances on full scale frequency (high to low) and right figure shows the variation at lower scale (high frequency).	192
Figure AII.3: Variation of bulk resistance with concentration for solutions of Fe ²⁺ , Fe ³⁺ and their mixed compositions (50-50 %).	192
Figure AII.4: Temperature & concentration variation of iron chloride solutions.	193
Figure AII.5: Conductivity variation of iron chloride solutions with concentration.	194
Figure AII.6: Variation in bulk resistance of KCl and KCl+biomatrix solutions with known concentration of KCl and unknown concentration of biomatrix.	194
Figure AII.7: Variation in molar conductivity of KCl and KCl+biomatrix solutions with known concentration of KCl and unknown concentration of biomatrix.	194
Figure AII.8: Comparative study of bulk resistance with concentration using EIS and DC measurement techniques.	195
Figure AII.9: Comparative study of molar conductivity with concentration using EIS and DC measurement techniques.	195

APPENDIX III

Figure AIII.1: Working methodology of PIXE imaging technique.	197
Figure AIII.2: Cooperation between PIXE and EDS spectrum.	197
Figure AIII.3: Sample preparation for PIXE measurements.	198
Figure AIII.4: PIXE analysis of longitudinal cross-section of root samples of A5.	199
Figure AIII.5: PIXE analysis of longitudinal cross-section of seed samples of A5.	200
Figure AIII.6: PIXE analysis of longitudinal cross-section of root samples of A6.	201
Figure AIII.7: PIXE analysis of transversal cross-section of root samples of A6.	202
Figure AIII.8: PIXE analysis of longitudinal cross-section of seed samples of A6.	203

ABSTRACT

Effect of Carbon Nanotubes in the Germination of Plants

Present thesis explains the brief description of the Nanomaterials in environmental and agricultural applications. Now a day's nanomaterials are used as an impliment to environmental, agricultural and food productions like water quality and availibity, plant germination, materials delivery and health care. This research shows the role of multiwalled carbon nanotube (MWCNT) in agricultural edible plants (Tomato and Maize). MWCNT is used, as an additive in bacteriological agar (BA) growth medium of different concentrations; 0, 5 10, 20 40 and 60 mg/l. The plants (Tomato and Maize) were grown for 7, 9, 14 and 27 days of germination time and biomasses and lengths were measured. We have used the plant germination in different media systems like BA and agarose (which contains no nutrient ions) to analyse the rate of growth in both mediums and how the ions transport takes place while introducing the MWCNT in the medium. We perform anaother set of exmeriment using Fe (Fe²⁺ and Fe³⁺ ion) concentration of 3×10^{-4} M in the agarose growth medium. Elemental concentration were analysed using polarised energy dispersive X-ray fluorescence pEDXRF spectrometry. Scannieng electron microscope (SEM) images shows, how MWCNT creates the pores and cavity on the cell membranes of the seeds. Fourier Transform Infrared spectroscopy (FTIR) is used to analyse the available chemical functional groups in the germinated plants. Raman and UV-Visible spectroscopy were used to analyze the metalicity, presence of carbon nanotubes and absorbance of powder and supernatant of MWCNT assisted plant samples. The results show that, MWCNT not only supports the water uptake but also promotes the nutrient delively, germination rate, growth and biomass of the germinated plants.

RESUMEN

Efecto de Nanotubos de Carbono en la Germinación de Plantas

En la presente tesis, se hace una breve descripción de nanomateriales en aplicaciones ambientales y agrícolas. En estos días, los nanomateriales se han utilizado en implementos para la producción agrícola y alimentaria; por ejemplo, en mejorar la calidad del agua, germinación de plantas y en el cuidado de la salud. Este trabajo de investigación muestra el papel de los nanotubos de carbono de pared múltiple (MWCNT) en plantas de alimentos agrícolas (Tomate y Maíz). MWCNT, se utiliza como aditivo en un medio de crecimiento (agar bacteriológico, BA) con diferentes concentraciones; 0, 5 10, 20 40 y 60 mg/l. Las plantas (tomate y maíz) se hicieron crecer durante 7, 14 y 27 días de tiempo de germinación y posteriormente, se midió sus biomásas y longitudes. También, se ha realizado la germinación de plantas en diferentes sistemas de crecimiento utilizando BA y agarosa (que no contiene iones de nutrientes) para analizar la tasa de crecimiento en ambos medios y la forma en que se da el transporte de iones cuando se hace la introducción de MWCNT en el medio. Se realizó otro conjunto de experimentos utilizando un medio de cultivo de agarosa con una concentración de 3×10^{-4} M Fe (iones de Fe^{2+} y Fe^{3+}). La concentración elemental de cada muestra se obtuvo mediante un espectrómetro de fluorescencia de rayos x polarizados de energía dispersiva (pEDXRF). Por otro lado, mediante un microscopio electrónico de Barrido (SEM), se muestra cómo MWCNT permiten la conformación de poros y cavidades en las membranas de las células de las semillas. Más adelante, al emplear espectroscopia infrarroja de la transformada de Fourier (FTIR), se analizan los grupos funcionales químicos que se encuentran en las plantas germinadas. Espectroscopia de Raman y UV-Visible se utilizó para analizar la metalicidad, la presencia de nanotubos de carbono y absorbencia de polvo y el sobrenadante de muestras de plantas asistida con MWCNT. Los resultados muestran que, MWCNT no sólo es compatible con la absorción de agua sino también promueve la entrega de nutrientes, la tasa de germinación, crecimiento y biomasa en las plantas germinadas.

GENERAL INTRODUCTION

The properties of nanomaterials and their potential applications are ever-increasing in all fields, particularly in agricultural biotechnology. Transport of certain nanoparticles is involved in a potential pathway of plants for beneficial outcome. However, investigations regarding the behavior of nanomaterials in plants and the mechanism of interaction effects and agricultural applications are still in rudimentary stage.

Carbon has the exceptional ability to organize itself into large number of allotropes and form amazing number of compounds. In the past few decades, nanotechnology and the recently discovered carbon nanostructures have fueled each other. The intense interest created in these materials, most notable being carbon nanotube (CNT) and graphene, has caused extensive studies on their use for several potential applications. There are two types of carbon nanotubes (CNTs): the single-walled (SWCNT) and multi-walled (MWCNT) carbon nanotubes. SWCNTs consisting of a single layer of graphene rings while MWCNT consisting of several layers of graphene rings telescoped one into the other. Many research have been done and new applications are being proposed every year. The structural applications of CNTs are numerous due to their extraordinary strength in application to; waterproof and tear-resistant textiles, fire protection, synthetic muscles, concrete strength and also increased the strength of sports equipments.

The uptake, bioaccumulation, biotransformation, and risks of nanomaterials (NMs) for edible crops and bio-agriculture are still not well understood. Very few nanomaterials and plant species have been studied. Very few references describe the biotransformation of nanomaterials in edible crops, and the possible transmission of the nanomaterials to the next generation of plants exposed to nanomaterials is unknown. The possible biomagnification of nanoparticles in the food chain is unknown. The particles could end up in the environment, settling in the soil, especially as fertilizers, growth enhancers and other nanoagricultural products hit the market. Some plants can take-up and accumulate nanoparticles, but it is unclear whether this poses a problem for plants or for the animals (like humans) that eat them.

The continuing researches on the applications of CNTs will likely produce countless other uses in the near future, not only in the fields of materials technology and electronics, but also in medicine, biology and agriculture. The scientists analyzed hundreds of scientific articles on the effects of different types of nanoparticles on edible plants. They found that the uptake and build-up of nanoparticles varies and these factors largely depend on the type of plant, size and chemical composition of the nanoparticles. This also confirms the plant toxicity of nanomaterials at the foundation stage; the work done is noting that the emerging field of nano-eco toxicology and development of agricultural food products. Scientists are continuing to study the toxicity of these CNTs but the general consensus is that, an overexposure may be a serious risk to human health. For example, a study from the University of Cambridge found that carbon nanotubes could cause cell death. Despite these worries, scientists continue to innovate, as the potential applications of these CNTs are too vast to consider stopping their research. One exciting new discovery has been the enhancement of seed germination and plant growth by CNTs. This might have significantly beneficial consequences for the increase of agricultural production. A serious concern for all countries is the question of the increase of agricultural production necessary to feed the growing world population and to counteract the effects of global climatic warming. Researchers have found that CNTs are able to penetrate the seed coats and accelerate their growth. The germination was found to be dramatically higher for seeds germinated in the medium containing MWCNTs than those of without MWCNTs. Analytical methods such as TEM and Raman spectroscopy showed that the MWCNTs had penetrated the seed coat and had enhanced water uptake by the cells of the germinating seed. While the exact mechanism is not yet understood, it is surmised that the CNTs could possibly augment the functioning of the aquaporin class of proteins in the cell membranes.

INTRODUCCIÓN GENERAL

Las propiedades de los nanomateriales y su potencial aplicación han sido un nuevo y excitante descubrimiento, en particular, en la mejora de la germinación de semillas y crecimiento de plantas con CNTs. Esto podría tener consecuencias significativamente beneficiosas para el aumento de la producción agrícola. Un motivo de gran preocupación en todos los países es lo referente al incremento de la producción agrícola necesaria para alimentar la población mundial creciente y contrarrestar los efectos del calentamiento climático global. Las propiedades de los nanomateriales y sus aplicaciones potenciales son cada vez mayores en todos los ámbitos, en particular, en la biotecnología agrícola. El transporte de ciertas nanopartículas está implicado en una vía potencial de plantas para obtener resultados beneficiosos. Sin embargo, las investigaciones sobre el comportamiento de los nanomateriales en las plantas y el mecanismo de interacción y sus aplicaciones agrícolas se encuentran todavía en estado rudimentario. El carbono tiene la capacidad excepcional para organizarse en gran número de alótropos y forma sorprendente número de compuestos. En las últimas décadas, la nanotecnología y las nanoestructuras de carbono recientemente descubiertas, han alimentado el interés mutuo. El intenso interés en estos materiales, siendo más notable en nanotubos de carbono (CNT) y el grafeno, ha causado extensos estudios sobre su uso en varias aplicaciones potenciales. Hay dos tipos de nanotubos de carbono (CNT): los nanotubos de carbono de pared simple (SWCNT) y multi-pared (MWCNT). SWCNTs que consta de una sola capa de anillos de grafeno mientras que MWCNT consiste en varias capas de anillos de grafeno telescópicamente uno dentro del otro. Muchas investigaciones se han hecho y se están proponiendo nuevas cada año. Las aplicaciones estructurales de los nanotubos de carbono son numerosas debido a su extraordinaria opción de aplicación; tal como, en textiles impermeables y resistente al rasgado, en protección contra incendios, en los músculos sintéticos, en la resistencia del concreto y en los equipamientos deportivos.

La captación, bioacumulación, biotransformación, y los riesgos en el uso de los nanomateriales (NM) para los cultivos de alimentos y la bio-agricultura aún no se comprenden bien. Son muy pocos los nanomateriales y especies de plantas que han sido estudiados. Muy pocas referencias describen la biotransformación de los nanomateriales en los cultivos de alimentos, y se desconoce la posible transmisión de los nanomateriales para la próxima

generación de plantas expuestas a estos nanomateriales. La posible biomagnificación de las nanopartículas en la cadena alimentaria es desconocida. Las partículas podrían terminar en el medio ambiente a través de su colocación en el suelo, al hacer uso de fertilizantes, mejorando el crecimiento de plantas u otros productos nanoagropecuarias que lleguen al mercado. Algunas plantas podría tomar nanopartículas que se acumulen, pero no está claro si esto representa un problema para las plantas o para los animales (como los humanos) que se alimentan de ellas. Los trabajos de investigación continúan enfocados en aplicaciones de nanotubos de carbono y probablemente producirán un sinnúmero de otros usos en un futuro cercano, no sólo en los campos de la tecnología de los materiales y la electrónica, sino también en la medicina, la biología y la agricultura. Los científicos han analizado cientos de artículos científicos sobre los efectos de diferentes tipos de nanopartículas en las plantas comestibles. Ellos encontraron que la absorción y la acumulación de las nanopartículas varían y estos factores dependen en gran medida del tipo de planta, el tamaño y la composición química de las nanopartículas. Esto también, confirma que la toxicidad de los nanomateriales en las plantas se da en la etapa de fundación. Los científicos continúan estudiando la toxicidad de los nanotubos de carbono, pero el consenso general es que, una exposición excesiva puede ser un riesgo grave para la salud humana. Por ejemplo, en un estudio de la Universidad de Cambridge, se encontró que los nanotubos de carbono podrían causar la muerte celular. A pesar de estas preocupaciones, los científicos continúan innovando, ya que las aplicaciones potenciales de los nanotubos de carbono son demasiado vastas como para considerar la suspensión de sus investigaciones. Un nuevo descubrimiento emocionante ha sido el aumento de la germinación de semillas y crecimiento de plantas por CNT. Los investigadores han encontrado que los nanotubos de carbono son capaces de penetrar en las cubiertas de las semillas y acelerar su crecimiento. También, se encontró que la germinación se da mucho más para las semillas germinadas en sistemas de cultivo que contienen MWCNTs que los que no tienen MWCNTs. Los métodos analíticos; tales como, TEM y espectroscopia de Raman mostraron que los MWCNTs penetran en la cubierta de la semilla y tenía una mayor absorción de agua por las células de germinación de la semilla. Aunque el mecanismo exacto no se conoce todavía, se parte de la suposición de que los nanotubos de carbono podrían posiblemente aumentar el funcionamiento de una clase de acuoporina de proteínas en las membranas de las células.

JUSTIFICATION

The available information of the mechanisms of CNT on plant germination and environmental applications are taking a crucial role but the exact dynamics of of water, nutrient and heavy metal elements uptake are unknown and unclear. The information available on literatures about plant growth and their concentration in the growth medium are also not very clear, for sure the CNTs support the plant growth of different plants but a small change in concentration causes a big difference on the germination rate. Also the purity of carbon nanotubes, growth media, and presence of nutrients in the growth medium are also a big issue. Looking forward to all these issues we have worked with standard multiwalled carbon nanotube (MWCNT) of various concentrations and different growth mediums (nutrients and without nutritive growth mediums). These experiments will confirm the exact mechanism of MWCNT concentration necessary for different plants in different media system and their role in transport to nutritive elements and increment in biomass. The mechanism of elemental retention in agricultural food plants plants indicates that the CNT adsorption adheres to charged sites of the cell membrane of the root cell structures as mycelium and vesicles. In plant roots, a small amount of CNT enters the cytoplasm of cortical cells (Black layer) by active or passive process and enters the symplast xylem.

JUSTIFICACIÓN

La información disponible sobre los mecanismos del CNT en la germinación de plantas y sus aplicaciones ambientales están tomando un papel crucial, pero la dinámica exacta acerca de la absorción de agua, nutrientes y elementos de metales pesados son desconocidos y poco clara. La literatura disponible sobre el crecimiento de plantas y su concentración en el medio de crecimiento tampoco es muy clara, con seguridad los CNT fomentan el crecimiento de la planta de diferentes plantas, pero un pequeño cambio en la concentración provoca una gran diferencia en la tasa de germinación. Asimismo, la pureza de los nanotubos de carbono, los medios de crecimiento y la presencia de nutrientes en el medio de cultivo son también un gran problema. Nosotros hemos observado todos estos aspectos al trabajar con nanotubos de carbono de pared múltiple estándar (MWCNT) de varias concentraciones y diferentes medios de crecimiento (medios de cultivo con y sin nutrientes). Estos experimentos confirmarán la pauta a seguir en la determinación de la concentración de MWCNT necesario para el crecimiento de distintas plantas en diferentes sistemas de medios de crecimiento y su papel en el transporte de elementos nutritivos e incremento de sus biomásas. El mecanismo de retención elemental en plantas agrícolas indica que la adsorción de CNT se da en sitios cargados de la membrana celular de las estructuras de las células de la raíz como podrían ser micelios y vesículas. En las raíces de las plantas, una pequeña cantidad de CNT entra en el citoplasma de las células corticales (Capa negra) a través de un proceso activo o pasivo y entra en el xilema simplástico.

HYPOTHESIS

Very little so far is known about how the CNTs function to enhance the growth of seedlings, in part because the discovery is recent. Researches indicate that CNTs enhance water delivery, it might be surmised that a similar mechanism might enhance the delivery of water-soluble external nutrients such as the heavy metal plant micronutrient. We hypothesize that the ability of CNTs to efficiently transport charged particles, as shown by their excellent and well-researched electromagnetic properties, might facilitate the transport of micronutrients such as Fe, Ca, Mg, Mn, Cu, Zn and Cl across the seed coat and cell membrane barriers. In this way they might act to enhance the efficiency of the ion channel proteins residing in the cell membranes, for the transport of metallic ions and similar charged species. Furthermore from the standpoint of heavy metal toxicity to plant cells, it is well known that in general, higher charge (oxidation) states are more toxic than lower oxidation states, because the former cause oxidative damage to the cells. We hypothesize further that the extensive p-bond networks that exist in the sp^2 hybridized orbitals of the graphene structures of the CNTs, might serve to act as electron donor/acceptor sites, thus enabling the reduction of higher metallic oxidation states to lower ones. The plant seeds that intended to be studied are the seeds of *Zea Maize* (di-coat seed and have sufficient biomass) and Tomato (mono-coat seed). The interest in the present research work is in Fe, Ca, Cu, Zn, Mn etc. because they are, (a) essential plant micronutrient (b) metallic and exhibits a number of stable oxidation states such as +3, +2, +1 (c) the analytical method of Polarised X-Ray Fluorescence Spectrometry (pEDXRF) available in the Radiation Laboratory of the IFM, UMSNH is particularly suitable for metals of the 4th and 5th period.

The second set of experiments concerns the growth of the Maize seedlings in petridishes pure agarose medium composed of only de-ionized (DI) water doped with a certain concentration of MWCNTs. The seedlings will be arranged around the periphery of the petridish. A certain concentration of dissolved Fe (II) and Fe (III) salt will be introduced at the gel medium. After a fixed period of time, the seedlings will be harvested. The seed coats will be separated. The pEDXRF system will be used to measure the concentrations of present

elements. Other experiments to view the structure of seedling tissue under the conditions of growth in media doped with MWCNTs and Fe solution will be conducted using the SEM/TEM coupled with x-ray microanalysis and Infra-Red analysis to look the intensity of the available elements in medium infrared region.

Another additional works have been done based on the ion transport and charge state analysis using Electro Chemical Impedance Spectroscopy (EIS). The entire study area is new as has been mentioned in Appendix. Using the electrochemical cell of the EIS spectrometer, calibration experiments will first be done using a fixed volume of Fe (II) and Fe (III) and K chloride solutions of graded concentrations in De-ionized water. The conductivity values for each metallic species of a given oxidation state, as a function of concentration, will be measured as well as the ionic mobilities. Calibration curves of concentration vs conductivity and mobility will be constructed. Using these curves the oxidation state of a certain unknown solution of the metal of a given concentration, will be determined. After the charge state calibration in pure de-ionized water, the germinated seedlings were crushed and their extract obtained by centrifugation and filtration. This biomatrix solution is mixed in Fe and K to make a fixed concentration and analyzed by using EIS. The subsequent EIS analysis of the Fe conductivities and mobilities in the seedling extract solutions and comparison with the calibration curves will yield information on the oxidation state of the Fe within the seedling tissue. The matrix of both the calibration and unknown solutions will simulate the composition of typical seedling extracts, i.e. it will be composed of soluble carbohydrates (e.g. glucose or sucrose) and proteins (e.g. the amino acid, lysine or glutamic acid). Eventually, we will use the use actual maize seedling extracts. The solutions of known concentration of the metal in a given oxidation state will be added to a known volume of this extract, the mixture will be centrifuged and filtered to obtain the solution.

HIPÓTESIS

Hasta la fecha, muy poco se sabe acerca de cómo los CNTs actúan en el incremento del crecimiento de plantas, debido a que el descubrimiento es reciente. Sin embargo, algunos investigadores indican que, los CNTs mejoran el suministro de agua. Cabe suponer que un mecanismo similar podría aumentar el suministro de nutrientes externos solubles en agua; tales como, el hierro (Fe). Hasta el momento, no existe algún trabajo en esta área. Se tiene la hipótesis de que la habilidad de los CNTs para mejorar el transporte de partículas cargadas (como lo muestran sus propiedades electromagnéticas investigadas), podrían facilitar el transporte de micronutrientes como Fe a través de la cubierta de la semilla y de las barreras de las membranas celulares. De esta manera, se podría actuar para mejorar la eficiencia de las proteínas de los canales iónicos que residen en las membranas celulares para el transporte de iones metálicos y especies de carga similar. Desde el punto de vista de la toxicidad de los metales pesados en las células vegetales, es bien sabido que en general, los estados de carga alta (en estado de oxidación) son más tóxicos que los estados de carga bajas, dado que el estado de oxidación causa daño en las células. Además, se postula que las extensas redes de enlaces π que existen en los orbitales de hibridación sp^2 en la estructura de grafeno de los CNTs, permiten actuar como electrón donante/receptor, permitiendo la reducción de estados de carga alta a estados de carga baja. Las semillas de las plantas que se piensan estudiar, son las semillas de Maíz y Tomate. El interés en este protocolo de investigación es el Fe, dado que: (a) Es un micronutriente esencial para las plantas. (b) Es un metal que presenta una serie de estados de oxidación estables; como: +3, +2, +1. (c) El método analítico de fluorescencia de rayos X polarizados de energía dispersiva (PEDXRF) se encuentra disponible en el Laboratorio de Radiación del IFM-UMSNH y es particularmente conveniente para detectar elementos metálicos del cuarto y quinto período.

La segunda fase de los experimentos tratados en este trabajo de investigación, se refieren al crecimiento de semillas germinadas de maíz en cajas petri en medios de cultivo compuestos solamente por agua desionizada dopada con una cierta concentración de MW-

CNTs. Las semillas germinadas se organizarán en la periferia de las cajas Petri. Una determinada concentración de sales de Fe (II) o Fe (III) será introducida en el medio de cultivo de cada caja petri. Después de un determinado periodo de tiempo, las plantas obtenidas son cosechadas. La cubierta de las semillas será separada. El pEDXRF será utilizado para medir la concentración de elementos presentes. La técnica de caracterización de SEM/TEM en conjunto con microanálisis de rayos X y espectrometría de infrarrojo serán utilizados para analizar los elementos y microestructura de las plantas.

La técnica de espectroscopia de impedancia electroquímica (EIS) es una técnica que se podría utilizar para la determinación del estado de oxidación y como su aplicación es nueva y en caso de tener éxito, se podría llevar a cabo una solicitud de patente. Como se ha mencionado anteriormente, en la sección del Apéndice. En primer lugar, se harán experimentos para caracterizar el estado de carga de los iones metálicos. Usando la celda electroquímica en el equipo de espectroscopia de impedancia electroquímica (EIS), los experimentos de calibración se realizarán primero, utilizando un volumen fijo de soluciones con diferentes concentraciones de Fe (III) y Fe (II). Empezaremos con experimentos de calibración con soluciones de Fe (II) y Fe (III). Con el fin de utilizar eficazmente el tiempo y antes de invertir en la compra de otros materiales, reactivos, herramientas y equipos necesarios. Se medirán los valores de conductividad de corriente directa para cada especie metálica con un estado de oxidación en función de la concentración. También, se medirá la movilidad iónica y se construirán curvas de calibración de la concentración frente a la conductividad y la movilidad. Se utilizarán las curvas del estado de oxidación para determinar la concentración en una solución con concentración conocida de metales y se determinarán las matrices tanto de las soluciones de calibración, como de las soluciones desconocidas. Se simulará la composición de los extractos de las semillas germinadas típicas, es decir, compuestos de carbohidratos solubles como la glucosa o la sacarosa y de proteínas como aminoácidos, lisina o ácido glutámico. Para esto, una vez que las semillas se encuentren desnudas, serán comprimidas y el extracto se separará por centrifugación y filtración. El análisis de muestras con respecto al tiempo dará concentraciones de Fe en la semilla-capa y así se podrá determinar la dinámica del transporte del Fe. Posteriormente, se hará un análisis por EIS para determinar la conductividad y movilidades del Fe en las soluciones del extracto de las semillas. Después, se hará la comparación con las curvas de calibración para obtener información sobre el estado de

oxidación del Fe en los tejidos. Eventualmente, utilizaremos extractos de semilla germinadas de maíz. Las soluciones de concentración conocida del metal en un tipo de estado de oxidación propuesta se añadirán a un volumen conocido de este extracto, la mezcla se centrifugará y se filtrará para obtener la solución. Los experimentos de calibración se llevarán a cabo como se describe anteriormente.

OBJECTIVES

GENERAL OBJECTIVE

To study the role of MWCNTs in the nutrient media with regard to the absorption, transport and charge state of the metallic micronutrient in the tissue of Maize and Tomato germinated seedlings.

SPECIFIC OBJECTIVES

- a) To study the concentration of the Fe species in the different anatomical tissues of the germinating seed and how this is affected by the presence of MWCNTs in the media.
- b) To study the dynamics of transport of the Fe across the seed coat with and without the presence of MWCNTs in the growth media.
- c) To study the oxidation state of the Fe species within the cellular fluid of the seedling tissue when the Fe (III) is introduced as Fe (II) in nutrient media doped by MWCNTs.

OBJETIVOS

OBJETIVO GENERAL

Estudiar el papel de los MW-CNTs en los medios nutritivos relacionados con la absorción, transporte y estado de carga de los micronutrientes metálicos en el tejido de las semillas germinadas de maíz y tomate.

OBJETIVOS ESPECÍFICOS

- a) Estudiar la concentración de las especies de Fe en los diferentes tipos de tejidos anatómicos de las semillas germinadas, y como éstas, son afectadas por la presencia de MW-CNTs en los medios nutritivos.
- b) Estudiar la dinámica de transporte de Fe a través de la corteza de la semilla con y sin la presencia de MW-CNTs en los medios de crecimiento.
- c) Estudiar los estados de oxidación de las especies de Fe dentro del fluido celular del tejido de las semillas germinadas, cuando el Fe es introducido como Fe (II) en medios nutritivos dopados con MW-CNTs.

CHAPTER 1
NANOMATERIALS, ENVIRONMENT AND PLANTS

CAPÍTULO 1
NANOMATERIALES, MEDIO AMBIENTE Y PLANTAS

CHAPTER 1

Nanomaterials, Environment and Plants

1.1 INTRODUCTION

The field of nanotechnology has advanced enormously in the past decade and, as a result, researchers have synthesized a large number of materials with at least one dimension in the nanoscale size regime for a diverse set of applications. Moreover, given societal needs in the 21st century and beyond, nanoscience and nanotechnology can provide many of the science and technology innovations and advances needed for global sustainability [44-53]. Because of the potential for increased and widespread use of nanomaterials in different applications and consumer products, the release of at least small quantities of nanomaterials into the environment during their product life cycle will be inevitable. The potential for environmental release raises concerns since little is known about the fate, transformation, and toxicity of the engineered materials [2, 3, 45, 46, 48]. To address these concerns, the Nanotechnology and several international consortia have increased their attention on the environmental health and safety issues associated with nanomaterials.

Analyzing nanomaterial-environment interactions depends on building a solid scientific model of nanomaterials [1, 48, 53] alone and on understanding their surface reactions with the complex environment. Nanomaterials themselves can take many forms and their size, composition, shape, structure, coatings, and surface chemistry will influence their nanomaterial-environment interactions in ways that are not yet well understood. For example, pristine nanomaterials may aggregate or change properties over time. Additionally, nanomaterials might sequester ions and transport them long distances and changes in environmental conditions might trigger the release of adsorbed contaminant species. An important example is the case of arsenate ions adsorbed onto iron oxide nanoparticles. *In situ* molecular-level studies are needed to fill knowledge gaps about chemical processes to understand the behavior of nanomaterials in complex environments [43, 46].

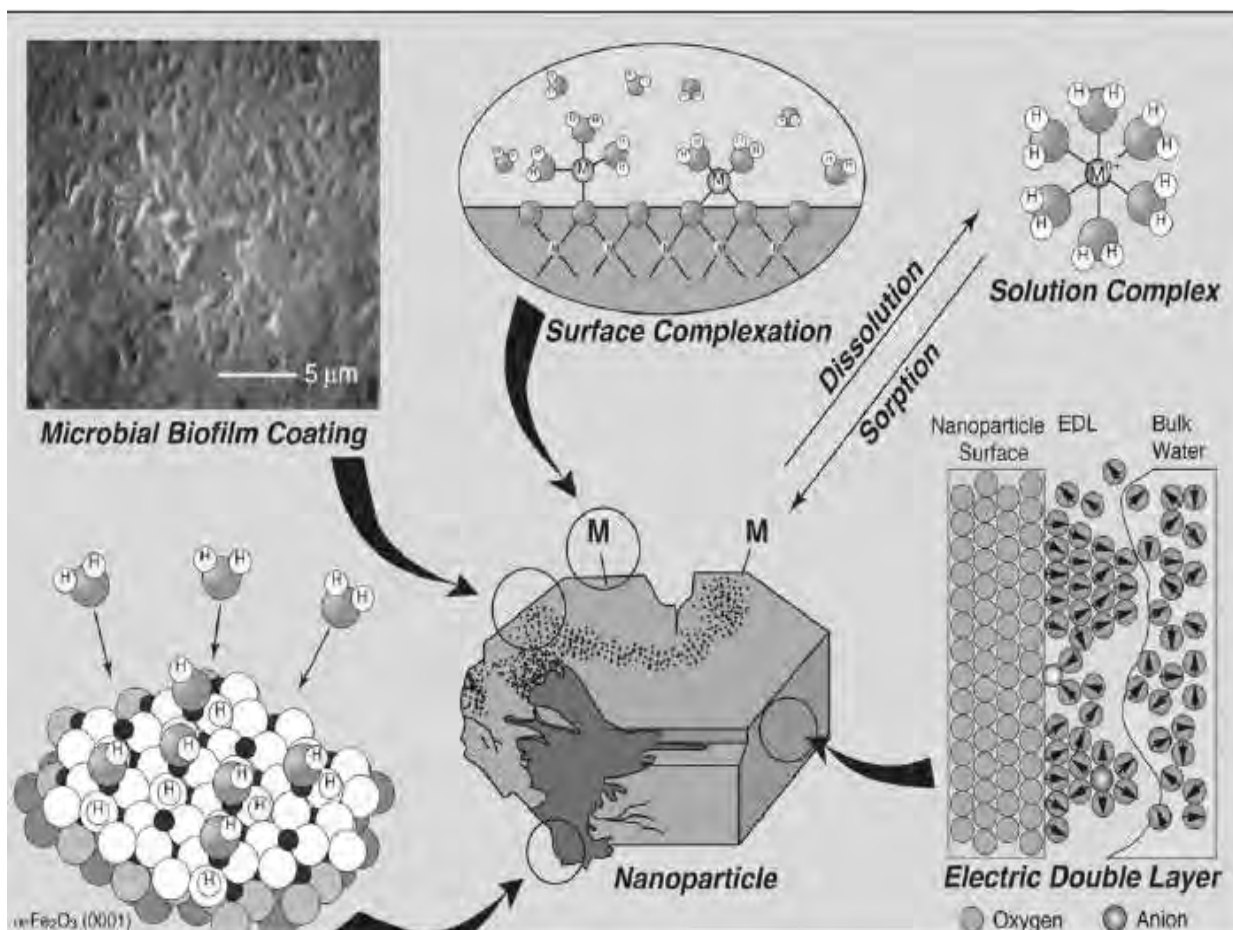


Figure 1.1: The schematic of a nanoparticle in aqueous solution illustrates some of the complexity at environmental interfaces. A close-up view of a highly simplified model of the electrical double layer at the nanoparticle-aqueous solution interface is also shown.

1.2 NANOMATERIALS AND NANOTECHNOLOGY

In the present atmosphere, nanotechnology is one of the most active fields in research and technology development. It is a field that has received tremendous attention and growth over the past few years, has thus far proven to be extremely beneficial encompassing many fields of science and engineering, thus causing some discrepancy in defining the terms [44-52]. There are, however, key words that are included in all definitions. Nanotechnology describes a broad discipline of research and technology development in nanoscale range (between 0.1-100 nm). Nanotechnology controls or manipulates individual atoms, molecules or structures in order to create and utilize devices and systems that possess novel properties and functions. Products formed and utilized in nanotechnology are classified as nanomaterials,

which are materials with at least one dimension in the nanoscale range. Nanomaterials are different from incidental or natural nanoparticles, which are produced as a byproduct of a manufacturing process or created by natural processes such as sea spray.

There have been various ways to categorize nanomaterials in the laboratories by grouping of their base material entailing four groups: carbon based, metal based, dendrimers and composites with other nanomaterials or bulk material. Another way for nanomaterials to be classified is by their nanometric dimensions, consisting of three groups: i) particles, which have three nanoscaled dimensions including fullerenes, dendrimers and polymers ii) tubes with two nanoscaled dimensions such as carbon nanotubes (CNT) [1, 3-10, 22, 26] inorganic nanotubes, nanowires and bipolymers and iii) films, plates and coatings with one nanoscaled dimension. Apart from the basis of the groupings, there are few similarities among each specific type of nanomaterials within each cohort like they have a nano-sized dimension and their properties are significantly different from other (bulk-type) materials.

1.3 POTENTIAL APPLICATIONS AND ENVIRONMENTAL EXPOSURE

Nanotechnology is not only beneficial in materials production, but has proven to be advantageous to the energy [18], medical [16, 28], environmental, food and agricultural industries [20-27]. Examples of products that are already in use in these industries include solar panels that increase energy with lighter materials, and batteries that provide cleaner, more efficient vehicles. Nanomaterials have been utilized in products that purify water from as, trichloroethylene and petroleum. Medically, nanomaterials are used for antimicrobial and anti-inflammatory purposes. Nanotechnology is utilized in pressure sensors for the delivery of babies and in kidney dialysis. Food packaging and food storage containers we infused with nanomaterials. Vitamins, fruit juices, infant fruit drinks and additives integrate nanomaterials. Current commercial applications of nano-chemicals in the agricultural industry may be unknown, as leading agri-chemical companies have not labeled their emulsion products containing the nanomaterials. Such products include plant growth regulators, fungicides and seed treatments. Nanomaterials have also enabled the use of pesticides that are released based on the environment, which may be in an insect's stomach.

Possibilities that are currently being tested range from specific delivery of drugs, pesticides, fungicides and nutrients. As they exponentially evolve they reveal their capability to revolutionize the environment, agriculture and food systems. Once amalgamated with other mediums and measures they have the ability to tackle some of the world's most crucial problems, especially in the sustainable development area. Problems could include ecosystem and biodiversity management, water, energy, health and environmental improvement and food and agriculture sustainability. Apart from intentional environmental applications nanomaterials can enter the environment from the waste. Waste can be from manufacturing plants to agitation of materials that contain nanomaterials to waste from the medical industry. With only a crude understanding of nanotechnology today the magnitude of its impact is endless as it has the potential to affect every material that we come in contact with on a daily basis. The most researches have been focused these days are based on "Environmental Remediation, Electronics and Energy applications" and most active nanomaterials predicted are carbon nanotubes [18, 47, 52].

With all the beneficial applications, there has been some, though relatively sparse in comparison, research done on the toxicity and hazardous effects associated with nanomaterials [17, 43, 48]. However far surpasses every other country globally. As aforementioned, when particle size decreases, properties like solubility, shape and surface chemistry are altered. This results in higher chemical reactivity and biological activity. Although advantages have been taken of these characteristics there is the possibility of related adverse affects for the very same reason. One of the main apprehensions is that nano-sized materials can be released into untargeted environments in as many ways as they can be used in production. For example, washing of antimicrobial clothing or washing machines with nano-silver may have nanomaterials in the water being distributed into effluents. Additionally, they have the potential to cause harm within their intended environments. For instance, nanomaterials are expected to aid in aquaculture ponds. However nanomaterials have caused a negative effect on fish [28]. Studies pertaining to toxicity of humans, inclusive of animal model studies, have far outweighed studies investigating the toxicity to environmental media. Nevertheless, knowledge on how nanomaterials could affect humans is currently very limited. There have been a few *in vivo* and *in vitro* laboratory studies, involving rodents and even fewer with humans that aim to determine toxic effects. *In vivo* studies saw high mortality of rats when

exposed intracheally to CNTs. CNTs also resulted in inflammation and granulomas in rats and immunological dysfunction in humans. In-vivo studies also exhibited effects on mice by Zn, while quantum dots were proven to be carcinogenic. *In vitro* studies have found cell death, cytotoxicity, mutagenic effects, decreased mitochondrial functions and increased cell proliferation in human and rat lung cells, brain microglia cells, alveolar, murine cells and liver cells by a wide variety of nanomaterials. Nanomaterials tested comprise of C60 fullerenes, carbon nanotubes (CNTs), zinc oxide (ZnO), aluminum trioxide (Al₂O₃), titanium dioxide (TiO₂), and silicon dioxide (SiO₂) nanomaterials. Overall, nanomaterials effects on humans and animals have shown significant accumulation in the brain, spleen, liver, lungs and bones. Nanomaterials have exhibited toxicity to human tissue and cell cultures [42]. With an increase of exposure, the knowledge gap will increase, as there is little ability to specifically define the dose to which animals and humans will be exposed.

Currently research has yet to determine how nanomaterials behave in environmental media such as soil, water or sludge. Once the environment is exposed to manufactured nanomaterials interaction is certain to behave differently than bulk particles. These associations whether biologically or chemically, will be different than with larger materials. Bioaccumulation could be a possibility once there is interaction with biological organisms. Nanomaterials are long-lived, mobile and insoluble in water, which make them ideal for bioaccumulation. The insight on hazards to environmental biological organisms is also extremely limited. Three additional factors that generate toxicity for the environment, are that i) the actual chemical composition is generally unknown and can differ for same nanomaterials with different sizes, ii) the potential for adhesion or incorporation to cells can cause cellular toxicity and iii) the shape of the nanomaterials can impale cells of all biological organisms.

Only a handful of research has been conducted on the effects of nanomaterials on plants. The research has indicated that nanomaterials can have a negative or positive effect on plants. Several studies have reported the positive effects of TiO₂ in spinach [17]. This was instigated from one of the first studies conducted on the effects of nanomaterials in plants. Researchers noted an increase in germination, photosynthesis and growth rate when spinach was exposed to TiO₂. Other research studies have proven the phytotoxicity of nanomaterials. Zn and ZnO nanomaterials at 2000 mg/l affect seed germination in ryegrass and corn

respectively [17]. These nanomaterials also just about ceased root elongation in 5 crop species, which includes rape and ryegrass with an IC50 (concentration where 50% of sample was inhibited) of 20 mg/l and in radish at 50 mg/l. A later study exposed ryegrass to ZnO nanomaterials. Researchers reported that seedling growth; biomass and root tips were negatively affected by exposure to ZnO. A study investigating the effects of Al₂O₃ on 5 crop species by nanomaterials also reported inhibition of root elongation. Copper oxide nanomaterials inhibited seedling growth in mung beans and wheat. The researchers reported that the Cu nanomaterials were in the root cell vacuoles. Iron oxide nanomaterials accumulated on the surface of and in the cells of pumpkin plants. C70 fullerenes were also accumulated in rice plants and they delayed flowering and negatively affected the weight of the seed produced. Plant growth of lettuce was also negatively affected when exposed to nanomaterials. This phytotoxic effect was induced by exposure to Cu, palladium, silicon and silver nanomaterials. Environmental hazards are not only in the biosphere but also in the atmosphere. The persistence and the ability of nanomaterials to agglomerate present themselves as perfect candidates for environmental hazards, especially for organisms like plants that are stationary and utilize the gases from the atmosphere.

1.4 CARBON NANOTUBES

Carbon Nanotubes are allotropes of carbon whose nanostructure is a hollow cylinder. The walls of the tubes consist of sp² hybridised C atoms interconnected to each other in the form of hexagonal graphene rings. The ends of CNTs are domed structures of six-membered rings capped by a five-membered ring. Generally speaking, there are two types of CNTs: the single-walled CNT (SW-CNT) consisting of a single layer of graphene rings, and the multiwalled CNT (MW-CNT) consisting of several layers of graphene rings telescoped one into the other. CNTs were first isolated and characterized by Ijima in 1991 [1]. Since then many research articles on CNTs have been published and new applications are being proposed every year.

The unique physical and chemical properties of CNTs such as structural rigidity [2] and flexibility, continue to generate considerable interest. Additionally, CNTs are extremely strong, about a 100 times stronger (stress resistant) than steel at one-sixth the weight. The structural applications of CNTs are numerous due to their extraordinary strength. Such applications include waterproof and tear-resistant textiles, increased concrete strength, fire

protection, increased strength in sports equipment, and synthetic muscles [3-5]. The structural application of nanotubes is a list that will continue to grow as companies innovate around the flexible molecules.

CNTs also act as either conductors or semiconductors depending on their chirality [6], possess an intrinsic superconductivity [7], are ideal thermal conductors [8], and can also behave as field emitters [9]. Given these unique electrical properties, CNTs have found use in the preparation of conductive films, magnets, solar cells, transistors, displays, and many other devices [10, 18]. CNTs are used in many chemical applications, including filters of air pollution, the storage of hydrogen, and water filters. In water filters, the microscopic tubes allow water molecules to pass through them while restricting larger particles [11].

1.5 APPLICATIONS OF CARBON NANOTUBE

We all know that the uniqueness of Nanotubes make them better than their competitors for specific applications. The combination of structure, topology and dimensions of Nanotubes takes an important role in their physical properties, which are unparalleled by most known materials. To discuss about the more details of carbon nanotubes here its important to describe the categories of nanotubes are well used these days are Multi-walled carbon nanotubes (MWCNTs) and single walled carbon nanotubes (SWCNTs). MWCNTs have shown the most promising appearance because of their utilities and characteristics. These were catalytically grown by Chemical Vapor deposition (CVD) multilayer graphite tubular structure that could be further annealed to decrease their defect density. The dimensions of these were several tens of nanometers in diameter, but occasionally smaller structure including the single –layer tubular structure were also observed. In early 1990 Iijima and others showed that high temperature arc-discharge process could produce smaller, highly graphite multiwall structures. Then comes the discovery of Single wall Carbon nanotubes (SWCNTs) in 1993 by the NEC and IBM groups. That suggested that catalytic vapor deposition can be controlled to make single layer tubular structures of graphene with diameters as small as 1 nm. The ability to grow such small defect free graphene tubes prompted peoples to suggest various applications for these structures, including that of electronic devices; chirality, defect free structure and small dimensions showed possibilities of their use as quantum wires.

Carbon based fibrillar structures at that point crossed over from the traditional graphite like materials to molecular structures with an applications domain expanding into nontraditional areas like nanoelectronics. These days, we are able to make nanotubes with a precisely tuned number of layers, such as SWCNTs and Multi-wall carbon nanotubes (MWCNTs) and a lot of progress has occurred in the scalable synthesis of this material. While we come to the application part of these materials, they divide between the traditional (like carbon fibers and other carbons) and nanotraditional (with unique property applications) uses.

1.6 ROLE OF CARBON NANOTUBE IN ENVIRONMENT

One exciting new discovery has been the enhancement of seed germination and plant growth by CNTs [12, 13, 16, 25]. This might have significantly beneficial consequences for the increase of agricultural production. A serious concern for all countries is the question of the increase of agricultural production necessary to feed the growing world population and to counteract the effects of global climatic warming. Khodakovskaya et al [12] have found that CNTs are able to penetrate the seed coats of tomato seeds and accelerate their germination and growth rates. The germination was found to be dramatically higher for seeds germinated in the medium containing MWCNTs (10-40 micro-g/ml). Analytical methods such as TEM and Raman spectroscopy showed that the MW-CNTs had penetrated the seed coat and had enhanced water uptake by the cells of the germinating seed. While the exact mechanism is not yet understood, it is surmised that the CNTs could possibly augment the functioning of the aquaporin class of proteins in the cell membranes.

The continuing researches on the applications of CNTs will likely produce countless other uses in the near future, not only in the fields of materials technology and electronics, but also in medicine, biology and agriculture. The technology is not without controversy however, and the possible toxicity of these CNTs has been cause for concern. Scientists are continuing to study the toxicity of these CNTs but the general consensus is that an overexposure may be a serious risk to human health. For example, a study from the University of Cambridge found that carbon nanotubes could cause cell death [13]. Despite these worries, scientists continue to innovate, as the potential applications of these CNTs are too vast to consider stopping their research.

1.7 PLANTS AND ENVIRONMENT

Plants are living things that reproduce and have needs such as sunlight, water, and food including carbon dioxide and minerals. We can measure the growth of plants by length and area. Plant behaviours are defined as rapid morphological or physiological responses to events, relative to the lifetime of an individual. Plants have a life cycle, just like all living things [27-31]. They begin as a seed, grow into a plant and then make new seeds.

Green plants produce carbohydrates and oxygen from water [27, 32-34] carbon dioxide, minerals and light energy through the process of photosynthesis. They take in carbon dioxide from the air, water and minerals from the soil and energy from sunlight. During photosynthesis, carbon dioxide and water unite in the presence of chlorophyll to form sugar and oxygen. The green plant uses some of the carbohydrates it makes to grow and produce leaves and other structures. The plant converts the remaining carbohydrates to starch and stores it. Plants contain a phytohormone called auxin that promotes the lengthening of plant cells. A buildup of auxin occurs on the dark side of the plant stem. The extra auxin causes the cells on the dark side to grow longer forcing the stems to bend toward the light. This movement toward light is called "phototropism". "Photo" means light and "tropism" means movement.

Plants are the only organisms able to sustain themselves by producing their own food. They also provide the food for animals and humans through the food chain. In ancient times plants were the main source of medicines and are still a very significant source of medicines today. Almost all plants have one common characteristic making them different from animals that they produce chlorophyll, a substance that allows to reduce CO₂. Some plants, however, are not able to use sunlight and soil to produce their own source of energy. Plants also have studied for their ability to cure illness. Peppermint is used for stomach ailments. Foxglove contains a medicine to treat heart disease, and the cinchona tree produces quinine that is used to treat malaria. There are some plants that produce products that can cure illness or promote death. Cocaine can be a powerful anesthetic, but it can also be deadly. The opium poppy produces morphine, codeine and heroin which if used appropriately can help people relieve pain, but these substances can also be deadly if misused. [32]

Most of the plants grow from the seeds but some plants do not have to grow from seeds; for example, a potato is not a seed, but it can reproduce itself by growing roots from a

specialized part of the potato, call to bercales. Other plants can begin to grow if a small piece of the plant falls on soil. Some plants send out underground rhizomes that send up new plants periodically. Nonflowering plants grow from spores. Like a seed, a spore develops into an embryo. Unlike a seed, the spore does not contain carbohydrates to enable the embryo to grow.

Flowering plants grow from seeds. A sprouting seed must absorb water before it will start to grow. Inside the seed is a tiny embryo, surrounded by stored food. When the embryo starts growing, roots grow downward and a stem grows upward. Once the stem breaks through the surface of the soil into the sunlight, the first two true leaves form and the plant begins to make its own food. When plants have water, sunlight and the proper minerals in the soil, they grow, manufacture their own food and give off oxygen.

The examples listed above all involve resource acquisition. Plants also display responses to environmental cues that are reflected in their reproductive behaviours. Individuals that fail to get pollinated may increase their investment in rewards that attract insect visitors. Plants that experience conditions that are unfavourable for pollination may respond by producing cleistogamous flowers that do not open and are self-pollinated. Individuals of *Ipomopsis aggregata* that failed to get pollinated shifted from being semelparous (flowering once and dying) to being iteroparous. These responses allow successful reproduction to occur under suboptimal conditions. Herbivory to reproductive tissues causes plants to selectively abort and/or regrow reproductive organs; flower damage generally shifts plants towards more femaleness. The timing of seed germination for many species is strongly affected by environmental conditions. The decision to germinate is a conditional response in contrast to the specific programs of developmental changes that occur during the germination process, which are fixed and therefore not considered as plant behavior. For instance, the number of hours of daylight determines may break dormacy in certain seeds and whether some species will germinate, whether vegetative growth is determinate or indeterminate. The spectral quality of light, temperature, fire, exposure to water, oxygen, CO₂, ethylene and other chemicals, passage through animal guts and attack by insects can all be important in determining breaking dormacy and whether seeds geminate. These conditional responses allow seeds to germinate into environments that are favorable for growth and to remain dormant when conditions are unfavorable [27, 30, 32].

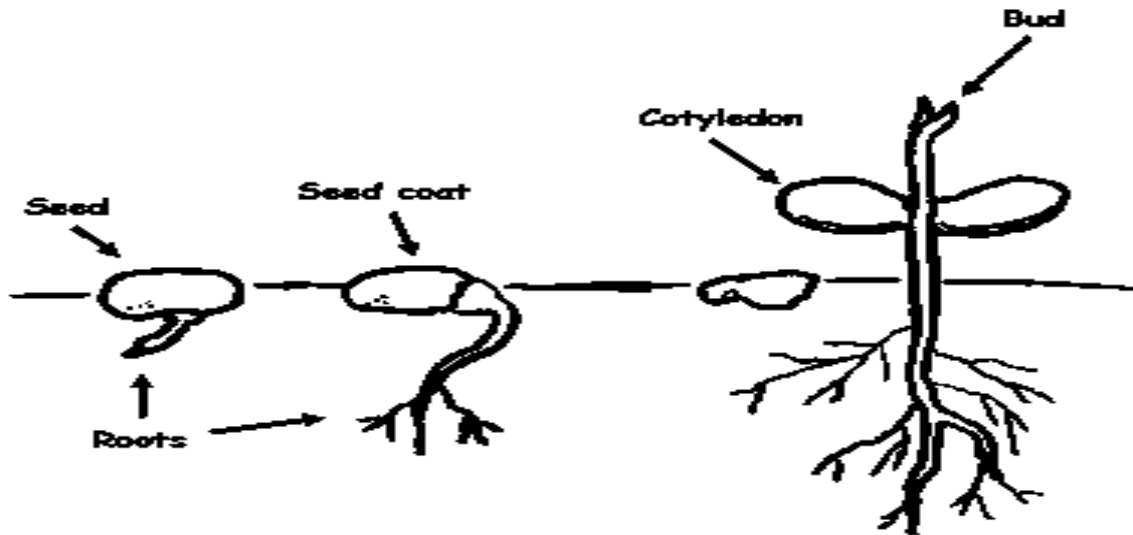


Figure 1.2: Seedling growth

1.8 WATER AND PLANT CELLS

The most abundant constituent of living plant cells is water. Water typically constitutes 80-95 % of the mass of growing tissues; common vegetables like carrots and lettuce may contain 85- 95 % water [32]. Wood, which is generally dead cell, has lower water percentage; sapwood, which has active Xylem transport, contains 35-75 % water, while heartwood, which does not transport water has slightly lower water content. Seeds with water content of 5-15 % are among driest of plant tissues [32, 33], yet before germinating they must absorb a considerable amount of water. Water serves several unique functions in the life of plants; it is most abundant and best solvent known. As a solvent it makes the medium for movement of molecules within and between cells and greatly influences the molecular structure and properties of proteins, membranes, nucleic acids and other cell constituents. Water is in the environment and in which most of the biochemical reactions in the cells occur and it participates in a number of essential reactions.

Plants continuously absorb and lose water, on a warm, sunny, dry day a leaf will exchange up to 100 % of its water in a single hour. The uptake of water is an important means of bringing dissolved soil minerals to the root surface for absorption. The fact that water is limiting is the reason for practice of crop irrigation. Water availability also limits the productivity of natural ecosystems. Thus an understanding of the uptake and loss of water by plants is of particular

importance. Polarity of water molecules gives rise to extensive intermolecular attraction “Hydrogen Bond”

Cell structure

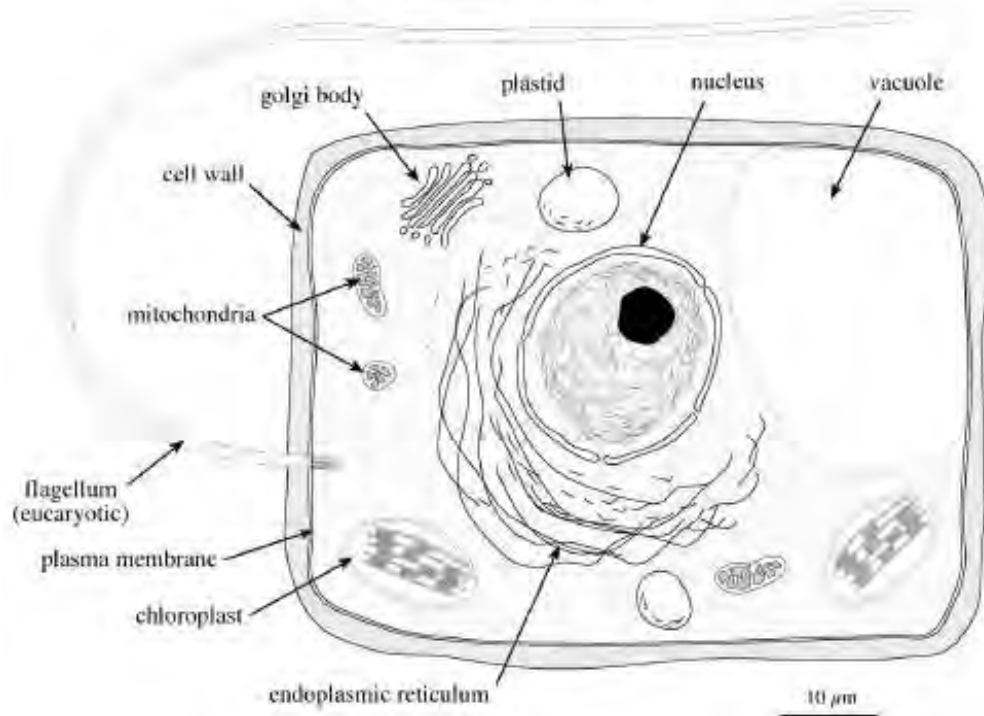


Figure 1.3: Plant cell structure

When water moves from the soil through the plant to the atmosphere, it travels through a widely variable medium, and the mechanism of transport also varies with the type of medium such as cell wall, cytoplasm, water channel and proteins. The water molecules in a solution are not static; they are in continuous motion, colliding with one and exchanging kinetic energy. Diffusion refers to the movement of molecules along a concentration gradient by random thermal agitation.

1.9 SEED GERMINATION AND DORMANCY

Seeds are a very important component of the world's diet grains and seed biology is one of the most extensively researched areas in plant physiology. Seed germination and dormancy

[36-41] are complex adaptive traits of higher plants that are influenced by a large number of genes and environmental factors. The use of quantitative genetics and other approaches has allowed the further genetic dissection of these traits. Molecular techniques, and especially expression studies and transcriptome and proteome analyses [36, 38,41] are novel tools for the analysis of seed dormancy and germination. The two fundamental promising questions which still catching the attention of researchers are:

- a) How does the embryo emerge from the seed to complete germination?
- b) How embryo emergence blocked so that seeds can be maintained in the dormant state?

The literature survey about Seed germination is far from comprehensive that's why it provides an overview of the essential processes that are associated with germination and a description of the possible impediments thereto that may result in dormancy.

The seed is the structure in which a usually fully developed plant embryo is dispersed and which enables the embryo to survive the period between seed maturation and seedling establishment thereby ensuring the initiation of the next generation. The dry dormant seed is well equipped to survive extended periods of unfavorable conditions. Seed dormancy is defined as the failure of an intact viable seed to complete germination under favorable conditions and is controlled by several environmental factors, such as light, temperature and the duration of seed storage (after ripening). Dormancy and germination are determined by the co-action of the growth potential of the embryo and the restraints imposed by the tissues surrounding it.

The seed, containing the embryo as the new plant in miniature, is structurally and physiologically equipped for its role as a dispersal unit and is well provided with food reserves to sustain the growing seedling until it establishes itself as a self-sufficient, autotrophic organism. The function of a seed is to establish a new plant; it may seem peculiar that dormancy, an intrinsic block to germination exists even in seemingly favorable conditions. For example, germination of annuals in the spring allows time for vegetative growth and the subsequent production of offspring, whereas germination in similar conditions in the fall could lead to the demise of the vegetative plant during the winter. Thus, dormancy is an adaptive trait that optimizes the distribution of germination over time in a population of seeds.

Seed dormancy is generally an undesirable characteristic in agricultural crops, where rapid germination and growth are required. However, some degree of dormancy is

advantageous, at least during seed development. This is particularly true for cereal crops because it prevents germination of grains while still on the ear of the parent plant (pre-harvest sprouting), a phenomenon that results in major losses to the agricultural industry. Extensive domestication and breeding of crop species have ostensibly removed most dormancy mechanisms present in the seeds of their wild ancestors, although under adverse environmental conditions, dormancy may reappear. By contrast, weed seeds frequently mature with inherent dormancy mechanisms that allow some seeds to persist in the soil for many years before completing germination.

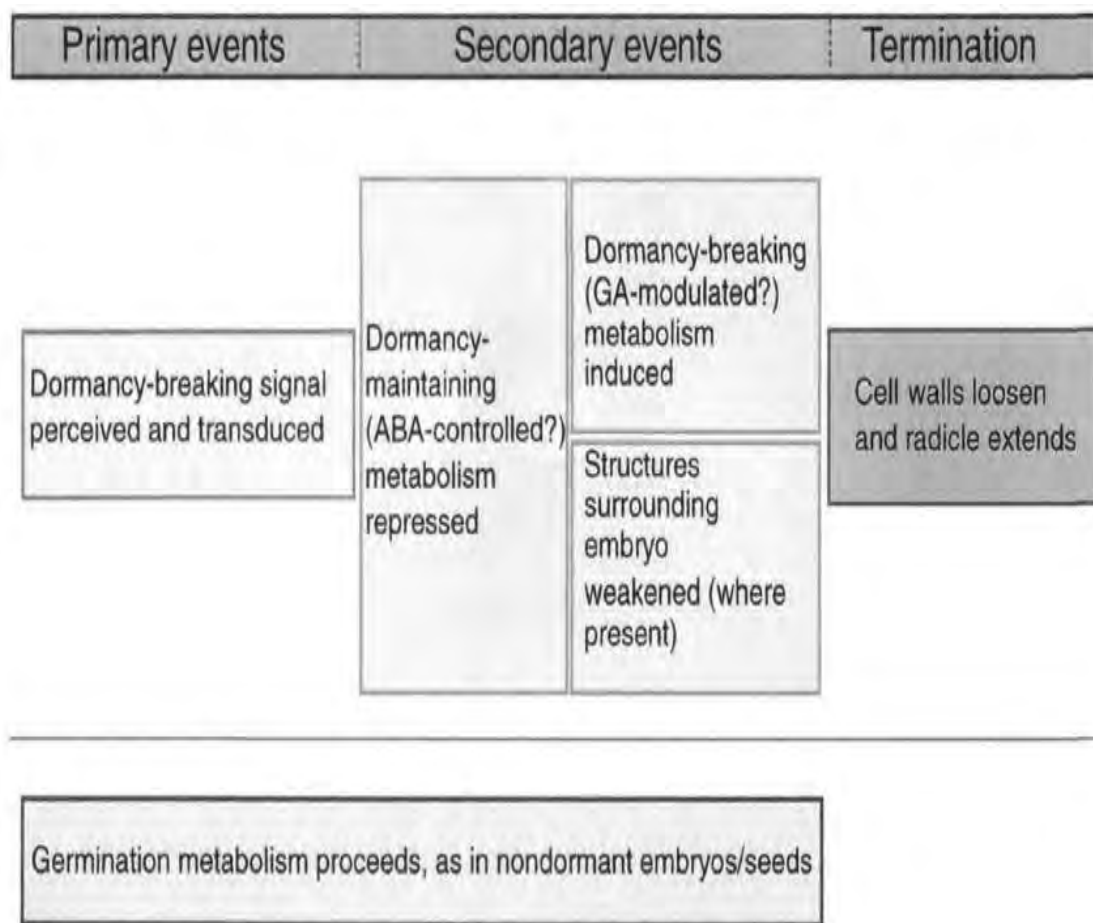


Figure 1.4: An overview of the major events that have been associated with the breaking of seed dormancy.

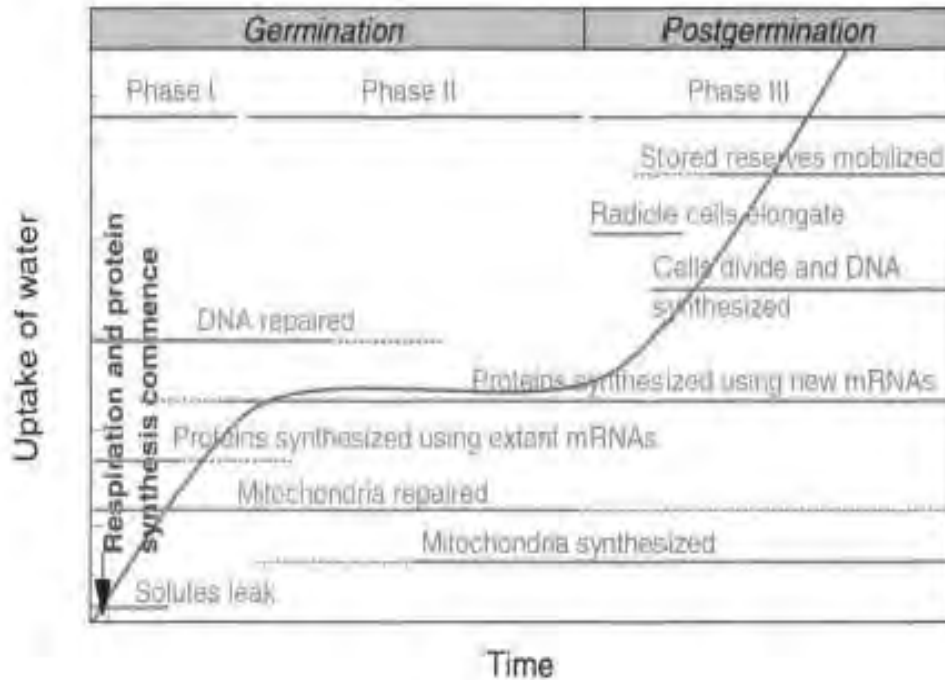


Figure 1.5: Time course of major events associated with germination and subsequent post germination growth.

Germination incorporates the events that commence with the uptake of water by the quiescent dry seed and terminate with the elongation of the embryonic axis (Bewley and Black, 1994). The visibility of completion of germination is usually the penetration of the structures surrounding the embryo by the radicle. Subsequent events, including mobilization of the major storage reserves are associated with the seedling growth. Virtually all of the cellular and metabolic events that are known to occur before the completion of germination of non-dormant seeds also occur in imbibed dormant seeds. The metabolic activities of the latter are from those of the formers. Hence, a dormant seed may achieve virtually all of the metabolic steps required to complete germination, yet for some unknown reason, the embryonic axis (i.e., the radicle) fails to elongate [37, 38]. Before considering dormancy, which imposes a block to the completion of germination, it is appropriate first to consider the processes that comprise germination. Germination commences with the uptake of water by the dry seed-imbibition and is completed when a part of the embryo, usually the radicle, extends to penetrate the surrounding structure.

In the germination process, the seed's role is that of a reproductive unit; it is the thread of life that assures survival of all plant species. Furthermore, because of its role in stand establishment, seed germination remains a key to modern agriculture. Thus, especially in a world acutely aware of the delicate balance between food production and world population, a fundamental understanding of germination is essential to crop production. Physiologically, germination is defined as the emergence of the radicle through the seed coat, which says nothing about other essential structures, such as the epicotyl or hypocotyls that become the above ground parts of a successful seedling. To the seed analyst, germination is "the emergence and development from the seed embryo of those essential structures which, for the kind of seed in question, are indicative of the ability to produce a normal plant under favorable conditions." This definition focuses on the reproductive ability of the seed, an essential objective in agriculture. Others consider germination to be the resumption of active growth by the embryo resulting in the rupture of the seed coat and emergence of a young plant. This definition presumes that the seed has been in a state of quiescence, or rest, after its formation and development. During this period of rest, the seed is in a relatively inactive state and has a low rate of metabolism. It can remain in that state until environmental conditions trigger the resumption of active growth. Regardless of which definition is preferred, it should be emphasized that one cannot actually see the process of germination unfold. Therefore all definitions include some measure of seedling development, even though this occurs subsequent to the germination event [36].

Based on the fate of the cotyledons, two kinds of seed germination usually occur, and neither appears to be related to seed structure. These two types are illustrated by the germination of bean and pea seeds. Although these seeds are similar in structure and are in the same taxonomic family, their germination patterns are quite different. Epigeal Germination. Epigeal germination is characteristic of bean and pine seeds and is considered evolutionarily more primitive than hypogeal germination. During germination, the cotyledons are raised above the ground where they continue to provide nutritive support to the growing points. During root establishment, the hypocotyls begins to elongate in an arch that breaks through the soil, pulling the cotyledon and the enclosed plumule through the ground and projecting them into the air. Afterwards, the cotyledons open, plumule growth continues and the cotyledons wither and fall to the ground [36, 38, 41].

1.10 FACTORS THAT AFFECT GERMINATION

a) Water and Germination

Water is a basic requirement for germination. It is essential for enzyme activation, breakdown, translocation, and use of reserve storage material. In their resting state, seeds are characteristically low in moisture and relatively inactive metabolically. That is, they are in a state of quiescence. Thus, quiescent seeds are able to maintain a minimum level of metabolic activity that assures their long-term survival in the soil and during storage. Moisture availability is described in various ways. Field capacity moisture is about optimum for germination in soil; however, germination varies among species and may occur at soil moistures near the permanent wilting point. Most seeds have critical moisture content for germination to occur. For example, this value in corn is 30%, wheat 40% and soybeans 50%. Once that critical seed moisture content is attained in the seed, sufficient water is present to initiate germination and the seed is committed to that event and can not turn back.

b) Gases balance

Air is composed of about 20% oxygen, 0.03% carbon dioxide, and about 80% nitrogen gas. If one provides different proportions of each of these gases under experimental conditions, it soon becomes clear that oxygen is required for germination of most species. Carbon dioxide concentrations higher than 0.03% retard germination, while nitrogen gas has no influence.

c) Temperature

Seed germination is a complex process involving many individual reactions and phases, each of which is affected by temperature. The effect on germination can be expressed in terms of cardinal temperature: that is minimum, optimum, and maximum temperatures at which germination will occur. The minimum temperature is sometimes difficult to define since germination may actually be proceeding but at such a slow rate that determination of germination is often made before actual germination is completed. The optimum temperature may be defined as the temperature giving the greatest percentage of germination in the shortest time. The maximum temperature is governed by the temperature at which denaturation of

proteins essential for germination occurs. The optimum temperature for most seeds is between 15 and 30°C. The maximum temperature for most species is between 30 and 40°C. Not only does germination have cardinal temperatures, but each stage has its own cardinal temperature; therefore, the temperature response may change throughout the germination period because of the complexity of the germination process. The response to temperature depends on a number of factors, including the species, variety, growing region, quality of the seed, and duration of time from harvest. As a general rule, temperate-region seeds require lower temperatures than do tropical-region seeds, and wild species have lower temperature requirements than do domesticated plants.

1.11 PATTERN OF SEED GERMINATION

Most seeds undergo a specific sequence of events during germination. Prior to germination, seeds are in a “maintenance” phase that is often characterized as dormancy being imposed by ABA, metabolic blocks or some other agent hindering the transition to germination. At some point, the seed becomes sensitive to the presence of “trigger” agents. A “trigger” agent such as light or temperature alterations shift the balance of inhibitors to favor promoters such as gibberellins. A “trigger” agent can be defined as a factor that elicits germination but whose continued presence is not required throughout germination. In contrast, a “germination” agent is a factor that must be present throughout the germination process. An example is gibberellic acid. The major sequence of events leading to germination is imbibition, enzyme activation, initiation of embryo growth, rupture of the seed coat and emergence of the seedling. Imbibition. The early stages of imbibition or water uptake into a dry seed represent a crucial period for seed germination. It is the first key event that moves the seed from a dry, quiescent, dormant organism to the resumption of embryo growth. Thus, any consideration of seed germination physiology and its resultant impact on stand establishment should focus initially on water uptake. The extent to which water imbibition occurs is dependent on three factors: (1) composition of the seed, (2) seed coat permeability, and (3) water availability. Composition of the seed. Seeds typically possess extremely low water potential attributed to their osmotic and matric characteristics. These potentials may be as low as – 400 MPa. The low water potentials are a consequence of the relationship of water with components of the seed. The temperature coefficient (Q₁₀) value of imbibition for most seeds

is 1.5 to 1.8 indicating that imbibition is a physical process not dependent on metabolic energy and related to the properties of the colloids present in seed tissues [32]. This is supported by the observation that imbibition occurs equally in dead and live seeds. Note in this figure that pea seeds have been heat killed and their rate of water uptake over time is essentially the same. The higher temperatures caused slightly greater rates of water increase due to the lower viscosity of water as temperatures increase. The principal component of seeds activated with the imbibition of water is protein. Proteins are zwitter-ions that exhibit both negative and positive charges that attract the highly charged polar water molecules. In contrast, this demonstrates that starches such as amylose have little affinity for water while lipids that have no charges on the molecular structure have no affinity for water.

Entry of water into seeds is greatly influenced by the nature of the seed coat (or pericarp). Water permeability is usually greatest at the micropylar area where the seed coat is ordinarily quite thin. The hilum of many seeds also permits easy water entry. Mucilages extruded from seed coats such as with this *Salvia* seed increase imbibition as do the cellulose and pectins located in the cell walls.

The environmental forces that determine the rate of water imbibition by seeds are complex. The ability to imbibe water is dependent on cell water potential and is a result of three forces:

- a) **Cell wall matric forces (represented by Ψ_m):** Cell membranes and intracellular inclusions such as mitochondria, ribosomes, and spherosomes are characterized by the presence of membranes. These membranes possess charges that attract water molecules and contribute to the total cell water potential.
- b) **Cell osmotic concentration (represented by Ψ_{II}):** The greater the concentration of soluble compounds, the greater the attraction for water.
- c) **Cell turgor pressure (represented by Ψ_p)** As water enters a cell, it exerts a swelling force on the cell wall called turgor pressure: Unlike the cell wall matric forces and osmotic concentration that attract water molecules into a cell, turgor pressure, which is a result of the restraining force of the cell wall, tends to retard water absorption.

It should be remembered that water always moves to more negative water potential and that the water potential of pure water is zero. The soils in which seeds are planted also exhibit

their own water potentials. The physical properties of soils determine the retention and conductivity of water. For example, it is well known that soils heavy in clays are able to absorb water more vigorously and retain it longer than those possessing high % of sand. In effect, as in this example, the difference between seed and soil water potential is quite large. The seed is at -14 MPa and the soil at -3 MPa. Thus, water flows into the seed. However, as imbibition continues, this difference is reduced in the immediate vicinity of the seed. If it were not for the conductive ability of soils, imbibition would be quickly halted. However, most soils exhibit a high degree of hydraulic conductivity that replenishes the available water surrounding the seed as it continues the process of imbibition. This is important since seeds are sessile and a continuous flow of water is essential for maximum imbibition. Associated with seed and soil water potential is the degree of seed-soil contact. The greater the intimate contact of the seed with the soil, the greater the amount of water imbibed. At least three mechanisms have evolved to improve seed-soil contact as demonstrated [32]. Differing kinds of seeds were exposed to decreasing water potentials using the matric forces of sintered glass plates that retained more water on their surface and germination under these conditions determined. Some seeds possess mucilage which is extruded from the epidermal cells of the seed as it imbibes water. The mucilage serves to increase the contact of the seed with the soil by increasing the number of pathways through which water may be absorbed by the seed that leads to increasing germination. Another mechanism to enhance seed-soil contact is to increase the amount of seed contact with a specific volume of soil. This can be accomplished by altering seed coat configuration. Seeds possessing textured seed coats are more likely to have a greater seed-soil contact than smooth-coated seeds, and thus they will imbibe water more rapidly resulting in greater germination. A final factor is seed size. Small seeds possess a greater surface area to volume ratio than large seeds. This greater surface area permits them to have access to a greater amount of water than larger seeds, which means they will hydrate and germinate more rapidly.

There are also differences among species in their ability to germinate at differing soil water content values. Seeds rarely attract water beyond 10 mm in most soils. Note that *Agropyron* and *Triticum* species are able to germinate at lower soil moisture contents than the others. Also, it is apparent that roots grow at lower soil water contents than shoots.

It would be expected that the process of water uptake would be uniform throughout the

seed. Yet studies to examine this process in soybean and corn seeds have demonstrated this is not the case. For example, the presence of an intact soybean seed coat is important to slow the uptake of water into the seed and it can delay water uptake for the first eight hours of soaking. The seed coat also directs water movement both tangentially and radially into the embryonic axis. The seed coat is the thinnest on the back of the seed, so water first moves into this structure as demonstrated by the wrinkling or swelling of the seed coat at this position.

The radial movement of water is attributed to the presence of a radical pocket that possessed a high incidence of hourglass cells. These cells may increase the water storage capacity around the radicle tip ensuring a ready source of water for turgor pressure essential for germination. The same appears true in many grass seeds, which possess a pericarp that completely surrounds the seed except at the pedicel end. This open, porous structure results in a more rapid hydration of the embryo that progressively moves from the radicle to the coleoptile end as demonstrated by staining in nitroblue tetrazolium chloride. Note at 6 hours, the radicle tip has already begun to turn color while the coleoptile region still remains white. A slower, more progressive wetting front simultaneously moves through the seed coat and into the endosperm that is not complete even after 48 hours imbibition.

1.12 METABOLISM OF GERMINATION

Several Studies have been conducted on the developmental changes that occur in seeds as they initiate embryo growth. Generally, the only substances taken up by the seedling during these early stages are water and oxygen. Because the seedling is underground and not photosynthetically active, there is a loss of CO₂ and leakage of seed materials that result in an overall loss in dry weight. As the seedlings initiate photosynthesis and have the capability to fix CO₂ into sugars, an increase in seedling dry weight occurs and there is a shift in sink strength within the seedling based on growth. Because monocot and dicot seeds are different in their morphological structure, it is not surprising that the alterations these seeds exhibit are unique.

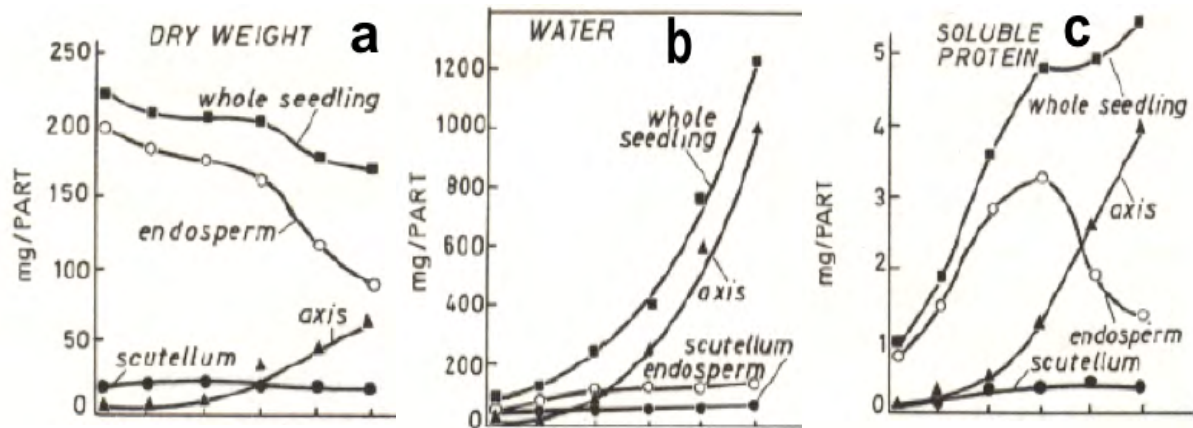


Figure 1.6: Metabolic process in maize seed germination, a, b and c represents the changes in dry weight, water uptake and soluble protein during time respectively.

Figure 1.6 represents the metabolic process of maize seed during 120 hours of germination. Monocot seeds generally display a germination pattern similar to that exhibited by corn. During the first 120 hours of germination, water uptake primarily occurs in the axis, which is high in protein content with little water uptake in the scutellum, which is high in oil content. Overall, there is a decrease in seedling weight initially with a marked decrease in dry weight of the endosperm and a concomitant increase in the dry weight of the embryonic axis. The scutellum shows little change in dry weight throughout the process. Soluble protein changes can be considered those associated with new enzyme formation. Note that there is a marked increase in soluble nitrogen formation throughout seedling growth. Initially, an increase in soluble nitrogen is found in the endosperm followed by a subsequent decrease in soluble nitrogen. Enzymes appear in the embryonic axis as it initiates growth and disappear, as the endosperm digestion is complete. The scutellum produces only a moderate increase in soluble nitrogen throughout this process.

a) Nucleic Acids Increase in both the Whole Seedling and Embryo Axis

These demonstrate that cells are dividing in this particular structure as growth is initiated. There is no change in the endosperm because this tissue is dead while the scutellum shows only a slight increase likely associated with the nucleic acids being transcribed for the synthesis of lipases.

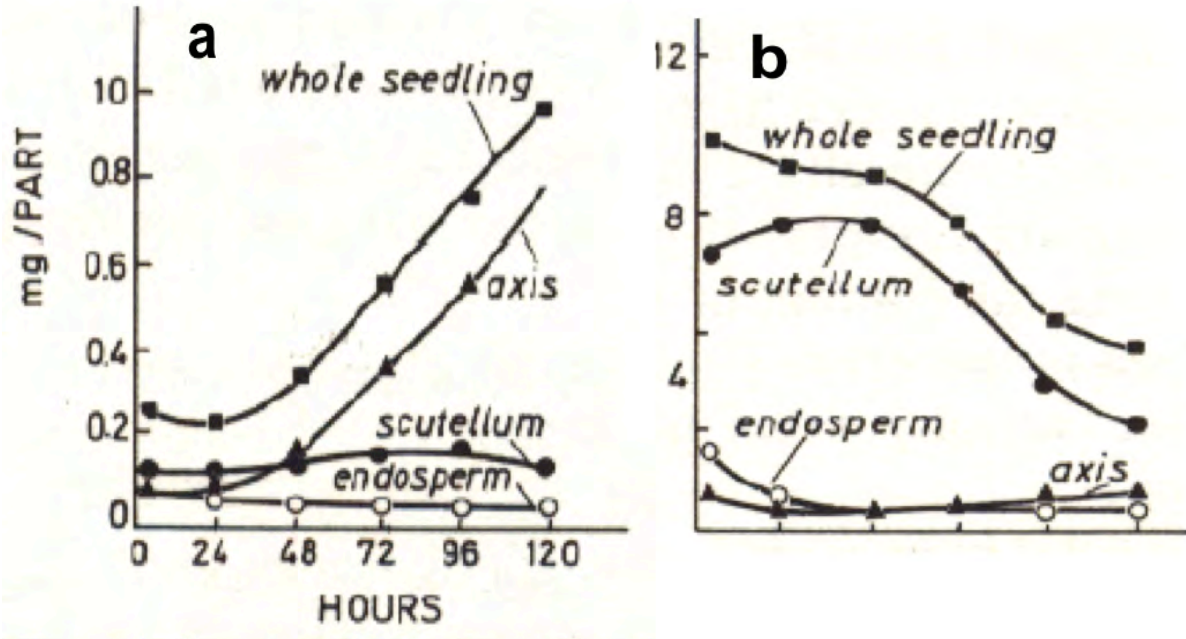


Figure 1.7: Nucleic Acid and Lipid changes during metabolism of 120 hours in Maize seed germination.

Lipid changes decrease during seedling growth because they are being degraded into fatty acids that are utilized during β -oxidation for the synthesis of energy. Most of these changes occur in the scutellum that is the primary oil storage structure in the corn seed. Little change in lipids is observed in the axis because this structure does not possess storage lipids.

Castor bean or *Ricinus communis* serves as an example of the physiological changes that occur in an oil-storage seed. In this seed, most of the oil is stored in the endosperm because the cotyledons are thin and leaf-like. To obtain energy from the lipids for seedling growth, mechanisms must be found where the lipids can be degraded for use in β -oxidation. This process is directed by the glyoxylate cycle that changes fatty acids ultimately to sucrose, which is a non-reducing sugar. Glucose and fructose, two molecules used in the TCA cycle to generate energy in lipid containing seeds, are reducing sugars. The graph on the left demonstrates that sucrose is first detected in the cotyledons where it is translocated to the embryo. Then it is hydrolyzed to glucose and fructose, which are used to generate energy for seedling growth.

b) The Fatty Acids are used in the Glyoxylate Cycle to Produce Sucrose

The disappearance of fatty acids from the endosperm where the greatest concentration of oil exists is documented in the following graph. The enzyme responsible for the degradation of oils to fatty acids is lipase. In protein containing seeds, protein hydrolysis is accomplished by proteases likely synthesized under the direction of gibberellins. The graph demonstrates that much of the protein degradation occurs in the cotyledons and then declines as the protein levels are exhausted with little activity present in the embryonic axis. The availability of high inorganic phosphorous levels during the early stages of seedling growth is essential for the production of phospholipids as well as energy rich molecules such as adenosine triphosphate (ATP). Approximately 80% of the phosphorous found in seeds is associated with the molecule phytin. To obtain this phosphorous, the hydroxyl group of phytin must be hydrolyzed by the enzyme phytase to release the inorganic phosphorous. With respect to nucleic acids, the initial stages of radicle protrusion through the seed coat are caused by cell elongation followed by cell division. As a result, deoxyribonucleic acid (DNA) synthesis is detected late after visible radicle protrusion. Initial enzyme synthesis is guided by the presence of long-lived or stored messenger ribonucleic acid (mRNA) that was synthesized during seed development and maintained in the seed until the germination event since the genetic code on DNA must be read and transcribed onto mRNA. During germination, the mRNA is translated into the synthesis of enzymes essential for germination.

c) Adsorption and Soaking Metabolism

Uptake of water by a mature dry seed is triphasic (Figure 1.4 & 1.5), with a rapid initial uptake (phase I) followed by a plateau phase (phase II). A further increase in water uptake occurs only after germination is completed, as the embryonic axes elongate. Because dormant seeds do not complete germination, they cannot enter phase III. The influx of water into the cells of dry seeds during phase I results in temporary structural perturbations, particularly to membranes, which lead to an immediate and rapid leakage of solutes and low molecular weight metabolites into the surrounding imbibition solution. This is symptomatic of a transition of the membrane phospholipid components from the gel phase achieved during maturation drying to the normal, hydrated liquid-crystalline state (Crowe and Crowe, 1992).

Within a short time of rehydration, the membranes return to their more stable configuration at which time solute leakage is curtailed. Upon imbibition, the quiescent dry seed rapidly resumes metabolic activity [32, 33, 34, 36]. The structures and enzymes necessary for this initial resumption of metabolic activity are generally assumed to be present within the dry seed having survived at least partially intact the desiccation phase that terminates seed maturation. Reintroduction of water during imbibition is sufficient for metabolic activities to resume with turnover or replacement of components occurring over several hours for achieving full metabolic status.

One of the first changes upon imbibition is the resumption of respiratory activity, which can be detected within minutes. After a steep initial increase in oxygen consumption, the rate declines until the radicle penetrates the surrounding. The time for events to be completed varies from several hours to many weeks, depending on the plant species and the germination conditions [37].

d) The Genetic Analysis of Differences in Seed Dormancy and Germination Characteristics

Genetic variation for seed dormancy within species is present both among accessions of wild plants and among varieties of cultivated plants. The substantial influence of environmental effects on the expression of germination characteristics and the involvement of many genes make dormancy a typical quantitative trait. Such traits are becoming more amenable to genetic analysis because the position of individual “*quantitative trait loci*” (QTL) and the relative contribution of these loci can now be determined. QTL analysis for seed dormancy requires permanent or immortal mapping populations, such as “*recombinant inbred lines*” (RILs), because these allow the testing of a large number of genetically identical seeds (i.e. seeds from the same RIL) in different environmental conditions. QTL analysis of seed dormancy has been reported for *Arabidopsis thaliana* [3], barley [4], rice [5] and wheat [6]. It appears that QTL identified for wheat co-locate with barley QTL but not with rice QTL [6]. Wild species often show stronger dormancy than cultivated genotypes, making crosses between wild and cultivated genotypes useful for QTL analysis [7,8]. QTL analysis can be followed by the study of individual genes (or chromosome regions) containing specific dormancy QTL and by fine mapping. Such studies have been initiated in barley [9,10] and

Arabidopsis (L Bentsink, unpublished data). It is expected that the study of such QTL will allow the molecular identification of genes that affect dormancy in these species by map-based cloning. However, the cloning of such dormancy QTL has not yet been reported.

Dry seeds are characterized by a remarkably low rate of metabolism that is undoubtedly attributable to their low moisture content that can be as low as 5 to 10% in unimbibed seeds. As soon as the seed becomes imbibed, however, marked changes in metabolism occur. A triphasic pattern of water uptake has been demonstrated during the germination of most seeds. Phase I occurs in dead or live seeds, an immediate release of gases is observed. It is not dependent on metabolism and is the result of matric forces and their attraction for water molecules inside the seed. Enzyme activation begins during Phases I and II of imbibition: During Phase II, there is a lag period in water uptake, but the seed undergoes many processes essential for germination. Finally, in Phase III, root elongation is observed: The root becomes functional during this phase and is responsible for the increased water uptake noted in Phase III. Interestingly, if respiration rates are observed, a similar triphasic pattern is found demonstrating the importance of water for enzyme activation. Here, pea seeds are followed with their seed coats intact (solid dots) or removed (open dots). When the seed coat is removed, respiration is more rapid because water uptake occurs more quickly. Note how there are three phases of respiration increase associated with the three phases of water uptake. The fourth phase in this graph is related to activities associated with lack of light and a decline in respiration due to the lack of photosynthesis since these seeds were germinated in the dark.

Respiration is the break down of sugars to produce energy molecules such as ATP. Based on these respiration findings, ATP production should also possess a triphasic pattern. In this study of imbibing lettuce seeds, the top graph documents the uptake of water and oxygen over time. Lettuce seeds initiate radicle protrusion based on this graph at 16 hours. In the lower graph, the production of ADP, ATP and total nucleotides is presented. Notice the expected triphasic increase for ATP and total nucleotides. Phase III occurred at 16 hours imbibition or the time of radicle protrusion.

Generally, enzymes that break down carbohydrates, lipids, proteins, and phosphorous-containing compounds are the first to be activated during Phase II of water uptake by seeds. The controlling mechanism for directing this storage tissue degradation has not yet been

clearly elucidated. In monocots, the following diagram depicts the transitions in chemistry with germination. Each circle represents the activity of a particular enzyme. Since the embryonic axis requires energy for growth, storage compounds must be hydrolyzed to soluble forms, translocated from the endosperm to the embryo, and transformed to energy molecules that can be immediately utilized by the embryonic axis. The endosperm initially becomes rich in soluble products such as glucose and maltose. These are then absorbed by the scutellum. In the scutellum, glucose and maltose are transformed by a series of in situ enzyme reactions to form sucrose. Sucrose itself is not hydrolyzed within the scutellum because the essential enzymes are not present. The sucrose molecule is then transported to the adjacent embryonic axis as the principal energy molecule for growth. In dicots, the hormonal regulation of storage product degradation is not as clear as monocots. This may be due to the absence of an aleurone-like tissue that synthesizes hydrolytic enzymes. Additionally, the role of hormones in dicot seed germination has been debated. In some instances, gibberellins are known to trigger hydrolytic enzyme synthesis, but the degree of activation is never as great as that noted in cereals. Some believe that germination is mediated by the growing embryonic axis. As the axis continues to grow, it incorporates breakdown products into the synthesis of new compounds. This reduces the concentration of compounds in the cotyledons, which in turn stimulates the hydrolysis of other storage reserves for use by the embryonic axis. Should this stimulation prove to be too great, and hydrolyzed storage products begin to accumulate, a feedback mechanism may be operative that retards further storage reserve hydrolysis. The mobilization and transfer of nutrients as shown in this diagram is through the conductive tissue of the cotyledons to the growing embryonic axis. Like grass seeds, storage compounds must initially be hydrolyzed to a soluble form before they can be translocated.

At this point the seedling is an autotrophic organism capable of growth without additional reserves. Germination is also ended by visible protrusion of the radicle and subsequent growth is attributed to seedling development.

1.13 GENOMICS AND PROTEOMICS IN SEED RESEARCH

Microarrays containing 2600 genes expressed in developing *Arabidopsis* seeds were described by Girke et al.. These microarrays revealed many genes of unknown function that are highly expressed in seeds. The analysis of protein patterns by 2D gel electrophoresis and

the subsequent identification of a number of those proteins, showed that among the 1300 seed proteins detected, 74 changed in abundance during the imbibition phase or during the radicle protrusion of Arabidopsis. Many of these proteins had previously been described as being involved in germination (e.g. in the mobilization of food reserves). In addition, proteins not previously associated with these processes were identified [32, 34, 37].

Germination incorporates those events that commence with the uptake of water by quiescent dry seed and terminate with the elongation of the embryonic axis. The visible sign that germination is complete is usually the penetration of the structures surrounding the embryo by radicle; the result is often called visible germination. Subsequent events, including the mobilization of the major storage reserves, are associated with growth of the seedling. Virtually all of the cellular and metabolic events that are known to occur before the completion of germination of nondormant seeds also occur in imbibed dormant seeds; indeed, the metabolic activities of the later are frequently only subtly different from those of the former. Hence, a dormant seed may achieve virtually all of the metabolic steps required to complete germination, yet for some unknown reason, the embryonic axis (radicle) fails to elongate.

In addition to the identification and subsequent cloning of genes through the use of mutants, genes controlling seed dormancy and germination can also be identified on the basis of their expression pattern. This may involve an unbiased search of genes with germination-specific expression or may focus on genes with assumed functions that are related to seed germination. During seed maturation the expression of many genes is altered and specific classes of mRNAs such as those of the late-embryogenesis-abundant (LEA) genes appear. However, none of these genes has a proven specific function in seed dormancy. Although it appears that seed maturation and post-germination growth have a distinct gene-expression profile, some genes that are highly expressed after germination are also expressed during the later stages of seed development, suggesting that some aspects of post-germination growth are initiated during maturation. To study genes that are activated during late embryo development and germination, mRNAs from immature siliques of the *abi3 fus3* double mutant were compared with those from wildtype siliques using a differential display [32]. The genes that were identified as being active during late embryo development and germination encode a variety of metabolic enzymes, regulatory proteins and a number of ribosomal proteins.

Cellular processes involved in growth, the activation of protection mechanisms (such as those involved in protection against oxidative stress), and storage-compound metabolism are expected to be related to germination. Germination in tomato and tobacco is controlled by interactions between the embryonic radicle tip and the enclosing endosperm cap. Weakening of the endosperm cap, by enzymatic hydrolysis, is required to allow radicle protrusion.

Dormancy and germination are complex traits that are controlled by a large number of genes, which are affected by both developmental and environmental factors [36, 37]. Seed dormancy and germination depend on seed structures, especially those surrounding the embryo, and on factors affecting the growth potential of the embryo. The latter may include compounds that are imported from the mother plant and also factors that are produced by the embryo itself, including several plant hormones. Genetic analysis has identified the crucial role of ABA in seed dormancy, as well as the requirement for GAs for germination. QTL and mutant analyses are identifying additional genes. Whether these genes with unknown functions are downstream targets of ABA and GA, or whether they affect seed dormancy/germination in an independent way is currently not known. The molecular identification of all these genes will be important, as will the identification of more target genes. Using whole transcriptome and proteome approaches will be the most efficient way to identify target genes.

1.14 REFERENCES

1. S. Ijima, *Nature*, 1991, 354, 56
2. G. Overny et al, *Z. Phys.*, 1993, D27, 93
3. Morinobu Endo et al, *Appl. Physics*, 2008, 111, 13
4. Srivastava et al, *Appl Mech Rev.*, 2003, 56, 215
5. Biological Materials Science: Bio-inspired Materials Design and Processing,
<http://www.programmaster.org/PM/PM.nsf/ViewSessionSheets?OpenAgent&ParentUNID=7C4B0CCD3C3C4C5685257611006AABC0>
6. N. Hamada et al, *Phys. Rev. Lett.* 1992, 68, 1579
7. C. Kociak et al, *Phys. Rev. Lett.*, 2001, 86, 2416
8. A.G. Rinzler et al, *Science*, 1995, 269, 1550
9. B. Cantor et al, *Scripta Mate.*, 2001, 44, 2055

10. V. Zhirnov et al, *J. Nanopart. Res.*, 1999, 1, 151-152.
11. Robert Meservy, www.chem.usu.edu/~tapaskar/Robert-Water%20Purification.pdf
12. M. khodakovskaya et al, *ACS Nano*, 2009, 3, 3221-3227
13. Carbon nanotubes found to increase plant growth,
<http://www.yearofscience.org/carbon-nanotubes-found-to-increase-plant-growth/>
14. Qiaoling Liu et al, *Nano Lett.*, 2009, 9, 1007
15. Daohui Lin et al, *Environmental Pollution*, 2007, 150, 243
16. Nucleoside transport and metabolism; <http://www.uni-kl.de/wcms/agn-research-ent.html>
17. Monique Long, The Effects of Single-Walled Carbon Nanotubes (SWNTs) on Plants, Texas Tech University, 2009.
18. Sandeep Agnihotr et al. Energy And Environmental Applications Of Carbon Nanotubes, Fuel Chemistry Division Preprints 2002, 47(2), 474
19. B. Šimić, S. Popović, M. Tucak, Influence Of Corn (*Zea Mays* L.) Inbred Lines Seed Processing On Their Damage, *Plant Soil Environ.*, 50, 2004 (4): 157–161
20. M. Janmohammadi Et Al. Seed Invigoration Techniques To Improve Germination And Early Growth Of Inbred Line Of Maize Under Salinity And Drought Stress, *Gen.Appl.* Psleaendtinpvhigyosriaotliongte,C2h0n0iq8u,Esptoeciimaplrriosvseuge,Er3m4in(3at-I4o)N,..2.15-226
21. Anatomy of the Mature Maize Seed, Maize Seeds In Situ Hybridization Database (<http://masish.uab.cat/masish/>)
22. Niraj Sinha et al., Carbon Nanotubes for Biomedical Applications, IEEE TRANSACTIONS ON NANOBIOSCIENCE, VOL. 4, NO. 2, JUNE 2005
23. DUBRAVKA NAUMOVSKI, Germination ecology of seeds of endemic species *Degenia velebitica* (Degen) Hayek (Brassicaceae), *Acta Bot. Croat.* 64 (2), 323–330, 2005
24. Guan et al. Seed priming with chitosan improves maize germination and seedling growth in relation to physiological changes under low temperature stress, *J Zhejiang Univ Sci B* 2009 10(6):427-433

25. Miguel Á. Copete et al. Seed germination ecology of the endemic Iberian winter annuals *Iberis pectinata* and *Ziziphora aragonensis*, *Seed Science Research*, Vol. 19, Issue 03, (2009) 155-169.
26. Richard Karban, Plant behaviour and communication, *Ecology Letters*, (2008) 11: 727–739 doi: 10.1111/j.1461-0248.2008.01183.x
27. Introduction to Plants, EED WACKERS! K-6 Educators Guide to Invasive Plants of Alaska
28. Alaska Department of Fish and Game (ADFG). 2005. Alaska Wildlife Curriculum, Alaska Ecology Cards. Anchorage, AK.
29. Carolin, R. 2005. *Incredible Plants*. Discoveries Series. Barnes and Noble Books, New York, NY.
30. Watts, B. 1987. *Dandelion*. Stopwatch Book Series. Silver Burdett Press, Englewood Cliffs, NJ.
31. Brussels, 6.5.2013 COM (2013) 262 Final, 2013/0137 (COD), Proposal For A Regulation of The European Parliament and of The Council on The Production And Making Available On The Market Of Plant Reproductive Material (Plant Reproductive Material Law) European Commission.
32. Taiz L., Zeiger E., *Plant Physiology* - 2002
33. Phytoremediation, LID Technical Guidance Manual for Puget Sound
34. Introduction to Phytoremediation, National Risk Management Research Laboratory Office of Research and Development U.S. Environmental Protection Agency Cincinnati, Ohio 45268, EPA/600/R-99/107 February 2000
35. Hinchman, Negri, and Gatliff, *Phytoremediation: Using Green Plants To Clean Up Contaminated Soil, Groundwater, And Wastewater*, Argonne National Laboratory Applied Natural Sciences, Inc.
36. J. Derek Bewley, Seed Germination and Dormacy, *The Plant cell*, Vol. 9, 1055-1066, July 1997, American Society of Plant Physiologists.
37. Maarten Koornneef et al. Seed Dormacy and Germination, *Curremnt Opinion in Plant Biology*, 5:33-36, 2012, Elsevier Science Ltd.
38. Loic Rajjou et al. Seed Germination and Vigor, *Annual Review of Plant Biology*, 6:507-33, 2012.

39. Y. Long et al. seed Dormancy and germination Characteristics of *Astragalus Arpobus* (Fabaceae, Subfamily Papilionoideae), a Central Asian Desert Annual Ephemeral, *South African Journal of Botany*, 83 (2012) 68-77.
40. Roger C. Styer et al. Dependence of Seed Vigor During Germination on Carbohydrate Source in Endosperm Mutants of Maize, *Plant Physiol.* (1984) 76, 196-200.
41. Bas J. W. Dekkers et al. Glucose delays Seed Germination in *Arabidopsis Thaliana*, *Planta* (2004) 218: 579-588.
42. Y. A. Kacar et al. Gelling Agents and Culture Vessels Affect in Vitro Multiplication of Banana Plantlets, *Genetics and Molecular Research* 9 (1): 416-424 (2010).
43. PS Warakagoda and S Subasinghe, In Vitro Culture Establishment and shoot Proliferation of *Jatropha Curcas L*, *tropical Agricultural Research & Extension* 12(2): 2009.
44. Nanotechnology and the environment: A mismatch between claims and reality, International POPs Elimination Network's Nanotechnology (IPEN) Working Group
45. Nanotechnology and the Environment, Report of a National Nanotechnology Initiative Workshop May 8–9, 2003, Arlington, VA
46. Nanotechnology and Environment: Beauty and the Beast?, Cynthia Folsom Murphy, David Allen, University of Texas, 2004.
47. Nanotechnology: Opportunities and Risks for Humans and the Environment, http://nanotech.law.asu.edu/Documents/2009/11/Germany%20nanotechnology%20opportunities%20and%20risk_385_7590.pdf
48. Beeta Ehdaie, Application of Nanotechnology in Cancer Research: Review of Progress in the National Cancer Institute's Alliance for Nanotechnology, *Int. Journal of Biological science*, 2007, 3(2): 108-110.
49. Woong Kim et al. Hysteresis Caused by Water Molecules in Carbon Nanotube Field-Effect Transistors, *Nano Letters*, DOI: 10.1021/nl0259232.
50. Mark C. Kalpin and Melissa Hoffer, Nanotechnology and the Environment: Will Emerging Environmental Regulations Stifle the Promise? US1DOCS 4975958v1
51. Ken Schmidt et al. Nanotechnology in the Environment Industry: Opportunities and Trends, Final Report and Bibliography for the Nano-Environmental Cross-Sector Initiative, March 4, 2005.

52. Mohammad Abdul Hameed Hyder, Potential Applications and Environmental Implications of Nanotechnology, Technical University of Hamburg-Harburg Germany.
53. Carbon Nanotubes and Graphene for Electronics Applications 2010-2020, By Ms Cathleen Thiele and Raghu Das, IDTechEx.com.

CHAPTER 2
MATERIALS AND CHARACTERIZATION TECHNIQUES

CAPÍTULO 2
MATERIALES Y TÉCNICAS DE CARACTERIZACIÓN

CHAPTER 2

Materials and Characterization Techniques

2.1 EXPERIMENTAL PROCEDURE

2.1.1 Materials Description

Multi-Walled Carbon Nanotube (MWCNT), carbon content > 95%, OD 6-9 nm, L 5 μ m: Produced by CoMoCAT[®] catalytic Chemical Vapor Deposition (CVD) process, number of walls are between 3-6, Black Powder, Diameter: 5.5 nm mode and 6.6 nm median, Melting Point: 3652-3697 °C, Density: ~2.1 g/ml (25°C), Bulk Density 0.22 g/cm³, Tube diameter determined from optical absorbance spectrum and AFM.

Multi-Walled Carbon Nanotube (MWCNT), Purity > 98% carbon basis, OD 6-13 nm, L 2.5-20 μ m: Preparation: CVD Method followed by HCl demineralization, average wall thickness ~ 7-13 graphene layers, Black Powder, Composition: Carbon >98% based on total metals impurities (X-ray Diffraction), Trace metal analysis \leq 20000 ppm, MWCNT: 99% (HRTM), Outer Diameter: 6-13 nm (HRTEM), Average Diameter: 12 nm (HRTEM), Inner Diameter: 2.0-6.0 nm (HRTEM), Length: 2.5-20 micron (TEM), Average Length: 10 micron (TEM), BET Surface Area: 2~20 m²/g (SSA), Melting Point: 3652-3697 °C, Density ~ 2.1 g/ml (25°C).

FeCl₂-4H₂O: Sigma-Aldrich [Purity \geq 99.0% (RT)], Sigma-Aldrich Quimica, S. de R.L. de C.V, Parque Industrial Toluca 2000, Calle 6 Norte No. 107, 50200 Toluca, Mexico.

FeCl₃-6H₂O: FeCl₃.6H₂O, PolystormorTM, AR ® (ACS), (97-102%) Mallinkrodt Inc. (Phillipsburg, NJ, USA).

MS Medium: MS Basal Medium (MS5519) Sigma Aldrich.

Agarose: Agarose (A9539), Sigma-Aldrich®, Sulphates \leq 0.15%, Impurities \leq 10% moisture content, Gel Strength \geq 1200 g/cm² at 1%, Gel Point 36°C(\pm 1.5°C), Electroendosmosis (EEM) 0.09-0.13.

Seeds: Maize (*Zea mays* var. *saccharata*) and Tomato (*Solanum lycopersicum*), Hortafloor, Rancho Los Molinos, S.A. de C.V.

Bacteriological Agar (BA): Bacteriological Agar, BD Bioxon, Becton Dickinson de Mexico, Cuatitlàn Izcalli, Edo. de Mèxico., Mèxico.

2.1.2 Medium Preparation using Autoclave and Seed Germination

Maize and Tomato seeds (Los Molinos) were cleaned by using ethanol solution (70% vol.) during 2 minutes on magnetic stirrer, after that, they were washed with deionized (DI) water. The seeds were also sterilized by using sodium hypochlorite solution (1% v/v in DI water) for 10 minutes and, washed several times by DI water. Before start the experiment sterilize all utilizes and containers (which are going to use) in the Autoclave. The first experimental set consisted of maize seedlings grown in agarose and BA gel medium spiked with different concentrations of MWCNT of purity 99% and 95 %. The agarose and BA powder were weighed and mixed with de-ionized (DI) water to obtain a concentration of 8 g/l and 15 g/l respectively. The agarose and BA were dissolved by heating the aqueous mixture at $\sim 95^{\circ}\text{C}$ with constant magnetic stirring about 2.5 hours. Upon complete dissolution, different aliquot volumes of the clear agarose solution were measured out. Appropriate masses of MWCNT were weighed out and mixed with aliquot volumes of the sterile agarose and BA solution by mechanical stirring for ~ 10 minutes in order to yield unvaried distributions of MWCNT in the gel of the different concentrations. The agarose and BA solutions containing the different concentrations of the MWCNT were then poured into replicate sterile petridishes to set as the gel substrate for seed growth. The environmental conditions of the samples were controlled by phytotron chamber (Temperature $23\text{-}25^{\circ}\text{C}$, Relative humidity $70\text{-}75\%$). The total numbers of seedlings in each set of experiment were described briefly in result section. The entire sets of plants were grown during a period of one to four weeks and dried at 60°C for 72 hours in an oven.

2.1.3 Medium Preparation using Magnetic Hot-Plate and Dark Germination of Seeds

The appropriate amount of bacteriological agar (BA) and agaose materials were weighed for concentrations 15 g/l and 8g/l respectively in distilled water and kept in beakers clean by HI-Clean protocol (first in 10% volume of Nitric acid for 8 hour and after that 24 hours in 1% volume of Nitric acid and after that clean with distilled water and dry in the oven). The

temperature of the magnetic heater was fixed 95-100⁰C and heated until the BA/Agarose completely melts (~3 hours). After complete melting of the medium divide it in separate beakers and weight MWCNT for concentrations 0, 5, 10, 20, 40 & 60 mg/l were mixed mechanically. While the MWCNT mixed homogenously in agar solution let it be cooled and before arriving to gel pore it in the sterilize petri dishes of sufficient replicated. After gelling the culture medium with and without MWCNT, embade the seeds at a seperate distance and keep in dark for germination of controlled temperature and humidity chamber**.

** The detailed descrrption of material prepararion for each set of experiments are explained in each chapter.

2.1.4 Nutrient Concentration and Dispersion of MWCNT

The MS medium is a highly concentrated nutrient medium. It is toxic to seedlings of some plants and like other nutrient recipes, is used in plant tissue culture media only to ensure nutrient supply for the growing plant [33, 34]. Monocotyledonous and gramminaceous plants like maize are particularly sensitive and show root burning (browning of the roots) and other symptoms of osmotic stress that impact the seedling's health [35, 34]. Maize seeds have enough intrinsic nutrients and can germinate successfully without a nutrient medium [35]. However, we need a **diluted** solution of MS in order to study the relative permeabilities of the various nutrient elements and how they are affected by the MWCNT.

The concentrations of elements in 1-MS (i.e. full strength MS) are very large, e.g. P is present in soil as 0.06 ppm [34] whereas in MS it is at the level of 38.75 ppm [1], an increase by a factor of 646. A ¼ dilution would reduce this to only 9.68 ppm, which is still ~ 161 times higher than naturally occurring P in soils. Considering that maize is a food grain that already is rich in nutritive elements unlike tomato seeds that are small and have little food value. That is possibly the reason why 1-MS was not toxic to tomato in the experiments of Khodakovskaya et al [36] but proved toxic to our maize seeds.

Therefore our interest is to ensure minimal damage to the health of the seedling, we reduce the concentration to **1/8 MS**. P will then be at 4.84 ppm, a manageable concentration. Now, BA already has some amount of nutrient salts [37] although at a much lower

concentration than MS. So 1/8 MS will be sufficient to allow the elements of interest to show up in the subsequent elemental analysis.

The effect of the toxicity of MWCNT on plants might be enhanced because of the combined effects of the purity of the MWCNT and the strength of the MS medium. Hence we use low concentrations of the high purity MWCNT in conjunction with low concentration of the MS (1/8 strength).

The dispersion of MWCNT has been done in 1/8 MS solution of pH 5.75, using ultrasonication for 2 hours at 48 kHz frequency.

2.1.5 Harvesting Germinated Seedling

Upon harvesting, the seedlings were gently rinsed with DI water, blotted dry with paper towels and their fresh weight (FW), root length (RL) and shoot length (SL) were measured. Then roots and shoots were cut and the FWs of these parts as well as of the seed body were measured. The seed body, root and shoot parts were dried at 60°C for 72h and dry weights (DWs) of these parts were measured too. A few seed bodies from the first experimental set were analyzed by Scanning Electron Microscopy (SEM).

2.1.6 Powder Preparations

The powder samples were prepared by using milling machine (Retsch, model MM-400) and 14 stainless steel balls. The milling conditions were a frequency of 25 Hz and time of 2 minutes till the entire mass appeared as a fine uniform powder.



Figure 2.1: Milling machine to prepare the powder samples

2.2 CHARACTERIZATION TECHNIQUES

The biomass and length measurements were analyzed by statistical software GraphPad Prism, version 5.0b with a significant probability (P) of < 0.05 (95 % confidence level). They were then assigned for analysis on the polarized energy dispersive x-ray fluorescence (pEDXRF) instrument (Spectro Analytical Instruments GmbH, Kleve, Germany, model Xepos III). After the non-destructive analysis by pEDXRF, the samples were recovered. A scanning electron microscope (SEM) JEOL JSM 7401F was employed to investigate the surface morphology of the samples. Fourier Transform Infra Red (Bruker Tensor 27) and Raman (LabRam II) Spectroscopy were used to analyse the presence of chemical functional groups, ionic transport and carbon nanotubes in the plant samples.

2.2.1 X-Ray Fluorescence (XRF) Spectroscopy

2.2.1.1 Fundamentals of XRF

The potential use of x-rays for qualitative and quantitative elemental assay was appreciated soon after x rays were discovered [3]. The early applications used Geiger Mueller tubes and elaborate absorber arrays or crystal diffraction gratings to measure x rays. Later, advances in semiconductor detectors and associated electronics opened up the field of energy-dispersive x-ray fluorescence (XRF) analysis for general elemental assay.

X-ray fluorescence (XRF) spectroscopy is an instrumental approach used to identify, and sometimes quantify, elements present in a substance. An element is identified by its characteristic X-ray emissions [3-7]. The quantification occurs by measuring the intensity of the characteristic emission line(s). As we have learned, all atoms have a fixed number of electrons arranged in orbitals around the nucleus, and the number of electrons in a given atom equals the number of protons in the nucleus. The number of protons is indicated by the atomic number in the Periodic Table of the elements. Each atomic number corresponds to a specific element. XRF analysis is based on the fact that the chemical elements emit characteristic radiation when subjected to appropriate excitation. The emission of characteristic line spectra can be induced by either the impact of accelerated particles such as electrons, photons, alpha particles and ions; or by the impact of high energy radiations from an X-ray tube or from a suitable radioactive source. Generally, direct electron excitation is used in electron microprobe

techniques, while radioisotope sources and proton generators are commonly associated with energy dispersion.

When a primary x-ray excitation source from an x-ray tube or a radioactive source strikes a sample, the x-ray can either be absorbed by the atom or scattered through the material. The process in which an x ray is absorbed by the atom by transferring all of its energy to an innermost electron is called the “photoelectric effect.” During this process, if the primary x-ray had sufficient energy, electrons are ejected from the inner shells, creating vacancies. These vacancies present an unstable condition for the atom. As the atom returns to its stable condition, electrons from the outer shells are transferred to the inner shells and in the process giving off a characteristic x-ray whose energy is the difference between the two binding energies of the corresponding shells. The emitted x-rays produced from this process are called “X-ray Fluorescence,” or XRF. The process of detecting and analyzing the emitted x-rays is called “X ray Fluorescence Analysis.” In most cases the innermost K and L shells are involved in XRF detection. A typical x-ray spectrum from an irradiated sample will display multiple peaks of different intensities.

The characteristic x-rays are labeled as K, L, M or N to denote the shells they originated from. Another designation alpha (α), beta (β) or gamma (γ) is made to mark the x-rays that originated from the transitions of electrons from higher shells. Hence, a $K\alpha$ x-ray is produced from a transition of an electron from the L to the K shell, and a $K\beta$ x-ray is produced from a transition of an electron from the M to a K shell, etc. Since within the shells there are multiple orbits of higher and lower binding energy electrons, a further designation is made as α_1 , α_2 or β_1 , β_2 , etc. to denote transitions of electrons from these orbits into the same lower shell.

The XRF method is widely used to measure the elemental composition of materials. Since this method is fast and non-destructive to the sample, it is the method of choice for field applications and industrial production for control of materials. Depending on the application, XRF can be produced by using not only x-rays but also other primary excitation sources like alpha particles, protons or high energy electron beams. Sometimes, as the atom returns to its stable condition, instead of emitting a characteristic x-ray it transfers the excitation energy directly to one of the outer electrons, causing it to be ejected from the atom. The ejected electron is called an “Auger” electron. This process is a competing process to the XRF. Auger

electrons are more probable in the low Z elements than in the high Z elements.

The x-ray intensity is proportional to both the elemental concentration and the strength of the ionizing source. Photon ionization, which is achieved using either an x-ray tube or radioisotope, is most applicable to the nondestructive assay of nuclear material. Other methods of ionization are generally prohibitive because of the physical size and complexity of the ionization source. XRF analysis is a complementary technique to densitometry. Densitometry measures photons that are transmitted through the sample without interaction, whereas XRF measures the radiation produced by photons that interact within the sample. The literature on XRF analysis includes several general references [3-7] that provide a thorough discussion of the method, with extensive bibliographies and information attenuation correction procedures and both energy and wavelength

2.1.1.2 Function of XRF

X-rays excite the atoms of the sample to emit radiation. This radiation is measured by a semiconductor detector. To achieve a higher sensitivity, the exciting radiation can be optimized using targets. The unit is delivered including an installed analysis method. Data are already stored in the unit's memory. The measured values are compared with these data. After the measurement is complete, the results relating to an unknown sample are displayed on the screen. The sample material can be solid, liquid or a powder. Targets emit radiation when they are hit by radiation themselves. Targets typically used include



Figure 2.2: XRF device used to characterize the powder samples

2.2.2 Scanning Electron Microscope (SEM)

2.2.2.1 Fundamental Principle

Scanning electron microscopy [8-10] is used primarily for the study of surface topography of solid materials. It permits a depth of field for greater than optical or transmission electron microscopy. The resolution of SEM is about 3 nm, approximately two orders of magnitude greater than the optical microscope and one order of magnitude less than the transmission electron microscope. Thus SEM bridges the gap between the other two techniques. A schematic diagram of the scanning electron microscope is shown in the Figure 2.3.

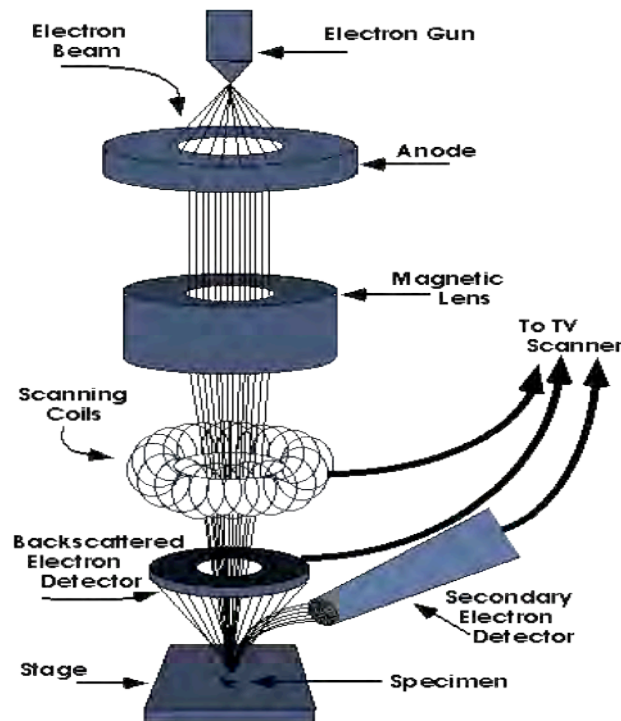


Figure 2.3: Schematic diagram of SEM

An electron beam passing through an evacuated column is focused by electromagnetic lenses on to the specimen surface [4, 5]. The beam is then rastered over the specimen in synchronism with the beam of a cathode ray tube display screen. In elastically scattered secondary electrons are emitted from the sample surface and collected by a scintillator, the signal from which is used to modulate the brightness of the cathode ray tube. In this way

secondary electron emission from the sample is used to form an image on the CRT display screen and the difference in secondary emission results from change in surface topography. If (elastically) backscattered electrons are collected to form the image, contrast results from compositional differences. Cameras are provided to record the images on the display screen.

2.2.2.2 Working Method

In a typical SEM, electrons are thermionically emitted from a tungsten or lanthanum hexaboride (LaB_6) cathode and are accelerated towards an anode, electrons can be emitted via field emission (FE). Tungsten is used because it has the highest melting point and lowest vapor pressure of all metals, thereby allowing it to be heated for electron emission. The electron beam, which typically has an energy ranging from a few hundred eV to 100 KeV, is focused by one or two condenser lenses into a beam with a very fine focal spot sized 0.4 nm to 5 nm. The beam passes through pairs of scanning coils or pairs of deflector plates in the electron optical column, typically in the objective lens, which deflect the beam horizontally and vertically so that it scans in a raster fashion over a rectangular area of the sample surface. When the primary electron beam interacts with the sample, the electrons lose energy by repeated scattering and absorption within a teardrop-shaped volume of the specimen known as the interaction volume, which extends from less than 100 nm to around 5 μm into the surface. The size of the interaction volume depends on the electrons' landing energy, the atomic number of the specimen and the specimen's density [8, 10].

2.2.2.3 Applications

Scanning electron microscopy has been applied to the study of fibrous materials, ceramics, catalysts, polymers and biological materials. Information may be obtained by examination of both the natural surface of materials and that exposed by either fracture or sectioning. Rough topographic features, void content and particle agglomerations are easily revealed as well as phase difference within a material.

Some examples of recent investigations are:

1. Metallographic investigations of amorphous metals and rapidly solidified brazing alloys to study magnetic domains, phase separation and corrosion.

2. Evaluation of textile finishes on fabrics and fibers, and the study of surface change resulting from various fiber treatments.
3. Characterization of optical fiber couplers and connectors; failure mode determination of optical fibers.
4. Correlation between processing conditions of ceramic materials and their ultimate microstructure.

2.2.2.4 Limitations

Samples to be studied must be solids that are not electron beam reactive and contain no highly volatile or corrosive components. Special specimen stages can handle specimens up to about 20 cm in diameter although conventional stages can accommodate samples only a few cm in diameter. Resolution limitation of the technique extends down to about 20 to 30 Angstrom.

2.2.3 Proton Induced X-Ray Emission (PIXE) Spectroscopy

2.2.3.1 Basics of PIXE

Particle induced x-ray emission (PIXE), is a powerful yet non-destructive elemental analysis technique now used routinely by geologists, archaeologists, art conservators and others to help answer questions of provenience, dating and authenticity [11]. Quantum theory states that orbiting electrons of an atom must occupy discrete energy levels in order to be stable. Bombardment with ions of sufficient energy (usually MeV protons) produced by an ion accelerator will cause inner shell ionization of atoms in a specimen. Outer shell electrons drop down to replace inner shell vacancies, however only certain transitions are allowed. X-rays of a characteristic energy of the element are emitted. An energy dispersive detector is used to record and measure these x-rays and the intensities are then converted to elemental concentrations [12-15].

2.2.3.2 Advantages of PIXE

a) High Sensitivity

Compared to electron based x-ray analytical techniques such as energy dispersive

spectroscopy (EDS), PIXE offers better peak to noise ratios and consequently much higher trace element sensitivities as seen in the spectra below. Absolute trace sensitivity to a given trace element is dependent upon a number of factors, such as matrix composition, detector efficiency and peak overlap. However, tests performed on the Harvard system have produced parts per million (ppm) level measurements for certain elements.

b) Measurements at Atmospheric Pressure

A MeV proton beam can be brought out from the high vacuum environment of the accelerator into the ambient of the laboratory. This technology makes it possible to measure a valuable artifact (see figure below) or precious material at atmospheric pressure out of the confines of an evacuated chamber without sampling. A possible disadvantage to running in this configuration is that low energy x-rays from lighter elements will be attenuated in air. However, we have the capability to purge the area between the sample and the detector with helium to minimize this effect. This is a gilded bronze vessel from the Han Dynasty (207 B.C. to 220 A.D.) from the Harvard University Art Museum's Asian Studies collection. A common technique to affix gold to a bronze base material incorporates a mercury amalgam to promote adhesion. Conservators were using PIXE to determine the method of gilding by seeing the presence or absence of a mercury signal.

c) Multi Element Capability

Major elemental analysis is performed for any element from sodium to uranium in a single spectrum on our system. X-rays from elements below sodium cannot be seen because they are absorbed in either the detector window, the atmosphere between the sample and the detector, or through any filters used. For trace element analysis, we choose a filter to attenuate the x-rays at the energies of the major elements allowing the detector to measure the trace elements with greater sensitivity. Usually these filters will cause an insensitivity to lighter elements, but will allow simultaneously analysis of any element above the filter's absorption edge.

d) The Proton Beam is Non-destructive

The Harvard system was designed to fulfill the needs of the archaeology and art

conservation community. We use the largest possible detector solid angle so that useful PIXE data can be acquired with relatively low beam currents. Usually these currents will cause only a few milliwatts of heating from the beam. The situation is improved even more by running it with a helium purge so that heat may be convected away.

e) The Use of Standards

Because of a lack of precise knowledge of critical system parameters such as absolute detector efficiency, x ray filter attenuation and integrated beam current, many PIXE systems rely on standards to determine accurate specimen compositions. Although we have had good results running in standardless mode for a variety of samples of known composition, we advise you to have a standard or set of standards in close approximation to that of the specimen. Many times it is easy to develop an internal standard to fit a particular measurement.

f) The Ideal Specimen

The ideal specimen should be flat and of uniform composition. Ceramic shards for example must be crushed mixed and pelletized. Since most of the characteristic x-rays emanate from the top few microns, for accurate measurements it is important that the sample be homogeneous to within the micron level. Real life samples do not always fit this ideal. A precious object may have a hidden layered structure, or not have a flat or even surface. Pelletization is obviously not an option. Here is advisable to analyze a number of spots and take the average. Such measurements are considered to be qualitative or at best semi-quantitative.

2.2.3.3 The Benefit of X-Ray Filters

At very high count rates, Si(Li) x-ray detectors will behave in a less than ideal fashion. Energy resolution could become significantly worse causing peaks to overlap. Pileup peaks may appear which manifest themselves as multiples of principle peaks. Spectrometer dead time may cause counting errors.

X-ray peaks from major elements can occupy much of the detectors useful counting capability. Dominant low energy x-rays may be filtered out so that the detector will only see

contributions due to the higher energy trace or minor elements. Beam current may now be increased with an overall effect of much greater trace element sensitivity while keeping the detector at a low count rate. In some cases single element foils may be used as "notch" filters to attenuate only a dominant matrix element but allow relatively high transmission of all other x-rays. A good rule of thumb in this case is that the best absorbing filter is lighter than the dominant matrix element by 2 atomic numbers. That is to say that the best filter for a Fe matrix would be a Cr foil.

2.2.3.4 System Description



Figure 2.4: PIXE device used for analysis

A finely collimated beam of protons is produced by a general ionex tandem ion accelerator and brought through a graphite plate with a series of closely spaced .3 mm holes. An o-ring seals a thin polymer window over this plate providing a vacuum barrier through which the beam is brought. The graphite block provides mechanical support to the film and helps to conduct heat away from it greatly increasing its lifetime under beam bombardment. Relative beam current integration is measured off of the graphite block providing accurate

normalization amongst samples. An internal Faraday cup provides secondary electron suppression. Because of this we can precisely measure and control the relative number of protons striking each sample.

Accurate sample placement relative to that of the beam is accomplished by the aid of a HeNe laser beam, which runs collinear to the ion beam. The sample is mounted on a block tilted as to provide the sample normal tilted 45 degrees from the incident ion beam. The sample area can be purged with He when looking for light elements with PIXE. A surface barrier detector is placed 60 degrees relative to the incident ion beam for RBS measurements at atmospheric pressure. A Si(Li) x-ray detector is placed 90 degrees relative to the incident ion beam and is used to determine x-ray peak energies and intensities. X-ray absorber filters are used to attenuate the dominant peaks and allow greater trace element sensitivity. GUPIX, an interactive software package is used to analyze and convert raw spectral data into elemental concentrations.

2.2.4 Infrared (IR) Spectroscopy

2.2.4.1 Fundamentals of IR Spectroscopy

Infrared (IR) spectroscopy [16-19] is one of the most common spectroscopic techniques used by organic and inorganic chemists. Simply, it is the absorption measurement of different IR frequencies by a sample positioned in the path of an IR beam. The main goal of IR spectroscopic analysis is to determine the chemical functional groups in the sample. Different functional groups absorb characteristic frequencies of IR radiation. Using various sampling accessories, IR spectrometers can accept a wide range of sample types such as gases, liquids, and solids. Thus, IR spectroscopy is an important and popular tool for structural elucidation and compound identification.

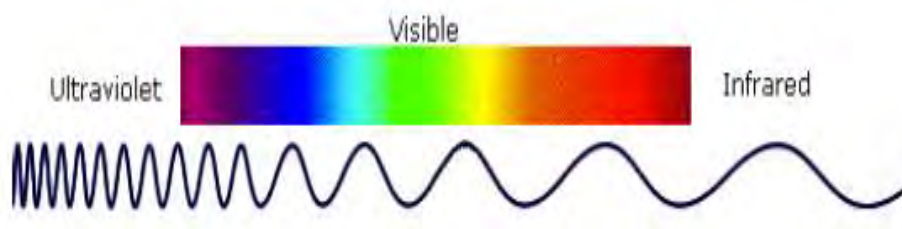


Figure 2.5: Spectrum

The light our eyes see is but a small part of a broad spectrum of electromagnetic radiation. On the immediate high energy side of the visible spectrum lies the ultraviolet, and on the low energy side is the infrared. The portion of the infrared region most useful for analysis of organic compounds is not immediately adjacent to the visible spectrum, but is that having a wavelength range from 2,500 to 16,000 nm, with a corresponding frequency range from 1.9×10^{13} to 1.2×10^{14} Hz.

Photon energies associated with this part of the infrared (from 1 to 15 kcal/mole) are not large enough to excite electrons, but may induce vibrational excitation of covalently bonded atoms and groups. The covalent bonds in molecules are not rigid sticks or rods, such as found in molecular model kits, but are more like stiff springs that can be stretched and bent. The mobile nature of organic molecules concerning conformational isomers, recognize that, in addition to the facile rotation of groups about single bonds, molecules experience a wide variety of vibrational motions, characteristic of their component atoms. Consequently, virtually all organic compounds will absorb infrared radiation that corresponds in energy to these vibrations. Infrared spectrometers, similar in principle to the UV-Visible spectrometer described elsewhere, permit chemists to obtain absorption spectra of compounds that are a unique reflection of their molecular structure. An example of such a spectrum is that of the flavoring agent vanillin, shown below [17, 19].

The complexity of this spectrum is typical of most infrared spectra, and illustrates their use in identifying substances. The gap in the spectrum between 700 & 800 cm^{-1} is due to solvent (CCl_4) absorption. Further analysis (below) will show that this spectrum also indicates the presence of an aldehyde function, a phenolic hydroxyl and a substituted benzene ring. The inverted display of absorption, compared with UV Visible spectra, is characteristic. Thus a sample that did not absorb at all would record a horizontal line at 100% transmittance (top of the chart).

The frequency scale at the bottom of the chart is given in units of reciprocal centimeters (cm^{-1}) rather than Hz, because the numbers are more manageable. The reciprocal centimeter is the number of wave cycles in one centimeter; whereas, frequency in cycles per second or Hz is equal to the number of wave cycles in 3×10^{10} cm (the distance covered by light in one second). Wavelength units are in micrometers, microns (μ), instead of nanometers for the same reason. Most infrared spectra are displayed on a linear frequency scale, as shown

here, but in some older texts a linear wavelength scale is used. A calculator for interconverting these frequency and wavelength values is provided on the right. Simply enter the value to be converted in the appropriate box, press "Calculate" and the equivalent number will appear in the empty box. Infrared spectra may be obtained from samples in all phases (liquid, solid and gaseous). Liquids are usually examined as a thin film sandwiched between two polished salt plates (note that glass absorbs infrared radiation, whereas NaCl is transparent). If solvents are used to dissolve solids, care must be taken to avoid obscuring important spectral regions by solvent absorption. Perchlorinated solvents such as carbon tetrachloride, chloroform and tetrachloroethene are commonly used. Alternatively, solids may either be incorporated in a thin KBr disk, prepared under high pressure, or mixed with a little nonvolatile liquid and ground to a paste (or mull) that is smeared between salt plates.

2.2.4.2 IR Frequency Range and Spectrum Presentation

Infrared radiation spans a section of the electromagnetic spectrum having wavenumbers from roughly 13,000 to 10 cm^{-1} , or wavelengths from 0.78 to 1000 μm . It is bound by the red end of the visible region at high frequencies and the microwave region at low frequencies. IR absorption positions are generally presented as either wavenumbers ($\bar{\nu}$) or wavelengths (λ). Wavenumber defines the number of waves per unit length. Thus, wavenumbers are directly proportional to frequency, as well as the energy of the IR absorption. The wavenumber unit (cm^{-1}) is more commonly used in modern IR instruments that are linear in the cm^{-1} scale. In the contrast, wavelengths are inversely proportional to frequencies and their associated energy. At present, the recommended unit of wavelength is μm , but μ (micron) is used in some older literature.

Wavenumbers and wavelengths can be interconverted using the following equation:

$$\bar{\nu} = \frac{1}{\lambda} \times 10^4 \quad (2.1)$$

IR absorption information is generally presented in the form of a spectrum with wavelength or wavenumber as the x-axis and absorption intensity or percent transmittance as the y-axis.

Transmittance T, is the ratio of radiant power transmitted by the sample (I) to the radiant power incident on the sample (I₀). Absorbance (A) is the logarithm to the base 10 of the

reciprocal of the transmittance.

$$A = \log_{10} \left(\frac{1}{T} \right) = -\log_{10} (T) = -\log_{10} \left(\frac{I}{I_0} \right) \quad (2.2)$$

The transmittance spectra provide better contrast between intensities of strong and weak bands because transmittance ranges from 0 to 100% T whereas absorbance ranges from infinity to zero. The analyst should be aware that the same sample will give quite different profiles for the IR spectrum, which is linear in wavenumber, and the IR plot, which is linear in wavelength. It will appear as if some IR bands have been contracted or expanded [18, 20].

The IR region is commonly divided into three smaller areas: near IR, mid IR, and far IR. The far IR requires the use of specialized optical materials and sources. It is used for analysis of organic, inorganic, and organometallic compounds involving heavy atoms (mass number over 19). It provides useful information to structural studies such as conformation and lattice dynamics of samples. Near IR spectroscopy needs minimal or no sample preparation. It offers high-speed quantitative analysis without consumption or destruction of the sample. Its instruments can often be combined with UV-visible spectrometer and coupled with fiberoptic devices for remote analysis. Near IR spectroscopy has gained increased interest, especially in process control applications.

2.2.5 UV-Visible Absorption Spectroscopy

2.2.5.1 Background

Ultraviolet and visible spectrometers have been in general use for the last 35 years and over this period have become the most important analytical instrument in the modern day laboratory. In many applications other techniques could be employed but none rival UV-Visible spectrometry for its simplicity, versatility, speed, accuracy and cost-effectiveness. This description outlines the basic principles for those new to UV-Visible spectrometry [21-25]. Absorption of light by solution is one of the oldest and still one of the more useful instrumental methods. The wavelength of light that a compound will absorb is characteristic of its chemical structure. Specific regions of the electromagnetic spectrum are absorbed by exciting specific types of molecular and atomic motion to higher energy levels. Absorption of microwave radiation is generally due to excitation of molecular rotational motion. Infrared absorption is associated with vibrational motions of molecules. Absorption of visible and

ultraviolet (UV) radiation is associated with excitation of electrons, in both atoms and molecules, to higher energy states. All molecules will undergo electronic excitation following absorption of light, but for most molecules very high energy radiation (in the vacuum ultraviolet, <200 nm) is required.

For molecules containing conjugated electron systems however, light in the UV-visible region is adequate (e.g., benzene absorbs in the 260 nm region). As the degree of conjugation increases, the spectrum shifts to lower energy. Thus naphthalene absorbs light up to 300 nm, and anthracene absorbs to about 400 nm. Because absorption spectra are characteristic of molecular structure, they can be used to qualitatively identify atomic and molecular species.

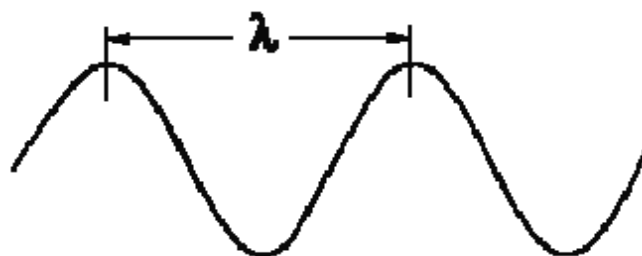


Figure 2.6: The wavelength λ of electromagnetic radiation.

Radiation is a form of energy and we are constantly reminded of its presence via our sense of sight and ability to feel radiant heat. It may be considered in terms of a wave motion where the wavelength, λ , is the distance between two successive peaks. The frequency, ν , is the number of peaks passing a given point per second. These terms are related so that:

$$c = \nu\lambda \quad (2.3)$$

where c is the velocity of light in a vacuum.

The full electromagnetic radiation spectrum is continuous and each region merges slowly into the next. For spectroscopy purposes, we choose to characterize light in the ultraviolet and visible regions in terms of wavelength expressed in nanometers. Other units which may be encountered, but whose use is now discouraged, are the Angstrom (\AA) and the millimicron ($\text{m}\mu$).

2.2.5.2 Absorption laws

Beer's law tells us that absorption is proportional to the number of absorbing

molecules; ie to the concentration of absorbing molecules (this is only true for dilute solutions) and Lambert's law tells us that the fraction of radiation absorbed is independent of the intensity of the radiation. Combining these two laws, we can derive the Beer-Lambert Law [21, 22]:

$$\log_{10} \frac{I_0}{I} = \epsilon lc \quad (2.4)$$

I_0 = the intensity of the incident radiation

I = the intensity of the transmitted radiation

ϵ = a constant for each absorbing material, known as the molar absorption coefficient (called the molar extinction coefficient in older texts) and having the units $\text{mol}^{-1} \text{dm}^3 \text{cm}^{-1}$, but by convention the units are not quoted

l = the path length of the absorbing solution in cm

c = the concentration of the absorbing species in mol dm^{-3}

The value of $\log_{10} (I_0 / I)$ is known as the absorbance of the solution (in older texts it is referred to as the optical density), and can be read directly from the spectrum, often as 'absorbance units'. A useful constant is the molar absorption coefficient (ϵ), because it is independent of concentration and path length, whereas absorption depends upon both. The other useful piece of information is the wavelength at which maximum absorption occurs. This is given the symbol λ_{max} . These two pieces of information alone are frequently sufficient to identify a substance, although identification is not the most common use of this technique. Conversely, if the values of ϵ and λ_{max} are known, the concentration of its solution can be calculated, this is the more common application. The values of both ϵ and λ_{max} are strongly influenced by the nature of the solvent, and for organic compounds, by the degree of substitution and conjugation.

2.2.5.3 Function of Spectrometer

Because only small numbers of absorbing molecules are required, it is convenient to have the sample in solution (ideally the solvent should not absorb in the ultraviolet/ visible range however, this is rarely the case). In conventional spectrometers electromagnetic radiation is passed through the sample which is held in a small square-section cell (usually 1

cm wide internally). Radiation across the whole of the ultraviolet/visible range is scanned over a period of approximately 30 s, and radiation of the same frequency and intensity is simultaneously passed through a reference cell containing only the solvent. Photocells then detect the radiation transmitted and the spectrometer records the absorption by comparing the difference between the intensity of the radiation passing through the sample and the reference cells [24, 25].

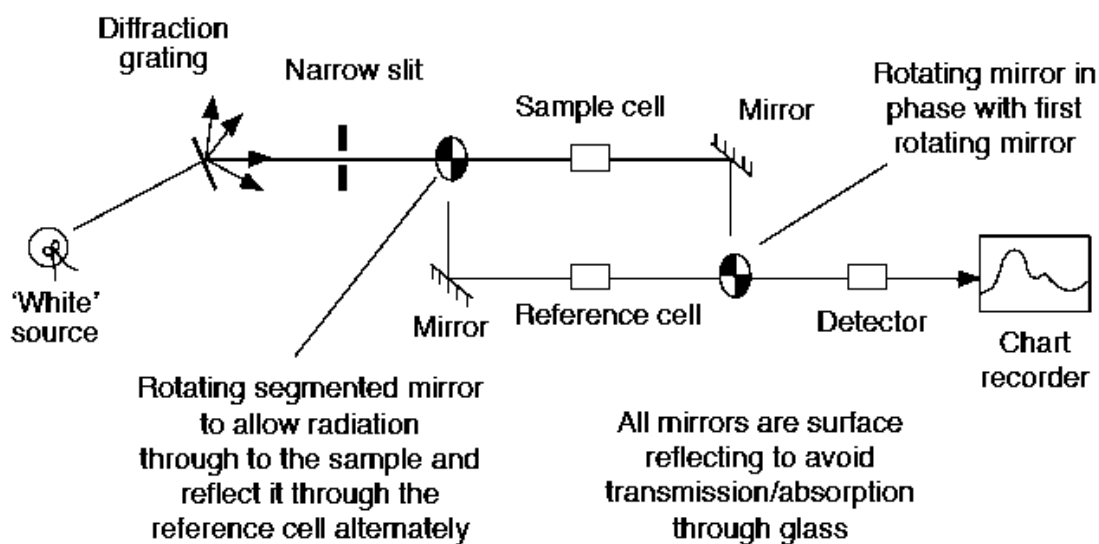


Figure 2.7: Function of ultraviolet/visible spectrometer.

No single lamp provides radiation across the whole of the range required, so two are used. A hydrogen or deuterium discharge lamp covers the ultraviolet range, and a tungsten filament (usually a tungsten/halogen lamp) covers the visible range. The radiation is separated according to its frequency/wavelength by a diffraction grating followed by a narrow slit. The slit ensures that the radiation is of a very narrow waveband i.e. it is monochromatic. The cells in the spectrometer must be made of pure silica for ultraviolet spectra because soda glass absorbs below 365 nm, and Pyrex glass below 320 nm. Detection of the radiation passing through the sample or reference cell can be achieved by either a photomultiplier or a photodiode, that converts photons of radiation into tiny electrical currents; or a semiconducting cell (that emits electrons when radiation is incident on it) followed by an electron multiplier similar to those used in mass spectrometers. The spectrum is produced by comparing the currents generated by the sample and the reference beams.

Modern instruments are self-calibrating, though the accuracy of the calibration can be checked if necessary. Wavelength checks are made by passing the sample beam through glass samples (containing holmium oxide) that have precise absorption peaks, and the absorption is calibrated by passing the sample beam through either a series of filters, each with a specific and known absorption, or a series of standard solutions.

2.2.6 Electrochemical Impedance Spectroscopy (EIS)

2.2.6.1 Basic Theory of EIS

This technique is based on analyzing the alternating current (AC) response of a circuit, comprising of a conducting material sandwiched between two blocking or non-blocking electrodes, to a sinusoidal electrical signal and subsequent calculation of the impedance as a function of frequency of the applied signal. The technique, broadly referred as “impedance Spectroscopy”, enables us to evaluate and separate the contribution to the overall electrical properties in the frequency domain due to electrode reaction at the electrode/electrolyte interface and the migration of ions through the bulk and across the grain boundaries of materials [26-28].

Electrochemical impedance theory is a well-developed branch of ac theory that describes the response of a circuit to an alternating current or voltage as a function of frequency. The mathematics of the theory is beyond the scope of this discussion, but we will present the basic theory here. In dc theory (a special case of ac theory where the frequency equals 0 Hz) resistance is defined by Ohm's Law:

$$E = I R \quad (2.5)$$

Using Ohm's law, we can apply a dc potential (E) to a circuit, measure the resulting current, and compute the resistance (R) or determine any term of the equation if the other two are known. Potential values are measured in volts (V), current in amperes or amps (A), and resistance in ohms (Ω). A resistor is the only element that impedes the flow of electrons in a dc circuit. In ac theory, where the frequency is non-zero, the analogous equation is:

$$E = I Z \quad (2.6)$$

As in Ohm's law, E and I are here defined as potential and current, respectively. Z is defined as impedance, the ac equivalent of resistance. Impedance values are also measured in ohms (Ω). In addition to resistors, capacitors and inductors impede the flow of electrons in ac

circuits. In an electrochemical cell, slow electrode kinetics, slow preceding chemical reactions, and diffusion can all impede electron flow, and can be considered analogous to the resistors, capacitors, and inductors that impede the flow of electrons in an ac circuit. Figure 2.8, shows a typical plot of a voltage sine wave (E) applied across a given circuit and the resultant ac current waveform. Note that the two traces are different not only in amplitude, but are also shifted in time with respect to each other that is, they are out of phase. In the case of a purely resistive network, the two waveforms would not be shifted. They would be exactly in phase, differing only in amplitude.

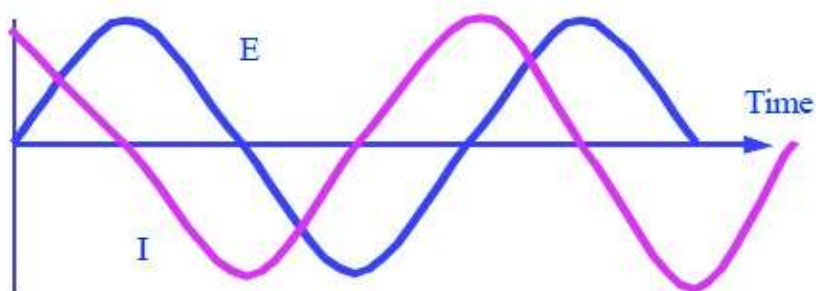


Figure 2.8: waveform of dI and dE

2.2.6.2 Impedance Response and Its Complex Behavior

Let us assume we have an electrical element to which we apply an electric field $E(t)$ and get the response $I(t)$, then we can disturb this system at a certain field E with a small perturbation dE and we will get at the current I a small response perturbation dI . In the first approximation, as the perturbation dE is small, the response dI will be a linear response as well (mirror at the tangent) of the $I(E)$ curve [26-32].

If we plot the applied sinusoidal signal on the X-axis of a graph and the sinusoidal response signal $I(t)$ on the Y-axis, an oval is plotted. This oval is known as a "Lissajous figure" (Figure 2.9). Analysis of Lissajous figures (Figure 2.9) on oscilloscope screens was the accepted method of impedance measurement prior to the availability of lock-in amplifiers and frequency response analyzers.

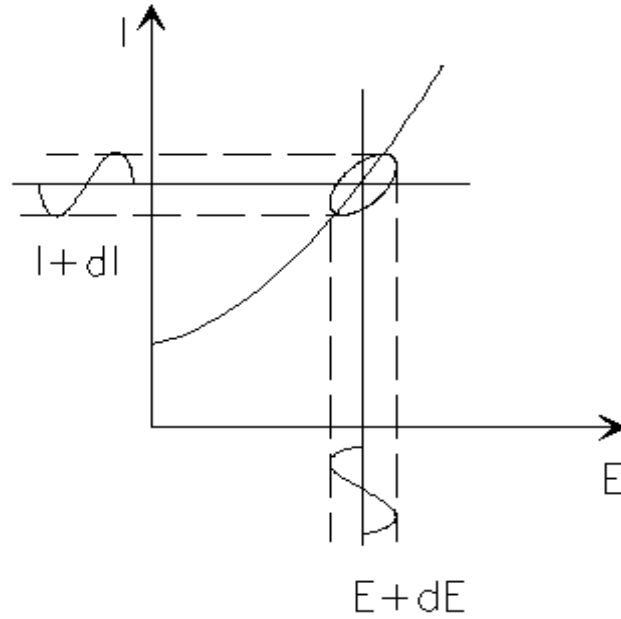


Figure 2.9: Lissajous figure

$$Z(t) = \frac{E(t)}{I(t)} = \frac{E_0 \cos(\omega t)}{I_0 \cos(\omega t - \phi)} = Z_0 \frac{\cos(\omega t)}{\cos(\omega t - \phi)} \quad (2.7)$$

Using Euler's relationship

$$\exp(i\phi) = \cos\phi + i \sin\phi \quad (2.8)$$

it is possible to express the impedance as a complex function. The potential is described as,

$$E(t) = E_0 \exp(i\omega t) \quad (2.9)$$

and, the current response as,

$$I(t) = I_0 \exp(i\omega t - i\phi) \quad (2.10)$$

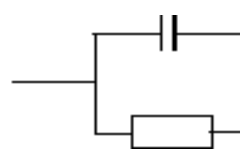
The impedance is then represented as a complex number:-

$$Z = \frac{E}{I} = Z_0 \exp(i\phi) = Z_0 (\cos\phi + i \sin\phi) \quad (2.11)$$

2.2.6.3 Nyquist Plot with Impedance Vector

The above expression for $Z(\omega)$ is composed of a real and an imaginary part. If the real part is plotted on the X-axis and the imaginary part on the Y axis, we get a "Nyquist plot", in this plot the y-axis is negative and that each point on the Nyquist plot is the impedance Z at

one frequency. On the Nyquist plot the impedance can be represented as a vector of length $|Z|$. The angle between this vector and the x-axis is ϕ . It has one major shortcoming. When you look at any data point on the plot, you cannot tell what frequency was used to record that point. Low frequency data are on the right side of the plot and higher frequencies are on the left. This is true for EIS data where impedance usually falls as frequency rises (this is not true of all circuits). The Nyquist plot results from the RC circuit. The semicircle is characteristic of a single "time constant". Electrochemical Impedance plots often contain several time constants. Often only a portion of one or more of their semicircles is seen [28, 31].



$$\frac{1}{Z} = \frac{1}{R} + \frac{1}{i\omega C} \quad (2.12)$$

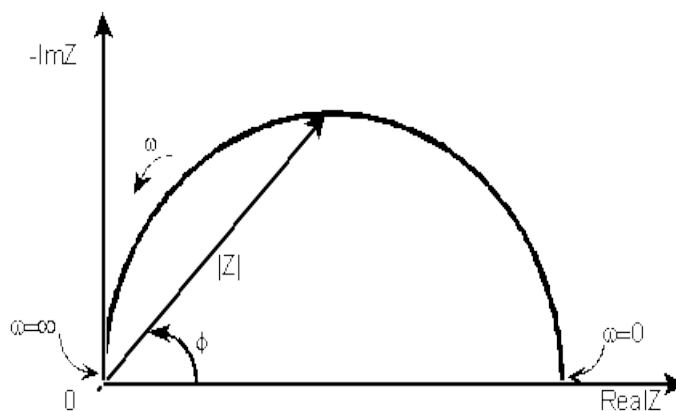


Figure 2.10: Nyquist Plot

Another popular presentation method is the "Bode plot". The impedance is plotted with log frequency on the x-axis and both the absolute value of the impedance ($|Z| = Z_0$) and phase-shift on the y-axis.

2.2.6.4 The Bode Plot

The Bode plot for the RC circuit is shown below. Unlike the Nyquist plot, the Bode plot explicitly shows frequency information.

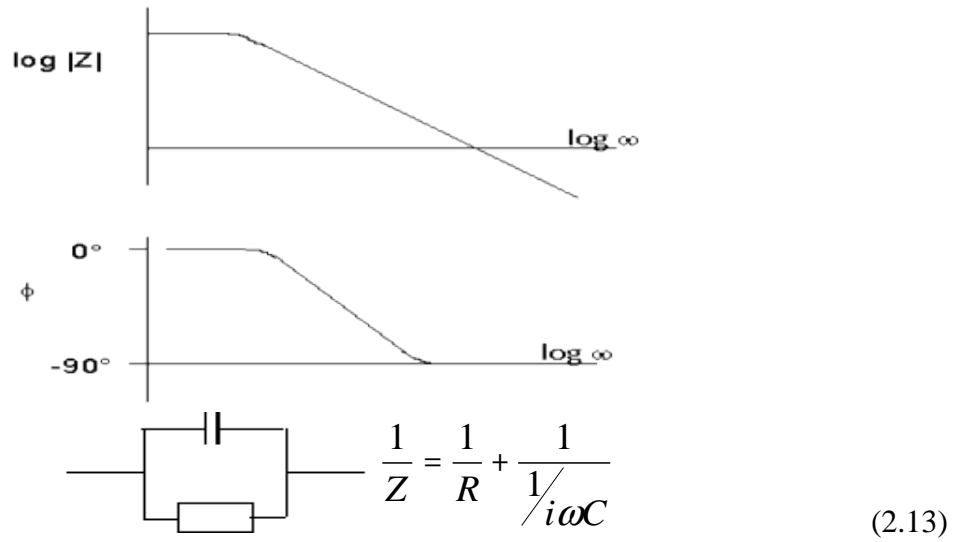


Figure 2.11: Bode Plot

Another popular presentation method is the "Bode plot". The impedance is plotted with log frequency on the x-axis and both the absolute value of the impedance ($|Z| = Z_0$) and phase-shift on the y-axis.

2.2.6.5 Cole-Cole Plot

When we plot the real and imaginary components of impedance in the complex plane (Argand diagram), we obtain a semicircle or partial semicircle for each parallel RC Voigt network:

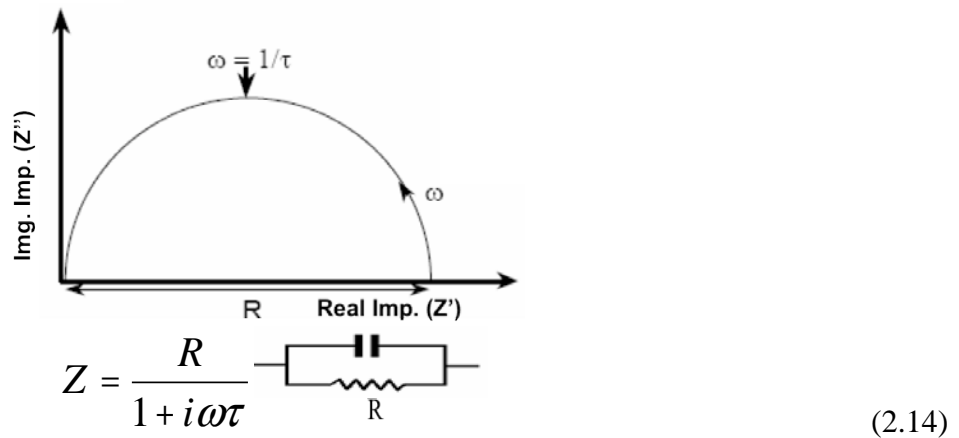


Figure 2.12: Cole-Cole Plot

The diameter corresponds to the resistance R.

The frequency at the 90° position corresponds to $1/\tau = 1/RC$

2.2.6.6 Examples of Nyquist and Bode Plot

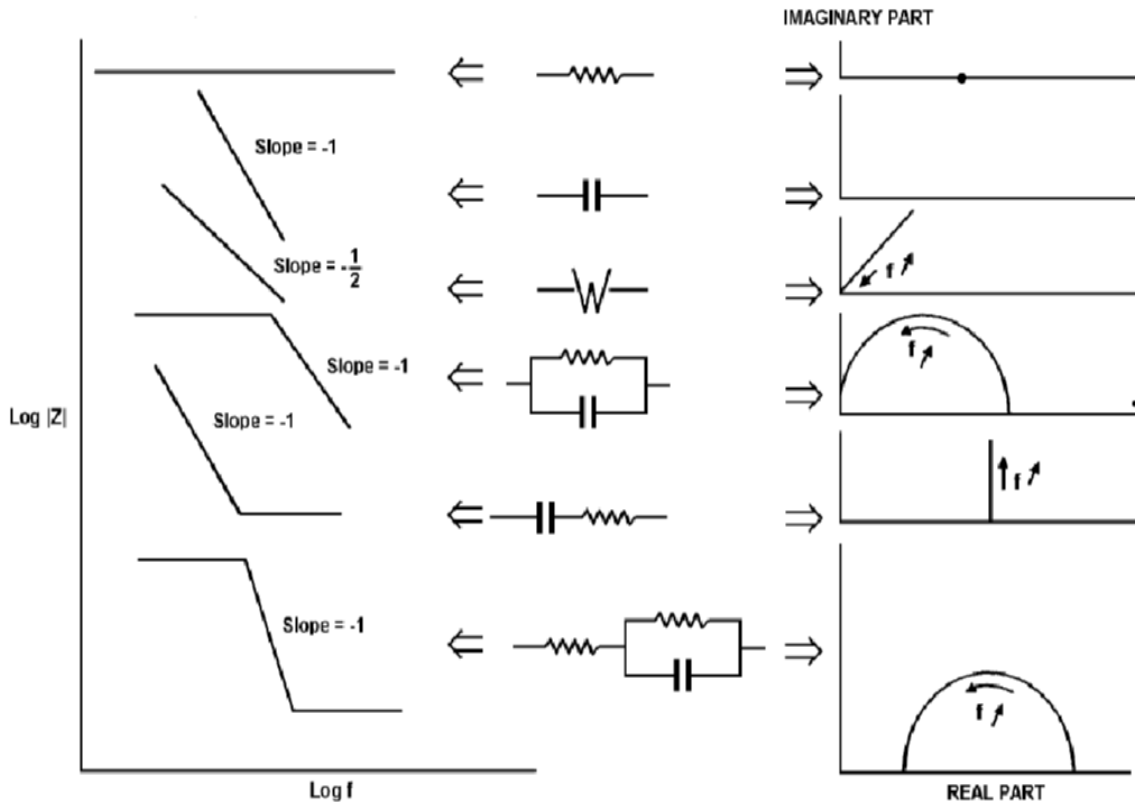
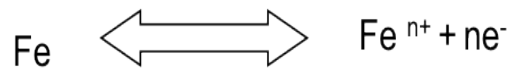


Figure 2.13: Nyquist & Bode Plot Presentation

2.2.6.7 Charge Transfer Reaction

Consider a metal substrate in contact with an electrolyte. Metal molecules can electrolytically dissolve into the electrolyte.



This charge transfer reaction has a certain speed. The speed depends on the kind of reaction, the temperature, the concentration of the reaction products and the potential. The

general relation between the potential and the current holds:

$$i = i_0 \left[\frac{C_o}{C_o^*} e^{\alpha \frac{nF\eta}{RT}} - \frac{C_R}{C_R^*} e^{-(1-\alpha) \frac{nF\eta}{RT}} \right] \quad (2.15)$$

i_0 = exchange current density

C_o = concentration of oxidant at the electrode surface

C_o^* = concentration of oxidant in the bulk

C_R = concentration of reductant at the electrode surface

n = number of electrons involved

F = Faradays constant

T = temperature

R = gas constant

a = reaction order

η = over-potential ($E - E_0$)

The Over-potential η , measures the degree of polarization. It is the electrode potential minus the equilibrium potential for the reaction. When the concentration in the bulk is the same as at the electrode surface, $C_o = C_o^*$ and $C_R = C_R^*$, this simplifies the last equation into:

$$i = i_0 \left[e^{\alpha \frac{nF\eta}{RT}} - e^{-(1-\alpha) \frac{nF\eta}{RT}} \right] \quad (2.16)$$

This equation is called the Butler-Volmer equation. It is applicable when the polarization depends only on the charge transfer kinetics.

Stirring will minimize diffusion effects. When η is very small and the electrochemical system is at equilibrium, the expression for the charge transfer resistance changes into:

$$R_{ct} = \frac{RT}{nFi_0} \quad (2.17)$$

i_0 can be calculated when R_{ct} is known.

Below in the table shows some common equivalent circuit models. The equation parameters for both the admittance and impedance are given for each element.

Table 2.1: Admittance and Impedance value calculation of different Circuit Arrangements.

Equivalent element	Admittance	Impedance
R	$1/R$	R
C	$i\omega C$	$1/i\omega C$
L	$1/i\omega L$	$i\omega L$
W (infinite Warburg)	$Y_0(i\omega)^{1/2}$	$1/Y_0(i\omega)^{1/2}$
O (finite Warburg)	$Y_0(i\omega)^{1/2} \coth(B(i\omega)^{1/2})$	$\tanh(B(i\omega)^{1/2})/[Y_0(i\omega)^{1/2}]$
Q (CPE)	$Y_0(i\omega)^\alpha$	$1/Y_0(i\omega)^\alpha$

2.2.7 RAMAN SPECTROSCOPY

Raman spectroscopy is a spectroscopic technique used to study the inelastic scattering of monochromatic light, usually from a laser source. Photons of the laser light are absorbed by the sample and then reemitted. Frequency of the reemitted photons is shifted up or down in comparison with original monochromatic frequency, which is called the Raman effect. This shift provides information about vibrational, rotational and other low frequency transitions in molecules. Raman spectroscopy can be used to study solid, liquid and gaseous samples. The intensity of the scattered light is dependent on the amount of the polarization potential change. Raman spectroscopy is used to study a material's chemical composition. Further applications are:

1. Mineral identification and structural characterization
2. Analyses of gemstones and archaeometric objects
3. Mineral inclusions

4. Speciation & concentration
5. Characterization of e.g., thermal maturity, metamictization, OH content, impurities

Advantages of Raman spectroscopy are its non-destructive nature, small sample amounts can be studied and no sample preparation is necessary.

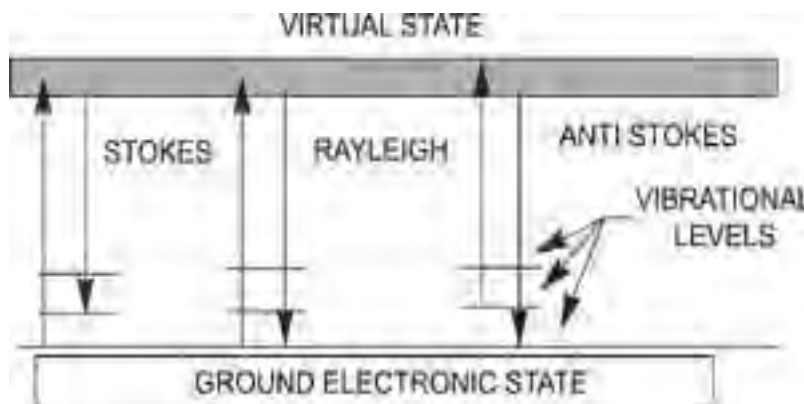


Figure 2.14: Energy level diagram of states in Raman signal.

2.3 REFERENCES

1. Introduction about Agar Growth Medium, http://www.bd.com/europe/regulatory/Assets/IFU/Difco_BBL/281230.pdf
2. Difco™ and BBL™ manual, 2nd Ed. http://www.bd.com/europe/regulatory/Assets/IFU/Difco_BBL/281230.pdf
3. M. C. Miller, X-Ray Fluorescence.
4. WinXRF Configuration Manual (AA83428), Fundamentals And Practice of XRF Analysis.
5. G. Gauglitz, T. Vo-Dinh, (Eds.), X-ray Analysis, The Handbook of Spectroscopy, Wiley-VCH, 2003, ISBN 3-527-29782-0, 1000 pp.
6. Koen H.A Janssens. R.E. Van Grieken (Eds.), Chapter 4 of "Non-destructive Microanalysis of Cultural Heritage Materials", Elsevier, Amsterdam, The Netherlands, 2004 - 800, ISBN 0-444-50738-8.
7. Peter Brouwer, Theory of XRF, 2010, PANalytical B.V., Almelo, The Netherlands
8. Practical Scanning Electron Microscopy; Goldstein, J.; Yakowitz, H.; Newbury, D.; Lifshin, E.; Colby, J.; Coleman, J., Plenum Press: New York; Plenum Press: New York, 1975.
9. Scanning Electron Microscopy; Wells, O.C., McGraw-Hill Book Company: New York, 1974.
10. Microscopy; Annemarie C. Reimschuessel, John E. Macur, Jordi Marti, Page 137-160.
11. Introduction to PIXE, PIXE-PAN Summer Science Program Notre Dame June, 2006, Larry Lamm, Research Professor
12. Particle Induced X-Ray Emission PIXE, Chapter 2.4,
13. Casimir Bamberger, Digital Imaging Mass Spectrometry, J. Am. Soc. Mass Spectrom. (2011) 22:1079Y1087, American Society for Mass Spectrometry DOI: 10.1007/s13361-

011-0120-1

14. Jiyeon Choi et al. Optical Coherence Microscopy for Nondestructive 3D Imaging of Femtosecond Laser Written Structures, Commercial and Biomedical Applications of Ultrafast Lasers IX, edited by Joseph Neev, Stefan Nolte, Alexander Heisterkamp, Rick P. Trebino, Proc. of SPIE Vol. 7203, 720317
15. Kelsey et al. PIXE Applications: Mesoamerican Pottery Analysis.
16. C. P. Sherman Hsu, Infrared Spectroscopy, *Separation Sciences Research and Product Development Mallinckrodt, Inc. Mallinckrodt Baker Division.*
17. Infrared Spectroscopy, CHEM 231 Lab, Technique Primer.
18. Zahra Monsef Khoshhesab, Reflectance IR Spectroscopy, *Payame Noor University Department of Chemistry Iran.*
19. Barbara Stuart, Infrared Spectroscopy: Fundamentals and Applications, Wiley Publication.
20. Introduction to Fourier Transform Infrared Spectroscopy, Thermo Nicolet Corporation.
21. Prof. Greenlief, UV-VIS Absorption Spectroscopy, *CH 4200, Fall 2004.*
22. UV-Vis Absorption Spectroscopy Theory,
teaching.shu.ac.uk/hwb/chemistry/tutorials/molspec/uvvisabl.htm
23. Prof. Subodh Kumar, Spectroscopy of Organic Compounds, Dept. of Chemistry Guru Nanak Dev University Amritsar -143005
24. Ultraviolet/visible spectroscopy, The Royal Society Of Chemistry, Uniliver
25. Basic UV-Vis Theory, Concepts and Applications, Thermo Spectronic
26. Basics of Electrochemical Impedance Spectroscopy, Princeton Applied Research.
27. B. V. Ratnakumar, M. C. Smart, S. Surampudi, Electrochemical Impedance Spectroscopy and its Applications to Lithium Ion Cells, Electrochemical Technologies Group, Jet Propulsion Laboratory, California Institute of Technology, California.
28. Electrochemical Impedance Spectroscopy, Zahner Mess Systeme (2013)
29. Utz Retter and Heinz Lohse, Electrochemical Impedance Spectroscopy, F. Scholz (ed.), *Electroanalytical Methods*, 2nd ed., 159 DOI 10.1007/978-3-642-02915-8_8, Springer-Verlag Berlin Heidelberg 2010.
30. Basics of Electrochemical Impedance Spectroscopy, Application Note, Gamry Instruments.
31. Andrzej Lasia, Electrochemical Impedance Spectroscopy and its Applications
32. Byoung-Yong Chang et al. Electrochemical Impedance Spectroscopy, Annual Reviews, 10.1146/annurev.anchem.012809.102211.
33. D. Weigel and J. Glazebrook, Arabidopsis, A Laboratory Manual. http://books.google.de/books?id=IfZAMNPWVv4C&pg=PA12&lpg=PA12&dq=phyta+agar+composition&source=bl&ots=76XQh4QrT7&sig=Znj2F5lru_MOnM1ZOQaO_jbAs0&hl=en#v=onepage&q&f=false
34. Taiz and Zeiger, Plant Physiology 5th ed., Chapter 5, Mineral Nutrients. (Palgrave-McMillan, 2010)
35. Research Gate forum
https://www.researchgate.net/post/MS_medium_and_in_vitro_seed_germination
36. M. Khodakovskaya et al, ACS Nano, 3, 3221 (2009).

CHAPTER 3

**INTERFACING CARBON NANOTUBES WITH PLANTS:
ENHANCEMENT OF GROWTH, WATER AND IONIC
NUTRIENT UPTAKE IN MAIZE (ZEA MAYS) AND
IMPLICATIONS FOR NANOAGRICULTURE**

CAPÍTULO 3

**INTERCONEXIÓN DE NANOTUBOS DE CARBONO CON
PLANTAS: INCREMENTO DEL CRECIMIENTO,
ABSORCIÓN DE AGUA Y SUSTANCIAS IÓNICAS
NUTRITIVAS EN MAÍZ (ZEA MAYS), IMPLICACIONES
PARA LA NANOAGRICULTURA**

ABSTRACT CHAPTER 3

The application of nano-biotechnology to crop-science/agriculture ('nanoagriculture') is a recent development. While CNTs have been shown to dramatically improve germination of some comestible plants, deficiencies in consistency of behavior and reproducibility arise, partially from the variability of the CNTs used. In this work, factory-synthesized multi-walled-CNTs (MWCNTs) of quality-controlled specifications were seen to enhance the germination growth of maize seedlings at low concentrations but depress it at higher concentrations. Growth enhancement principally arose through improved water delivery by the MWCNT. Polarized EDXRF spectrometry showed that MWCNTs affect mineral nutrient supply to the seedling through the action of the mutually opposing forces of inflow with water and retention in the medium by the ion-CNT transient-dipole interaction. The effect varied with ion type and MWCNT concentration. The differences of the Fe tissue concentrations when relatively high equimolar Fe^{2+} or Fe^{3+} was introduced, implied that the ion-CNT interaction might induce redox changes to the ion. The tissue Ca^{2+} concentration manifested as the antipode of the Fe^{2+} concentration indicating a possible cationic exchange in the cell wall matrix. SEM images showed that MWCNTs perforated the black-layer seed-coat that could explain the enhanced water delivery. The absence of perforations with the introduction of $\text{FeCl}_2/\text{FeCl}_3$ reinforces the idea of the modification of MWCNT functionality by the ion-CNT interaction. Overall, in normal media, low dose MWCNTs were seen to be beneficial, improving water absorption, plant biomass and the concentrations of the essential Ca, Fe nutrients, opening a potential for possible future commercial agricultural applications.

Key words: MWCNT, maize, germination, ion, nano-biotechnology, nanoagriculture.

RESUMEN CAPÍTULO 3

La aplicación de nano-biotecnología en la ciencia del cultivo de plantas ('nanoagricultura') es de desarrollo reciente. Aunque se ha demostrado que los CNT ayudan a mejorar drásticamente la germinación de algunas plantas comestibles, las deficiencias en la consistencia y reproducibilidad surgen, parcialmente a partir de la variabilidad de los nanotubos de carbono utilizados. En este trabajo, los nanotubos de pared múltiple-CNT (MWCNTs) elaborados de fábrica con especificaciones de calidad controlada se utilizaron para mejorar el crecimiento y germinación de plantas de maíz en bajas concentraciones. La espectrometría de pEDXRF mostró que MWCNTs afectan el suministro de nutrientes minerales al semillero a través de la acción de fuerzas que se oponen mutuamente al flujo de entrada de agua y la retención en el medio por la interacción transitoria-dipolo de iones-CNT. El efecto varía con el tipo de iones y la concentración de MWCNT. Las diferencias en las concentraciones de Fe cuando se introduce en forma relativamente alta de Fe^{2+} equimolar o Fe^{3+} , implicaba que la interacción ion-CNT podría inducir cambios redox del ión. La concentración de Ca^{2+} que se manifiesta como antípolar de la concentración de Fe^{2+} indica un posible intercambio catiónico en la matriz de la pared celular. Imágenes de SEM mostraron que los MWCNTs perforaron la cubierta de la semilla (capa negra), lo cual podría explicar la distribución de agua. La ausencia de perforaciones con la introducción de $\text{FeCl}_2/\text{FeCl}_3$ confirma la idea de la modificación de la funcionalidad de los MWCNT debido a la interacción de iones-CNT. En general, en los medios de cultivo normales, dosis bajas de MWCNTs se observaron que son beneficiosos, ya que mejoran la absorción de agua, la biomasa vegetal y las concentraciones de Ca y nutrientes de Fe. Con todo esto, se abre un mar de posibles aplicaciones agrícolas comerciales futuras.

Palabras Clave: MWCNT, Maíz, Germinación, Ion, Nano-biotecnología, Nanoagricultura.

Interfacing Carbon Nanotubes with Plants: Enhancement of Growth, Water and Ionic Nutrient Uptake in Maize (*Zea Mays*) and Implications for Nanoagriculture

3.1 INTRODUCTION

During the last decade noteworthy advances have been reported in the study of the fundamental characteristics of nanomaterials and their utilization for a multitude of applications. In medicine and biology, nanomaterials have been investigated for diverse end-uses such as gene and drug delivery, bio-sensing and diagnostic and tissue engineering [1-4]. Since their discovery [5], carbon nanotubes (CNT) amongst all nano materials, have attracted a major share of the interest because of their unique mechanical, electrical, thermal and chemical properties [6]. Most studies of CNTs in the biosciences have focused on their influence on animal and human cells [7, 8]. Relatively scant attention has been paid to the effect of CNTs on plant cells and the way they might influence the physiology and the development of plants. Yet plants are fundamental to higher life on earth – they are the geo-physico-chemical transducers that produce food and oxygen that sustain life in the biosphere. They are also end-receivers of environmental contaminants including the CNT-based ones. Thus the plant-CNT interaction needs to be thoroughly investigated from the cellular to the organismic level to understand its multifaceted complexity. This knowledge will also serve to develop the technology of ‘nanoagriculture’ – a nascent area of nano-biotechnology that holds promise for growth acceleration and higher biomass yields of crop plants [9].

At the cellular level there has been substantial interest in the possibility of CNTs penetrating the plant cell wall to work as a smart delivery system of chemicals to the cell. The ability of single-walled-CNTs (SWCNTs) to penetrate the cell wall and membrane of tobacco cells [10] and of cup-stacked cellulase impregnated CNTs to penetrate the cell wall and transport intracellularly through cellulase-induced nanoholes [11], have been demonstrated. At the whole plant level, a number of researchers have reported the dramatic effects on seed

germination and plant growth by multi-walled CNTs (MWCNTs). MWCNTs have been shown to penetrate the seed-coat and stimulate the growth of tomato seeds [12, 13] as well as the growth of mustard seeds [14], while water soluble MWCNTs (wsMWCNT) have been shown to exhibit the same dramatic improvement of the growth of gram plants [15]. More efficient water uptake induced by the CNT has been implied as the growth stimulator [12-15]. On the other hand there exist contradictory reports that show the toxicity of CNTs to the growth of a number of different plants [16-18]. MWCNT reduced the root fresh weights (FW) of rice and cucumber seedlings while the root lengths (RL) varied in a non-orderly manner with MWCNT concentration (rice) or decreased (cucumber) [16]; the germination rate of maize and rye grass decreased with 2000 mg/l of MWCNT but their RLs increased [17]; MWCNT increased the FW and RLs of wheat seedlings but had no effect on seed germination and shoot lengths (SL) [18].

The contradictory observations are a result of the variability between the experimental entities employed in the studies. The effect of the MWCNT will principally vary with the type of plant studied, the type of growth medium and ambient growth conditions, the type of MWCNT (pristine or functionalised), its concentration, and the ultrasonication and associated techniques used to obtain the aqueous dispersion of the MWCNT. The dependence of seedling growth on the first three factors is well known in plant physiology. An assortment of media have been used in the aforesaid works – wet filter paper [14, 17, 18], agar with MS nutrients [12,13] and hydroponics with Hoagland's nutrients [16] or without [15]. Pristine MWCNTs are hydrophobic and form aggregates in aqueous media that reduce their aspect ratio and hence their effectiveness. To disperse their CNTs the researchers in the aforesaid studies had functionalised their CNTs with different hydrophilic groups [12-15] or had used a surfactant (PEG) [13], and had used different protocols for ultrasonication [12-15, 17 and 18]. Functionalization and micellar cage formation by a surfactant [19] alter the surface chemistry of the CNT, which changes the way it interacts with the plant [13]. Furthermore, different durations or intensities of ultrasonication will change the degree of dispersion of the CNT, introducing its component to the variability. Too vigorous an ultrasonication has been supposed damage the CNT [19]. In yet another variation, ultrasonication had been replaced by bead milling [16]. Pristine MWCNTs where used were pure, but were individualistic in type because they had been fabricated in the researchers' own laboratories with different

techniques, resulting in MWCNTs with different morphologies or remnant functional groups. Thus the substantial variability in the characteristics of the CNTs used, amongst other factors, is a reason for the variable

To define the basic response of the given plant to the MWCNT unambiguously, a baseline study that can be easily replicated across independent laboratories becomes necessary. Such a study would incorporate standard components of controlled specifications that are universally available, utilize minimal processing, and for the plant growth, employ a simple well-established protocol. Such a baseline could also serve as reference to more elaborate studies involving different processing techniques, growth protocols and other features. The general goal of the present work is a baseline-type study with add-ons as described further below. Also, if CNT-driven nanoagriculture is to be developed as a large-scale commercial venture, consistency and reproducibility of results acquire added importance.

We report the study of maize (*Zea mays*) seedlings grown in nutrient agar gel under controlled ambient conditions with the gel being treated by different concentrations of pristine MWCNT non-ultrasonically distributed within it. The MWCNT were obtained from an established chemicals company and possessed reliable, quality-controlled specifications. Maize is one of the species recommended by the USEPA [20] for the determination of the ecological effects of toxic substances. Moreover, it is an important food and agro-industrial crop such that an enhancement of its growth rate and biomass production (if CNTs do indeed promote these) would be highly beneficial. Few studies of CNT affected seed germination have been conducted on maize. The objective of the present study was to observe the effect of the MWCNT on the indices of growth and water absorption of the whole seedling as well as its morphological parts and to determine the mineral nutrient concentrations in the seedling. Seedling growth in the initial phases of seed germination is principally driven by water imbibition [21]. If the mechanism of the CNT-seed interaction is through the facilitation of water uptake, then this is also expected to enhance mineral nutrient uptake and affect growth. However, given the fact that CNTs purportedly display a marked interaction with ions and polar molecules [22, 23], it would be interesting to see how enhanced water delivery versus ion-CNT interactions play out as far as seedling nutrient uptake is concerned. The mechanism of ionic interactions with the CNT surface [22] implies that redox type changes of the nutrient

ion of a given oxidation state might take place with the MWCNTs in the medium. This is explored in the later part of this work with the introduction of the important mineral nutrient iron as Fe(II) and Fe(III) chloride in agarose gel. Agarose was chosen because it retains the gel platform of the previous study but is practically nutrient free so that the effects on iron will not be obscured by interference by other ions or polar species. The initiation of germination is not affected by the lack of substrate nutrients because it is driven by the stored food in the seed endoderm / cotyledon [21]. The growth experiments were terminated after 7 days of growth because up till ~7 days, the phases I – III of germination predominate where as stated before, water imbibition is of paramount importance.

3.2 EXPERIMENTAL SECTION

3.2.1 Materials

MWCNTs were purchased from Sigma-Aldrich® (St. Louis, MO, USA), purity >95%, OD 6-9 nm, L 5 µm. Bacteriological agar (BA) (Bioxon®) was purchased from Becton-Dickinson (BD de Mexico, Mexico City, Mexico) and Agarose from Sigma-Aldrich® (A9539). BA contains a certain level of mineral nutrients as ionic or polar species [22] but their levels in agarose are negligible. The reagents FeCl₂.4H₂O (>99% pure) and FeCl₃.6H₂O (≥ 97% pure) were purchased from Sigma-Aldrich® and Mallinckrodt Inc. (Phillipsburg, NJ, USA) respectively. Maize (sweet corn) seeds were purchased from a local seed supply company (Hortafloor, Rancho Los Molinos SA de CV, Mexico).

3.2.2 Substrate Preparation and Seedling Growth

The first experimental set (EXP-1) consisted of maize seedlings grown in BA gel medium spiked with different concentrations of MWCNT.

The BA powder was weighed and mixed with de-ionised (DI) water to obtain a concentration of 15g/l then autoclaved at 120⁰C for 20 mins. Appropriate masses of MWCNT were weighed out and mixed with aliquot volumes of the sterile BA solution by mechanical stirring for ~ 10 minutes in order to yield unvaried distributions of MWCNT in the gel of the different concentrations listed in Table 3.1. The BA solutions containing the different concentrations of the MWCNT were then poured into replicate sterile petridishes to set as the gel substrate for seed growth.

Table 3.1: Concentrations of the MWCNT ([MWCNT]) prepared in the bacteriological agar (BA) medium.

Sample name	Carbon nanotube concentration (mg/l)
0	0
5	5
10	10
20	20
40	40
60	60

Maize seeds were cleaned by magnetic stirring in a 70% ethanol solution for 2 minutes and washed with DI water. They were then surface sterilized in a 1% v/v solution of sodium hypochlorite by gentle stirring for 10 mins, then washed several times with DI water. The seeds were blotted dry in sterile paper towels and implanted into the set gel substrates described previously. The petridishes were sealed with tape and appropriately labeled. These operations were done in the laminar flow-hood. The petridishes were then transferred to a climate-controlled chamber (temperature 23-25⁰C, Relative humidity (RH) ~ 71.5%, photoperiod 16h light- 8h dark) and the seeds allowed to germinate and grow for 7 days. The total number of seedlings was 108 with each MWCNT case listed in table 3.1 containing 18 seedlings.

The second experimental set (EXP-2) was identical to the first except that only the Control and the MWCNT concentration of 20mg/l were used and a subset of seedlings was harvested periodically for the time-series analysis of the growth. The progress of seedling development in the two experimental sets was monitored photographically.

The third experimental set (EXP-3) consisted of maize seedlings grown in agarose gel medium spiked with Fe(II) and Fe(III) chloride with or without the simultaneous presence of MWCNT at the concentration of 20 mg/l.

Agarose powder was weighed and mixed in DI water, so as to correspond to a concentration of 8 g/l. The agarose was dissolved by heating the aqueous mixture at <95⁰C with constant magnetic stirring for about 2.5 hours. Upon complete dissolution, different

aliquot volumes of the clear agarose solution were measured out and the appropriate masses of Fe(II) and Fe(III) chloride as well as the appropriate mass of the MWCNT were mixed in by magnetic stirring for ~ 10 minutes to yield the concentrations as presented in Table 3.2.

Table 3.2: Concentrations of Fe(II) and Fe(III) introduced as their chlorides and the concentration of the MWCNT in the agarose medium.

Sample name	Additive concentration
A0	--
A1	MWCNTs (20 mg/l)
A2	Fe (II) 3×10^{-4} M
A3	Fe (II) 3×10^{-4} M + MWCNTs (20 mg/l)
A4	Fe (III) 3×10^{-4} M
A5	Fe (III) 3×10^{-4} M + MWCNTs (20 mg/l)

The Fe concentration of 3×10^{-4} M (16.8 mg/l) approximated the MWCNT concentration of 20 mg/l. The agarose solutions containing these different species were then poured into replicate sterile petridishes to set as the gel substrate for seed growth. The protocol for seed implantation was the same as in the first experimental set. The total number of seedlings in this set was 243 with each of the cases listed in table 3.2 containing 40-41 seedlings. The growth for all seedlings were carried out in the dark for 7 days at the ambient conditions of ~ 23⁰C and a RH of ~ 55%. Growth in the dark was necessary to prevent the photo-oxidation of Fe(II) [25]. Like many cultivated species, maize seeds are able to germinate equally well in light or dark.

3.2.3 Morphological Measurements and Microscopy

Upon harvesting, the seedlings were gently rinsed with DI water, blotted dry with paper towels and their FW, RL and SL measured. The roots and shoots were then cut and the FWs of these parts as well as of the seed body were measured. A few seed bodies from the third experimental set were analysed by Scanning Electron Microscopy (SEM). The seed parts were then oven dried at 60⁰C for 72h. The dry weights (DW) of these parts were then measured.

The SEM analysis was performed for the surface topography of the pericarp/seed-coat near the black-layer of the maize seed where the radicle emerges. The seed body was copper coated by vacuum deposition and analysed in the field emission SEM (JSM 7401F, JEOL Ltd. Tokyo, Japan) at 15KV with a working distance of 28-30 mm.

3.2.4 Elemental Analysis of The Seedling Tissue By Polarised Energy Dispersive X-Ray Fluorescence Analysis (PEDXRF)

pEDXRF is an advancement in EDXRF instrumentation first proposed in the mid-1990s [26] with commercial instruments sold since the early 2000s. The operating principle is based on the cancellation of the Bremsstrahlung background by the double polarisation of the initial x-ray beam. Consequently the analytical sensitivity markedly improves, permitting trace level analysis. We have shown [27] that samples of masses lower than the recommended mass for ideal analysis (as frequently occur in the biosciences), can be analysed for relative elemental concentrations with sufficient accuracy. The detectable elemental range is from Na to U. The advantages of pEDXRF lie in its non-destructive, multielemental and rapid trace analysis capabilities.

Dry plant parts were ball milled (model MM-400, Retsch GmbH, Germany) at 25 Hz for 2 minutes till the entire mass appeared as a fine powder. The elemental analysis of the powders was carried out by the pEDXRF spectrometer SpectroXepos III (Spectro Analytical Instruments GmbH, Kleve, Germany) using the TurboQuant™ analytical routine. It is important to remember that for the low sample dry mass yields as in the present work, the quantity of interest is the relative magnitude of the element's concentration corresponding to the different treatments.

3.2.5 Data Analysis

Averages and standard errors were computed over 3 sets of replicates for each case listed in the table 3.1 and 3.2 with the number of seedlings for each set as cited previously. Tests of statistical differences were carried out by the Student's t-test at 95% confidence level, except where stated differently. The softwares [28] ORIGIN 6 and SIGMAPLOT 10 were used for data reduction and analysis.

3.3 RESULTS

Figures 3.1a-d show the various indices studied in this work as they vary with the MWCNT concentration ([MWCNT]) in the BA medium for the fixed period of germination of 7 days (EXP-1).

The % water was calculated as: $\{(FW-DW)/FW\} \times 100$. The MWCNT increased the water content of the root but less unequivocally for the whole seedling (figure 3.1a). The sudden increase at low [MWCNT] continued in a gradual manner or attained a near constancy at the higher [MWCNT]. For the shoot however, after a spurt in the %water at the [MWCNT] of 10mg/l, the water content decreased gradually. The trace for the seedling follows the combined response of the root and shoot. The FWs (Figure 3.1c) follow the trends of the water contents, which is reasonable due to FW being largely composed of tissue water. The DWs (Figure 3.1d) for each morphological part are not much different at the low [MWCNT] but show a sudden spurt at 20 mg/l [MWCNT] particularly for the root, while slowly declining at the higher [MWCNT]. Figure 3.1b shows that the RLs increased markedly with root %water; for the SLs the increase with shoot %water was weaker and more “noisy”.

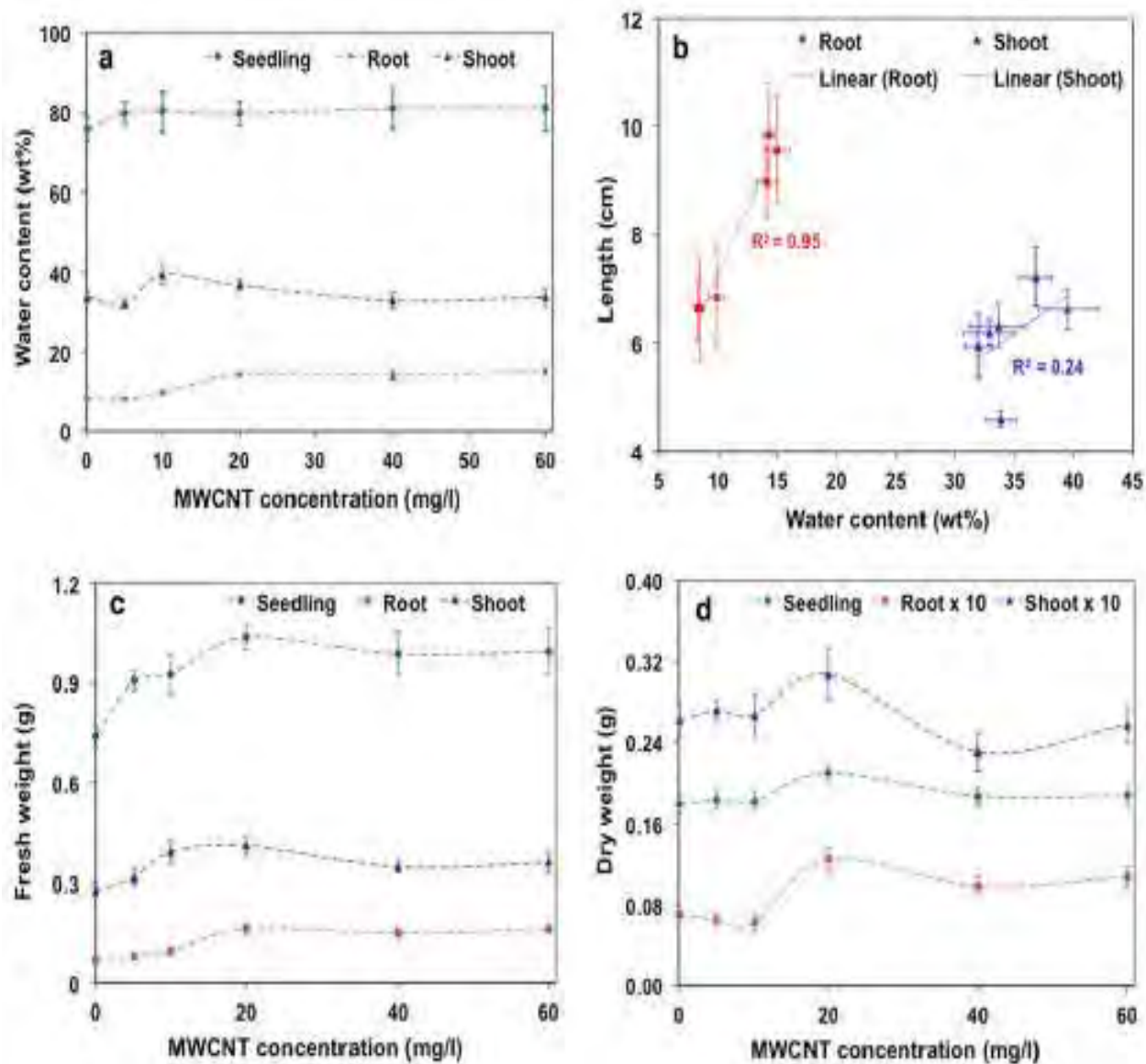


Figure 3.1: Effect of multi-walled carbon nanotubes (MWCNT) on the 7-day germination and growth of maize in the BA medium (see table 3.1). ($n=18$). (a) % Water content of the whole seedling, the root and the shoot versus the [MWCNT]. (b) Root (RL) and shoot lengths (SL) with respect to their % water contents (c) dry weights (DW) and (d) fresh weights (FW) of the different morphological parts versus the [MWCNT]. The root and shoot DWs have been multiplied by 10 to accommodate them in the same graph. The dashed lines in (a), (c) and (d) are splined connectors only. The dotted lines in (d) are the linear regression fits to approximately quantify the trends.

Figures 3.2a-d refer to the time (t)-series analysis at the fixed [MWCNT] of 20 mg/l (EXP-2).

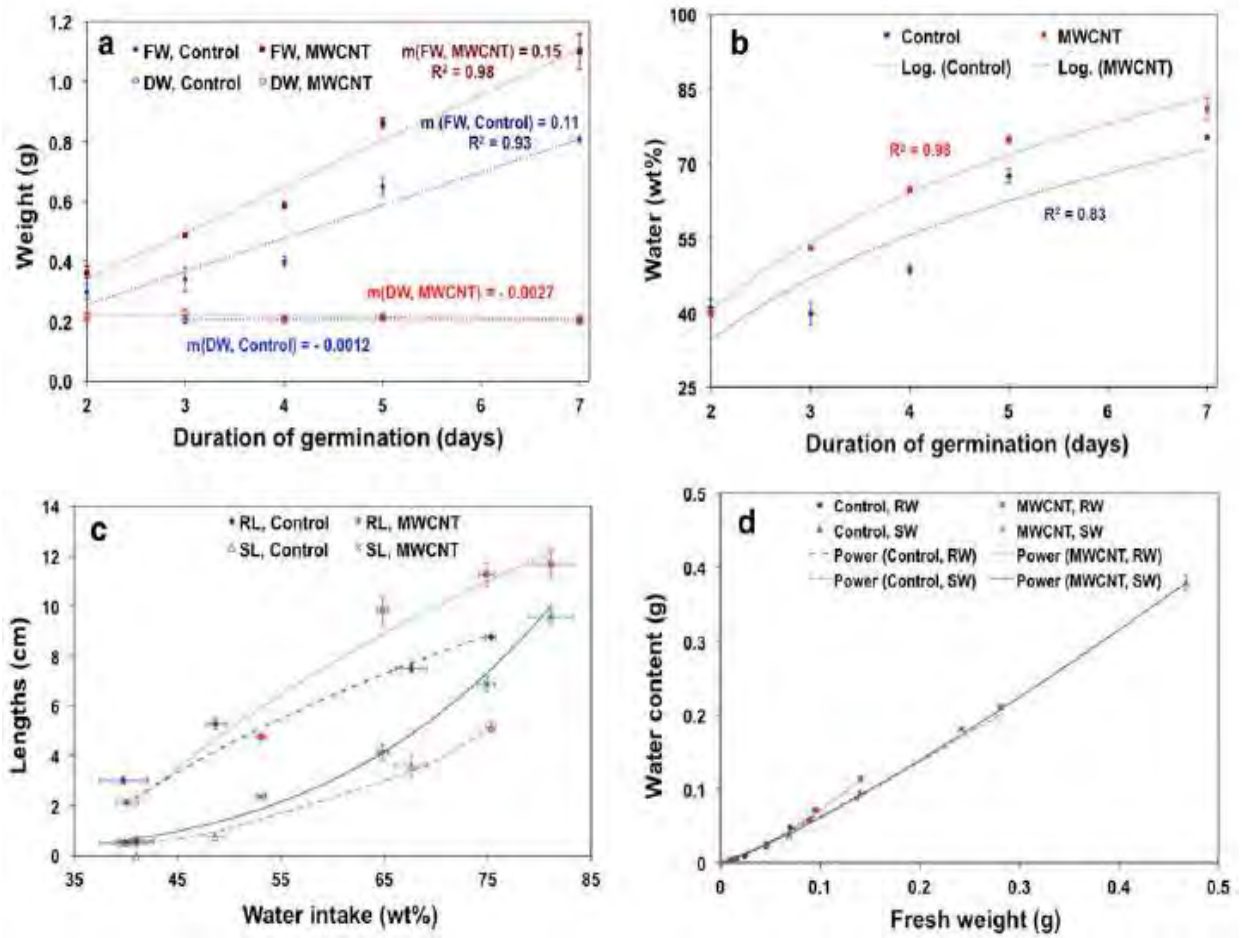


Figure 3.2: Variation of growth indices with duration of germination of maize seedlings grown in BA with/without(=Control) 20 mg/l MWCNT. (a) FW and DW. The dotted lines are the linear regression fits with the slopes (m) and correlation coefficient (R^2) values as shown. (b) % Water intake. The dotted lines are the logarithmic fits. (c) RL and SL with respect to %water intake by the seedling. The dotted and the dot-dashed lines are the logarithmic fits to the RL, the solid and dashed lines are the power-law fits of the SL, for the MWCNT and Control. The R^2 values respectively are 0.96, 0.88, 0.98, 0.98. (d) Test of universal allometric power law scaling of biology. The y-axis is the net water content of the shoots and roots, SW and RW respectively. The dotted, dot-dashed, solid and dashed lines are the power-law fits to the RW and SW with and without the MWCNT respectively. The R^2 values in sequence are, 0.986, 0.998, 0.998, 0.999.

With the exception of one pair of data points the seedling DWs for the MWCNT treated medium and the control (Figure 3.2a) are not different statistically. The seedling FWs on the other hand increase as they should as in any growing organism. Figure 3.2b re-affirms the higher water intake by the seedling in the presence of the MWCNT and indicates a decreasing rate of intake with time (logarithmic fits). Figure 3.2c in a sense is a “corollary” of Figure 3.1b: the [MWCNT] is fixed but the observations correspond to the different growth periods (the seedling water content is a parametrically time-dependent quantity (Figure 3.2b)), showing the variation of the root and shoot lengths with water content where the latter is the key entity affected by the MWCNT (Figure 3.2b). The plots in figure 3.2d were constructed to test the validity of the universal allometric power-law scaling of biology [31] for the water content versus the root and shoot FWs in the context of MWCNT mediated growth, given that water is the principal actuator of germination and metabolism [21, 30].

The seedling water content in the agarose medium (Figure 3.3a) of EXP-3 did not show a high degree of variation with respect to the control except when ferrous chloride alone (A2) or ferric chloride with MWCNT (A5) were added.

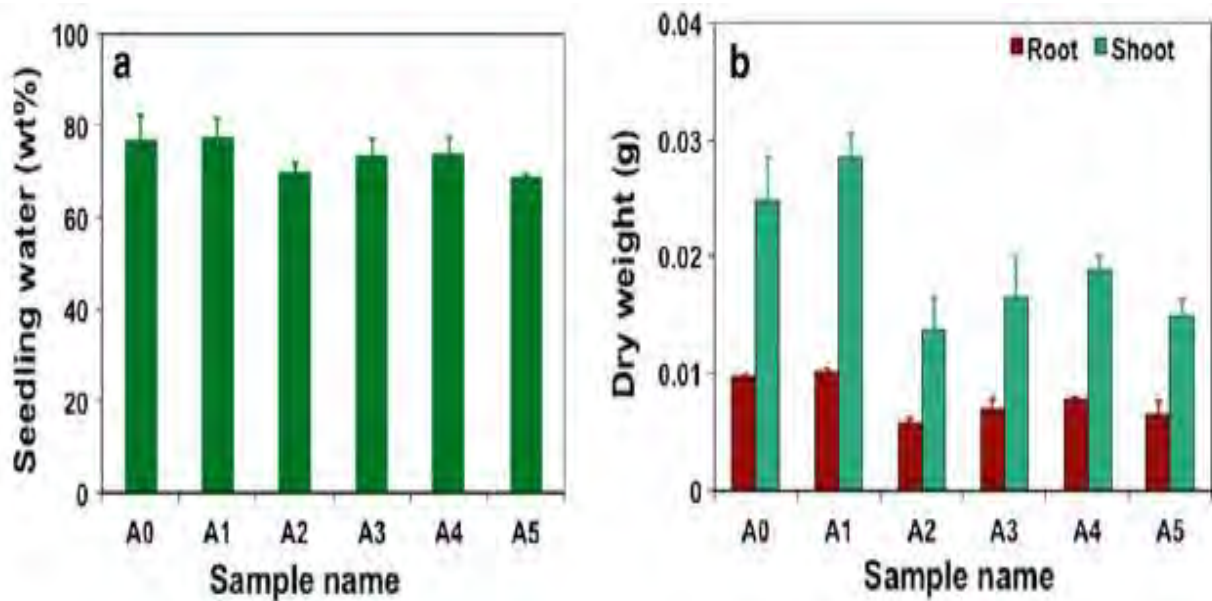


Figure 3.3: Seedlings grown in agarose media (see table 3.2). ($n=40$ or 41). (a) Variation of %water of the seedling (b) Root and shoot DWs.

The trend of the water content was mirrored in the root and shoot DWs (Figure 3.3b) albeit more sensitively particularly for the shoot.

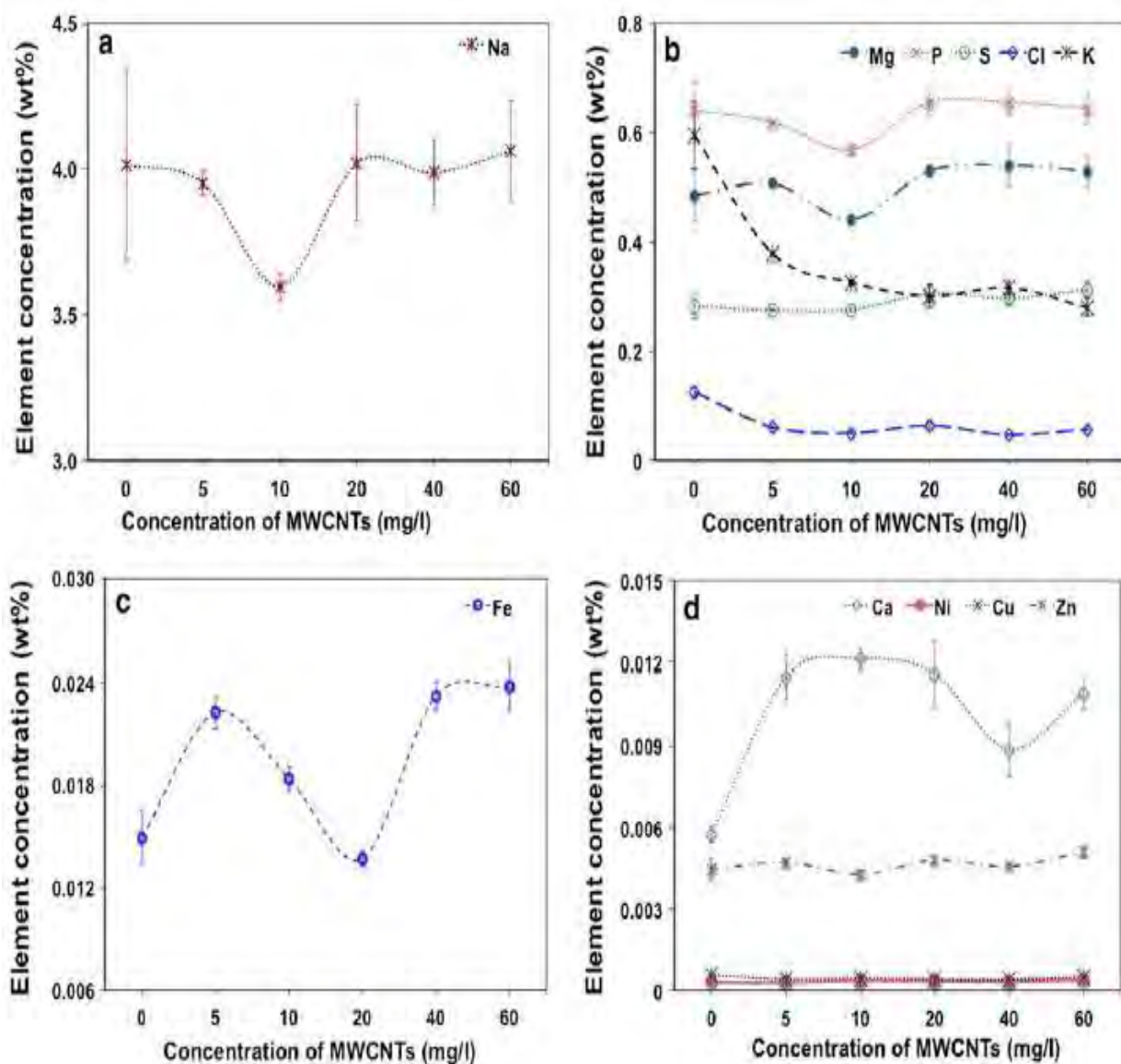


Figure 3.4: Elemental concentrations of the seedling samples corresponding to table 3.1 obtained using polarised energy dispersive x-ray fluorescence spectrometry (pEDXRF).

Figure 3.5 shows the pEDXRF elemental analysis of the seedlings of EXP-3 for the same set of macro and micro mineral nutrients. Other than Ca, Fe and Cl, tissue concentrations of all elements of the set are unchanged regardless of the medium (Figure 3.5b).

The elemental analysis of the seedlings of EXP-1 by pEDXRF (Figure 3.4) yielded the tissue concentrations of the macro and micro mineral nutrients of the 3rd and 4th periods of the Periodic Table.

With the exception of Cl, K, Ca and Fe, there is no statistically significant difference between the Control and the lowest [MWCNT] of 5 mg/l. Only in the cases of Cl and K does the Control have the highest concentration of the element in the plant tissue. As the MWCNT is introduced, the tissue Cl and K concentrations fall till 10 mg/l and 20 mg/l of [MWCNT] respectively then gradually level off. For all other elements the tissue elemental concentrations display a minimum at 10 mg/l [MWCNT] except for Ca and Fe for which the minima occur at 40 mg/l and 20 mg/l. After the minimum, the tissue elemental concentration rises and maintains a level that is not statistically significantly different between the different higher [MWCNT], except for Ca.

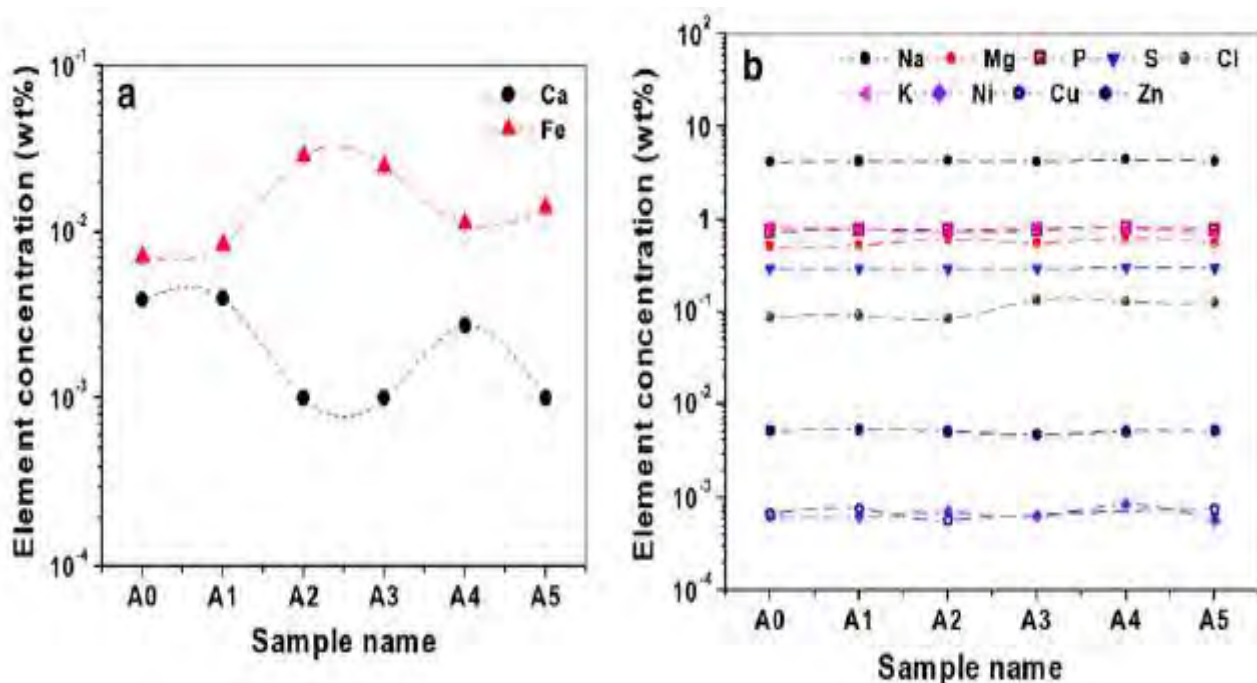


Figure 3.5: Elemental concentrations of the seedling samples corresponding to table 3.2 obtained using pEDXRF. The small errors bars are not visible, however the coefficients of variation averaged over all [MWCNT] are 0.1% to 3.2% for the different elements.

This is expected because the agarose is nearly completely free of extraneous elements. Thus none of these elements can be brought in to a significant measure from the external

medium and therefore retain their intrinsic concentrations in the seedling for which the type of external medium is inconsequential. The difference in the Cl concentrations compared to the Control show up in the media A3 (Fe(II) + MWCNT), A4 (Fe(III)) and A5 (Fe(III) + MWCNT). The most interesting cases are of the Ca and Fe concentrations whose trends are near mirror images of each other. Since Fe and not Ca is present in the agarose and Ca only in the cell walls and intracellular compartments of the seedling, the non-constant concentration of Ca is likely a result of the Fe, Ca interaction in the media and plant cells with mediation by the MWCNT. Although Fe is frequently used as a catalyst in the manufacture of CNTs, the closeness of the Fe concentration of the agarose medium containing the MWCNT (A1) with the Fe for the plain agarose medium (A0, Control) as well as the purity of > 95% of the MWCNT used in this work makes contamination by the Fe from such a source unimportant.

Figure 3.6 shows the SEM images of the black-layer region corresponding to the treatments in the agarose medium (EXP-3). The most interesting feature is how the pure MWCNT modifies the surface topography (Figure 3.6c) of this region and how the relatively high ionic concentrations of iron and chloride ions in the medium change the capacity of the MWCNT to modify this surface topography (Figures 3.6d and 3.6e).

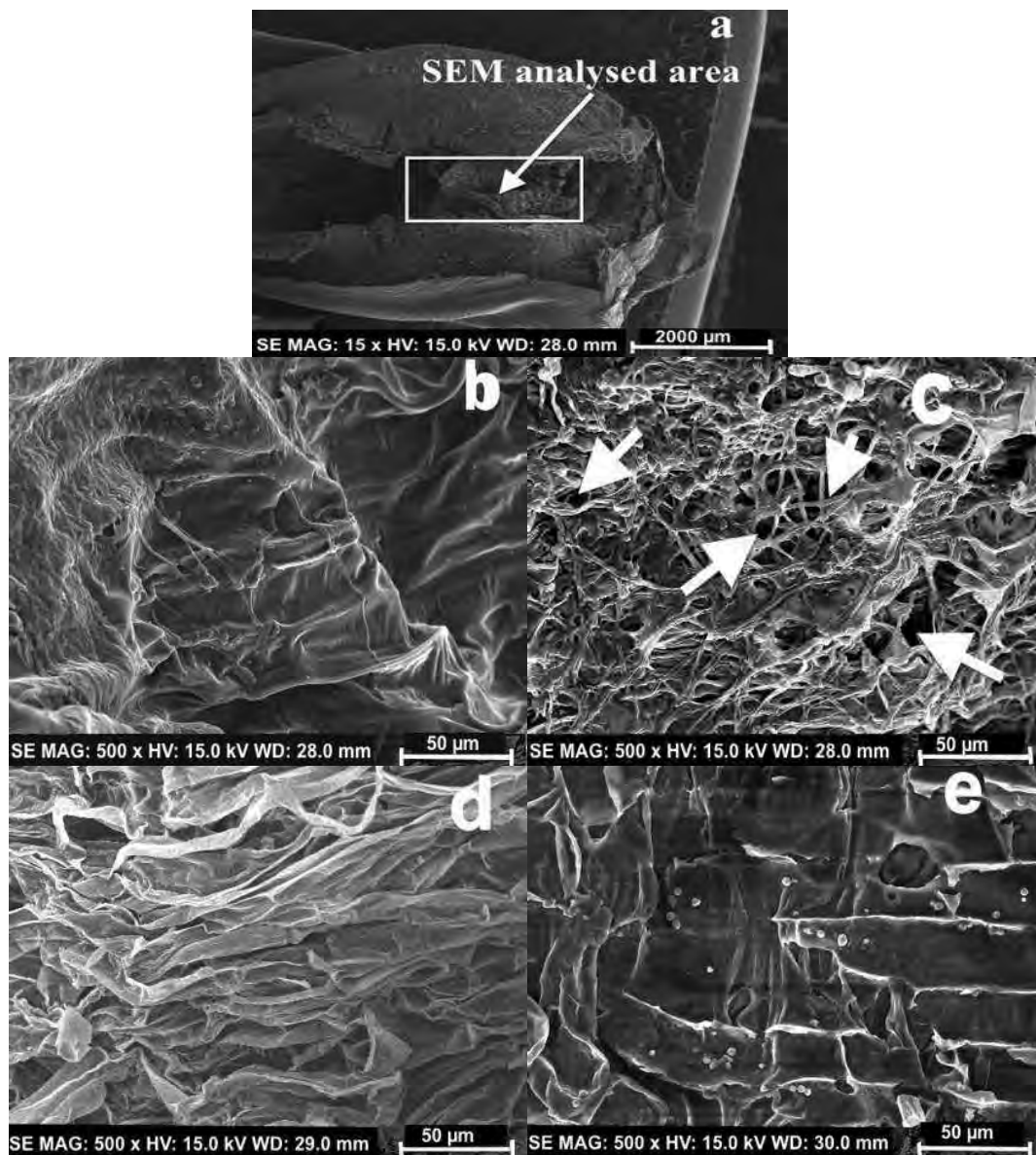


Figure 3.6: SEM images of the topography of the black-layer region of the seed-coat of the 7 day germinated maize seedling grown in agarose gel with some of the additives of table 3.2. (a) The analysed area near the black-layer (b) Control medium (c) MWCNT (20 mg/l) medium; the white arrows indicate the pores (d) Fe(III) ($3 \times 10^{-4} M$) medium (A4) (e) Fe(II) ($3 \times 10^{-4} M$) + MWCNT(20 mg/l) medium (A3).

3.4 DISCUSSION

3.4.1 Water Content And Growth Indices (EXP-1)

The region of the black-layer of the pericarp/seed-coat where the radicle emerges is the first point of entry of water and oxygen molecules in the germinating maize seed [32]. The MWCNTs suspended in the gel medium as well as the dissolved ions and other species (Fe^{2+} , Fe^{3+} and Cl^- only, in the agarose gel media) would be carried along with the water and are likely to show their effects prominently here. In particular if the MWCNT can penetrate seed coats [12] they would find it the easiest to do in this part because of the propensity of this region to allow the entry of external molecules. Transmission electron microscopy (TEM) and Raman spectrometry [13-15] have shown the penetration into seedling tissue (except the shoots) by the MWCNT. The difference that the MWCNT make to the surface of the seed's black-layer is evident in the comparison between the Figure 3.6c and 3.6b. A high degree of porosity and a partial dismemberment of the surface structure are seen upon introduction of the MWCNT (Figure 3.6c). Such pores would greatly facilitate the entry of water, nutrients and oxygen as well as the dispersed aqueous phase MWCNT themselves into the germinating seed. It is well known that scarification aids the germination of seeds. Visually, the appearance of the effect of the MWCNT at the black-layer region (Figure 3.6c) seems akin to scarification at the microscopic scale.

The seed body and root are directly in contact with the gel medium. The higher water permeation upon introduction of low [MWCNT] due to the aforesaid pores is likely the cause for the higher uptake of water implicit in the Figures 3.1a and c, 3.2a and b. Higher [MWCNT] would be logically expected to increase the penetrability and hence the water content. However the water contents are seen to follow the trends described in Figure 3.6c indicates numerous large pores at the [MWCNT] of 20mg/l (size of the order of μm), thus the putative increase of porosity with [MWCNT] ≥ 20 mg/l is not expected to substantially enhance the water content. Furthermore, at the higher [MWCNT] in the medium, the nanotubes would aggregate more (particularly in the absence of induced exfoliation) resulting in the diminution of functionality such as their capacity to increase water delivery to the parts in contact with the medium. These factors may account for the scant variation of the % water at the [MWCNT] ≥ 40 mg/l. The shoots are not immersed in the medium so water enters the shoot as for all plants by capillary action driven by the root water pressure. Aggregation of the

MWCNT in the extracellular or intracellular spaces within the root, that is likely to scale with the [MWCNT] [19], would impede this normal upward flow and affect the physiology of shoot water transport at the higher [MWCNT]. The initial formation of intracellular aggregates within the root of gram plants even by the wsMWCNTs, has been observed [15]. Oxidative damage at the higher [MWCNT] concentrations [33] consequent to the penetration of the plasma membrane of the seedling cells by the CNT [10] may also play a role in the reduction of the water content and FW of the shoot (Figure 3.1c) at the higher [MWCNT]. The combination of the facilitation of water entry at low [MWCNT] and but its 'obstruction' at higher [MWCNT] makes the trace of the shoot water content pass through a broad maximum at the [MWCNT] of ~20 mg/l.

The root length shows a clear ($R^2 = 0.95$, $p < 0.05$) and steep dependence on the quantity of water imbibed which in turn, as seen in the foregoing, is correlated with the [MWCNT]. Water increases the cell turgor pressure that triggers cell elongation and the production of hormones (e.g. gibberellic acid (GA) and auxin) that promote root growth [21, 30]. The weaker and noisier increase ($R^2 = 0.24$, $p < 0.05$) of shoot length with water content may be a consequence of two factors. While water uptake induces shoot growth also through the aforesaid physiological processes [21, 30], the uptake by the shoot is indirect and dependent on the upward water transport by the root. The latter would be affected by the [MWCNT] in the manner described in the previous paragraph. Additionally, other independent factors such as light intensity are also involved in shoot growth [30]. The combination of the different factors produces a noisier and weaker response of the shoot length to just the water content.

Figure 3.4 shows that for most nutrients (except Cl and K) the concentrations rise at [MWCNT] > 10 mg/l (at > 0 mg/l [MWCNT] in the case of Ca). The [MWCNT] of ~ 20 mg/l is also the concentration where the water content for the different parts, particularly the root, reaches the maximum (Figure 3.1a). The rise in imbibed water brings in more mineral nutrients from the medium and also signals enhanced enzyme and hormone activity [21], factors that are expected to benefit tissue development. This consequence of the water absorption is seen in the rise of the relative concentrations of most mineral nutrients (Figure 3.4) and in the DWs (Figures 3.1d) where a maximum is reached at the [MWCNT] of 20 mg/l. Root and seedling water content hold nearly steady after 20 mg/l [MWCNT] (Figure 3.1a) so

the water borne increase of mineral nutrients is not expected to increase after this concentration, which indeed is broadly the case (Figure 3.4). However increased [MWCNT] is a possible source of oxidative cell damage as discussed in the preceding as well as causing perforations in the seed epidermal matrix (Figure 3.6c). These factors may impact the metabolic activity adversely resulting in a decline of the root and shoot DW with increased [MWCNT].

Thus the benefits of the MWCNT in this work are observed for the lower end of the concentration range (≤ 20 mg/l). Toxicity effects [17, 33] diminish the usefulness of the MWCNT to the plant at higher concentrations. The effect of the MWCNT on plant health therefore appears to be one of chemical hormesis, a phenomenon that has been observed for normally toxic substances in areas such as toxicology and homeopathy [34].

3.4.2 Time Series Analysis (EXP-2) of Water Absorption and Growth Indices

The overall tendency of the data for the FWs in Figure 3.2a may be qualitatively inferred from the slopes of the trend lines. The magnitudes of the slopes indicate that the FW in the MWCNT medium increases ~ 1.4 times faster than the control. These results are reasonable given the observation of the MWCNT aiding water imbibition (section 3.4.1) and due to FWs being mostly water. Likewise the approximate overall tendency of the seedling DWs in Figure 3.2a may be inferred from the trend lines whose slopes differ statistically ($\leq 70\%$ confidence level). The DWs in both the MWCNT and control media show a decreasing trend with time (negative slope) in keeping with the physiology of seed germination before photosynthesis sets in [21]. The magnitudes of the slopes show that the DW of the MWCNT treated seedlings decrease at almost double the rate of the Control seedlings. This would indicate that the higher water imbibition caused by the MWCNT triggers a higher rate of metabolic activity and respiration through the activation of enzymes and hormones [21] leading to a faster DW decline.

Water enters the cells of the gel submerged parts of the seedling by passive diffusion driven by the difference of the water potential across the gel-seedling barrier [30]. As more water fills the cellular spaces with time, the magnitude of the potential difference decreases resulting in a lowered rate of water entry or a saturation effect, in keeping with Fick's second

law of diffusion [30]. The saturation effect shows up clearly for both the control and the MWCNT treated seedling in Figure 3.2b. The MWCNT treated seedlings consistently absorbed more water than the control. To qualitatively indicate the non-linear or saturative behaviour, the data were fitted to log functions that were seen to produce the most acceptable fits. The MWCNT data produced a better quality of fit (R^2 value). In fact the better statistics of all data sets concerning the MWCNT is a feature that stands out. Statistically, the degree of orderliness in the data values (precisions) is indicated by how low the average coefficient of variation (CV for the set) is. The CV values for the water contents and growth indices studied in this experiment for the MWCNT treated seedlings were consistently lower, of the order of 0.5-0.7 times the values for the corresponding control data sets. Molecular dynamics simulations of water in CNTs show that CNTs act as molecular channels for water where the hydrophobicity confines the water molecules to ordered files of polarized chains and moves them in a pulsatile fashion [35]. In an attempt to investigate this phenomenon experimentally, Tripathi et al [15] have shown that their wsMWCNT aligned themselves in the vascular bundles of the roots of gram plants and enhanced plant water uptake possibly by the ensuing channeling action. It is possible then that the enhanced water uptake shown in this work and the orderliness of the behaviour consequent to MWCNT application, might also result from a similar alignment and channeling in contrast to the normal random thermal motion of the water molecules in the Control.

In Figure 3.2c the rate of root length increase diminished with the increase of seedling water content (logarithmic fit) which at first seems aberrant. However the *in vitro* growth constrains the downward elongation of the root – a situation that is not encountered in field plants. Such a confinement is less rigorous for the upward elongation of the shoot. For both media, the SL rapidly increases (power-law fit) as a consequence of water imbibition and phototropism. However, one observes that for the same water content (i.e. same values of %water on the fitted curves), the RL and SL for the MWCNT case are higher than for the control. The same water content implies that all water related growth factors would be invariant. Thus, MWCNTs at low concentrations seem to interact with the seedling cells at more levels than just the facilitation of water delivery, to enhance growth.

In a landmark study [31a] West, Brown and Enquist (WBE) have argued that mass is the prime determinant of variation in physiological behaviour when different organisms are

compared over many orders of magnitude. Scaling with mass then, they show follows a simple power-law,

$$Y = Y_0 \cdot M_b^b \quad (3.1)$$

where Y is some observable metabolism-related quantity, Y_0 is a normalisation constant and M_b is the mass of the organism. At the core of this allometric scaling law is the axiom that the exponent b takes on a limited set of values, typically simple multiples (n) of $1/4$. For the fluid volumes in trees [31b], b is seen to be $25/24 = 4.17(1/4)$ or rounded to the nearest integer, it is $4(1/4)$. We have seen in the current experiment that the water content is a crucial metabolic driver in germination and early growth and is affected by the presence of the MWCNT. In Figure 3.2d we explore the question of whether the same $1/4^{\text{th}}$ behaviour carries over to seedlings in the artificial environment of the MWCNT and if different, how much different from the control. The fluid being principally water, its weight (g) would approximate closely the volume (ml) at room temperature and pressure. Figure 3.2d shows that the power-law fitted the experimental data of the variation of the water contents (in g) in the morphological parts versus their FWs, rather well (R^2 values as indicated). The plots for all parts whether or not treated by the MWCNT are nearly identical with only small variations in the exponent values. The values of $\{Y_0, b\}$ for the root(control), root(MWCNT), shoot(control), shoot(MWCNT) were respectively, $\{1.354, 1.288\}$, $\{1.527, 1.331\}$, $\{0.829, 1.118\}$, $\{0.932, 1.184\}$. Rounding the b values to the nearest integral multiple of $1/24$ we get b as, 31, 32, 27, and 28 times the fraction $1/24$ respectively for the sequence. An average of these multiples of $1/24$ rounded to the nearest integer yields (30 ± 2) . In other words the fluid (water) volume obeys eqn (1) with the exponent as $\sim 30/24$ or $5(1/4)$. (*N.B.* If the shoot alone is considered, the exponent is closer to $25/24$, being ~ 27 or 28 times $1/24$). Thus the seedling follows the expected universal scaling law just as the giant trees, many orders of magnitude its size, do. The perturbation brought in by the xenobiotic MWCNT to the seedling's physiology does not make it deviate from the law. The value of b however is one integer unit in excess of the b value typical for trees showing that water constitutes the masses of these young plants more than for the older trees. WBE point out that it is not so much the closeness of the value of b to $n \cdot 1/4$ is but rather its approximation over a great range of sizes and conditions (e.g. our seedlings vs. giant trees) that is important and that the residual variation may throw light on the secondary factors that cause the deviation from the exact $n \cdot 1/4$ value. Seen in this light, we

note that the b for the MWCNT cases are consistently somewhat higher than for the control. We posit that a detailed logging of the values of b in such types of experiments for various Y may empirically allow the quantification (and thereby prediction) of the effects of the given MWCNT.

3.4.3 Elemental Concentrations in Seedling Tissue (EXP-1 and EXP-3)

The salts of the mineral macro and micronutrients of the BA in the aqueous gel medium present the elements principally as ions or polar molecules to the plant tissue. The flow of water into the plant (principally the root) facilitated by the MWCNT as seen in the foregoing, brings in the dissolved ions where the inflow varies as shown in Figure 3.1a. However the MWCNT surfaces in the medium may attach the ions through the ion-transient dipole (ITD) interactions between charged/polar species and the π -electron clouds in the CNT molecular structure as has been documented in the literature (see for example, [36]). The strength of these interactions will vary with the type of ion and CNT, CNT concentration, state of CNT aggregation etc. in a complex way. Hence the profile of the elemental concentrations (Figure 3.4) is likely the result of a trade-off between these 2 contrary forces - increase by water inflow vs. retention (adsorption) by the medium's MWCNT. We proceed to describe the specific cases vis à vis this probable mechanism.

For the maximally electro-positive and negative ions in the medium (K^+ and Cl^-) the introduction of the different [MWCNT] only serves to decrease their concentrations up till a broad minimum after which the concentrations flatten out (Figure 3.4b). The ITD interaction is likely to dominate over water inflow for these highly electro-active ions restricting their ingress into the seedling. A saturation is seen at $[MWCNT] \geq 20$ mg/l possibly because of increased MWCNT aggregation that reduces the surface area despite the increase of [MWCNT]. For other ions except Fe and Ca, the attractive force appears to dominate up till ~ 10 mg/l of MWCNT. At $[MWCNT] \geq 20$ mg/l the increased water inflow (Figure 3.1a) dominates, increases the elemental concentrations, which then level off as a consequence of the plateau in the water content (Figure 3.1a) and the MWCNT aggregation. In the case of Fe the [MWCNT] of 5 mg/l causes a sharp rise but for $[MWCNT] > 5$ mg/l the interplay between the adsorptive forces, the increase of water inflow and MWCNT aggregation as for the other

ions, makes the profile pass through a minimum (20 mg/l) with the subsequent rise and leveling off. The case for Ca is similar except that its high concentration spans a broad plateau up till 20 mg/l and the minimum occurs for the higher [MWCNT] of 40 mg/l. Increased water transport finally prevails (at [MWCNT] 60 mg/l) increasing the Ca concentration but lingering adsorptive effects likely make the value less than at the plateau region. These examples show the specific nature of the ion (polar molecule)-CNT interaction and the role of water flux in the overall ionic transport into the seedling.

We have seen that Fe and Ca are the 2 nutrients that show some of the most sensitive responses to the MWCNT (Figures 3.4 c and d). EXP-3 in the agarose medium was constructed to inspect the behaviour of Fe without the interference of the other ions at the [MWCNT] of 20 mg/l where the CNT displays a strong adsorptive effect (Figure 3.4c) and where water inflow is relatively high (Figure 3.1a). We hypothesize that the strong CNT-Fe interaction if guided by the ITD would be affected by the charge state of the Fe; hence a difference would presumably show up between Fe^{2+} and Fe^{3+} introduced at the same concentrations. The plant's own preferential absorption of Fe^{2+} would also factor into the overall response. In plants typically the enzyme iron reductase secreted by the root plasma membrane, reduces Fe^{3+} to Fe^{2+} to facilitate Fe uptake [30]. Figure 3.5a shows that the plant absorbs distinctly more Fe^{2+} (A2) than Fe^{3+} (A4) in the absence of the MWCNT. When the MWCNT is introduced, the seedling Fe concentration from Fe^{2+} is slightly reduced (A3 lower than A2, Figure 3.5a) despite the better water delivery in A3 compared to A2 (Figure 3.3a) possibly because of the adsorption of Fe^{2+} onto the MWCNT in the medium. In the case of Fe^{3+} with the MWCNT however, the Fe concentration within the plant slightly increases (A5 more than A4, Figure 3.5a) despite the reduced water delivery in A5 compared to A4 (Figure 3.3a). If the Fe were to remain as Fe^{3+} then the combined effect of the plant's low-affinity for Fe^{3+} and the higher electrostatic attraction by the electron cloud in the MWCNT for the higher positive charge, would have reduced the plant Fe concentration further. The contrary observation, *viz.* the increase, may then possibly be due to the reduction of 3+ to 2+ by the CNT's electronic density thereby facilitating the uptake of Fe by the plant. The differences in Fe concentrations and seedling %water contents cited here are statistically different at 95% confidence level for the concentrations and at 80-90% confidence level for the %water.

Ca is present in the cell wall matrix of the seedling largely in the binding heteropolysaccharide pectin, as calcium pectate [30]. The addition of MWCNT alone (A1) makes no change to the Ca content in the seedling, as it should be. However when Fe^{2+} is added either alone (A2) or with the MWCNT (A3) a relatively high reduction in the Ca content in the seedling takes place in a diametrically opposite manner to the Fe contents (Figure 3.5a). This suggests that Ca is cationically exchanged by the Fe^{2+} in the cell wall matrix leading to a reduction in the seedling Ca content. When Fe^{3+} alone is introduced, the Ca concentration rises markedly almost exactly mirroring the reduction of Fe content in the seedling tissue (Figure 3.5a). The non-equivalent positive charges between Fe^{3+} and Ca^{2+} makes the replacement of Ca^{2+} less probable by cation exchange (e.g. in the bonds with the pectate groups [30]). However, when the Fe^{3+} is introduced with the MWCNT, the Ca content falls, again mirroring the rise in Fe content (Figure 3.5a). If the Fe^{3+} -CNT interaction causes some reduction of the Fe^{3+} to Fe^{2+} which in turn exchanges with the Ca^{2+} in the cell wall matrix, it would explain these aforesaid observations. The Ca concentration profile therefore provides further support to the possibility of the CNT surface promoting the Fe^{3+} reduction. Calcium bound to pectin has a structural and hydrating role in the cell wall and also functions in cellular metabolic regulation and signaling [30]. Excess heavy metals (e.g. the Fe^{2+} in EXP-3) are known to modify the stability of Ca channels causing an increase of cellular Ca fluxes [37]. Given these functions, one may expect that the possible efflux of Ca out of the seedling would reduce its DW and the water content, particularly of the root. This expectation is supported by the observations of Figure 3.3 that show that the root DW and total %water content are the least as compared to the Control for the samples that possess the least Ca concentrations (A2 and A5 of Figure 3.5a).

The interdependence of the $\text{Fe}^{2+}/\text{Fe}^{3+}$ and Ca^{2+} concentrations is contrasted with the near constancy of the Cl^- concentrations where Cl^- is the counterion to the Fe^{2+} and Fe^{3+} in the system. The rise of Cl in the plant tissue for A3, A4 and A5 as compared to A2 is probably due to the effects of higher water inflow in A3 and A4 (Figure 3.3a) and the higher mole ratio of Cl to Fe in FeCl_3 compared to FeCl_2 .

3.4.4 Water Contents, DWs and Surface Topography of Seedlings in EXP-3

The ratios of the %water contents of (a) A0 to the Control in EXP-1 (b) A1 to the [MWCNT] of 20 mg/l in EXP-1 are (a) 1.01 ± 0.08 and (b) 0.97 ± 0.06 which are both close to 1. The ratio in (a) proves that there is no intrinsic difference between the two types of gel media in their ability to supply water to the seedling. The second ratio shows the water transport to the total seedling by the MWCNT at 20 mg/l behaves in the same manner in the two media.

The SEM image of the seed coat in the black-layer area in the medium A4 (FeCl_3) shows little physical change as compared to A0 (Control, figure 3.6b), except a more striated or puckered surface (figure 3.6d). The introduction of the medium A3 (FeCl_2 with the 20 mg/l MWCNT) also leaves the seed coat intact with apparently even less layer folding (figure 3.6e). These images are in contrast to figure 3.6c (A1 medium) that show seed coat perforation which has earlier been linked to more facile water delivery (sections 3.4.1 and 3.4.2). The similar surface topographies of A3 and A4 suggest the seedling water contents in A3 and A4 might be close which in fact is the case (figure 3.3a). The more intriguing feature is the difference that the FeCl_2 makes to the surface topography when the background concentration of the MWCNT is the same (figure 3.6e vs. figure 3.6c). The ITD force alluded to before (section 3.4.3) may result in the adsorption or localization of some of the Fe^{2+} (and other ions) on the surface of the MWCNT, thereby altering its functionality so that it cannot so effectively cause the surface pores on the black-layer of the seed-coat (figure 3.6e). Such an alteration of the surface chemistry of the MWCNT may affect its ability to deliver the metal ion (Fe^{2+}) to the seedling and perhaps may also affect water delivery since the CNT surface affects water conduction (section 3.4.2). A3 is seen to have a slightly lower Fe concentration than A2 (figure 3.5a). While the effect on the DWs by the treatment in A3 versus the one in A1, is strong (figure 3.3b: DWs of A3 lower than A1), the corresponding decrease in the % water content in A3 relative to A1 (figure 3.3a) is less prominent although the difference is statistically significant ($\leq 80\%$ confidence level). It is possible that the aforesaid change in MWCNT functionality may also affect its enhancement of germination and growth. DWs are a result of metabolic processes. In figure 3.3b we see that the metabolic processes that

contribute to root and shoot DWs were the highest for the pure MWCNT treated seedlings. The introduction of FeCl_2 and FeCl_3 only depreciated the DW enhancement by the MWCNT.

Overall the findings of EXP-3 suggest that the pristine MWCNT (medium A1) are more potent for seedling growth than MWCNT in media with high concentrations of ions or polar groups.

3.5 SUMMARY AND CONCLUSION

We have shown that the germination of maize seedlings is affected by the MWCNT in a concentration dependent manner: lower concentrations are beneficial, higher ones prove toxic in what appears to be chemical hormesis. At the concentration of 20 mg/l, the pristine MWCNTs increased the growth indices and the water contents of the morphological parts, most prominently for the root, which was directly in contact with the medium. Higher MWCNT concentrations were less effective possibly because of increased CNT clumping which impacted their potency and/or the toxicity of high MWCNT concentrations. The latter was more marked for the shoot.

The growth and water imbibition rates were found to be higher with the application of the MWCNT (at 20 mg/l). However, for the same water contents the lengths were higher for the MWCNT plants indicating the benefit of the low dose of the MWCNT to the physiology in more ways than only water delivery. The consistently high statistical orderliness of the MWCNT measurements was conjectured to support the prevalent idea of the property of CNTs to act as molecular water channels. The MWCNT's water delivery capabilities may be useful to future strategies of arid-zone agriculture. The 20 mg/l MWCNT was found not to cause departures from the universal allometric scaling law of biology applied to plant water volumes, indicating that as a xenobiotic, the MWCNT does not fundamentally alter the plant's physiology.

The capacity of the MWCNT to affect the nutrient element delivery to the seedlings was investigated via Polarized EDXRF spectrometry. The concentrations of all ionic nutrients were seen to pass through a narrow or broadly defined minimum with respect to the MWCNT concentration. We argue that this behaviour likely points to the action of 2 contrary forces: one the CNT ion-transient-dipole (ITD) interaction that tends to restrain entry of the ion/polar species into the plant and the other the water inflow that facilitates entry. The relatively high

concentrations of most nutrients generally at ~ 20 mg/l of MWCNT tied in with the increase of fresh and dry weights at this MWCNT concentration.

Using pEDXRF spectrometry the interaction of the MWCNT (at 20 mg/l) with the +2 and +3 oxidation states of Fe in relation to the delivery of Fe as nutrient to the seedling in agarose media was investigated. The results indicated that the ITD interaction between the CNT and the Fe ions may have a role in the reduction of the 3+ to the 2+ oxidation state. Ca²⁺ concentrations showed a high inverse correlation with Fe²⁺ suggesting some sort of Ca efflux from the seedling cells with a possible mechanism being cation exchange in the cell wall matrix. The dry weights and % water contents generally followed the Ca elemental concentration trend as would be expected in view of the central role of Ca in metabolism and cell wall properties.

The surface structure near the black-layer of the pericarp-seed coat in the presence/absence of the MWCNT and Fe²⁺/Fe³⁺, was inspected by SEM. The surface topography showed fairly dense pore-like structures for the pure MWCNT treated case. These pores may account for the enhanced water delivery by the MWCNT. The presence of Fe²⁺ and Fe³⁺ ions either without or with the MWCNT showed no such structures. We argue that the adsorption of the Fe ions on the CNT surface may impact its functionality such as its perforation of the seed-coat and its enhancement of germinative growth. The results of the experiment show that the introduction of the Fe and Cl ions depreciated the MWCNT's ability to enhance dry weight and to a lesser extent, deliver water to the whole seedling.

We conclude that pristine MWCNTs at low concentrations benefit the growth of maize seedlings by enhancing water, nutrient transport and biomass but that their potency could be diminished by high concentrations of ions/polar species in the medium. These findings suggest a potential for the utilization of CNTs for optimizing water transport in arid-zone agriculture and of improving crop biomass yields.

3.6 REFERENCES

1. J. Panyam, V. Labhatsevar, *Biodegradable nanoparticles for gene and drug delivery to cells and tissue*, *Advanced Drug Delivery Reviews*, 55, 329-47 (2003).
2. A. Merkoçi (ed.), *Biosensing using nano materials*, Wiley, 2009. DOI: 10.1002/9780470447734

3. A. Tiwari and A. Tiwari (eds.), *Nano materials in drug delivery, imaging and tissue engineering*, Wiley-Scrivener (2013). ISBN: 978-1-1182-9032-3
4. B.W. Lee, R. Schubert, Y.K. Cheung, F. Zannier, Q. Wei, D. Sacchi, S.K. Sia, *Strongly binding cell-adhesive polypeptides of programmable valencies*, *Angewandte Chemie*, 49, 1971-75 (2010)
5. S. Iijima, *Helical micro-tubules of graphitic carbon*, *Nature*, 354, 56-58 (1991)
6. M. S. Dresselhaus, G. Dresselhaus, A. Jorio, *Unusual properties and structure of carbon nano tubes*, *Annual Review of Materials Research*, 34, 247-78 (2004).
7. K. Donaldson, R. Aitken, L. Tran, V. Stone, R. Duffin, J. Forrest, A. Alexander, *Carbon Nanotubes: A Review of Their Properties in Relation to Pulmonary Toxicology and Workplace Safety*, *Toxicological Sciences*, 92, 5-22 (2006).
8. V. Martinelli, G. Cellot, F.M. Toma, C.S. Long, J.H. Caldwell, L. Zentilin, M. Giacca, A. Turco, M. Prato, L. Ballerini, L. Mestroni, *Carbon nanotubes promote growth and spontaneous electrical activity in cultured cardiac myocytes*, *ACS Nano Letters*, 12, 1831-38 (2012).
9. C. Srinivasan, R. Saraswathi, *Nanoagriculture – carbon nanotubes enhance tomato seed germination and plant growth*, *Current Science*, 99, 274-5 (2010).
10. Q. Liu, B. Chen, Q. Wang, X. Shi, Z. Xiao, J. Lin, X. Fang, *Carbon nanotubes as molecular transporters for walled plant cells*, *Nano Letters*, 9, 1007-10 (2009).
11. M.F. Serag, N. Kaji, M. Tokeshi, Y. Baba, *Introducing carbon nanotubes into living walled plant cells through cellulase-induced nanoholes*, *RSC Advances*. 2, 398-400 (2012).
12. M. Khodakovskaya, E. Dervishi, M. Mahmood, Y. Xu, Z. Li, F. Watanabe, A.S. Biris, *Carbon nanotubes are able to penetrate plant seed coat and dramatically affect seed germination and plant growth*, *ACS Nano* 3, 3221-27, (2009). {Article retracted, *ACS Nano*, 6, 7541 (2012) }
13. H. Villagarcia, E. Dervishi, K. de Silva, A.S. Biris, M.V. Khodakovskaya, *Surface chemistry of carbon nanotubes impacts the growth and expression of water channel protein in tomato plants*, *Small*, 8, 2328-34 (2012)

14. A. Mondal, R. Basu, S. Das, P. Nandy, *Beneficial role of carbon nanotubes on mustard plant growth: an agricultural prospect*, Journal of Nanoparticle Research, 13, 4519-28 (2011).
15. S. Tripathi, S.K. Sonkar, S. Sarkar. *Growth stimulation of gram (Cicer arietinum) plant by water soluble carbon nanotubes*, Nanoscale, 3, 1176 (2011).
16. P. Begum, R. Ikhtiari, B. Fugetsu, M. Matsuoka, T. Akasaka, F. Watari, *Phytotoxicity of multi-walled carbon nanotubes assessed by selected plant species in the seedling stage*, Applied Surface Science, 262, 120-4 (2012).
17. D. Lin, B. Xing, *Phytotoxicity of nanoparticles: Inhibition of seed germination and root growth*, Environmental Pollution, 150, 243-50 (2007).
18. X. Wang, H. Han, X. Liu, X. Gu, K. Chen, D. Lu, *Multi-walled carbon nanotubes can enhance root elongation of wheat (Triticum aestivum) plants*, Journal of Nanoparticle Research, 14, 841-51 (2012).
19. L. Vaisman, H. Daniel Wagner, G. Marom, *The role of surfactants in dispersion of carbon nanotubes*, Advances in Colloid and Interface Science, 128-130, 37-46 (2006).
20. U.S. Environmental Protection Agency (USEPA), 1996, *Ecological effects test guidelines (OPPTS 850.4200): Seed germination/root elongation toxicity test*, Available from: http://www.epa.gov/opptsfrs/publications/OPPTS_Harmonized/850_Ecological_Effects_Test_Guidelines/Drafts/850-4200.pdf
21. M. B. MacDonald, *Physiology of seed germination* (2007).
http://seedbiology.osu.edu/HCS631_files/4A%20Seed%20germination.pdf;
http://seedbiology.osu.edu/HCS631_files/4B%20Seed%20germination.pdf; Private communication, February 2013.
22. Z. I. Miskovic, *Interactions of ions with carbon nano-structures*, Journal of Physics: Conference Series 133, 012011 (2008). doi:10.1088/1742-6596/133/1/012011.
23. A.I. Frolov, K. Kirchner, T. Kirchner, M.V. Fedorov, *Molecular-scale insights into the mechanisms of ionic liquids' interactions with carbon nanotubes*, Faraday Discussions. 154, 235-47 (2012).
24. Difco™ and BBL™ manual, 2nd Ed;
http://www.bd.com/europe/regulatory/Assets/IFU/Difco_BBL/281230.pdf.

25. P.S. Brateman, A. Graham Cairns-Smith, R.W. Sloper, T. George Truscott, M. Craw, *Photo-oxidation of Fe(II) in water between pH 7.5-4.0*, Journal of the Chemical Society, Dalton Transactions, 7, 1441-45 (1984)
26. J. Heckel, M. Haschke, M. Brumme, R. Schindler, *Principles and applications of energy dispersive x-ray fluorescence analysis with polarized radiation*, Journal of Analytical Atomic Spectrometry. 7, 281-86 (1992).
27. C. J. Alvarado, W.A. Abuhani, T. Whelan, O.S. Castillo, S. Landsberger, L.M. Villaseñor, S.E. Borjas, S.L. Bribiesca, S.A. Alexander, N. Dasgupta-Schubert, *Comparative analysis of the lead and copper concentrations of metal accumulating plants with or without mycorrhizae*, Communications in Soil Science and Plant Analysis (*in press*).
28. (a) *OriginLab Data analysis and graphing software*, OriginLab Corp, Northampton, MA, USA <http://www.originlab.com/>; *SigmaPlot Statistical data analysis software*, SysStat Software Inc., San Jose, CA, USA; <http://www.sigmaplot.com/products/sigmaplot/sigmaplot-details.php>
29. *Spectro Analytical Laboratory*
http://www.spectro.com/pages/e/p0105yt001_TurboQuant_Video.htm
30. L. Taiz , E. Zeiger, *Plant Physiology, 4th Edition*, Sinauer Associates Inc. Publishers, Sunderland, MA, USA (2006)
31. (a) G.B. West, J.H. Brown, *The origin of allometric scaling laws in biology from genomes to ecosystems: towards a quantitative unifying theory of biological structure and organization*, The Journal of Experimental Biology, 208, 1575-92 (2005). (b) B.J. Enquist, *Universal scaling in tree and vascular plant allometry: toward a general quantitative theory linking plant form and function from cells to ecosystems*, Tree Physiology, 22, 1045-64 (2002).
32. M.B. McDonald, J. Sullivan, M.J. Lauer, *The pathway of water uptake in maize seeds*, *Seed Science and Technology*, 22. 79-90 (1994)
33. C. Lin, Y. Su, M. Takahiro, B. Fugetsu, *Multiwalled carbon nanotubes induce oxidative stress and vacuolar structure changes to Arabidopsis T87 suspension cells*, Nano Biomedicine, 2, 170-181 (2010).
34. E.J. Calabrese, L.A. Baldwin, *Chemical hormesis: its historical foundations as a biological hypothesis*, Human and Experimental Toxicology, 19, 2-31 (2000).

35. A. Alexiadis, S. Kassinos, *Molecular Simulation of water in carbon nanotubes*, Chemical Reviews, 108, 5014-34 (2008).
36. T. A. Beu, *Molecular dynamics simulations of ion transport through carbon nanotubes. III. Influence of the nanotube radius, solute concentration and applied electric fields on the transport properties*, The Journal of Chemical Physics. 135, 044516 (2011).
37. A. Manara, *Plants and Heavy Metals*. A. Furini (ed.), Springer Briefs in Biometals, Springer (2012).

CHAPTER 4
STUDY OF CULTURE MEDIUM AND PURITY OF CARBON
NANOTUBES IN PLANT GROWTH

CAPÍTULO 4
ESTUDIO DEL MEDIO DE CULTIVO Y PUREZA DE
NANOTUBOS DE CARBONO EN EL CRECIMIENTO DE
PLANTAS

ABSTRACT CHAPTER 4

Carbon Nanotubes (CNTs) among all nanomaterials have attracted a major interest because of their mechanical, electrical and chemical properties. Most studies of CNTs in bioscience have focused on their influences in animal and human cells. Relatively scant attention has focused on the effect of CNTs in the development of agriculture; plant growth and their influences with plant cells.

This study shows the effect of multi-walled carbon nanotubes (MWCNTs) in maize growth and their interaction with nutritive elements. MWCNTs were used as a substrate mixed in agar nutritive medium with a purity of 95% and 99%. The experiments were carried out for samples containing MWCNTs of; 0, 10, 20, 40 and 60 mg/l concentration for one week seedling. The use of MWCNT were showed higher rate of growth in comparison to the medium containing no MWCNT. The percentage element concentrations were measured by pEDXRF analytical techniques. The samples assisted with MWCNT have variation in the percentage elemental concentration than those without MWCNT. Morphological study of the samples germinated with MWCNT assisted media were analysed by SEM technique. Raman spectroscopy technique has been used to analyse the presence of metal ions and carbon nanotube in treated samples.

Keywords: Nano-biomaterial, Concentration, Elements, Germination, Nanoagriculture, pEDXRF, SEM.

RESUMEN CAPÍTULO 4

Los nanotubos de carbono (CNT) de entre todos los nanomateriales han atraído un gran interés debido a sus propiedades mecánicas, eléctricas y químicas. La mayoría de los estudios de CNT en la biociencia se han centrado en sus influencias en las células humanas y animales. Relativamente poca atención se ha centrado en estudiar el efecto de los nanotubos de carbono en el desarrollo de la agricultura; crecimiento de plantas y su influencia con células de planta.

Este estudio muestra el efecto de los nanotubos de carbono de pared múltiple (MWCNT) en el crecimiento del maíz y su interacción con elementos nutritivos. Los MWCNTs que se utilizaron como sustrato mezclado con un medio de cultivo compuesto de agar nutritivo cuentan con una pureza de 95% y 99%. Los experimentos se llevaron a cabo para muestras que contienen una concentración de MWCNTs de 0, 10, 20, 40 y 60 mg / l y un periodo de crecimiento de las plantas de una semana. El uso de MWCNT para el crecimiento de plantas, mostró una tasa de crecimiento mayor que aquellas plantas que crecieron en un medio de cultivo sin MWCNT. Las concentraciones porcentuales de elementos fueron medidas por técnicas analíticas como pEDXRF. Las muestras que contienen MWCNT tienen variación en la concentración porcentual elemental que aquellas sin MWCNT. Un estudio morfológico de las muestras germinadas en medios de cultivo con MWCNT se realizó mediante la técnica SEM. Técnica de espectroscopia Raman se ha utilizado para analizar la presencia de iones metálicos y de nanotubos de carbono en las muestras tratadas.

Palabras Clave: Nano-biomaterial, Concentración, Elementos, Germinación, Nanoagricultura, pEDXRF, SEM.

CHAPTER 4

Study of Culture Medium and Purity of Carbon Nanotubes in Plant Growth

4.1 INTRODUCTION

Carbon nanotubes are molecular-scale tubes of graphitic carbon with outstanding properties. They are among the stiffest and strongest fibers known, and have remarkable electromechanical properties and many other unique characteristics. For these reasons they are widely popular in scientific research circles and have attracted huge academic and industrial interests. One important advantage of carbon nanotube is that they can easily penetrate membranes such as cell walls (Srinivasulu Morla et al., 2011). The carbon nanotubes are usually quite short, and tend to form clusters. The nanotubes are long-narrow shape, quite short, and tend to form clusters, so it makes sense that they can function like a needle at the cellular level (Sandeep Agnihotri et al., 2002; Atanu Bhattacharyya et al., 2010). Another interesting advantage of CNT is that their electrical resistance changes significantly when other molecules attach themselves to the carbon atoms (Riyaz Ahmad Dar, 2011; Chiu-wing Lam et al., 2006). These studies are using a variety of different biological matter including glucose, hydroxyapatite, porous silicon and even vegetables such as chickpea and tomato plants (Shadin Ishag et al., 2009; Hector Villagarcia et al., 2012).

The study on the effects of nanoparticles in plant science is a newly emerging area of research. At present, many different studies are being performed all over the world (Mariya Khodakovskaya et al.; 2009; Khodakovskaya et al., 2012; Allah Ditta, 2012; X. Wang et al., 2012; E.A. Smirnova et al., 2012; Zheng L et al., 2005; Hediat M. H. Salama, 2012) to deduce the use of nanotubes in the production of agriculture; such as chickpea and tomato plants, which involves the employment of nanoparticles with the ambition of beneficial effects to the crops. Compared to plant cell walls and membranes, the penetration of nanoparticles into seeds is expected to be difficult due to the significantly thick seed coat covering the whole seed (Srinivasulu Morla et al., 2011; D. K. Tiwari et al., 2013). In spite of this prospective

obstruction Hector Villagarcia et al., 2012 demonstrated that CNTs could effectively penetrate seed coat thereby influencing the seed germination and plant growth. These studies commendably established that exposure of seeds to CNTs results the enhanced germination and growth rate with an exception of the toxic possibility that come through carbon nanotubes. Remembering all this steps of purity and functionalization we worked using standard MWCNT (Sigma Aldrich) to standardize the purity and their specific concentration necessary for plant germination. In our experiments we are focused on the two principles facts; (a) Role of MWCNT (99% pure) concentration in different gel medium (agarose and bacteriological agar {BA}) and (b) Purity of MWCNT (95 and 99%) in agarose medium. These two factors are the most important issues because agarose medium is nutrient free while BA agar contains sufficient nutrient for preliminary days of germination (until 15 days) without any additional nutrients (MS basal medium). This study shows the clear information about kinetics of plant growth, water uptake, nutrient transport and its variability with purity concentration of MWCNT mixed in BA and agarose substrate medium.

4.2 EXPERIMENTAL

4.2.1 Materials

MWCNTs were purchased from Sigma-Aldrich® (St. Louis, MO, USA), purity >95 % (OD 6-9 nm, L 5 µm) and 99% (OD 6-13 nm, L 2.5-2 µm). Bacteriological agar (BA) (Bioxon®) was purchased from Becton-Dickinson (BD de Mexico, Mexico City, Mexico) and Agarose from Sigma-Aldrich® (A9539). BA contains a certain level of mineral nutrients as ionic or polar species (T. A. Beu, 2011) but their levels in agarose are negligible. Maize (sweet corn) seeds were purchased from a local seed supply company (Hortaflo, Rancho Los Molinos SA de CV, Mexico).

4.2.2 Medium Composition and Germination

The first experimental set consisted of maize seedlings grown in agarose and BA gel medium spiked with different concentrations of MWCNT of purity 99%. The agarose and BA powder were weighed and mixed with de-ionised (DI) water to obtain a concentration of 8 g/l and 15 g/l respectively. The agarose and BA were dissolved by heating the aqueous mixture at ~95°C with constant magnetic stirring about 2.5 hours. Upon complete dissolution, different

aliquot volumes of the clear agarose solution were measured out. Appropriate masses of MWCNT were weighed out and mixed with aliquot volumes of the sterile agarose and BA solution by mechanical stirring for ~10 minutes in order to yield unvaried distributions of MWCNT in the gel of the different concentrations listed in Table 4.1. The agarose and BA solutions containing the different concentrations of the MWCNT were then poured into replicate sterile petridishes to set as the gel substrate for seed growth.

Table 4.1: Sample description of MWCNT assisted Samples in Agarose and BA Medium.

Sample name	Medium	MWCNT Concentration (mg/l)
A-0	Agarose	0
A-10		10
A-20		20
A-40		40
A-60		60
BA-0		Bacteriological Agar
BA-10	10	
BA-20	20	
BA-40	40	
BA-60	60	

Maize seeds were first surface sterilized using 70% ethanol for 2 minutes, washed with DI water and then 1% v/v solution of sodium hypochlorite for 10 minutes on magnetic stirrer after that washed several times with DI water. The seeds were implanted into the set gel substrates and petridishes were kept for germination in dark for 7 days at ambient condition (Temperature ~ 24°C & Relative humidity (RH) ~ 55%). The total number of seedlings in this set was 360 listed in table 4.1. In another experiment the material preparation and germination protocol was same as earlier except the mediums used were agarose (8 g/l) with control (only pure agarose) and the MWCNT concentration (20 mg/l) of purity 95% and 99% (Table 4.2). The progresses of seedling development were continued for 7 days with same number of seedlings and ambient condition as previous.

Table 4.2: Sample description of MWCNT concentration of 20 mg/l with purity of 95 and 99 %.

Sample name	Additives description
Control	---
MWCNT-95	MWCNT (95 % purity) of 20 mg/l concentration
MWCNT-99	MWCNT (99 % purity) of 20 mg/l concentration

Upon harvesting, the seedlings were gently rinsed with DI water, blotted dry with paper towels and their fresh weight (FW), root length (RL) and shoot length (SL) were measured. Then roots and shoots were cut and the FWs of these parts as well as of the seed body were measured. The seed body, root and shoot parts were dried at 60°C for 72h and dry weights (DWs) of these parts were measured too. A few seed bodies from the first experimental set were analysed by Scanning Electron Microscopy (SEM).

4.2.3 Analysis of Relative Element Concentration using Polarized Energy Dispersive X-Ray Fluorescence (pEDXRF) Technique

The operating principle of pEDXRF is based on the cancellation of the Bremsstrahlung background by the double polarisation of the initial x-ray beam. The samples of masses lower than recommended masses can be analysed for relative elemental concentrations with sufficient accuracy. The detectable elemental by pEDXRF is ranging from Na to U and the advantage of this technique is of its non-destructive, multi-elemental and rapid tracing capability.

Dry plant parts together ball milled (model MM-400, Retsch GmbH, Germany) at 25 Hz for 2 minute until all mass appeared as a homogeneous microsize powder. The elemental analysis of the powders was carried out by the pEDXRF spectrometer SpectroXepos III (Spectro Analytical Instruments GmbH, Kleve, Germany) using the TurboQuant™ analytical routine. The elements concentrations with and without MWCNT were calculated for agarose and BA medium germinated plants. The relative elemental concentration was calculated for MWCNT with respect to their control (pure medium).

4.2.4 Morphological Measurements and Microscopy

The scanning electron microscopy (SEM) analysis was performed for the surface morphology of the seed body part (seed-coat) near the hilum and micropyle (where the root and shoot separate). The seed coat is thinnest in this region and makes the water and MWCNT permeation easily. The SEM of seed body was analysed using field emission SEM (JSM 7401F, JEOL Ltd. Tokyo, Japan) at 15 kV by copper coated vacuum deposition with a working distance of 28-31 mm, magnification of 200 and 100 μm scale.

4.2.5 Data Analysis

Averages and standard errors were computed over 3-6 sets of replicates with each set contains average of 5 seedlings listed in the Table 4.1 and 4.2. The data reduction and statistical analyses were carried out at 95% confidence level using software's GraphPad Prism (v-5.0 b) and Excel.

4.3 RESULTS

4.3.1 Role of Culture Medium with the Presence of MWCNT

Figure 4.1a-c shows the role of MWCNT for various parameters to maize plant germination in agarose and BA medium for fixed germination of 7 days. In figure 4.1a the variation of root and shoot length with respect to respective water content. The % water calculation is done on FW basis as: $\left(\frac{FW-DW}{FW}\right) \times 100$ and we can see that there is higher uptake of water permeation upon the introduction of MWCNT at certain concentration in agarose and BA medium.

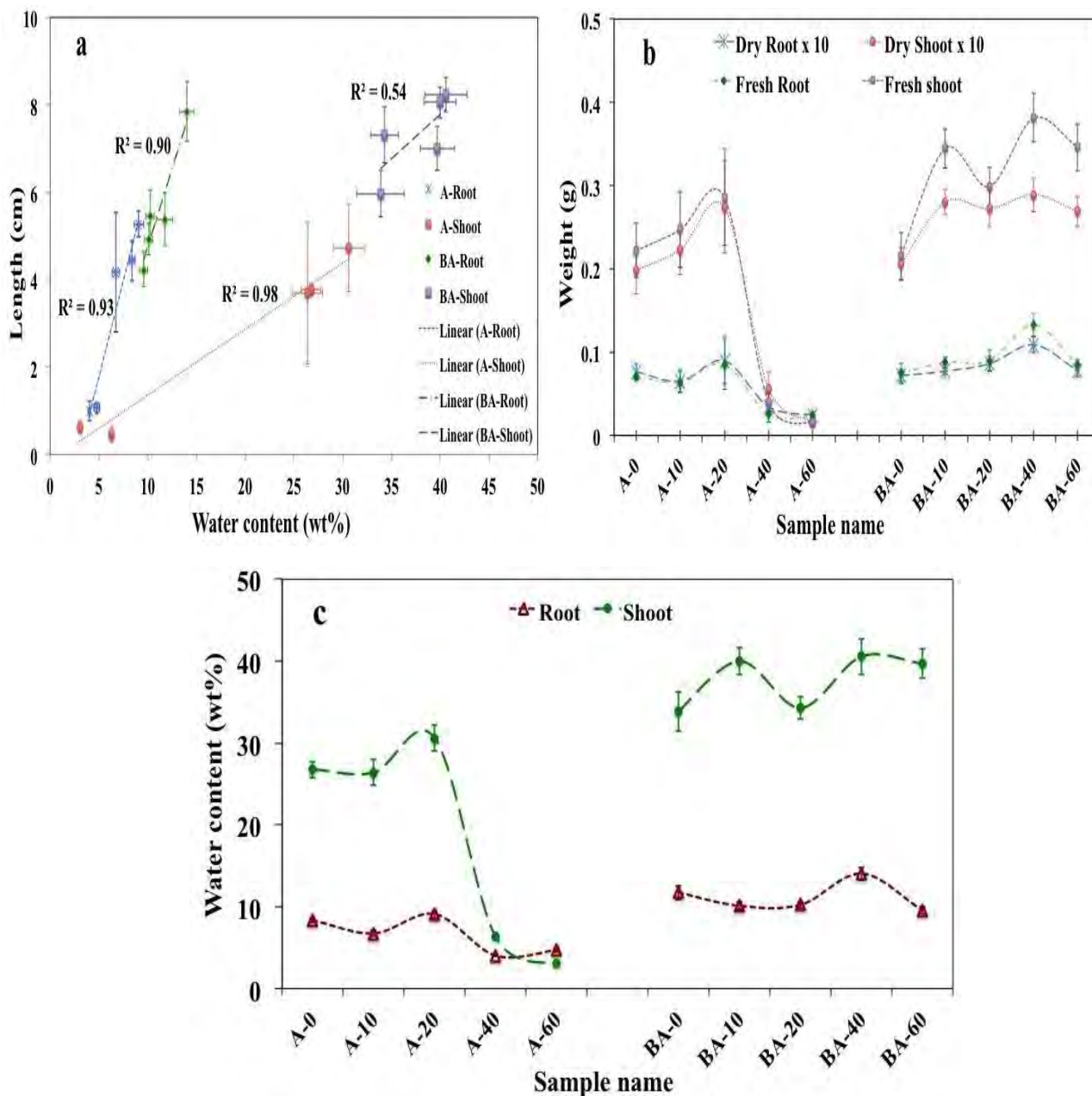


Figure 4.1: MWCNT concentration to plant germination in agarose and BA medium. (a) Length variation with respect to % water content. (b) Fresh and dry weight measurement for BA and Agarose germinated medium in presence of MWCNT. (c) Water availability in roots and shoots of 2 different germinated media system.

4.3.2 Relative Element Concentration

Figure 4.2 shows the relative concentration of elements in germinated seeds, treated in BA and agarose medium. Since agarose contains very less concentration of nutritive elements

and BA has sufficient nutrients and the germinated plants have elemental concentration varying with the additive medium and concentration of the MWCNT. In case of agar the maximum concentration is about MWCNT of 20 mg/l, which is also the same concentration of better germinated medium while in BA some elements have higher concentration at MWCNT of 10 mg/l and some are at 40 mg/l concentration and others are decreasing with the concentration of MWCNT.

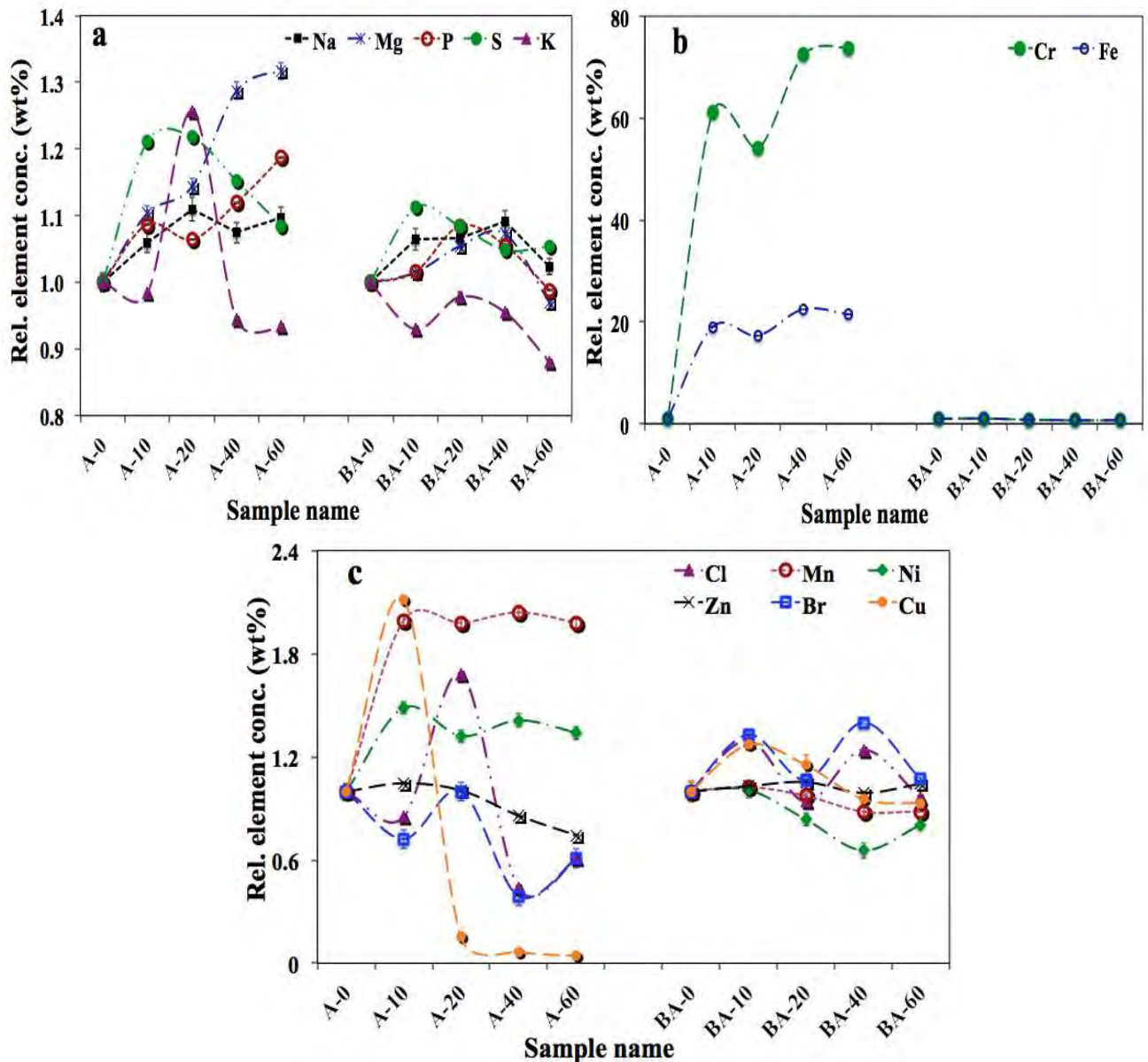


Figure 4.2: Relative concentration of present elements and incremental transport of selected elements with and without MWCNT.

4.3.3 Comparative Study with Purity of MWCNT

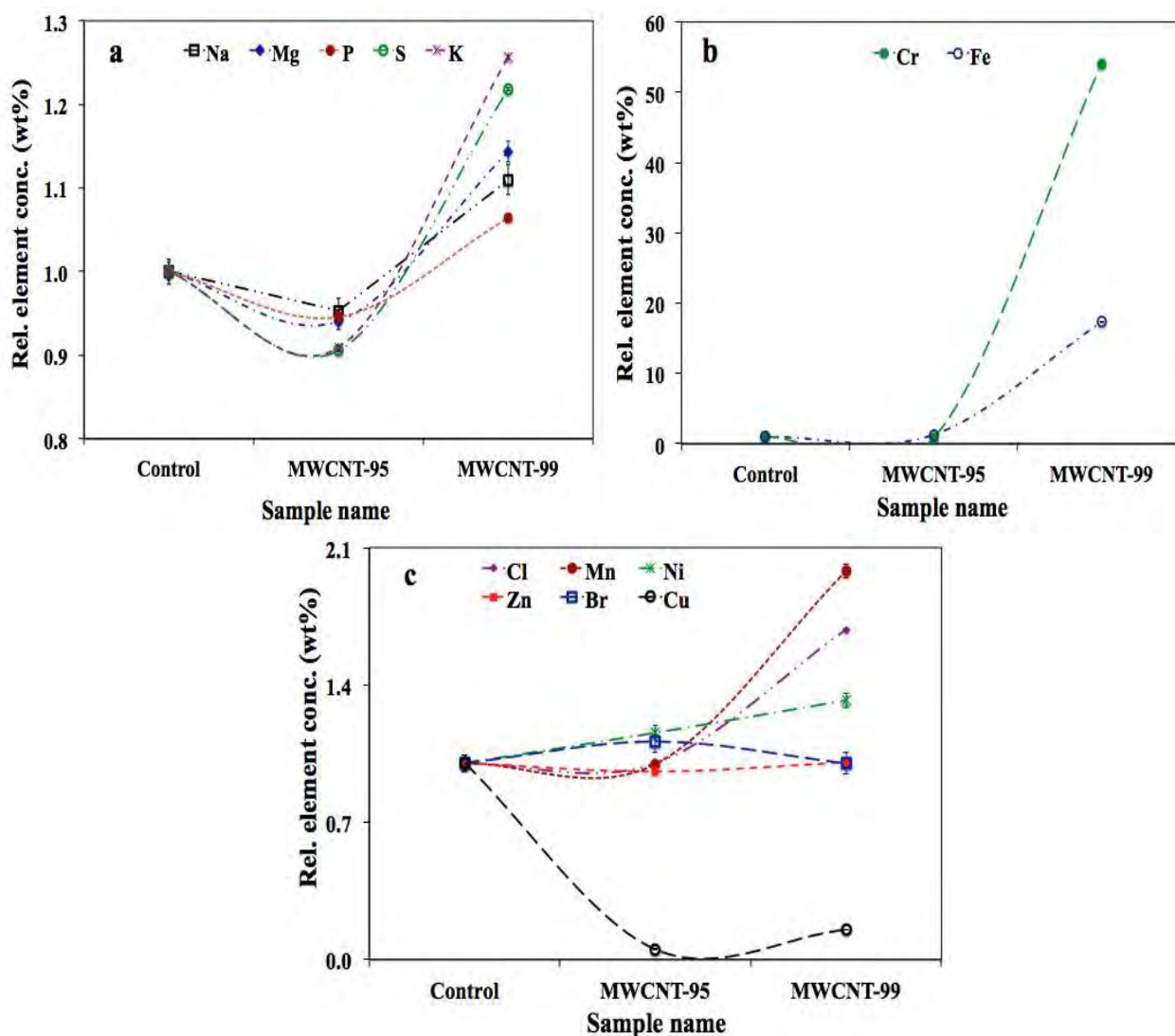


Figure 4.3: comparative study of elemental transport with MWCNT purity in agarose medium germinated plants.

Figure 4.3 shows the maize plant germinated in agarose medium with different purity of MWCNT concentration at 20 mg/l. The pEDXRF analysis shows that using high pure MWCNT (99%) the transport of elements in germinated plants have much higher % concentration comparatively with control (without MWCNT) and MWCNT of 95% purity. only in case of Cu, Zn and Br the convention is relatively low or equal to control and MWCNT of 95%. This clearly explains that the MWCNT of 99% purity transports the nutritive more effectively than of control and MWCNT of 95% purity.

4.3.4 Morphology of MWCNT Assisted Germination

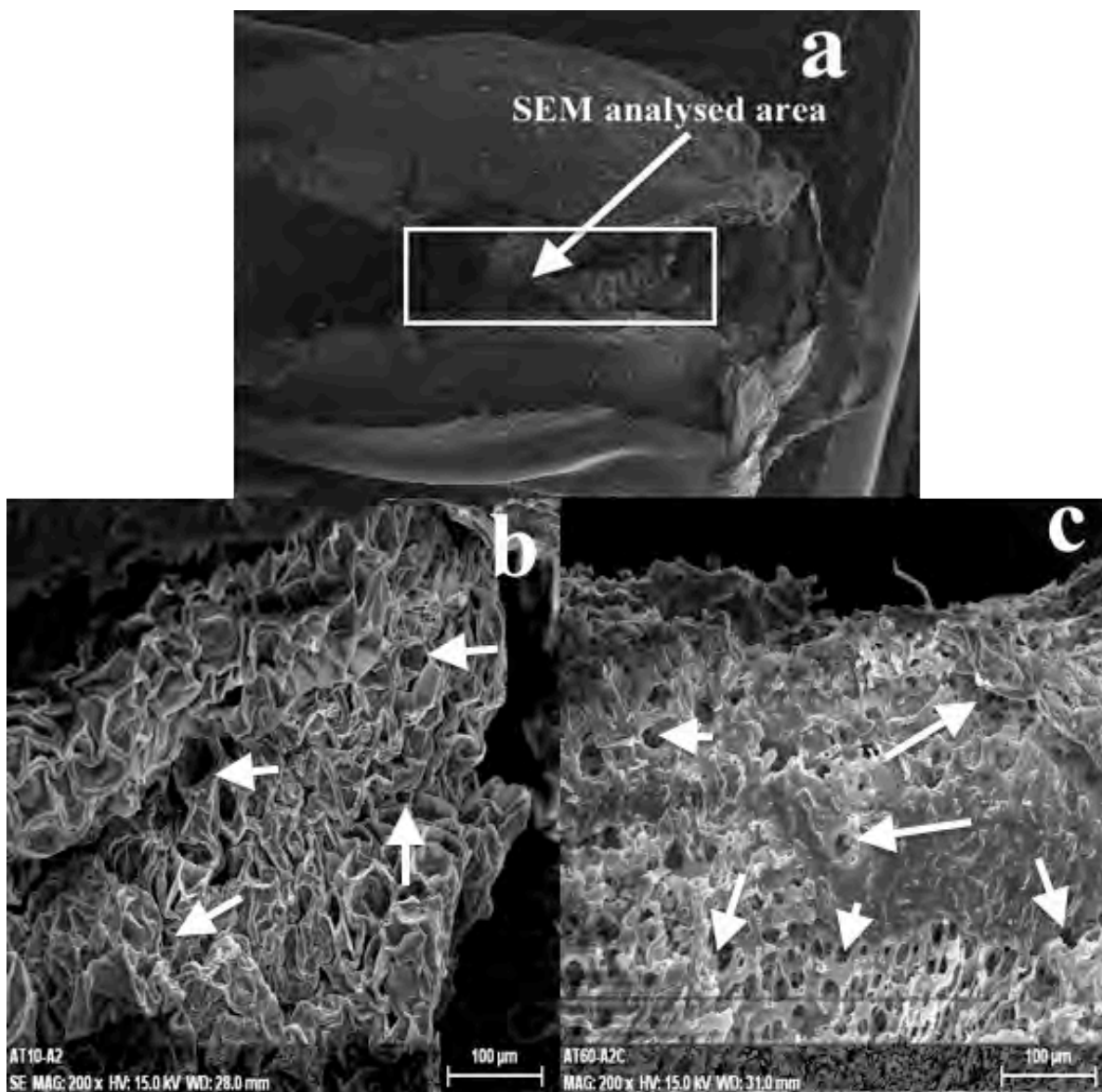


Figure 4.4: SEM image of MWCNT treated seed bodies. (a) Analyzed area. (b) Presence of MWCNT 10 mg/l concentration. (c) Presence of MWCNT 60 mg/l concentration.

The SEM images of the MWCNT assisted plant germination in agarose gel medium were shown in figure 4.4. The importance of this is how the high pure MWCNT concentration affects the surface morphology of the seeds during germination. Figure 4.4a indicates the

imaging area used for SEM and figure 4.4b and 4.4c shows the morphology of the surface treated with MWCNT concentration of 10 and 60 mg/l.

4.3.5 Raman Analysis of Powder Samples of Plants

The Raman analysis of plant and MWCNT samples has been carried out using two wavelengths, 514.5 nm (green laser) and 488 nm (blue laser) and the results are shown in figure 4.5 and 4.6.

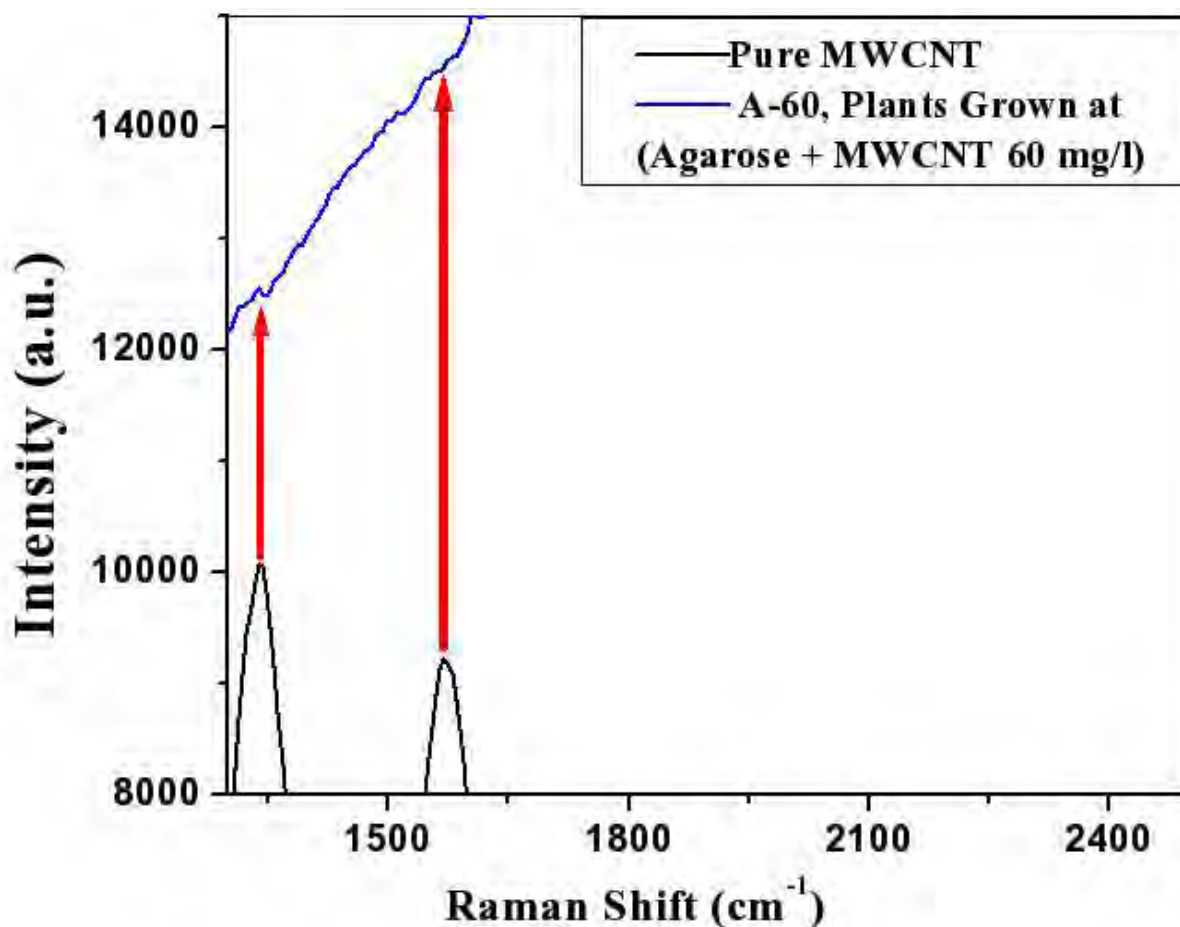


Figure 4.5: Raman analysis of pure MWCNT (95 %) and powder sample of plant germinated in agarose culture medium containing 60mg/l concentration of MWCNT. Raman measurement has been taken using 514.5 nm (green) laser of counts for 0.1 second.

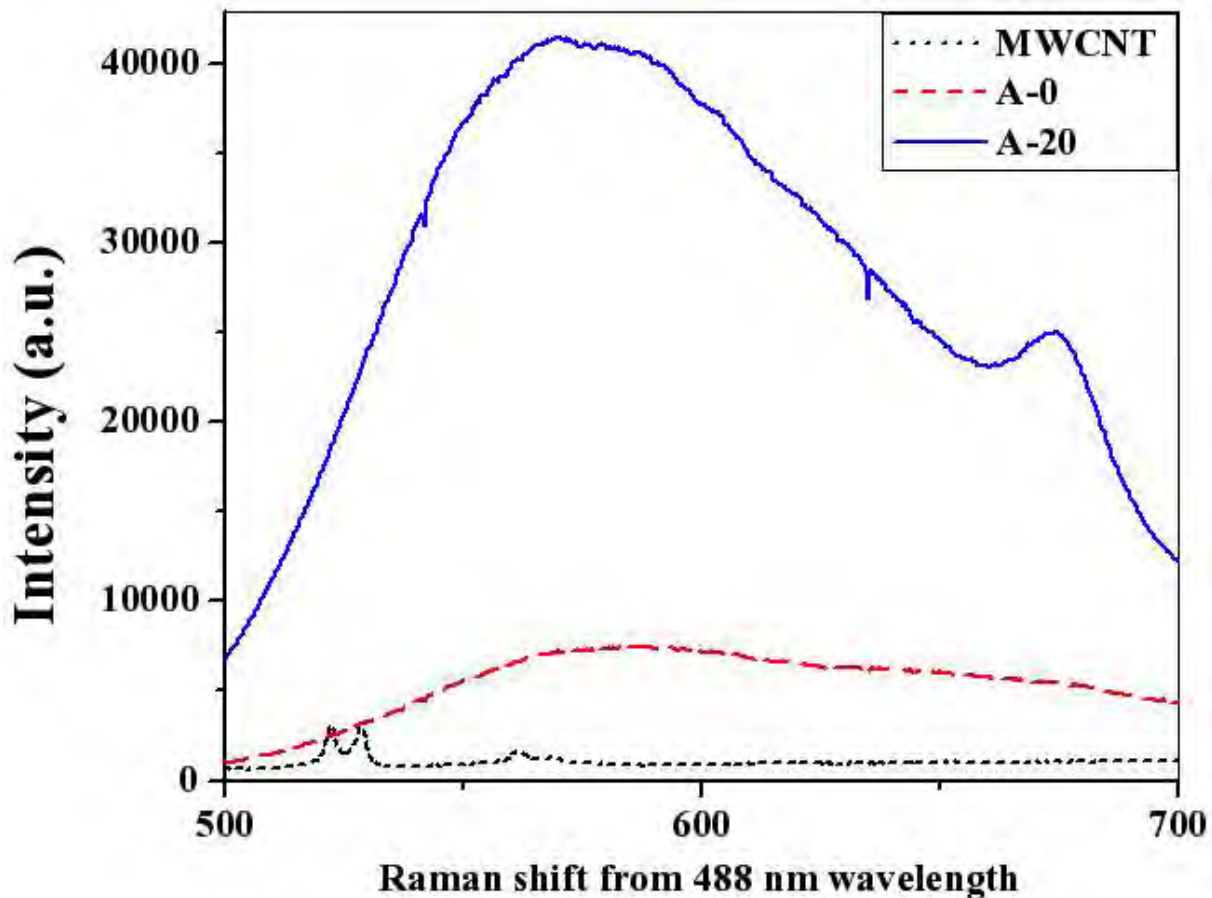


Figure 4.6: Luminescence analysis of MWCNT 95 % pure (Black line), powder sample of control medium germinated plants (Red line) [Table 4.1, A-0] and powder sample of MWCNT, 20 mg/l concentration assisted plants (Blue line) [Table 4.1, A-20].

4.4 DISCUSSION

4.4.1 Weight, Length, and Water Content Statistics

The experiments performed with two different gel mediums (agarose and BA) and the concentration of MWCNT chosen. In our study the germination performed specially on two basis; first the role of the medium with and without presence of nutrients and second the role of MWCNT concentration beneficial for plant germination in two mediums. Literally agarose is nutrient free while BA contains sufficient nutrients necessary for plants during initial days germination (Difco™ and BBL™ manual, 2nd Ed). MWCNT of selected concentrations were spiked with agarose and BA medium without any external addition of nutrient medium. Figure 1a shows that the RLs increased markedly with root %water; for the SLs the increase with

shoot %water (BA medium) were more “noisy”. The root and shoot length with respect to %water content for agarose and BA ($R^2 \geq 0.90$, $p < 0.05$) except BA shoot. The noisier increase ($R^2 = 0.54$, $p < 0.05$) of shoot length with water content (BA shoot) may be a consequence of two factors. Water absorption increases the cell rigidity pressure that triggers cell elongation and the production of hormones (e.g. gibberellic acid (GA) and auxin) that promote root growth (Shadin Ishag et al., 2009). Water uptake by the shoot is indirect and dependent on the upward water transport by the root (Allah Ditta, 2012). The latter would be affected by the MWCNT concentration. Additionally, other independent factors such as light intensity are also involved in shoot growth. The MWCNT increased the water content of the shoots for BA in comparison to control system while for agarose with very high concentration of MWCNT the water % decreases, its because of the toxic nature and dipolar activity (Chiu-wing Lam et al., 2006) of MWCNT (figure 4.1c). The %water in shoot spurt in the at the MWCNT of 20 mg/l for agarose, while for the BA medium the water content decreased gradually at 20 mg/l while for other concentrations, it is higher than the respective control. From the figure 4.1b it is clearly visible that for the agarose medium there is sudden increase in fresh and dry shoot weight (until MWCNT 20 mg/l concentration while for higher concentration there is big decrease in growth) compared to pure medium (without MWCNT) while for the BA medium the increment in fresh and dry shoot weight is much higher than the agarose. The DW of plant indicating the growth and vigour, maximum dry weight accumulation shows the maximum growth as well as vigour comparison to other. The rise in imbibed water brings in more mineral nutrients from the medium and also signals enhanced enzyme and hormone activity (G.B. West & J.H. Brown, 2005), factors that are expected to benefit tissue development. This consequence of the water absorption is seen in the rise of the relative concentrations of most mineral nutrients (figure 4.2) and in the DWs (figures 4.1b) where a maximum is reached at MWCNT of 20 mg/l concentration (agarose). These factors may impact the metabolic activity adversely resulting in a decline of the root and shoot DW with increased MWCNT concentration. Thus the benefits of the MWCNT of purity 99% are observed for the lower end of the concentration range (≤ 20 mg/l) for agarose while for BA the interacts differently. Toxicity effects diminish the usefulness of the MWCNT to the plant at higher concentrations. The effect of the MWCNT on plant health therefore appears to be one

of chemical hormesis, a phenomenon that has been observed for normally toxic substances in areas such as toxicology and homeopathy (Chiu-wing Lam et al., 2006; D. K. Tiwari et al.). The seed body and root are directly in contact with the gel medium. The higher water permeation upon introduction of low MWCNT due to the aforesaid pores is likely the cause for the higher uptake of water implicit in the figures 4.1a and 4.1c. Higher MWCNT concentration would be logically expected to increase the penetrability. Furthermore, at the higher MWCNT in the medium, the nanotubes would aggregate more (particularly in the absence of induced exfoliation) resulting in the diminution of functionality such as their capacity to increase water delivery to the parts in contact with the medium. These factors may account for the scant variation of the %water at the MWCNT \geq 40 mg/l in agarose medium. The shoots are not immersed in the medium so water enters the shoot as for all plants by capillary action driven by the root water pressure. Aggregation of the MWCNT in the extracellular or intracellular spaces within the root, that is likely to scale with the MWCNT concentrations would impede this normal upward flow and affect the physiology of shoot water transport at the higher MWCNT. Oxidative damage at higher MWCNT concentrations consequent to the penetration of the plasma membrane of the seedling cells by the CNT (Khodakovskaya et al., 2012) may also play a role in the reduction of the water content and FW of the shoot (figure 4.1c) at higher concentration of MWCNT. The combination of the facilitation of water entry at low MWCNT concentration but its ‘obstruction’ at higher MWCNT concentration makes the trace of the shoot water content pass through a broad maximum at MWCNT concentration of \sim 20 mg/l.

4.4.2 Relative Elemental concentrations

The elements concentration of samples [table 4.1 and 4.2] were analysed using pEDXRF for total seedlings (root, shoot and seed-body). The relative elemental concentrations of samples (MWCNT $\{\geq 99\%$ } assisted in agarose and BA medium) were calculated with respect to their respective controls. The tissue concentrations of the macro and micro mineral nutrient elements of the 3rd and 4th periods of the periodic table were shown for MWCNT with respect to elements respective concentration of control medium (Figure 4.2 and 4.3). With the exception of Cl, K, Ca and Fe, there is no statistically significant difference between the Control and the lower concentration of MWCNT for BA agar. In the cases of Cr and Fe

(Figure 4.3b) shows a drastic change with MWCNT for agarose medium approx 60-80 times for Cr and 20 times for Fe, while for BA the relative concentration is constant (Aditi Singh et al., 2008; Z. I. Miskovic, 2008; T. A. Beu, 2011).

Agarose Medium: In case of Agarose medium the relative elemental concentration increases with respect to control except the K, Cl, Br, Cu and Zn; that mean the with the introduction of MWCNT in gel medium the transport of elements is more precise. In case of Cl and Br have the same trend with the presence of MWCNT, which shows the slight decrease with MWCNT concentration of 10 mg/l but at 20 it have an increase and then again decrease it might be because of the impurity of the medium which may consist some dipolar effect with the MWCNT or can be the absolute error of the instrumental observation of micro nutritive elements. Cu concentration increases with MWCNT of Conc. 10 mg/l after that decrease with the higher concentration and remains constant.

For the maximally electro-positive and negative ions in the medium (K^+ and Cl^-) the introduction of the different [MWCNT] only serves to decrease their concentrations up till a broad minimum after which the concentrations flatten out (figure 4.3b). The ion-transient dipole interaction is likely to dominate over water inflow for these highly electro-active ions restricting their ingress into the seedling. A saturation is seen at $MWCNT \geq 20$ mg/l possibly because of increased MWCNT aggregation that reduces the surface area despite the increase of [MWCNT]. For other ions except Fe and Ca, the attractive force appears to dominate up till ~ 10 mg/l of MWCNT. At $[MWCNT] \geq 20$ mg/l the increased water inflow (figure 4.1a) dominates, increases the elemental concentrations, which then level off as a consequence of the plateau in the water content (figure 4.1a) and the MWCNT aggregation. In the case of Fe the [MWCNT] of 5 mg/l causes a sharp rise but for $[MWCNT] > 5$ mg/l the interplay between the adsorptive forces, the increase of water inflow and MWCNT aggregation as for the other ions, makes the profile pass through a minimum (20 mg/l) with the subsequent rise and leveling off. The case for Ca is similar except that its high concentration spans a broad plateau up till 20 mg/l and the minimum occurs for the higher [MWCNT] of 40 mg/l. Increased water transport finally prevails (at [MWCNT] 60 mg/l) increasing the Ca concentration but lingering adsorptive effects likely make the value less than at the plateau region. These examples show the specific nature of the ion (polar molecule)-CNT interaction and the role of water flux in the overall ionic transport into the seedling (A.I. Frolov et al., 2012).

BA Medium: From the figure 4.2, when MWCNT introduced in the medium the effect is not so much cleared and shows a noisy effect its because of BA medium which contains all nutrients and the purity can not be clarify so that the transport of elements is not so precise as agarose medium. As the MWCNT is introduced, the tissue K and Cl concentrations fall at 20 mg/l and 60 mg/l of MWCNT respectively. The salts of the mineral macro and micronutrients of the BA in the aqueous gel medium present the elements principally as ions or polar molecules to the plant tissue.

The flow of water into the plant (principally the root) facilitated by the MWCNT as seen in the foregoing, brings in the dissolved ions where the inflow varies as shown in Figure 4.1a. However the MWCNT surfaces in the medium may attach the ions through the ion-transient dipole interactions between charged/polar species and the π -electron clouds in the CNT molecular structure as has been quoted (J. Heckel et al., 1992). The strength of these interactions will vary with the type of ion and CNT, CNT concentration, state of CNT aggregation etc. in a complex way. Hence the profile of the elemental concentrations (figure 4.2) is likely the result of a trade-off between these 2 contrary forces increase by water inflow vs. retention (adsorption) by the medium's MWCNT.

Figure 4.3 shows the pEDXRF elemental analysis of the seedlings of control and MWCNT of purity 95 and 99 % for the same set of macro and micro mineral nutrients in agarose medium. In case of Cu the relative concentration is decreasing with the presence of MWCNT in comparison to control but with MWCNT of 99 % purity there is slight increment than MWCNT 95%. Fe and Cr, tissue concentrations with MWCNT 99% are highly increasing (figure 4.3b). This is because the agarose is nearly completely free of extraneous elements and purity of MWCNT, which transporting the minimum amount of Fe and Cr to the plants because these are so important elements to make plant survive, most probably this nutrients comes in medium through the DI water. Thus none of these elements can be brought in to a significant measure from the external medium and therefore retain their intrinsic concentrations in the seedling for which the type of external medium is inconsequential. Except Cu, Zn and Br, plants germinated by assisting MWCNT of 99 % purity have highest increment in concentrations of all elements. Since Fe and not Cr is present in the agarose Although Fe is frequently used as a catalyst in the manufacture of CNTs. The closeness of the Fe concentration of the agarose medium containing for the plain agarose medium (Control) as

well as the purity of > 95% and 99 % of the MWCNT used in this work makes contamination by the Fe from such a source unimportant.

4.4.3 Surface topography

Figure 4.4 shows the SEM images of the seed coat corresponding to the treatments in the agarose medium. The most interesting feature is how the pure MWCNT modifies the surface topography of the seed coat and how the relatively high ionic concentrations of iron and chloride ions in the medium change the capacity of the MWCNT to modify this surface topography.

The hilum and the micropyle (H/M) are parts of the seed anatomy where water and the essential oxygen for the germinating seed most easily enter because the seed coat is the thinnest here. The MWCNTs suspended in the gel medium would be carried along with the water and are likely to show their effects prominently. In particular if the MWCNT can penetrate the seed coat they would find it the easiest to do in this part because of the thinness of the seed coat. A high degree of porosity and a partial dismemberment of the surface structure are seen upon introduction of the MWCNT (figure 4.4). Such pores would greatly facilitate the entry of water, nutrients and oxygen as well as the dispersed aqueous phase MWCNT themselves into the germinating seed. It is well known that scarification aids the germination of seeds. Visually, the appearance of the effect of the MWCNT at the H/M region seems a kin to scarification at the microscopic scale.

4.4.4 Raman Analysis

Figure 4.5 and 4.6 shows the intensity of MWCNT and plant samples with respective shift in wavelength. The Raman analysis of plant samples has been carried out using two wavelengths, 514.5 nm (green laser) and 488 nm (blue laser) and the results of plant samples of Table 1 are shown in figure 4.5 and 4.6. Since for biological samples the background effect is too large and compared to pure MWCNT the concentration used to growth medium of plants was too small. Figure 4.5 shows presence of MWCNT of high concentration used growth medium, while figure 4.6 shows the photoluminescence phenomena. The peak at 680 nm appearing in CNT assisted grown plants, which is showing the presence of Cr ion but that is absent in control plants.

4.5 CONCLUSION

We have shown that the germination of maize seedlings is affected by the MWCNT in a concentration dependent manner: lower concentrations are beneficial, higher ones prove toxic in what appears to be chemical hormesis. At the concentration of 20 mg/l in agarose medium and 40 mg/l for BA, the high pure MWCNT increased the growth indices and the water contents of the morphological parts, most prominently for the shoot. Higher concentrations of MWCNT were less effective possibly because the increased concentration clumps and increase their potency. The comparative study of germinating medium (agarose and BA) the BA medium which contains more nutrient facilitate the water content more easily with the presence of MWCNT but also the water content is higher for control medium too in comparison to agarose germinated medium, it is because of the nutrient element make interaction with seed coat and make delivery through MWCNT for easier than no nutrient medium (agarose).

The capacity of the MWCNT to affect the nutrient element delivery in seedlings via enhanced water delivery was investigated by means of Polarised Energy Dispersive X-ray Fluorescence (pEDXRF) spectrometry. The concentrations of all ionic nutrients were seen to pass through a narrow or broadly defined minimum with respect to the MWCNT concentration, this behaviour points the two contrary forces, one the CNT ion-transient-dipole interaction that tends to restrain entry of the ion/polar species into the plant and the other the water inflow entry. The relatively high concentrations of most nutrients at approx 20 mg/l of MWCNT with the increase of fresh and dry weight (agarose assisted system) while for BA it is completely different for example only in case of 20 mg/l these is a slightly lower tendency but except that it is higher than the respective control. The interaction of the MWCNT (20 mg/l) with the 95 and 99% purity were added in agarose germination medium were investigated by pEDXRF spectrometry. The dry weights and % water contents generally followed the Ca elemental concentration trend as would be expected in view of the central role of Ca in metabolism and cell wall properties. The surface morphology of germinated seed body parts were looked by scanning electron microscopy (SEM). The SEM showed fairly dense pore-like structures for the pure MWCNT treated case. These pores may account for the enhanced water delivery by the MWCNT. Raman analysis shows that higher concentration of

MWCNT in culture medium indicates the presence of nanotubes in germinated plants. Thus we conclude that high pure MWCNT at low concentrations benefit the germination of the maize seedling by enhancing water and nutrient transport but that their potency could be diminished by high concentrations of ions/polar species in the medium.

4.6 REFERENCES

1. Sandeep Agnihotri et al, Energy And Environmental Applications of Carbon Nanotubes, *Fuel Chemistry Division Preprints* (2002), 47 (2), 475.
2. Atanu Bhattacharyya et al, Nano-particles - A recent approach to insect pest control, *African Journal of Biotechnology* (2010), Vol. 9(24), pp. 3489-3493.
3. Riyaz Ahmad Dar, Adsorptive stripping voltammetric determination of podophyllotoxin, an antitumour herbal drug, at multi-walled carbon nanotube paste electrode, *J. Appl Electrochem* (2011) 41:1311–1321, [doi:10.1007/s10800-011-0346-4].
4. Chiu-wing Lam et al, A Review of Carbon Nanotube Toxicity and Assessment of Potential Occupational and Environmental Health Risks *Critical Reviews in Toxicology, Taylor and Francis Group* (2006), 36, 3, 189.
5. D. K. Tiwari et al, Interfacing carbon nanotubes (CNT) with plants: enhancement of growth, water and ionic nutrient uptake in maize (*Zea mays*) and implications for nanoagriculture, *Applied Nanoscience*, Springer (Under Review).
6. Srinivasulu Morla et al, Factors Affecting Seed Germination and Seedling Growth of Tomato Plants cultured in Vitro Conditions *J. Chem. Bio. Phy. Sci.* (2011), 1 (2), 328-334.
7. Shadin Ishag et al, Effects of Growth Regulators, Explant And Genotype on Shoot Regeneration in Tomato (*Lycopersicon esculentum* c.v. Omdurman), *Int. J. Sustain. Crop Prod.* (2009), 4 (6), 7-13.
8. Hector Villagarcia et al, Surface Chemistry of Carbon Nanotubes Impacts the Growth and Expression of Water Channel Protein in Tomato Plants, *small* 2012, 8, No. 15, 2328–2334.
9. Mariya Khodakovskaya et al, Carbon Nanotubes are Able To Penetrate Plant Seed Coat and Dramatically Affect Seed Germination and Plant Growth, *ACS Nano* (2009), 3, 3221.
10. Khodakovskaya et al, Carbon Nanotubes Induce Growth Enhancement of Tobacco Cells *ACS Nano* (2012), 6 (3), 2128–2135.

11. Allah Ditta, How helpful is nanotechnology in agriculture? *Adv. Nat. Sci.: Nanosci. Nanotechnol.* (2012), 3.
12. X. Wang et al, *Multi-walled carbon nanotubes can enhance root elongation of wheat (Triticum aestivum) plants*, *Journal of Nanoparticle Research* (2012), 14, 841-51.
13. E.A. Smirnova et al, *Multi-walled Carbon Nanotubes Penetrate into Plant Cells and Affect the Growth of Onobrychis arenaria Seedlings*, 11 International Meeting on Cholinesterases, ActaNature (2012).
14. Zheng L et al, *Effect of Nano-Tio(2) On Strength of Naturally Aged Seeds and Growth Of Spinach*, *Biol. Trace Elem. Res.* (2005), 104, 83.
15. Hediat M. H. Salama, *Effects of silver nanoparticles in some crop plants, Common bean (Phaseolus vulgaris L.) and corn (Zea mays L.)*, *International Research Journal of Biotechnology* (2012), 3 (10), 190-197.
16. Difco™ and BBL™ manual, 2nd Ed
http://www.bd.com/europe/regulatory/Assets/IFU/Difco_BBL/281230.pdf
17. Aditi Singh et al, *Environmental Impact Assessment for Potential Continuous Processes for the Production of Carbon Nanotubes*, *American Journal of Environmental Sciences* (2008), 4 (5), 522-534.
18. Z. I. Miskovic, *Interactions of ions with carbon nano-structures*, *Journal of Physics* (2008): Conference Series 133, doi:10.1088/1742-6596/133/1/012011
19. A.I. Frolov et al, *Molecular-scale insights into the mechanisms of ionic liquids' interactions with carbon nanotubes*, *Faraday Discussions* (2012), 154, 235-47.
20. J. Heckel et al, *Principles and applications of energy dispersive x-ray fluorescence analysis with polarized radiation*, *Journal of Analytical Atomic Spectrometry* (1992), 7, 281-86.
21. G.B. West and J.H. Brown, *The origin of allometric scaling laws in biology from genomes to ecosystems: towards a quantitative unifying theory of biological structure and organization*, *The Journal of Experimental Biology* (2005), 208, 1575-92.
22. T. A. Beu, *Molecular dynamics simulations of ion transport through carbon nanotubes. III. Influence of the nanotube radius, solute concentration and applied electric fields on the transport properties*, *The Journal of Chemical Physics* (2011), 135, 044516, [doi:10.1063/1.3615728].

CHAPTER 5
MATHEMATICAL MODELING OF WATER ABSORPTION
KINETICS

CAPÍTULO 5
MODELO MATEMÁTICO DE LA CINÉTICA DE ABSORCIÓN
DE AGUA

ABSTRACT CHAPTER 5

This chapter explains the mathematical modeling of water sorption by seeds in initial days (7 days) of germination in control and MWCNT of concentration 20 mg/l mediums. Water is the most studied material on earth, but some of its characteristics and properties are still not completely understood. This depends on the fact that water has some unique features, which make it an incredibly anomalous substance. A large number of “hypothetical” models for water have been proposed during the years. Generally, each model is developed to fit well one particular physical characteristic of water (e.g., density, radial distribution, or critical parameters) at the expenses of others. The choice of carbon-oxygen parameters is crucial to the calculated behavior of confined water. Hummer et al. found that a minute reduction in the attraction between carbon and oxygen could lead to consistent differences in the results

We are so used to dealing with water in our everyday life that it is difficult to believe how differently this substance can behave in confined nanospace. If the diameter of the nanotube is comparable to the size of H₂O molecules, in fact, water molecules inside the CNT cannot cross each other and they can only move as a single file. The structure of water in larger CNTs, on the other hand, shows a typical layered structure, which covers the internal walls of the nanotube. Based on all this literatures studies we have measured the water absorption by maize seedling in standard and MWCNT assisted medium to know the if the MWCNT delivers the water in food plants in same ratio or have any significant variation compared to the medium without MWCNT. The calculation is based on the Peleg's kinetic modeling to obtain the rate of water absorption in food plants.

Keywords: Peleg Equation, Kinetic Modeling, Water Absorption.

RESUMEN CAPÍTULO 5

En este capítulo, se explica el modelado matemático de la absorción de agua a través de semillas en días iniciales (7 días) de germinación en muestras de control y muestras con una concentración de MWCNT de 20 mg / l en los medios de cultivo. El agua es el material más estudiado en el mundo, pero algunas de sus características y propiedades siguen sin ser totalmente conocidas. Esto depende del hecho de que el agua tiene algunas características únicas, que lo convierten en una sustancia increíblemente anómala. Se han propuesto un gran número de modelos hipotéticos para el agua durante los últimos años. En general, cada modelo está desarrollado para satisfacer una característica física particular del agua (por ejemplo, densidad, distribución radial o parámetros críticos). La selección de los parámetros de carbono-oxígeno es crucial para el comportamiento calculado de aguas confinadas. Hummer y colaboradores encontraron que una reducción pequeña en la atracción entre el carbono y el oxígeno podría conducir a diferencias consistentes en los resultados.

Estamos tan acostumbrados a tratar con el agua en nuestra vida cotidiana que es difícil de creer lo diferente de cómo se puede esta sustancia comportar en un nanospacio confinado. Si el diámetro del nanotubo es comparable al tamaño de las moléculas de H₂O, las moléculas de agua dentro de los CNT no pueden cruzarse entre sí y que sólo se pueden mover como un único ente. Por otro lado, La estructura del agua en nanotubos de carbono más grandes, muestra una estructura de capas típicas, que cubren las paredes internas del nanotubo. En base a todos estos estudios, hemos medido la absorción del agua a través de plantas de maíz en medios de cultivo estándar y MWCNT para conocer si los MWCNT llevan el agua a las plantas en la misma proporción que tienen cualquier planta en medios de cultivo sin MWCNT. El cálculo se basa en la modelación cinética Pelegs para obtener la tasa de absorción de agua en las plantas agrícolas.

Palabras Clave: Ecuación Peleg, Absorción de Agua, Modelización Cinética.

Mathematical Modeling of Water Absorption Kinetics

5.1 INTRODUCTION

Water is one of the most important substances on earth. All plants and animals must have water to survive. Water molecule plays an important role in the life of Plants. Water helps to: a) Germination of seeds. b) Photosynthesis. c) The transport of nutrients. d) The maintainance of plant stucture by providing the appropriate pressure to the plant tissue. It affects the strength, permeability, and thermal stability of all plants. In the life of Plants, the water content should also be controlled at a proper level. Therefore, study on the interaction between water and plant cells is of great importance both in theory and in application. The absorption of water into the grains during germination is influenced by the soaking of water from the mediums. From an engineering point of view, one is interested not only in knowing how fast the absorption of water can be accomplished, but how it will be affected by processing variables such as supporting medium, temperature [1, 2] and also how one can predict the soaking time under given conditions. Thus, quantitative data on the effect of processing variables are necessary for practical applications to optimise and characterise the soaking conditions, design food processing equipment and predict water absorption as a function of time, temperature and rate of water absorption. Peleg's model [1-4] was successfully applied to experimental data and the corresponding parameters were obtained and correlated with germinating medium.

Maize is one of the most produced and consumable food product world wide, particularly in Mexìco and all other the Latin American countries. It is one of the important plant of three sisters group (Squash, Maize and climbing beans). Maize root system is generally shallow, so that plant is dependent on soil moisture. As a C4 plant (a plant that uses C4 Carbon fixation) maize is a considerably more water-efficient crop than C3 Plants like the small grans, alfa-alfa and soyabeans. IT provides support for beans, and the beans provided nitrogen derived from the nitrogen fixing Rhizobia bacteria which lives on the roots and other

Legumes. C4 Carbon fixation is one of three biochemical mechanism along with C3 and CAM photosynthesis used in carbon fixation. Carbon fixation is the conversion of inorganic carbon to organic compounds by living organism, most prominent example is photosynthesis.

5.2 PELEG EQUATION

The kinetics of the water absorption has been studied during germination and the mathematical modeling is important to design and optimize the process during germination time [1, 4-6]. In 1988 Pelegp proposed a two parameter based sorption equation to calculate the water Adsorption of food products; the equation is:

$$M_t = M_0 + \frac{t}{K_1 + K_2 t}$$

$$\frac{1}{(M_t - M_0)} = K_1 \left(\frac{1}{t} \right) + K_2 \quad (5.1)$$

K_1 =Peleg Rate Constant ($t\%^{-1}$)

K_2 = Peleg Capacity Constant ($\%^{-1}$)

M_t = Moisture Content at time t (%)

M_0 =Initial Moisture Constant (%)

t = Time (Day)

Peleg's Equation is based on non-exponential model and its parameters are in hydration kinetics that applied to weight gain during rehydration.

5.3 STATISTICAL DATA ANALYSIS

In our experiments we have used Control and the MWCNT (20mg/l) growth medium maize seedling of 7 days. The seedlings were harvested periodically for the time-series analysis of the growth. Calculated parameters for kinetics of water modeling and plots were compared using Sigma plot 10. The parameters were calculated and fitted on a linear regression. The moisture content; % Fresh Basis (%fb) indicates that the rate of water absorption is initially rapid then slows down as a equilibrium approaches. This asymptotic

behavior is related to decrease of driving forces for water transfer.

5.4 RESULTS AND DISCUSSION

5.4.1 Kinetics of Water Supply: Peleg's Equation for Seedling

The water absorption data of the samples in terms of moisture content [1, 3, 5, 8, 9] under the experimental condition fitted to Peleg's eq., The linear fit of data $1/\text{Time}$ vs. $1/(M_t - M_0)$ for control and MWCNT assisted media system were calculated as shown in plot. The Peleg's constant vales for control and MWCNT media systems were calculated by statistical analysis of the data and given below in table 5.1.

Table 5.1: Peleg coefficient values of water sorption on total seedling of maize plants germinated in control and MWCNT mediums during 7 days.

Seedling	Coefficient	Std. Error	t	P	R2
Control, K_2	0.01	0.00	2.21	0.11	0.73
Control, K_1	0.04	0.01	2.85	0.06	
CNT, K_2	0.01	0.00	7.77	0.00	0.99
CNT, K_1	0.05	0.00	19.27	0.00	

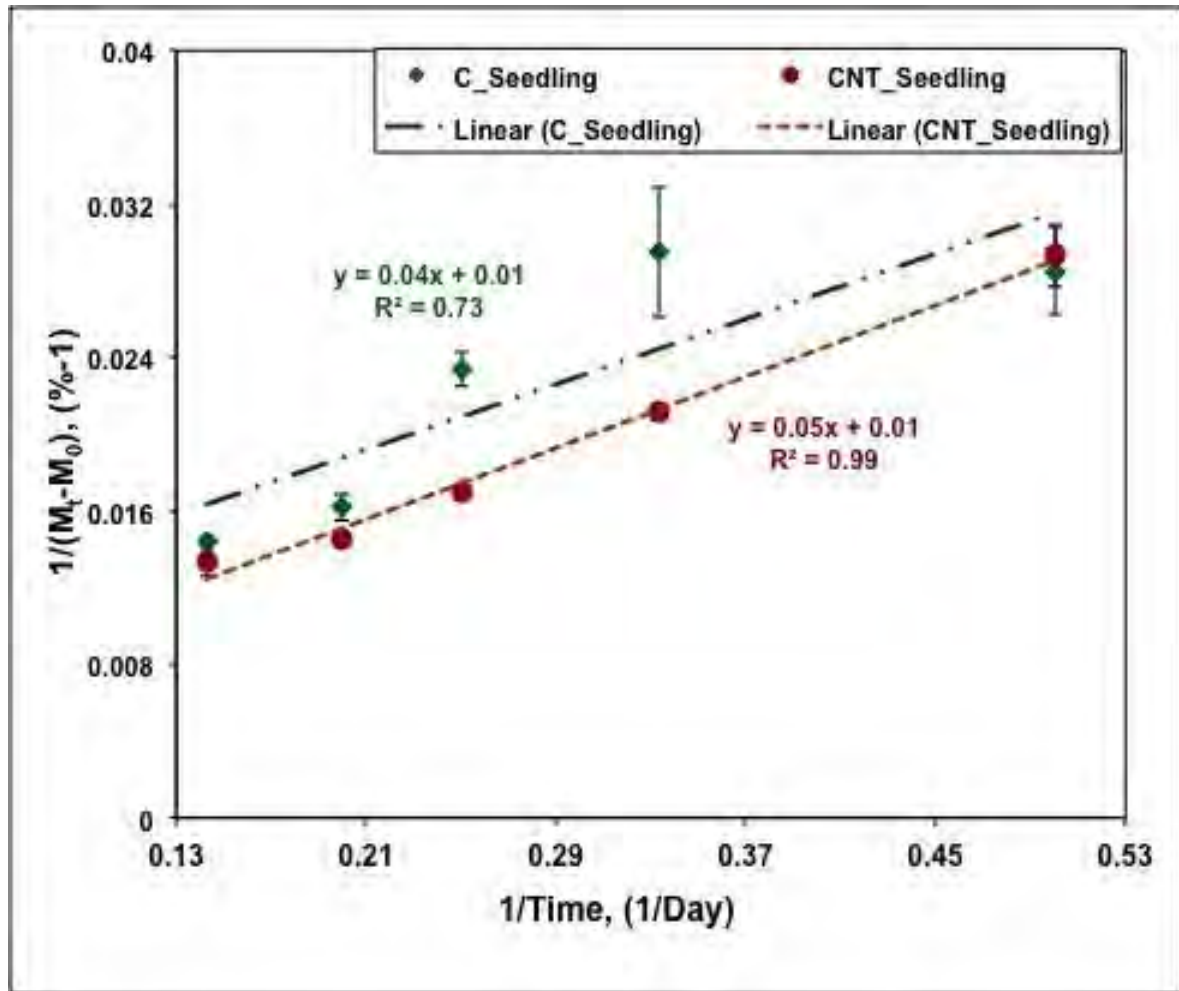


Figure 5.1: Water absorption on maize seedling of 7 days germination in control and MWCNT assisted growth media system.

5.4.2 Peleg's Equation In Root and Shoot Water Absorption

In case of root and shoot $M_0=0$.

So the Peleg's equation for root and shoot will be considered as;

$$M_t = M_0 \pm \frac{t}{K_1 + K_2 t}$$

$$\frac{1}{M_t} = K_1 \left(\frac{1}{t} \right) + K_2$$

The R2 Values less than 0.99 confirms the adequacy of the equation to describe the water absorption Kinetics

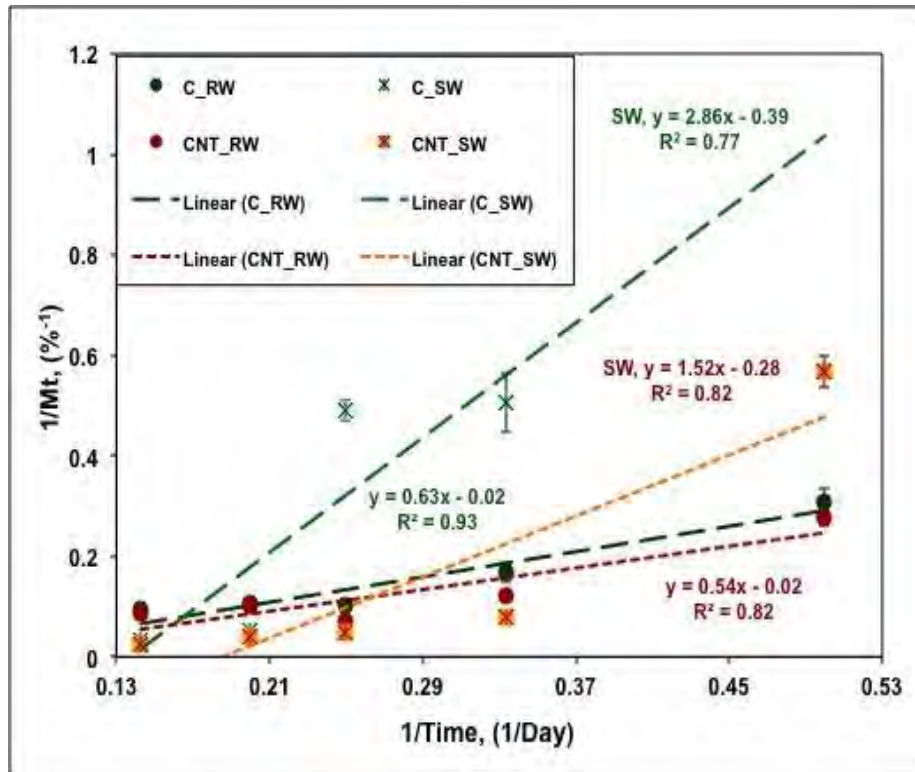


Figure 5.2: Water absorption on 7 days germinated root and shoots of maize seedling in control and MWCNT assisted growth media system.

Table 5.2: Peleg coefficient values of water sorption on 7 days control and MWCNT germinated roots and shoots of maize plants.

Root Water (RW)	Coefficient	Std. Error	t	P	R ²
Control, K ₂	-0.02	0.03	-0.75	0.51	0.93
Control, K ₁	0.63	0.10	6.23	0.01	
CNT, K ₂	-0.02	0.05	-0.48	0.66	0.82
CNT, K ₁	0.54	0.15	3.68	0.03	
Shoot Water (SW)	Coefficient	Std. Error	t	P	R ²
Control, K ₂	-0.39	0.17	-2.27	0.15	0.77
Control, K ₁	2.86	0.55	5.15	0.04	
CNT, K ₂	-0.28	0.13	-2.17	0.12	0.82
CNT, K ₁	1.52	0.42	3.64	0.04	

5.4.3 Water Absorption Modeling of Seed Body (SB)

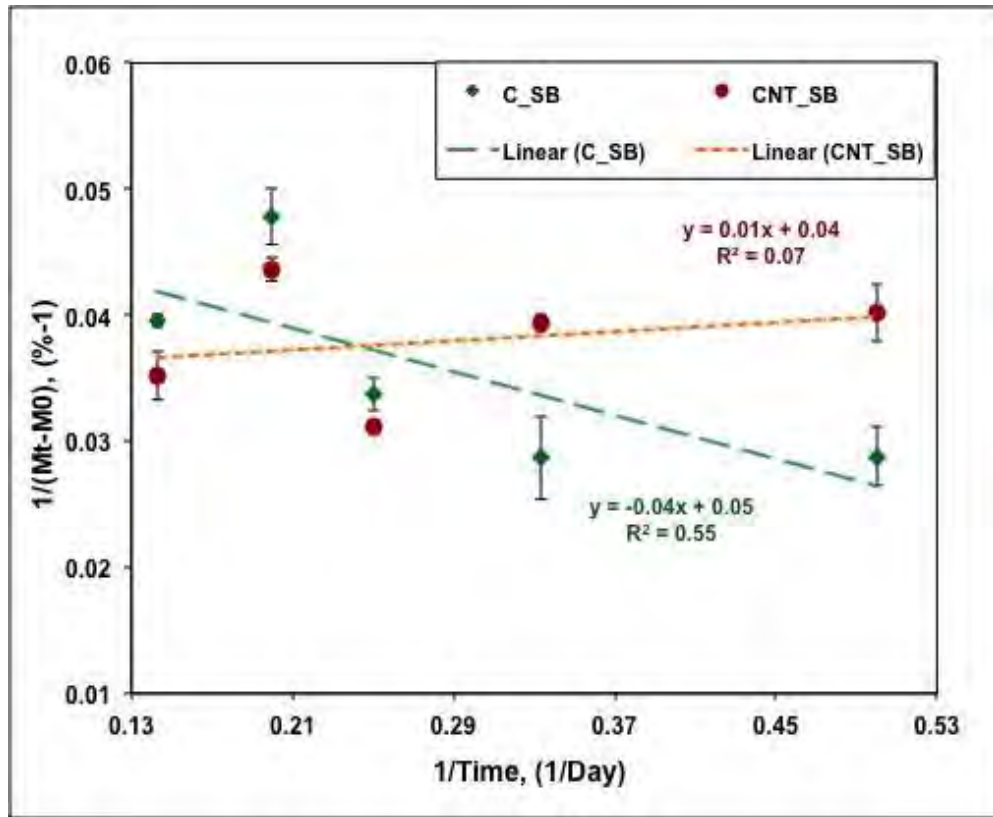


Figure 5.3: Water absorption on 7 days germinated seed body of maize seedling in control and MWCNT growth mediums.

Table 5.3: Peleg coefficient values of water sorption on 7 days control and MWCNT germinated seed body of maize plants.

Seed Body (SB)	Coefficient	Std. Error	t	P	R2
Control, K ₂	0.05	0.01	6.83	0.01	0.55
Control, K ₁	-0.04	0.02	-1.91	0.15	
CNT, K ₂	0.04	0.01	5.90	0.01	0.07
CNT, K ₁	0.01	0.02	0.47	0.67	

5.5 CONCLUSION

Peleg's equation represents the Kinetic behavior of water absorption for Maize seedling, root and shoot, during 7 days of time period for control and MWCNT assisted media.

The % Coefficient of variation (%CV) calculation for Control and MWCNT assisted media shows that the % CV values obtained for MWCNT System with standard deviation is lower than the control system that means the MWCNT not only promotes the water supply but also behaves as a molecular channel for the continuous supply.

Table 5.4: *Coefficient of variation on water sorption of maize seedlings germinated during 7 days on control and MWCNT growth medium.*

	C- Seedling	C- SB	CNT- Seedling	CNT- SB	C- Root	C- Shoot	CNT. Root	CNT- Shoot
CV %	5.83	5.84	3.29	3.31	5.88	5.28	3.31	3.32
Std. Dev.	3.98	3.97	1.90	2.06	3.99	4.41	2.09	2.08

The kinetic analysis of the water absorption modeling shows that the MWCNTs makes a molecular channel to continuous supply of water while in seedling while in case of Control system is random.

5.6 REFERENCES

1. M. Kashiri et al. Modeling Water Absorption Of Sorghum During Soaking, Latin American Applied Research, 40:383-388 (2010).
2. R.C. Verma And Suresh Prasad, Kinetics Of Absorption Of Water By Maize Grains, Journal Of Food Engineering 39 (1999) 395-400.
3. Ali Yildirim et al. Modeling Of Water Absorption Of Ultrasound Applied Chickpeas (*Cicer Arietinum* L.) Using Peleg's Equatio, Journal Of Agricultural Sciences, 16 (2010) 278-286
4. M. C. Quicazán et al. Applying Peleg's Equation To Modelling The Kinetics Of Solid Hydration And Migration During Soybean Soaking, Ingeniería E Investigación Vol. 32 No. 3, December 2012 (53-57)
5. Chris J. Meyer et al. Patterns And Kinetics Of Water Uptake By Soybean Seeds, J Ournal Of Experimental Botany, Vol. 58, No. 3, Pp. 717–732, 2007
6. X. Zhang And G. H. Brusewitz, Water Absorption By Cracked Mustard, Cereal Chem. 70(2): 133-136.

7. J. Khazaei, Water Absorption In Three Wood Varieties, *Ercetari Agronomice In Moldova* Vol. Xli , No. 2 (134) / 2008
8. C.S. Ethmane Kane, Moisture Sorption Isotherms And Thermodynamic Properties Of Tow Mints: *Mentha Pulegium* And *Mentha Rotundifolia*, *Revue Des Energies Renouvelables* Vol. 11, No2 (2008) 181–195.
9. Ricardo D. Andrade et al. Models Of Sorption Isotherms For Food: Uses And Limitations, *Vitae, Revista De La Facultad De Quimica Y Farmaceutica*, Vol 18, No. 3, 2011.

CHAPTER 6
INTERACTION OF CARBON NANOTUBES WITH MINARAL
NUTRIENTS FOR THE PROMOTION OF TOMATO
SEEDLINGS

CAPÍTULO 6
INTERACCIÓN DE NANOTUBOS DE CARBONO CON
NUTRIENTES MINERALES PARA EL INCREMENTO EN EL
CRECIMIENTO DE LAS PLÁNTULAS DE TOMATE

ABSTRACT CHAPTER 6

The study on the effects of nanoparticles in plant science is a newly emerging area of research and compared to plant cell walls and membranes, the penetration of nanoparticles into seeds is expected to be difficult due to the significantly thick seed coat. This study shows the effect of pristine multi-walled carbon nanotube (MWCNT) and ultrasonically dispersed multi walled carbon nanotube (dMWCNT) on germinated tomato plants in standard nutrient media. MWCNTs were used as an additional promoter mixed in a substrate medium and the medium prepared for tomato seedlings were different in each set of experiments. The experiments carried out for samples containing MWCNTs of concentrations 0, 10, 20, 40 and 60 $\mu\text{g/ml}$ and germination were carried out for one week, two week and four weeks. The use of MWCNTs were showed higher rate of growth in comparison to the medium containing no MWCNT and the percentage element concentrations transported during germination were analyzed by pEDXRF analytical technique. The samples assisted with MWCNT interact differently with macro/micro elements than those without MWCNT.

Keywords: Biomaterial, Carbon Nanotubes, Concentration, Elements, MWCNT, pEDXRF. Tomato plants.

RESUMEN CAPÍTULO 6

El presente trabajo, realiza un estudio sobre los efectos de las nanopartículas en la ciencia de plantas, el cual es un área emergente de la investigación y en comparación con las paredes celulares de las plantas y de las membranas, se espera que la penetración de las nanopartículas en las semillas sea difícil debido a la cubierta de la semilla significativamente gruesa. Este estudio muestra el efecto de los nanotubos de carbono de multipared (MWCNT) y la dispersión por ultrasonido de nanotubos de carbono de pared múltiple (dMWCNT) en plantas de tomate germinadas en medios de cultivo estándar. Los MWCNTs fueron utilizados como un promotor adicional mezclados en un medio de cultivo y dicho medio de cultivo preparado para plantas de tomate fueron diferentes en cada conjunto de experimentos. Los experimentos se hicieron para muestras que contienen MWCNTs de concentraciones de 0, 10, 20, 40 y 60 $\mu\text{g} / \text{ml}$ y la germinación se llevó a cabo durante una semana, dos semanas y cuatro semanas. El uso de MWCNTs mostró una mayor tasa de crecimiento en comparación con los medios de cultivo que no contiene MWCNT y para la determinación de las concentraciones de los elementos transportados durante la germinación se empleó la técnica analítica de pEDXRF. Las muestras que contienen MWCNT interactúan diferentes a aquellas que no contienen MWCNT.

Palabras Clave: Biomateriales, Nanotubos de Carbono, Concentración, Elementos, MWCNT, pEDXRF. Plantas de Tomate.

CHAPTER 6

Interaction of Carbon Nanotubes with Mineral Nutrients for the Promotion of Tomato Seedlings

6.1 INTRODUCTION

Carbon nanotubes are molecular-scale tubes of graphitic carbon with outstanding properties, which have attracted a major interest in exploitation to diverse applications. Some carbon nanotubes can be extremely efficient conductors of electricity and heat, some act as semiconductors, depending on their configurations. Carbon nanotubes can conduct heat and electricity far better than copper, and are already being used in polymers to control or enhance conductivity, and in antistatic packaging. Most studies of CNTs in bioscience have focused on their influences in animal and human cells but relatively scant attention has focused on the role of CNT in agrosience; plant growth and their influences with plant cells [Ditta Allah; Rico et al.; Morla et al.; Miskovic]. Recent studies show the penetration of Carbon Nanotubes with plant cells and delivery of necessary elements to plants in support of their growth [Tiwari et al.; Mondal et al.].

The study on the effects of nanoparticles in plant science is a newly emerging area of research and compared to plant cell walls and membranes, the penetration of nanoparticles into seeds is expected to be difficult due to the significantly thick seed coat. At present, many different studies are being performed all over the world to elucidate the contribution of CNT in agricultural and environmental applications. The most popular studies in this area are the production of biofuel, glucose oxides, hydroxyapatite and in plant growth. The Carbon Nanotubes penetrate the thick outer seed coat of the plants and this interaction facilitates differently for different plants, depending on the seed coat thickness and bonding with plant cell structure. Because of their direct interaction with seeds and size of the tubes; carbon nanotubes are easily able to form a capillary action from the substrate to seeds in the transport of water and dissolved micronutrient elements in them. Since, in the initial days of germination embryo contains sufficient nutrient and there is need of water availability for fast

growth. The results of our previous experiments of maize plants shows result that presence of mwcnt, increase the rate of seed germination and the roots start coming within 48 hours of the germination time while in controlled system (without mwcnt) root start after 72 hours or more. Except all these beneficial effects [Agnihotri et al.; Mondal et al.; Morla et al.] there is some drawbacks, considering the human health and toxicity of mwcnts in food because of their direct interaction [Naiya et al.; Rico et al. The previous studies shows that the contribution of mwcnt is very effective during the initial stage of germination; the mwcnt affects the germination in different manner: a) Concentration in the medium. b) Purity of the mwcnt. c) Presence of nutrients in the substrate medium. d) Ambient growth conditions.

Considering all these factors; this articles shows the effect of mwcnt on initial days of germination of tomato plants: a) without presence of any nutrients in the substrate medium. b) Presence of nutrient medium. c) Various concentration of mwcnt mixed in the agar substrate. d) Role of MWCNT during period of germination.

6.2 EXPERIMENTAL

6.2.1 Materials

Standard Murashige & Skoog (MS) medium (M5519) and MWCNT (purity >95%, OD 6-9 nm, L 5 μ m) were purchased from Sigma-Aldrich®, St. Louis, MO, USA. Bacteriological agar (BA) (Bioxon®) [Difco™ and BBL™ manual] was purchased from Becton-Dickinson (BD de Mexico, Mexico City, Mexico), which contains a certain level of mineral nutrients as ionic or polar species. Tomato seeds were purchased from a local supplier (Hortaflor, Rancho Los Molinos SA de CV, Mexico).

6.2.2 Medium Preparation and Plant Growth

a) Plain Medium, With and Without MWCNT

The first experimental sets were consist of tomato seedlings grown in bacteriological agar (BA) gel medium spiked with different concentrations of MWCNT. The appropriate masses of weighed MWCNT were mixed with deionized (DI) water for different concentration of mediums mentioned in Table 6.1. Weighted BA powder for concentration of 15 g/l was added with very slow rate to mwcnt mixed solutions and finally autoclaved at 120⁰C for 20 minutes. The BA solutions containing the different concentrations of the MWCNT were then

poured into replicate sterile petridishes to set as the gel substrate for seed growth. Tomato seeds were cleaned by magnetic stirring in a 70% ethanol solution for 2 minutes and washed with DI water. They were then surface sterilized in a 1% v/v solution of sodium hypochlorite by gentle stirring for 10 minutes, then washed several times with DI water. The seeds were blotted dry in sterile paper towels and implanted into the gel substrates described previously. The petridishes were covered and appropriately labeled. These operations were done in the laminar flow-hood. The petridishes were then transferred to a climate-controlled chamber (temperature 23-25⁰C, Relative humidity (RH) ~ 71.5%, photoperiod 16 h light- 8 h dark) and the seeds are allowed to germinate for 7 days. The total number of seedlings was 78 with each case listed in table 6.1 containing 13 seedlings.

Table 6.1: Sample description of germinated tomato plants in BA medium assisted with and without mwcnt.

Sample name	Growth medium and time	mwcnt concentration (µg/ml)
C0	7 days germinated plants in BA growth medium with and without mwcnt (C)	0 (Standard)
C5		5
C10		10
C20		20
C40		40
C60		60

b) Plant Growth in Presence of Nutrient Medium and dMWCNT

The second experimental set shows the tomato plant growth using mwcnt ultrasonically dispersed in 1-MS medium of pH 5.75 for 2 hour. First, make a stock solution of 1-MS basal nutritive medium solution of pH 5.75 then the appropriate masses of the mwcnt were mixed in 100 ml of 1-MS medium solution and ultrasonicate for 2 h. After dispersion, use this 100 ml solution mixed in bacteriological agar medium solution of concentration 8 g/l [table 6.2]. Other processes were identical to the first set of experiment as mentioned in section 2.2 a. The total number of seedlings were 60 with each case listed in table 6.2

containing 10 seedlings, and the ambient condition was same as of previous set of experiment (section 6.2.2 a).

Table 6.2: Sample description of germinated tomato plants in nutrient added and dmwcnt introduced BA growth medium.

Sample name	Growth medium and time	dmwcnt concentration (µg/ml)
T0	14 days germinated plants in nutritive (1-MS) BA medium with and without dmwcnt (T)	0 (Control)
T5		5
T10		10
T'0	27 days germinated plants in nutritive (1-MS) BA medium with and without dmwcnt (T')	0 (Control)
T'5		5
T'10		10

6.2.3 Elemental Analysis using pEDXRF Spectrometry

pEDXRF spectrometry were applied for the elemental analysis of the germinated tomato plant samples. The operating principle is based on the cancellation of the bremsstrahlung background by the double polarization of the initial x-ray beam. The advantages of pEDXRF lie in its non-destructive, multi-elemental and rapid trace analysis capabilities.

Dry plant parts were milled in grinder for 5-10 minutes till the entire mass appeared as a fine powder. The elemental analysis of the powders was carried out by the pEDXRF spectrometer SpectroXepos III (Spectro Analytical Instruments GmbH, Kleve, Germany) using the TurboQuant™ analytical routine. It is important to remember that for the low sample dry mass yields as in the present work, the quantity of interest is the relative magnitude of the element's concentration corresponding to the different treatments.

6.2.4 Fourier Transform Infra Red (FT-IR) Spectroscopy

Infrared (IR) scans were run at resolution of, 4 cm⁻¹ between 400-4000 cm⁻¹ range using Bruker tensor 27 FT-IR spectrometer. Powder samples of whole seedlings (germinated plants) of different concentration and medium treated were used.

6.2.5 Data Analysis

Averages and standard errors were computed over 10 sets of replicates for each case listed in the Table 6.1 and 6.2 with the number of seedlings for each set as cited previously. Tests of statistical differences were carried out by the Student's t-test at 95% confidence level, except where stated differently. The softwares; GraphPad Prism, Excel, and Origin were used for data reduction and analysis.

6.3 RESULTS AND DISCUSSION

6.3.1 Without Nutrient Medium and Undispersed MWCNT

Figure 6.1 shows the effect of pristine MWCNT on tomato plant germination for 7 days. We placed the sterile tomato seeds in without nutrient BA medium with different concentration of MWCNT. The medium without mwcnt (0 μ g/ml) germinated plants were used as standard germinated medium compared with MWCNT treated systems. In this experiment we have used the various concentration of MWCNT to know, the effect of various concentration on germination and what will happen if exceeds the availability of MWCNTs in growth medium. The root and shoot length statistics of 7 days germinated plant seedlings are shown in figure 6.1a with respect to MWCNT presented medium. The root length shows that there is no statistical variation with presence of MWCNT-germinated plants compared with standard medium germinated plants. The medium containing MWCNT of concentration 20 μ g/ml and 60 μ g/ml have decrease in the root length than other media systems. Since MWCNT added without dispersion and there is not any clear information about homogeneous distribution of MWCNT in the medium. Sometimes MWCNTs are elongated in the medium and much availability of MWCNT causes the toxic effect in the medium, which is already explained in our previous work [Tiwari et al.]. Shoot length distribution with respect to MWCNT concentration (Figure 6.1a) shows that, even without nutrients in the germinated medium MWCNT affects the growth more compared with standard medium germinated plants. From figure 6.1a, we can see that there is better germination at concentration of 40 μ g/ml and 60 μ g/ml of MWCNT. The root and shoot lengths are decreasing, this is because of the high availability of MWCNT.

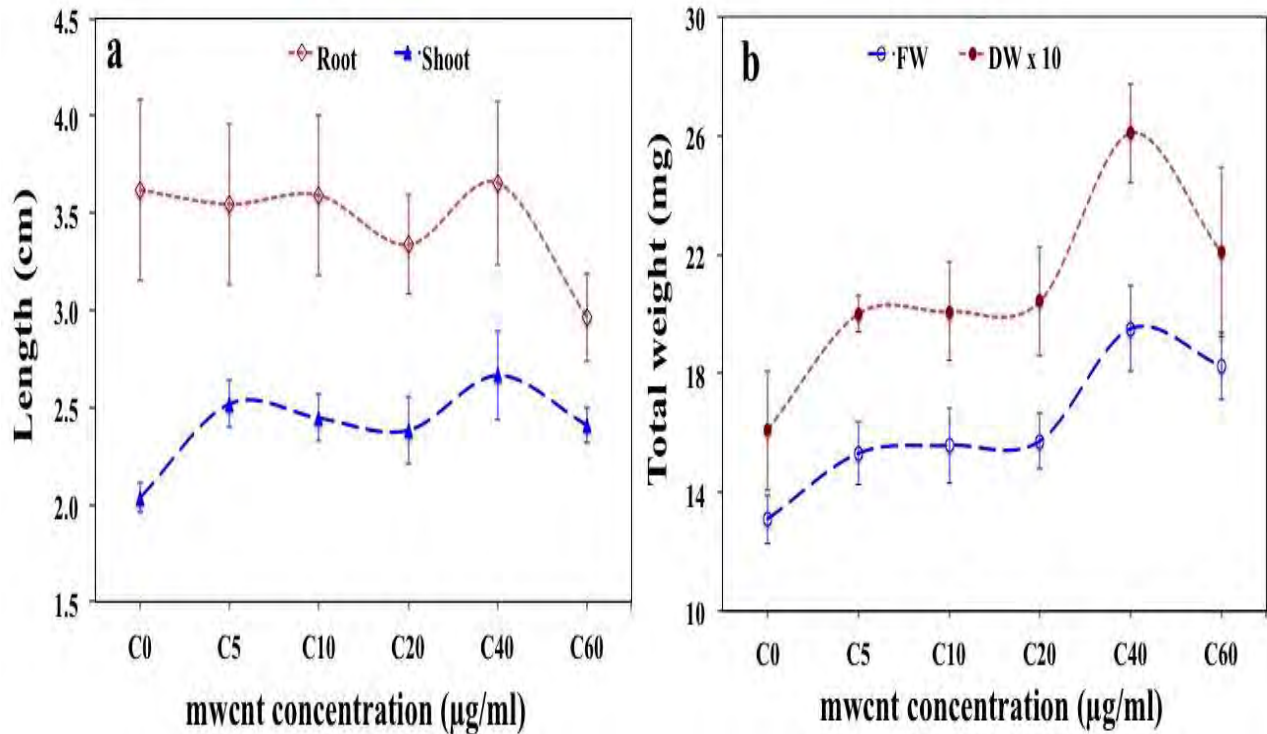


Figure 6.1: Effect of pristine mwcnt on 7 days germinated tomato seedlings. a) Length of root and shoot growth on a medium with and without mwcnt. b) Total fresh and (dry x 10) weight measurement with respect to mwcnt concentration.

Figure 6.1b shows the total fresh and dry weight measurement with MWCNT concentration, the dry weight data with respect to MWCNT concentrations are shown with their respective concentration multiplied by 10, its because to plot fresh and dry weight measured data on same plot. Total fresh and dry weight a measurement shows that, presence of MWCNT not only affects the growth of tomato seedlings but also affects the biomass. From figure 6.1 we find better germination (length) and biomass (fresh and dry weight) at MWCNT concentration of 40µg/ml presented medium.

6.3.2 Nutrient-rich and dMWCNT Growth Medium Affects Better Germination

Figure 6.2 shows the effect of dmwcnt in 14 and 27 days of tomato germination. Since figure 6.1 explains that, pristine mwcnt affects the growth in initial days of germination and here we are interested to find the role of mwcnt on tomato plants in a medium containing; a)

Nutrients (1-MS strength). b) Using mwcnt dispersed in 1-MS strength, to make the homogeneous distribution of mwcnt in the nutrient-rich growth medium. c) How dmwcnt affects the growth of tomato plants in longer days of germination.

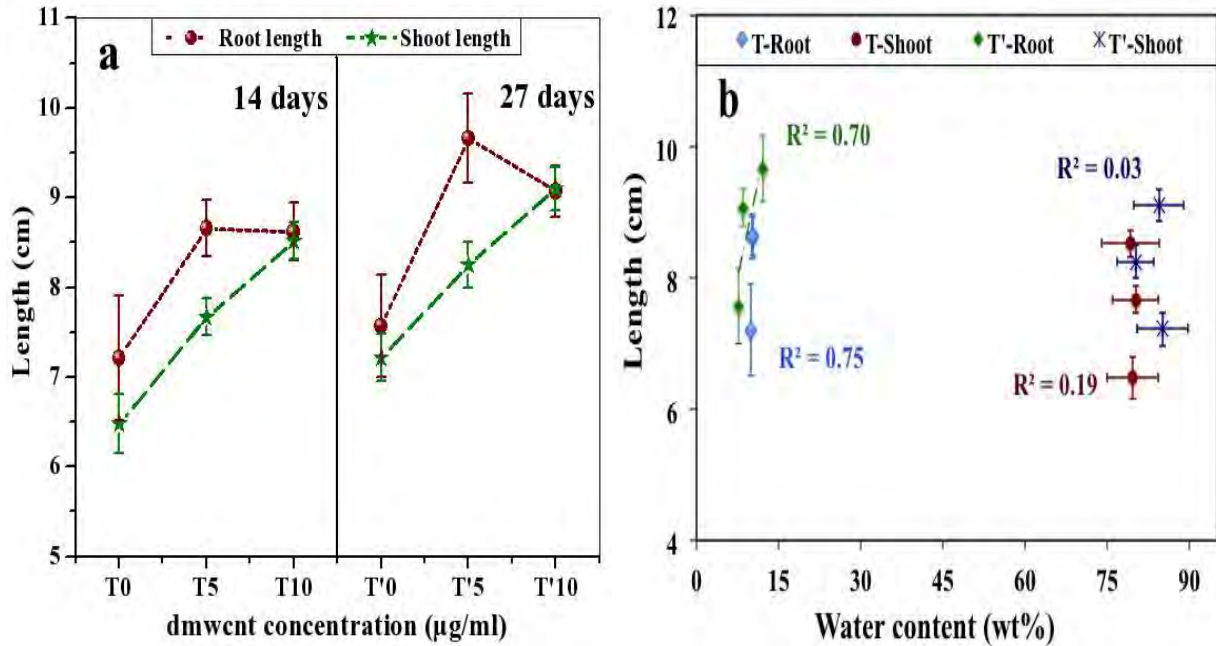


Figure 6.2: Tomato germination with the presence of dmwcnt of 14 and 27 days of seedlings. a) Root and shoot length measurement. b) Root and shoot length variation with respect to % water content. Results are shown average \pm SE of 10 plants per each treatment.

Figure 6.2a, shows the germination of tomato plants in full nutritive medium with and without dmwcnt. The presence of dmwcnt shows the better germination than respective control system. Since here we are doing our analysis for longer days of germination and mentioned by [Mc. Donald] 2nd and 4th weeks (14 and 27 days) are IInd and IIIrd stage of seedlings, where the growth rate is less and biomass consumption takes place in all edible plants. The root and shoot length is better in dmwcnt assisted growth medium of concentration 5 µg/ml and 10 µg/ml than without dmwcnt but there is not any significant difference between 5 and 10 µg/ml concentration for root system while for shoot these two concentrations affects the germination for 14 and 27 days of seedlings. If we compare, the rate of germination for 27 days of seedling, growth of different concentrations of dmwcnt than their respective concentration of 14 days seedlings; we can see that the rate of germination is lower as explained earlier. Figure 6.2b shows the root and shoot length statistics for 14 and 27 days of

seedlings with respect to their % water availability, which shows that the root length follows the better linear trend with % water content, while in case of shoots the trend is not very fit. The linear fit of root and shoot length variation with respect to % water content is given as: root, $y = 3.69x - 29.04$, $R^2 = 0.75$, shoot; $y = -0.93x + 81.47$, $R^2 = 0.19$, of 14 days germinated plants and root, $y = 0.39x + 5.12$, $R^2 = 0.70$, shoot; $y = -0.06x + 13.50$, $R^2 = 0.03$, for 27 days germinated plants. The R^2 vale of linear fit for shoot shows that, in early days (14 days) follow better trend than that of 27 days, this is because all the germination done in closed circular magenta boxes of controlled photo-condition (16 h light, 8 h dark) and for longer days of germination, it is not only depends on the nutrient and water transport, there might happen photosynthesis too.

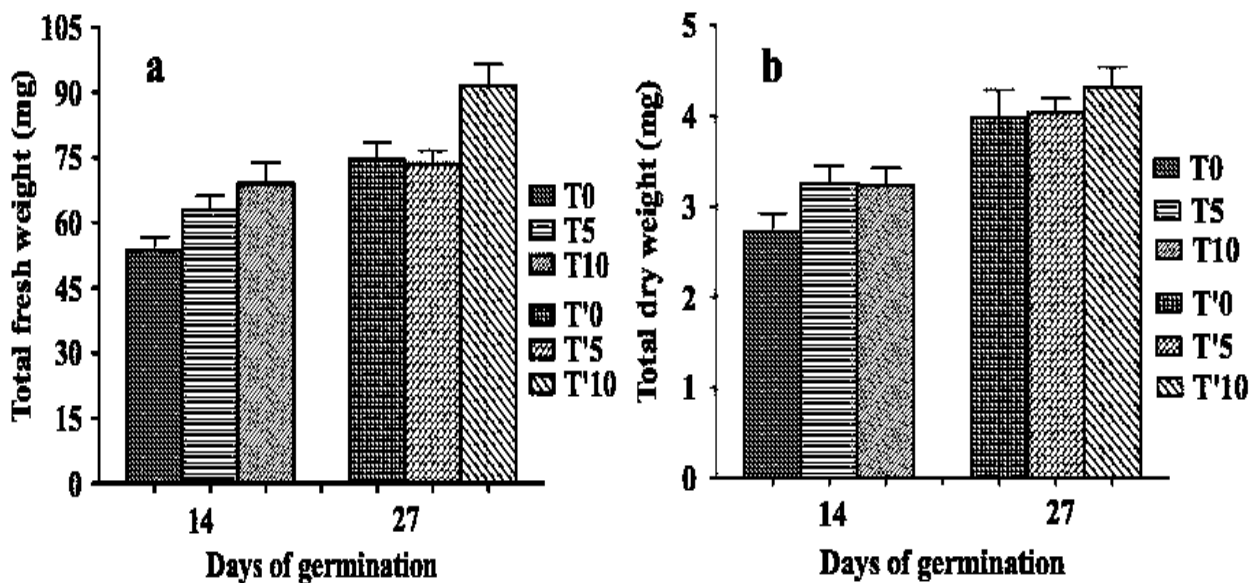


Figure 6.3: Effect of dmwcnt on growth and development of tomato plants for 14 & 27 days of germinated seedlings. a) Total fresh weight. b) Total dry weight. Results are shown average \pm SE of 10 plants per each treatment.

Total fresh and dry weight measurements of root and shoots are shown in figure 6.3. Figure 6.3a and 3b shows the total fresh and dry weight of 14 and 27 days germinated plants. For 14 days of germinated plants the dmwcnt of concentration 5 and 10 $\mu\text{g/ml}$ have high fresh weight than their respective control medium while for 27 days of germinated plants the control and dmwcnt of 5 $\mu\text{g/ml}$ approaches same fresh weight while 10 $\mu\text{g/ml}$ have better response, that means for longer days of germination the higher concentration of dmwcnt affects better

responses in biomass gain than that of control and lower concentration. If we compare the growth of 27 days seedlings with their respective of 14 days, we can see that the control medium germinated plants gain weight in better ratio than that of dmwcnt, 5 $\mu\text{g/ml}$, while higher concentration (10 $\mu\text{g/ml}$) have better response. Dry weight measurement of total seedlings (Figure 6.3b) shows that, for longer days of germination the higher concentration of dmwcnt is beneficial for growth rate and also in biomass.

6.3.3 % Elemental Concentration Analysis

The availability of nutrient elements in the germinated plants as explained in section 6.2.2a and b (Table 6.1 and 6.2) were analyzed using pEDXRF spectrometer shown in Figure 6.4. Since plants get carbon, hydrogen and oxygen from the air and water, considered as a non-mineral nutrient, except all these nutrients, there are certain minerals nutrients are very important for plants to grow and develop which they get from the soil medium. The measured macro and Micro nutrient elements are K, Ca, Mn, Fe, Cu and Zn, which plays very crucial role in the plants life. The detailed description of these nutrients and their availability in nutrient and MWCNT assisted growth medium is explained below.

Potassium (K): K is primary macronutrient very important for plants to help, building protein, photosynthesis and reduction of disease. K also plays a key role in maintenance of plant water balance and a vast array of physiology process vital for plant growth. Figure 6.4 shows clearly that plant germinated with nutrient growth medium contains high concentration (4-5 %) while without nutrient medium have much lower concentration (0.25%) of K. Presence of MWCNT concentration in nutrient growth medium shows higher percentage than respective control, while plants grown without nutrients have high concentration at 20 $\mu\text{g/ml}$. The K deficiency to tomato plants exhibits uneven fruit ripening, poor texture and soft fruits.

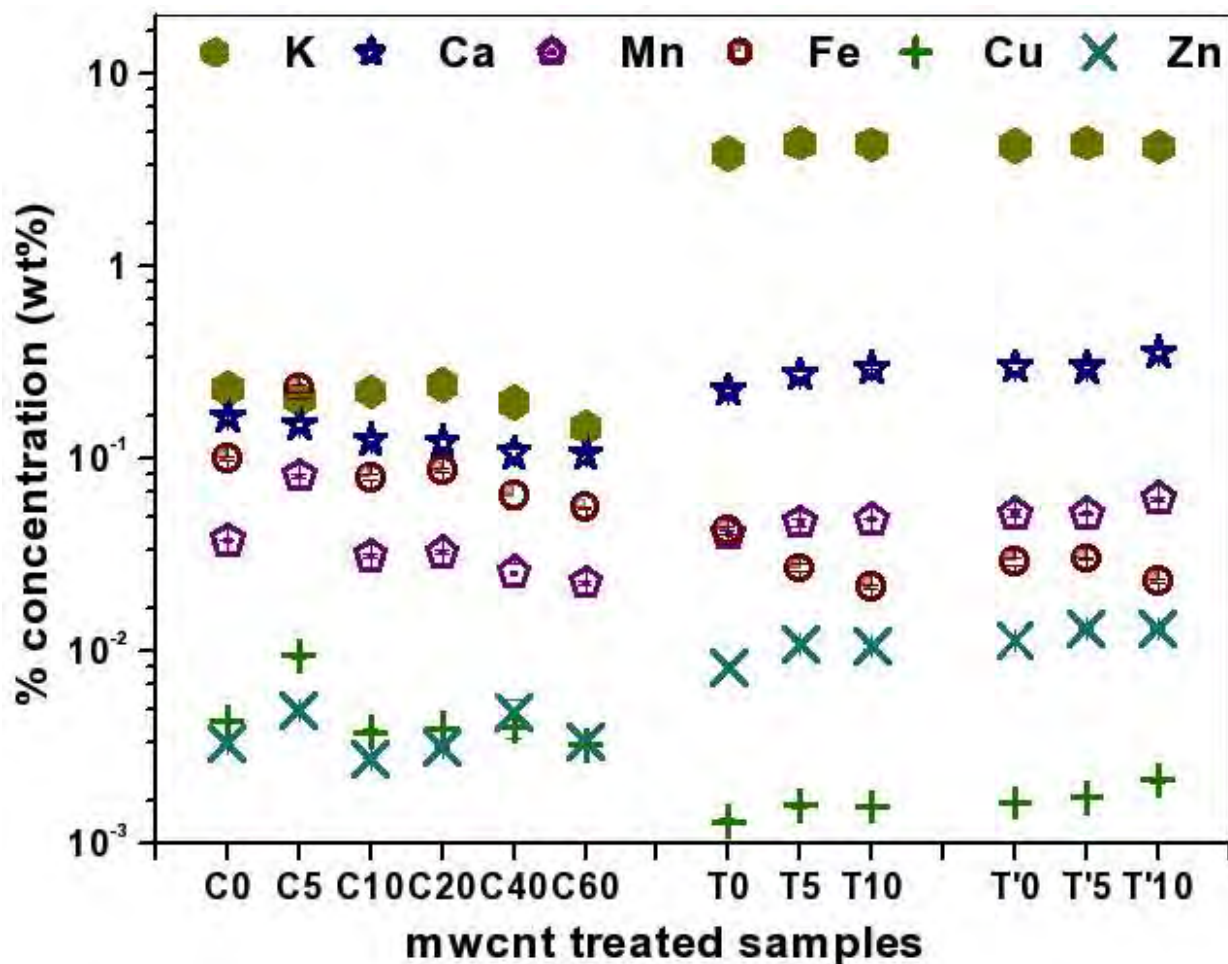


Figure 6.4: Percentage concentration of nutrient elements present in germinated tomato plants. C0-60 shows the samples germinated for 7 days with varying MWCNT concentration from 0 to 60 $\mu\text{g/ml}$ and without using any additional nutrient in the growth medium (Table 6.1). T0-10 are the sample germinated for 14 days in presence of 1-MS nutrient in growth medium and dMWCNT concentration 0-10 $\mu\text{g/ml}$ (Table 6.2). T'0-10 are the samples of 27 days germinated plants in presence of 1-MS nutrient and dMWCNT 0-10 $\mu\text{g/ml}$ Concentration in the growth medium (Table 6.2).

Calcium (Ca): Ca is an important secondary nutrient essential for plants to provide the expansion of cell walls. It also helps to transport and retention of other elements as well as strength. Ca concentration of plants, germinated without nutrient medium decreases with increase of MWCNT concentration (Figure 6.4) while for nutrient media germinated plants Ca

concentration increases with increase of dMWCNT concentration. That shows dMWCNT not only affects the germination but also promotes the nutrient elements (Ca) during germination.

Iron (Fe): Fe is a micronutrient, essential to plant growth, formation of chlorophyll and acts as an oxygen carrier. From Figure 6.4, Fe concentration decreases with introduction of MWCNT and dMWCNT except MWCNT 5 µg/ml.

Manganese (Mn): Mn functions with enzyme system involved in breakdown of carbohydrates and nitrogen metabolism. Mn concentration follows the same trend as Fe with presence of MWCNT concentration, while in nutrient germinated plants dMWCNT increase the transportation rate than without dMWCNT treated system. This means dMWCNT support the delivery of Mn element same as Ca.

Copper (Cu): Cu concentration in the germinated plants are random and their delivery and presence is not highly affected by MWCNT or dMWCNT. Only the MWCNT with concentration of 5 µg/ml shows high availability of Cu while in other cases it is decreasing and almost close to the plants germinated without MWCNT, and in dMWCNT it is slightly higher % ratio than their respective control. From Figure 6.4, we notice that in the nutritive medium the Cu concentration is much lower than that of without nutritive medium of early days of germination, that means this Cu concentration is not because of the nutrient availability but because of the presence in the cell matrix of seeds. While the seeds are start germination there availability in seed cell matrix is high while the plants start growing this Cu nutrient transported by natural transport statistics of seed cell process to make plants strong and availability getting less.

Zinc (Zn): The Zn concentration varying with the growth medium, with the MWCNT concentration of 5 and 20 µg/ml (C), the Zn concentration increases relatively then other growth medium. While the plants grown in MS nutritive medium and dMWCNT the concentration of Zn is highly differ from those germinated with MS medium and with the presence of dMWCNT the concentration increasing compared with their control germinated plants. This shows clearly that dMWCNT promotes the Zn availability within plants in higher

ratio than that of without dMWCNT. Another aspect of this is, if we compare only the control system germinated plants of C0 (without nutrient), T0 (MS germinated plants of 14 days) and T'0 (MS germinated plants of 27 days), the concentration on Zn increasing with time and also the presence of nutrients promotes the transport of Zn elements itself my seeds without any promoter like MWCNT but while medium is introduced by MWCNT or dMWCNT the promotion of Zn elements is higher.

6.3.4 FTIR Analysis

The results of FTIR of germinated plants are shown in Figure 6.5. We can see that the peaks obtained for the germinated plants are different from the peaks of MWCNT (solid dark yellow trace). The FTIR measurements were made of whole germinated plants have 14 and 27 days (Table 6.2) and there is not any presence of MWCNT. This result is consistent with the recent observations made by Miralles et al., who also detected practically no presence of MWCNTs in their plant tissue.

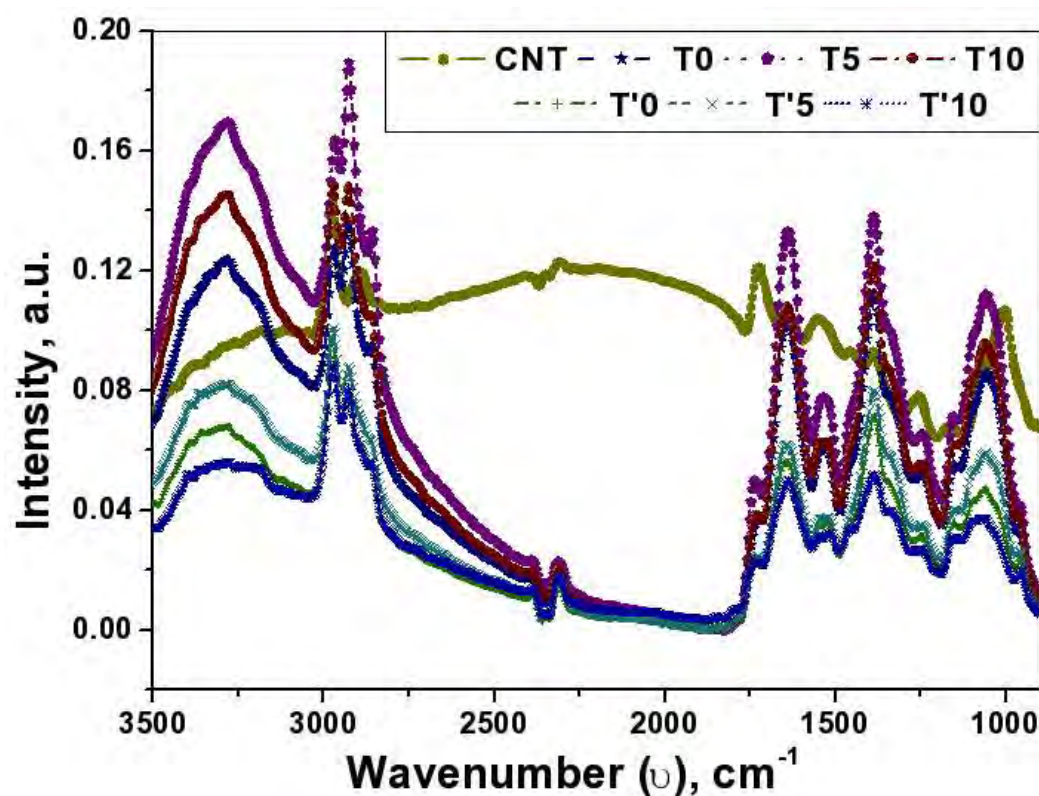


Figure 6.5: Detection of MWCNT in 14 and 27 days (Table 6.2) tomato seedlings using infrared spectrometer.

6.4 CONCLUSION

Result demonstrates that MWCNT and dMWCNT both promotes the tomato plant germination. The plants grow with MWCNT and without any addition nutrient growth medium are beneficial but the rate of germination is lower in comparison to those containing nutrient growth medium and ultrasonically dispersed MWCNT (dMWCNT). The promotion of nutrient elements is depends on the there status in periodic table and ionic interaction. To early days of germination (7 Day) the MWCNT of 40 µg/ml concentration is more beneficial for biomass gain as well as shoot growth, when we using the dMWCNT and standard nutrients growth medium the rate of germination is higher comparatively with MWCNT and without nutrient medium. We see that carbon nanotubes (MWCNT & dMWCNT) are highly effective to tomato seed germination and their development than control medium also promotes the nutrients in germinated plants. For longer days of germination higher concentration of dMWCNT is more effective than lower concentration and promotes germination, biomass and some nutrient elements.

6.5 REFERENCES

1. **Agnihotri Sandeep et al. (2002)** Energy and Environmental Applications of Carbon Nanotubes. Fuel Chemistry Devison Preprints, 47(2) 474.
2. **Difco™ and BBL™ manual**, 2ndEd
3. http://www.bd.com/europe/regulatory/Assets/IFU/Difco_BBL/281230.pdf
4. **Ditta Allah (2012)** How Helpful is Nanotechnology in Agriculture? Adv. Nat. Sci.: Nanosci. Nanotechnol. 3, 033002 (10pp).
5. **Khodakovskaya M.V. et al (2009)** Carbon nanotubes are able to penetrate plant seed-coat and dramatically affect seed germination and plant growth: ACS Nano. 2009 Oct 27; 3(10):3221-7. doi: 10.1021/nn900887m. Retraction in: ACS Nano. 2012 Aug 28; 6(8): 7541.
6. **MacDonald M. B (2007)** Physiology of Seed Germination; http://seedbiology.osu.edu/HCS631_files/4A%20Seed%20germination.pdf ;
7. **Miskovic Z. I. (2008)** Interactions of Ions with Carbon Nano-Structures. Journal Of

Physics: Conference Series 133, 012011. Doi:10.1088/1742-6596/133/1/012011

8. **Mondal Anindiyta et al. (2011)** Beneficial Role of Carbon Nanotubes on Mustard Plant Growth: An Agricultural Prospect. *J. Nanopart Res*, 13:4519-4528.
9. **Morla Srinivasulu et al. (2011)** Factors Affecting seed Germination and Seedling Growth of Tomato Plants Cultured in Vitro Conditions, *J. Chem. Bio. Phy. Sci.* Vol. 1, No.2, Sec. B.328-334.
10. **Naiy Remya et al. (2010)** Nanoparticulate Material Delivery to plants. *Plant Science*, 179, 154-163.
11. **Rico Cyren M. (2011)** Interaction of Nanoparticles with Edible Plants and their Possible Implications in the Food Chain. *Jopurnal of Agricultural and Food Chemistry*, 59, 3485-3498
12. **Tiwari D. K. et al. (2013)** Interfacing Carbon Nanotubes (CNT) With Plants: Enhancement of Growth, Water and Ionic Nutrient Uptake in Maize (*Zea Mays*) and Implications for Nanoagriculture. *Applied Nanoscience* (Springer), DOI 10.1007/s13204-013-0236-7.

CHAPTER 7

**SPECTROSCOPIC ANALYSIS OF IONIC AND METAL
TRANSPORT ON PLANT SAMPLES GERMINATED WITH
MULTI-WALLED CARBON NANOTUBES**

CAPÍTULO 7

**ANÁLISIS ESPECTROSCÓPICO DEL TRANSPORTE
IÓNICO Y DE METALES EN MUESTRAS DE PLANTAS
GERMINADAS CON NANOTUBOS DE CARBONO DE PARED
MÚLTIPLE**

ABSTRACT CHAPTER 7

This chapter explains a detailed study of "Tomato" and "Maize" Plants germination in a culture medium containing 1/8 MS strength nutrients and various concentrations of dispersed multiwalled carbon nanotubes (MWCNT). Germinated plants were milled to make a microsize powders and Turbo Quant X-ray fluorescence method were used to analyze the elemental concentration of plant samples. The Powders were also analysed using FTIR, UV-Visible and Raman Spectroscopy for the confirmation of presence on chemical functional groups, catalyst, metal elements and MWCNT in plant samples.

RESUMEN CAPÍTULO 7

En este capítulo, se explica un estudio detallado de la germinación de plantas de "Tomate" y "Maíz" en un medio de cultivo que contiene nutrientes forzados de 1/8 MS y diversas concentraciones de nanotubos de carbono de pared múltiple dispersos. Las plantas germinadas se molieron para hacer un polvos de tamaño micrónico y el método TurboQuant de fluorescencia de rayos X se utilizó para analizar la concentración elemental de muestras de plantas. Los polvos también se analizaron mediante espectroscopia de FTIR y espectroscopia Raman para la confirmación de la presencia en MWCNT en muestras de plantas.

Spectroscopic Analysis of Ionic and Metal Transport on Plant Samples Germinated with Multi-Walled Carbon Nanotubes

7.1 INTRODUCTION

There is a growing need to increase the global food supply and maximize profitability from their crops. As a result of this growing need, there has been a surge in the use of pesticides, fungicides, and herbicides on crops in recent decades to aid in preventing crop spoilage from insects, weeds, microbes, and fungi and improve the life of the crop. In recent days, Research find that there has been a drastic change in plant cells and the way they might influence the physiology and development of plants by using carbon nanotubes (CNTs). Most studies of CNTs in the biosciences have focused on their influence on animal and human cells. Relatively scant attention has been paid to the effect of yet plants are fundamental to higher life on earth; they are the geo-physico-chemical transducers that produce food and oxygen that sustain life in the biosphere. They are also end-receivers of environmental contaminants including the CNT-based ones. Thus the plant-CNT interaction needs to be thoroughly investigated from the cellular to the organismic level to understand its multifaceted complexity. This knowledge will also serve to develop the nascent technology of ‘nanoagriculture’.

However the effect of the CNT will principally vary with the type of plant studied, the type of growth medium and ambient growth conditions, the type of CNT, its concentration and associated techniques used to obtain the better homogeneity of the CNT in the assisted medium.

7.2 MATERIALS AND METHOD

First Make a stock solutions of Murashige & Skoog (MS) basal Medium of strength 1 and 1/8-MS and fix the Ph to 5.75 after that MWCNTs for concentrations 0, 1, 2.5, 5, 10 mg/l were weighed. The weghted MWCNTs of concentrations were added in 50 ml pH adjusted MS solution and dispersed ultrasonically for 2 hour at 48 kHz frequency. Bacteriological Agar

of concentration 8 g/l was weighted separately for each treatment of with and without MWCNT solution and mixed in 5.75 pH adjusted MS solution. Finally the dispersed MWCNT solutions of each concentration were added to separate solutions of BA added MS solution of related concentration of MWCNT and autoclaved at 120⁰C for 20 min. After autoclaving pore the solutions to replicate magenta boxes for each treatment and seed germination were done in same way as explained in Chapter 2 section 2.1.2. Every set of experiment will have 3 replicates with 6 seeds/Magenta boxes and the fresh and dry weight measurements were measured for 10-12 germinated plants of maize and tomato. The dry plants after biomass analysis were grinded to make microsize powder, in this set of experiments for the maize plants the roots, shoots and seed body were powdered separately while for tomato the root and seed body were grinded together and shoots separately. The treatment of the maize and tomato plants used for germination are given in Table 7.1.

Table 7.1: Sample description of maize and tomato plants treatments used for germination.

Plants	Sample Name	MS-Strength	MWCNTs	Agar
			(mg/l)	(g/l)
Maize	M ₀	1/8-MS	0	8
	M ₁	1/8-MS	1	8
	M ₂	1/8-MS	2.5	8
	M ₃	1/8-MS	5	8
	M ₄	1/8-MS	10	8
Tomato	T ₀	1/8-MS	0	8
	T ₁	1/8-MS	1	8
	T ₂	1/8-MS	2.5	8
	T ₃	1/8-MS	5	8
	T ₄	1/8-MS	10	8

Table 7.2: Description of powder samples of root, shoot and seed body of germinated plants of maize and tomato.

Reference Name	Sample Type	Plant Type
M0-CM	Culture Medium	Bacteriological Agar
M1-CM		
M2-CM		
M3-CM		
M4-CM		
M0-R	Root	Maize (Zea Mays)
M1-R		
M2-R		
M3-R		
M4-R		
M0-S	Shoot	
M1-S		
M2-S		
M3-S		
M4-S		
M0-SB	Seed Body	
M1-SB		
M2-SB		
M3-SB		
M4-SB		
T0-R	Root + Seed Body	Tomato
T1-R		
T2-R		
T3-R		
T4-R		
T0-S	Shoot	
T1-S		
T2-S		
T3-S		
T4-S		

7.3 RESULTS AND DISCUSSION

7.3.1 Plant Germination with MWCNT Assisted Nutrients Medium

Figure 7.1 shows the total fresh and dry biomass of germinated maize plants with varying concentrations of MWCNTs as mentioned in Table 7.1. The result shows that the MWCNT germinated plants contains more biomass than control system. The dry biomass is plotted, multiplied by 10 of the real weight to see the variation compared with fresh biomass. The dry biomass results shows that with the introduction of MWCNT the biomass changes but after a certain concentration of MWCNT (M2), the biomass starts decreasing.

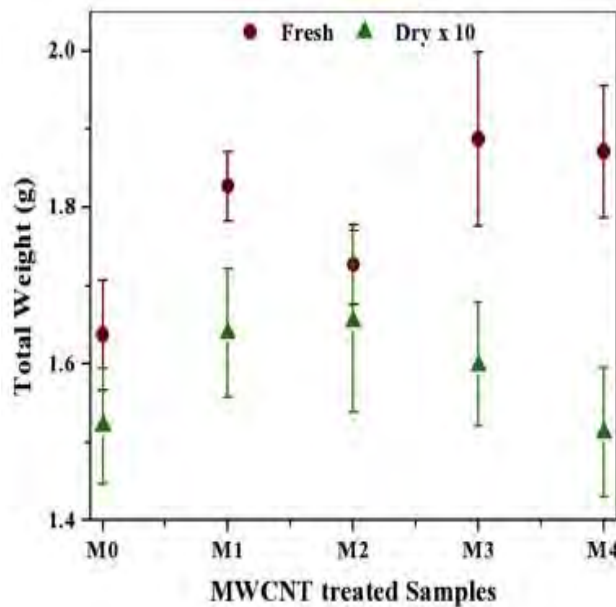


Figure 7.1: Fresh and dry x 10 weights of 9 days germinated maize plants as mentioned in Table 7.1. The results are shown average \pm SE of 10 plants.

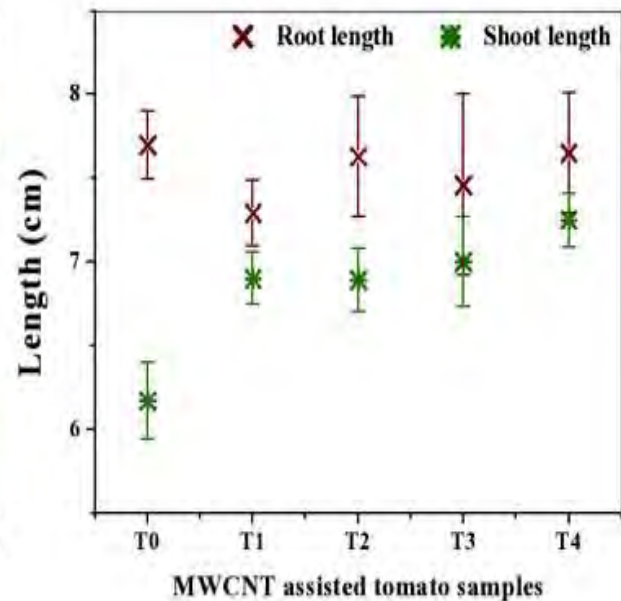


Figure 7.2: Root and shoot lengths of 9 days germinated tomato plants of Table 7.1. Results are shown average \pm SE of 10 plants.

Figure 7.2 shows the root and shoot length of the germinated tomato plants (Table 7.1). It is clear from the figure that MWCNT treated plants shows high increment in the shoots while the root is lower or relatively same as control system. For the tomato plants as the MWCNT concentration increases in growth medium the rate of germination also increases.

7.3.2 XRF Analysis

Figure 7.3 shows the XRF results of germinated maize plants. The XRF analysis carried out for the plants part; root shoot and seed body separately. From figure 7.3 we can see that the % concentration of elements is different for different parts of plants and there is increase or decrease in the elemental concentration (depending on elements) while germinated with MWCNT mixed growth medium.

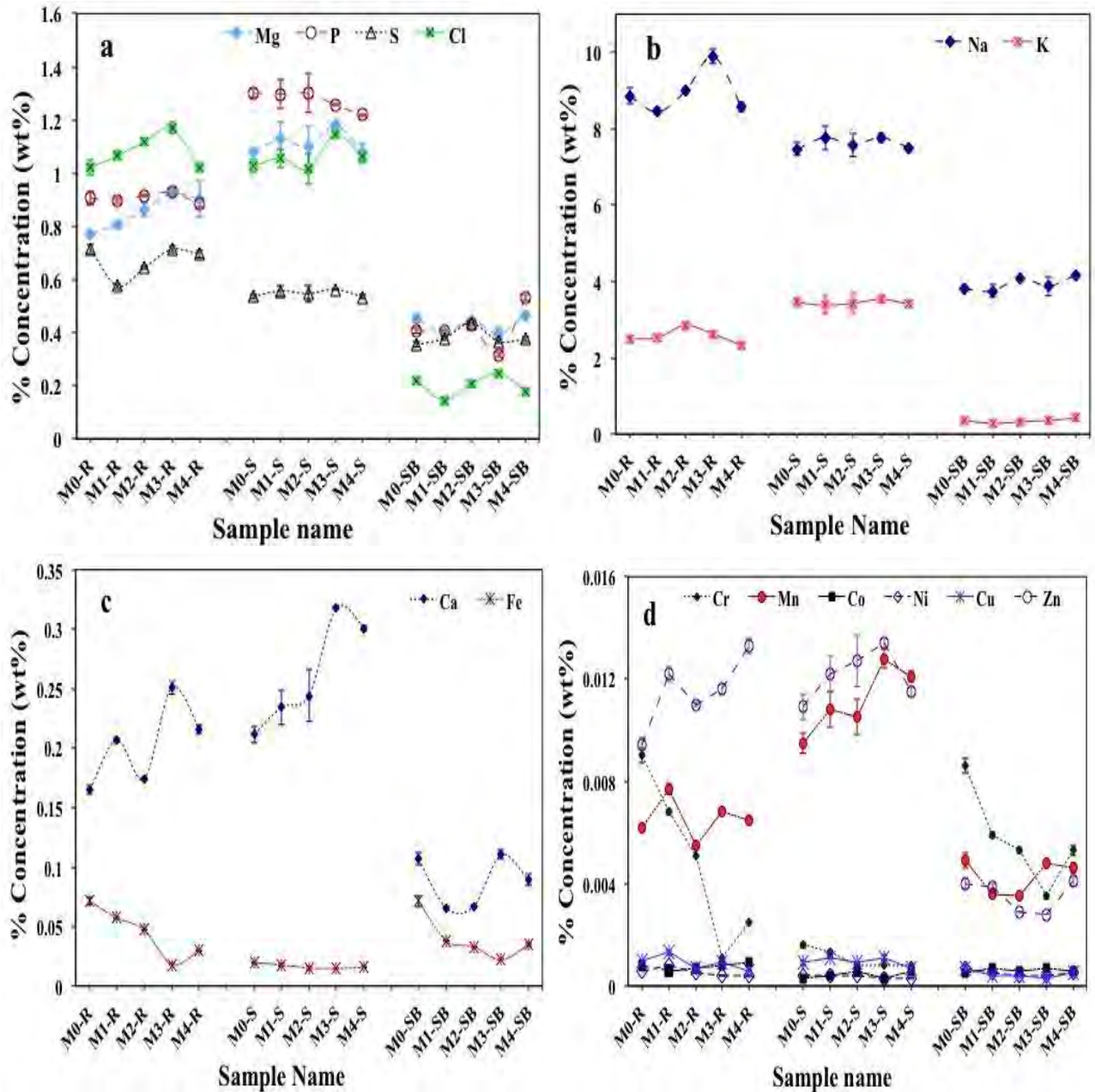


Figure 7.3: XRF measurement of plant samples of Maize (Table 7.2). Figures, a, b c and d explains the presence of different elements of plants samples of Table 7.1.

7.3.3 FTIR Measurements

Infrared measurements of powder samples of maize plants of different treated system has been carried out and shown in Figure 7.4. The presence of functional groups are different in intensity for different treatments and also varying with part os plant samples. The black lines in the plots of different measuremets are showing the results for pure MWCNT (95%). The peaks at 2978 cm^{-1} are more prominent in MWCNT treated roots while disappearing in control treated plants.

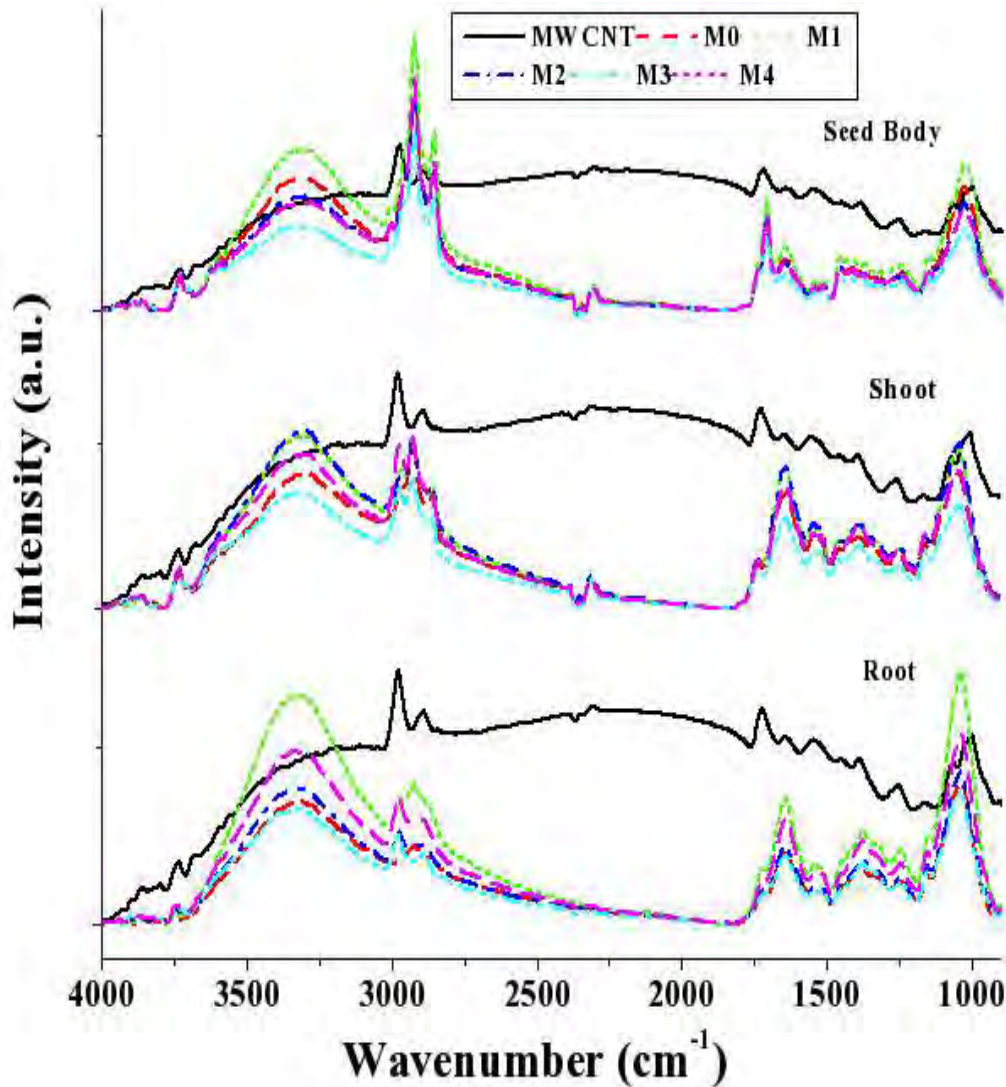


Figure 7.4: IR analysis of parts of maize plants (root, shoot and seed body) (Table 7.1/7.2).

FTIR results of germinated plants of tomato are shown for root and shoots in Figure 7.5a and b. The results for root system are showing clear variation in for control and MWCNT

treated plants. The root samples treated with MWCNT contains highly reactive functional groups while control system sample lacking.

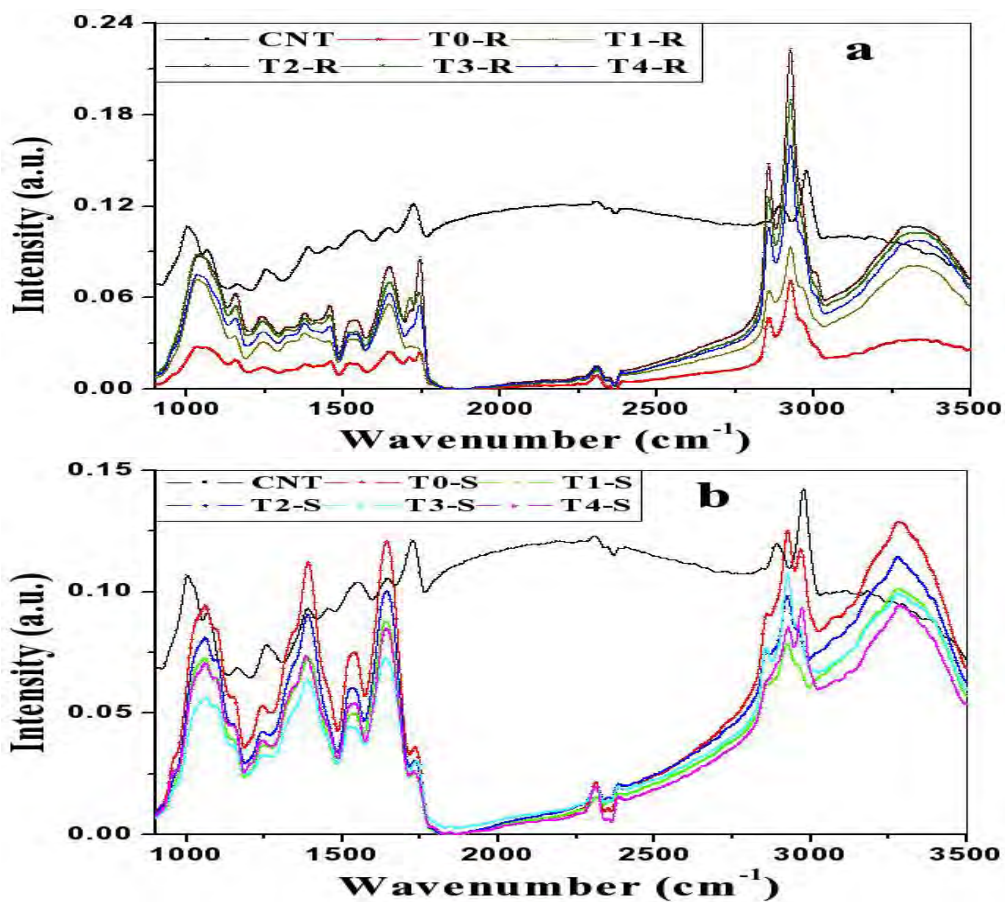


Figure 7.5: IR analysis of parts of tomato plants. a) Root+Seed Body (R). b) Shoots (S) (Table 7.2).

7.3.4 Raman Analysis

Raman measurements were done using LabRam II Dilor, Raman spectrometer. The wavelength of the lasers used to analyse the samples were; Green (514.5 nm) and Blue (488nm). The analyses of the different sample (Table 7.2) measurements are shown in figures, 7.6, 7.7 and 7.8). The results show that the plants germinated using MWCNT contains more metals than control germinated. The presence of metals in seed body is disappearing in control while present in MWCNT contained medium, this shows that MWCNT transported these metals through the vascular system of plants. The presence of metals in root and shoot systems

are also more while introducing with MWCNT compared to control, its because some of these metals desolved in water and uptake through water.

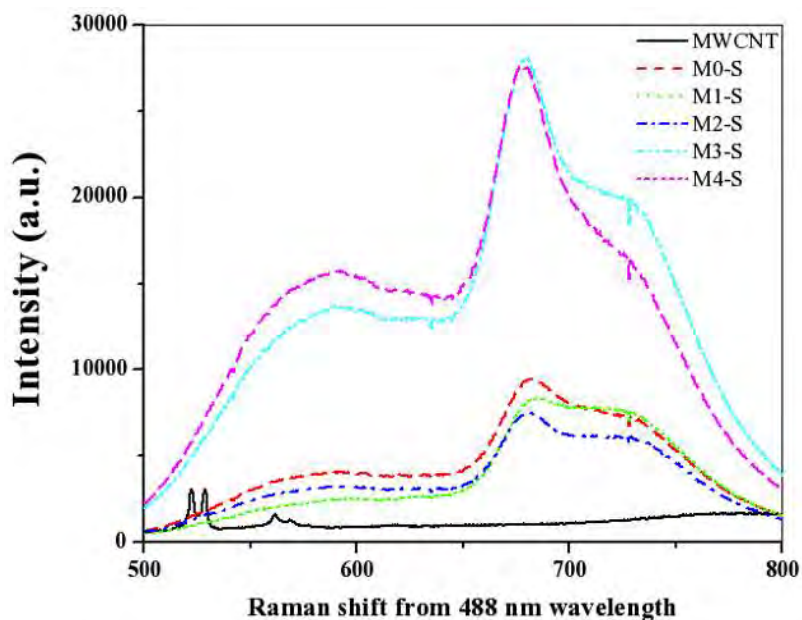


Figure 7.6: Raman analysis of powder samples of shoot part of maize plants germinated with and without MWCNT (Table 7.2), pure MWCNT (black line) is used as a reference.

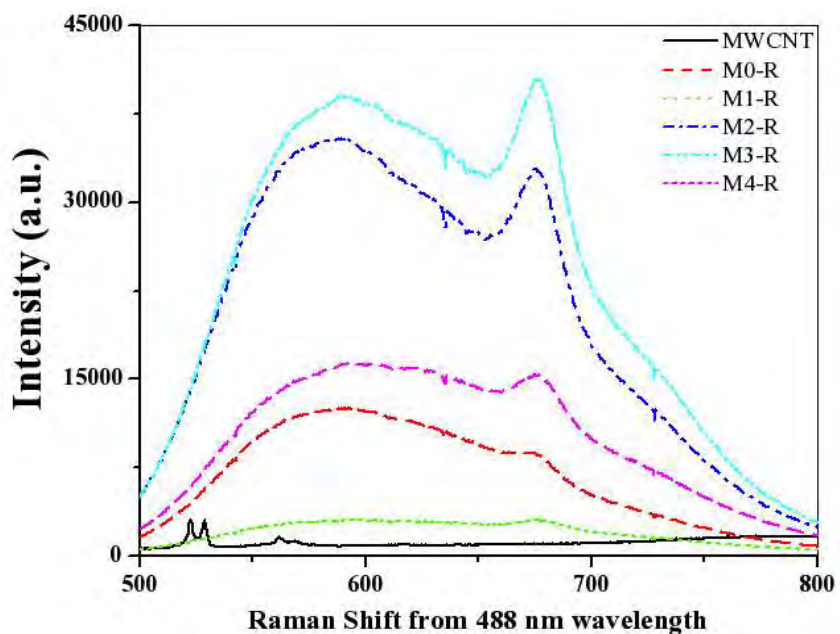


Figure 7.7: Raman analysis of powder samples of root part of maize plants germinated with and without MWCNT (Table 7.2), pure MWCNT (black line) is used as a reference.

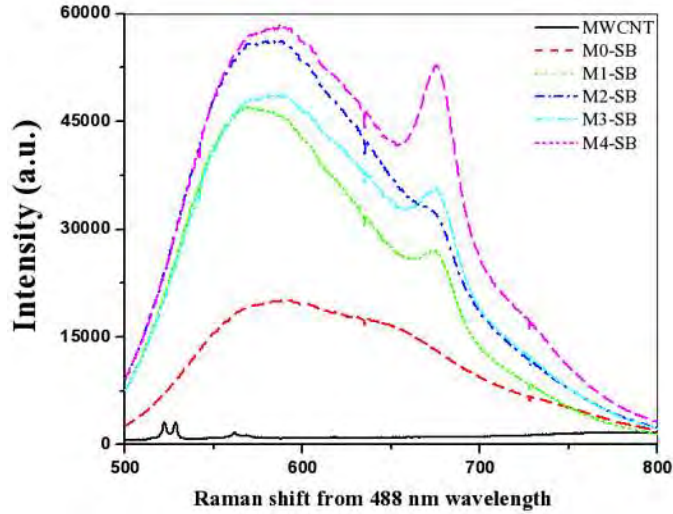


Figure 7.8: Raman analysis of powder samples of seed body after 9 days of germination with and without MWCNT (Table 7.2), pure MWCNT (black line) is used as a reference.

7.3.5 UV-Visible Analysis

UV-Visible analysis is carried out with the supernatants of the plants and culture mediums (Table 7.2). The supernates of the culture medium obtained by dissolving 0.052g weight per 1 ml (0.052 g/ml) deionised water and heating at 95⁰c for 3 hours and then centrifuge it for 30 min.

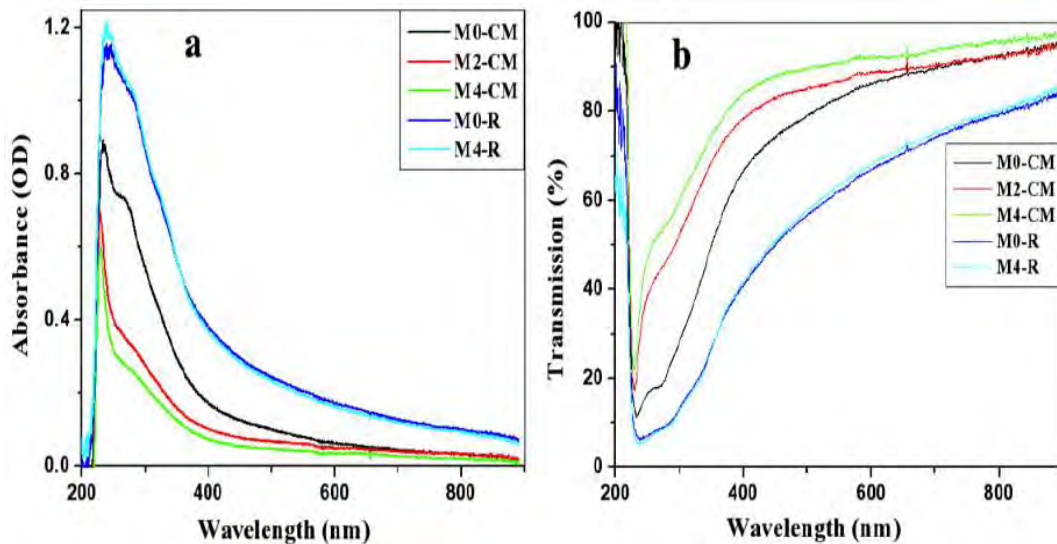


Figure 7.9: Absorbance and transmission measurement of the samples listed in Table 7.2 using UV-Visible analysis.

The supernatants of the root were obtained by crushed to very fine and then mixing in deionized water (0.052 g/ml) and centrifuge for 30 minutes. Finally obtained supernatants were analysed in quartz cuvettes using Specro Photometer USB-4000, Ocean Optics. From Figure 7.9, we see that the absorbance and transmission for culture mediums and roots of MWCNT and control.

7.4 CONCLUSION

The plants germinated with and without MWCNT for 9 days, which is the time period of weight gain and biomass development shows that the MWCNT assisted plants have higher weight with respect to control germinated plants (maize and tomato). XRF, FTIR and Raman spectroscopic measurement were carried out to analyse the % elemental concentration, presence of functional groups, metalicity and presence of MWCNT in germinated plant. Since the biological sample got a lot of signal to noise ratio in Raman test compared to pure MWCNT, and the concentration of MWCNT used was too low and that mixed in culture medium but except that the results shows some ionic presence of MWCNT assisted plant samples. The ionic presence in plant samples might be because of MWCNT promotes water uptake and those ions enter through uptake by desolving in water. Another interesting result we find in the FTIR analysis that MWCNT assisted plant contains more functional groups than those without MWCNT. In summary, the presence of MWCNT in plant samples is not clear but there are clear evidences to the promotion of metallic elements, chemical functional groups, and ionic transport together with the higher rate of germination, fresh and dry biomasses. The dispersion of MWCNT was useful to make the culture medium more homogeneous and that helps to avoid the cluster formation, which causes toxic effect in our previous results.

FINAL CONCLUSIONS

This research work is to develop an effective method to explore the role of pristine and dispersed multiwalled carbon nanotubes (MWCNT & dMWCNT) in seed germination and their development (plant growth) in different growth mediums (*in Vitro*) such as; BA, agarose and Fe ion mixed medium, applying mechanical stirring. Results obtained through experiments shows that MWCNTs are interacting the outer cell walls of seeds and promoting the plant germination in higher ratio than that of respective control media system. The general objective of this research work concerns the influence of different concentrations of highly pure MWCNT on the germination and growth of maize seedlings as well as on the concentrations and transport of mineral nutrients into the seedling. It also explains the mechanism of metal ion transport mediated by the MWCNTs using the two-oxidation states of Fe (II and III) as markers. All the studies reported are intended to optimize the various experimental conditions. This is so because many aspects of the experiments have no precedents. For a rigorously quantitative study, optimization and reproducibility of all experimental parameters are essential. Maize (*Zea mays* L.) ranks third in global cereal production and is considered as an essential food crop. Previous studies on the effect of nanomaterials (NMs) in maize reveal improved growth parameters but the effects of NMs on maize physiological components and their distribution in roots and shoots are essential to understand the functional properties of mineral fertilizers in detail. Determination of essential regulatory and defense compounds in maize such as proteins and phenols is necessary to ascertain the biotic and abiotic tolerance mechanisms adapted through NMs fertilization. For application of NMs for plant growth enhancement, the availability of an economical silica source with increased functional properties is currently a demanding task. Moreover the degree of NMs solubility depends on particle size and chemical compositions. To understand the function of NMs it is preferable to study the phytochemical changes of maize cultivars differing in NMs absorption and its effect on maize metabolic defense compounds.

The first chapter (Chapter 1) is an overview of Nanomaterials their wide applications in environmental research and concepts we use in our work. This knowledge was accumulated during years of research in and outside our lab, and forms the foundation from which, started

the exploration of the carbon nanotubes in plant Science.

Chapter 2 describes the parts of the development of the experimental procedures and a brief introduction of the characterization techniques used during my research, in which I was involved, both during the initial set-up stage and throughout the following years. In addition to this chapter, Appendix lists many of the suppliers we have used to build and upgrade the apparatus (e.g. Electrochemical Impedance Spectroscopy and X-Ray fluorescence spectroscopy).

Chapters 3 through 7, covers research done using multi walled carbon nanotubes in different ratio, different purity and in different media systems in "*In Vitro*" condition to analyze their role in germination of maize and tomato plants in different growth conditions.

Chapter 3 explains the experiments done using higher concentrations of MWCNT in controlled growth chamber and the concentrations of Fe^{2+} and Fe^{3+} in the agarose growth medium were used to see the interaction of these ions with MWCNT and their reaction with maize seeds; such as oxidation or reduction. The SEM analysis shows that, MWCNT seedlings contain many pores and fraction on cell membranes than those without MWCNT.

The results obtained from chapter 4, shows that the plants grown on bacteriological agar (contains more nutrients) have high rate of germination than those on agarose (nutrient less) medium. FTIR analysis shows that the MWCNT germinated plants contains more functional groups. Another factor is the purity of MWCNT, which shows that high pure carbon nanotubes transports the % concentration of elements more than those of comparatively less pure. Raman measurement of the samples shows the presence of MWCNT in plant samples, germinated using high concentration (60 mg/l) of MWCNT in agarose culture mediums. The luminescence analysis also gives clear information of metal presence in MWCNT germinated plants while that is disappeared in control system germinated plants.

Results of chapter 5 give a clear information that carbon nanotubes not only promotes the growth and ions (chapter 3 & 4) but also the nutrient delivery and water transport in a continuous rate during period of germination which is proved by Mathematical formulation using Pelegs kinetics equation.

Chapter 6 shows the germination, growth and development of tomato plants using MWCNT and dMWCNT in nutrient less and highly rich nutrient medium. The results show that the lower concentration of dMWCNT is beneficial for early days of germination and higher

concentration is useful to longer period, while plants gain sufficient biomass.

The experimental results of chapter 7, shows the maize and tomato plants germination in nutrient medium using dispersion of MWCNT in 1/8 MS Basal medium. The dispersion of MWCNT has been done in MS Basal medium because, it contains many nutrient elements and organic chemical groups that also help to formalise the MWCNT. The XRF, FTIR, UV-Visible and Raman spectroscopic measurements were carried out to verify the presence of metal elements, chemical functional groups, ions and nanotubes in the germinated plants treated differently. The results obtained shows that the nanotubes are able to penetrate the plant cell walls, promotion of plant growth, enzyme activation and also increment in the fresh & dry biomasses. The interaction of nanotubes for maize and tomato plants are different such as; delivery of water, nutrients and metal transportation. The results also show that the interactions of carbon nanotubes with elements are selective. The FTIR results shows the presence of different functional groups in the different part of germinated plant samples are different, also varies with the plants and culture medium used. The Raman measurements for luminescence shows a peak broadening at $\sim 680\text{ cm}^{-1}$ wavenumber in the samples germinated using MWCNT, which shows the metallic presence in those samples. UV-Visible measurement shows the absorbance and transmittance of the samples.

CONCLUSIONES FINALES

Este trabajo de investigación se realizó para desarrollar un método eficaz para explorar el efecto de los nanotubos de carbono de pared múltiple (MWCNT y DMWCNT) en la germinación de semillas y su desarrollo (crecimiento de plantas) en diferentes medios de crecimiento (in vitro), tales como: medios de cultivo de BA, agarosa e ión de Fe mezclado utilizando agitado mecánico. Los resultados obtenidos a través de los experimentos hechos, muestran que los MWCNTs interactúan con las paredes celulares externas de las semillas y promueven la tasa de germinación de las plantas en comparación con sistemas de cultivo sin nanotubos. El objetivo general de este trabajo de investigación se refiere a la influencia de diferentes concentraciones de MWCNT (alta pureza) sobre la germinación y el crecimiento de las plantas de maíz, así como, en concentraciones y transporte de nutrientes minerales en la planta. También, se explica el mecanismo de transporte de iones metálicos a través de los MWCNTs utilizando dos estados de oxidación del Fe (II y III). Todos los estudios realizados están enfocados en optimizar las diferentes condiciones experimentales. Esto es así, debido a que muchos aspectos de los experimentos realizados no tienen precedentes. Para un estudio cuantitativo riguroso, la optimización y la reproducibilidad de todos los parámetros experimentales son esenciales. El maíz (*Zea mays* L.) ocupa el tercer lugar en la producción mundial de cereales y es considerado como un cultivo alimenticio esencial. Estudios previos sobre el efecto de los nanomateriales (NM) en el maíz, muestran mejoras en los parámetros de crecimiento, pero los efectos de los componentes fisiológicos del maíz y su distribución en las raíces y frutos son esenciales para comprender las propiedades funcionales de fertilizantes minerales en detalle. Para la aplicación de NMs en la mejoría del crecimiento de planta, la disponibilidad de una fuente de sílice económica con el incremento de propiedades funcionales es actualmente es una tarea demandante. Por otro lado, el grado de solubilidad de los NMs depende del tamaño de partículas y composición química. Finalmente, Para entender el funcionamiento de los NMs es preferible estudiar los cambios fitoquímicos de cultivos de maíz defiriendo en la absorción y su efecto en el metabolismo del maíz.

El primer capítulo (Capítulo 1) es un resumen de aplicaciones de los nanomateriales en la investigación ambiental y conceptos básicos empleados en este trabajo. Este conocimiento adquirido se ha ido acumulado durante años de investigación dentro y fuera de nuestro

laboratorio, y constituye la base de la que partimos en la exploración de los nanotubos de carbono en la ciencia de plantas.

El capítulo 2 describe las partes del desarrollo de los procedimientos experimentales y una breve introducción relacionada a las técnicas de caracterización utilizados durante nuestro trabajo de investigación, en la que estuve involucrado, tanto durante la fase de configuración inicial y a lo largo de los años siguientes. Además, en este capítulo, el apéndice enumera muchas de las fuentes que hemos utilizado para construir y modernizar el sistema (por ejemplo, impedancia electroquímica y espectroscopia de fluorescencia de rayos x).

Los Capítulos 3 al 7 cubren la investigación realizada utilizando nanotubos de carbono de pared múltiple en diferentes proporciones, diferentes purezas y en diferentes sistemas de medio de cultivo en condiciones "in vitro" para analizar su papel en la germinación de diferentes plantas en diferentes condiciones de crecimiento.

Capítulo 3 explica acerca de los experimentos realizados con altas concentraciones de MWCNT en una cámara de crecimiento controlada. También, explica sobre las concentraciones de Fe^{2+} y Fe^{3+} en el medio de cultivo de agarosa que se utilizaron para ver la interacción de los iones de hierro con MWCNT y sus reacciones en las semillas de maíz, tales como la oxidación o la reducción. El análisis por SEM muestra que las semillas germinadas con MWCNT contienen muchos poros y las membranas celulares se encontraron desquebrajadas o agrietadas que aquellas que no fueron germinadas con MWCNT.

Los resultados obtenidos en el capítulo 4 muestra que las plantas cultivadas en medio de cultivo nutritivo (BA) da mejor germinación que en aquellas semillas que se encuentran en el medio de agarosa. El Análisis de FTIR muestra que las plantas germinadas con MWCNT contienen mayor número de grupos funcionales químico. Otro factor importante es la pureza de MWCNT, la cual demuestra que los nanotubos de carbono con pureza alta promueve la presencia de mayor concentración de elementos en comparación con aquellas muestras que contienen nanotubos de carbono con menor pureza. La medición por Raman de las muestras indica la presencia de MWCNT en muestras de plantas germinadas usando alta concentración (60 mg / l) de MWCNT en medios de cultivo de agarosa. La medición de luminiscencia también da una idea clara de la presencia iónica de metales pesados en plantas germinadas con MWCNT mientras que no hay dichos iones presentes en las muestras de control de plantas germinadas.

Los resultados obtenidos del capítulo 5 dan una clara información de que los nanotubos de carbono no sólo promueven el crecimiento y la presencia de iones de metales pesados (capítulo 3 y 4), sino también, el transporte de agua y elementos disueltos en agua en una forma continua durante el periodo de germinación, lo cual es probado a través de la cinética Pelegs y el modelo matemático de absorción de agua.

El capítulo 6 muestra el germinado, crecimiento y desarrollo de plantas de tomate usando MWCNT y dMWCNT en medios de cultivo con alto y bajo contenido de nutrientes. Los resultados obtenidos muestran que cuando la concentración es baja de dMWCNT, es benéfico para los primeros días de germinación. Sin embargo, mientras que una concentración más alta es útil debido a que se puede obtener mayor cantidad de biomasa y funciona mejor para un período más largo de germinación.

Los experimentos del capítulo 7, muestra que las plantas de maíz y de tomate de plantas germinadas en medio nutritivo mediante dispersión de MWCNT en un octavo del medio de MS basal. La dispersión de MWCNT se ha hecho en medio basal MS porque contiene muchos elementos nutrientes y grupos químicos orgánicos, que también ayudan a formalizar a los MWCNT. Los análisis de XRF, FTIR, UV-Visible y Raman se llevaron a cabo para verificar la presencia de elementos metálicos, grupos funcionales químicos, iones y nanotubos en las plantas germinadas de los diferentes tratamientos. Los resultados obtenidos muestran que los nanotubos son capaces de penetrar las paredes celulares de plantas, promueven el crecimiento de las plantas, promueve la activación de la enzima y también incrementa la cantidad de biomasa seca. El fenómeno de interacción de los nanotubos para el maíz y para el tomate son diferentes, tales como: la entrega de agua y el transporte de los nutrientes y metales. Los resultados también muestran que la interacción de los nanotubos de carbono no son los mismos para todos los elementos, que varía con ciertos elementos selectivos. Los resultados de FTIR muestran la presencia de diferentes grupos funcionales en diferentes partes de las muestras de plantas germinadas los cuales son diferentes. También, hay variaciones con las plantas y medios de cultivo utilizados. Las mediciones de Raman por luminiscencia ampliada muestra un pico de número de onda aproximada de $\sim 680 \text{ cm}^{-1}$ en las muestras germinadas usando MWCNT, lo cual indica la presencia de iones en esas muestras. El análisis por UV-Visible muestra la absorbancia y transmitancia de dichas muestras.

APPENDIX I

PLANT GERMINATION USING ACTIVATED CARBON (AC)

ANEXO I

GERMINACIÓN DE PLANTAS UTILIZANDO CARBÓN ACTIVADO (AC)

APPENDIX I

Plant Germination using Activated Carbon (AC)

AI.1 INTRODUCTION

Activated carbon (AC) is widely used in ecological studies for neutralizing allelopathic compounds. However AC has direct effects on plants because it alters substrate parameters such as nutrient availability and pH. These side-effects of AC addition may interfere with allelopathic effects. In this study we analyzed three widely used commercial AC and analyzed their effects on Tomato and Maize plants (*Solanum Lycopersicum* and *Zea Mays* Var. *Saccharata*) germination. Finally, AC addition to substrates had differential effects on seed germination. A set of control experiment has been performed together with AC assisted medium to compare the role of substrate parameter and plant performance. The effect of basic inorganic Elements available in the MS based culture medium, AC, light and dark on the germination rate and protocorm formation was investigated.

AI.2 MATERIALS AND METHODS

Seeds obtained from rancho de los molinos were cultured on basic inorganic media which were Murashige and Skoog (MS) medium (Murashige and Skoog, 1953), one eighth of MS (1/8 MS) medium together with or without 0, 5 and 10 mg/l activated carbon and 8 g/l concentration of bacteriological agar (BA) gel. The pH of the 1/8 MS solutions was adjusted to 5.75 and AC of required concentrations were dissolved in MS solution using ultrasonication for 2 hour at 48 kHz Frequency. The dispersed AC solutions were mixed in 1/8 MS mixed bacteriological agar and autoclaved at 120°C for 20 min. After autoclaving the final mixtures were pored to already sterilize majenta boxes and waited until the medium form gel. After the forming the gel the seeds were planted and close the lids of majenta boxes with 2 holes on top of the lid, which was sealed by parafilm. The seed germination was done in controlled chamber at fix temperature of 23-25°C and humidity 55-60%. The dry plants after biomass analyses were grinded to make microsize powder of roots, shoots and seed body separately (Table AI.1).

Table AI-1: Sample description of experiment performed

Plants		Tomato			Maize		
Sample Name		T'	T''	T'''	M'	M''	M'''
MS-Strength		1/8-MS	1/8-MS	1/8-MS	1/8-MS	1/8-MS	1/8-MS
AC	(mg/l)	0	5	10	0	5	10
Bact. Agar	(g/l)	8	8	8	8	8	8

AI.3 RESULTS & DISCUSSION

AI.3.1 Activated Carbon Promotes the Plant Germination

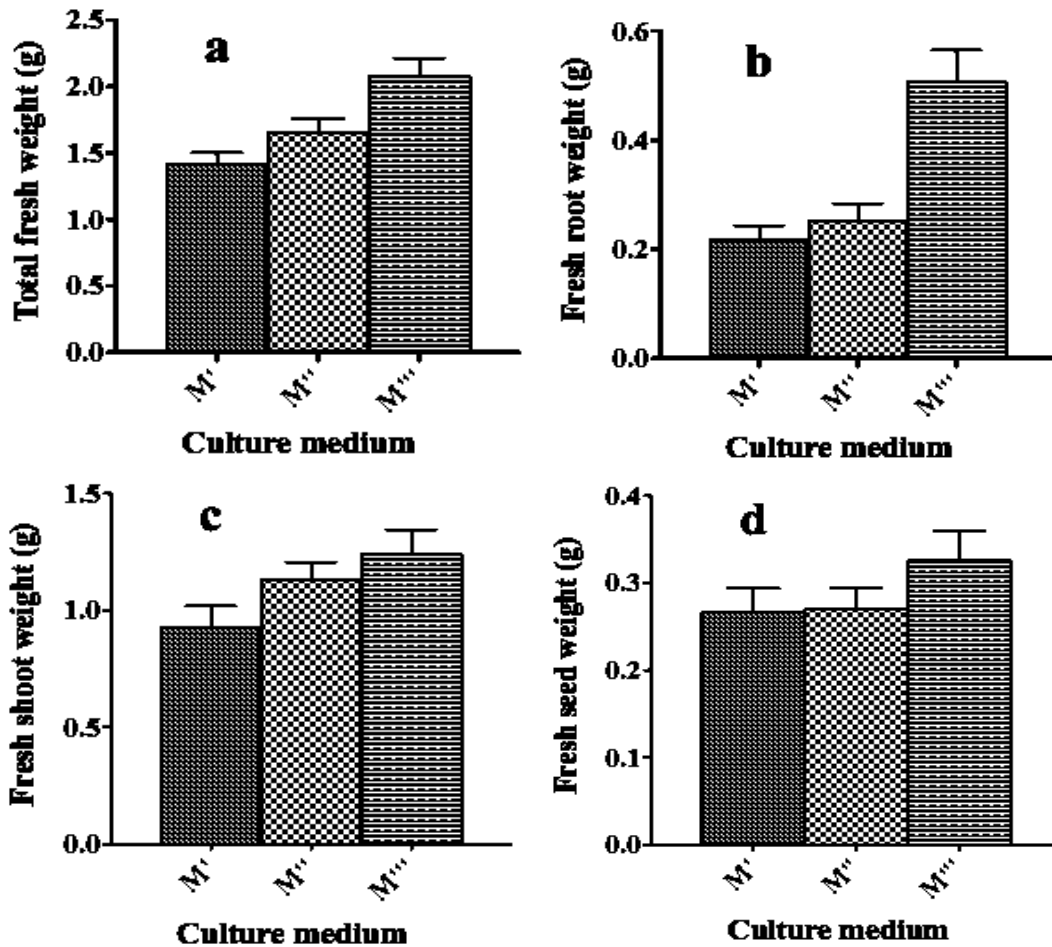


Figure AI-1: Germination analysis of 9 days germinated Maize plants in activated carbon (AC) assisted culture medium. a) Total fresh weight measurement. b) Fresh root weight measurement. c) Measure of fresh shoot weight. d) Weight of fresh seed body. Results are shown average \pm SE of 7 plants per each treatment.

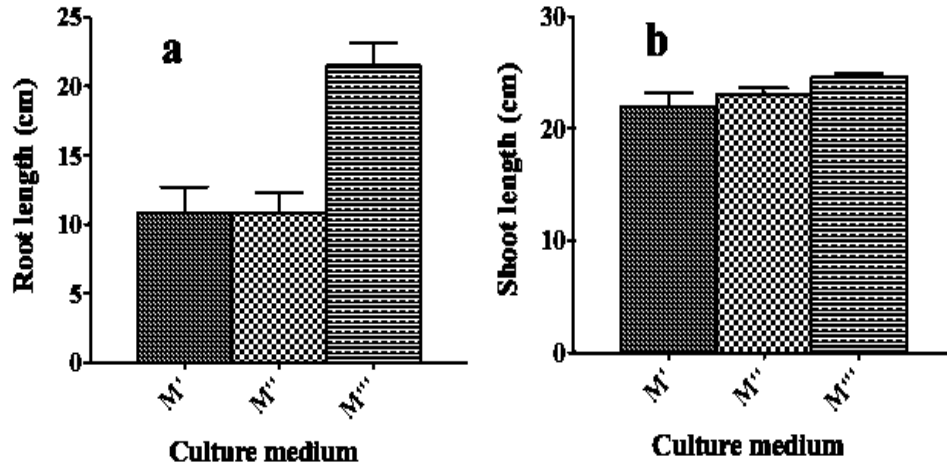


Figure AI-2: Growth of 9 days germinated Maize plants in (AC) assisted culture medium. a) Measure of root length. b) Measure of shoot length. Results are shown average \pm SE of 7 plants to each treatment.

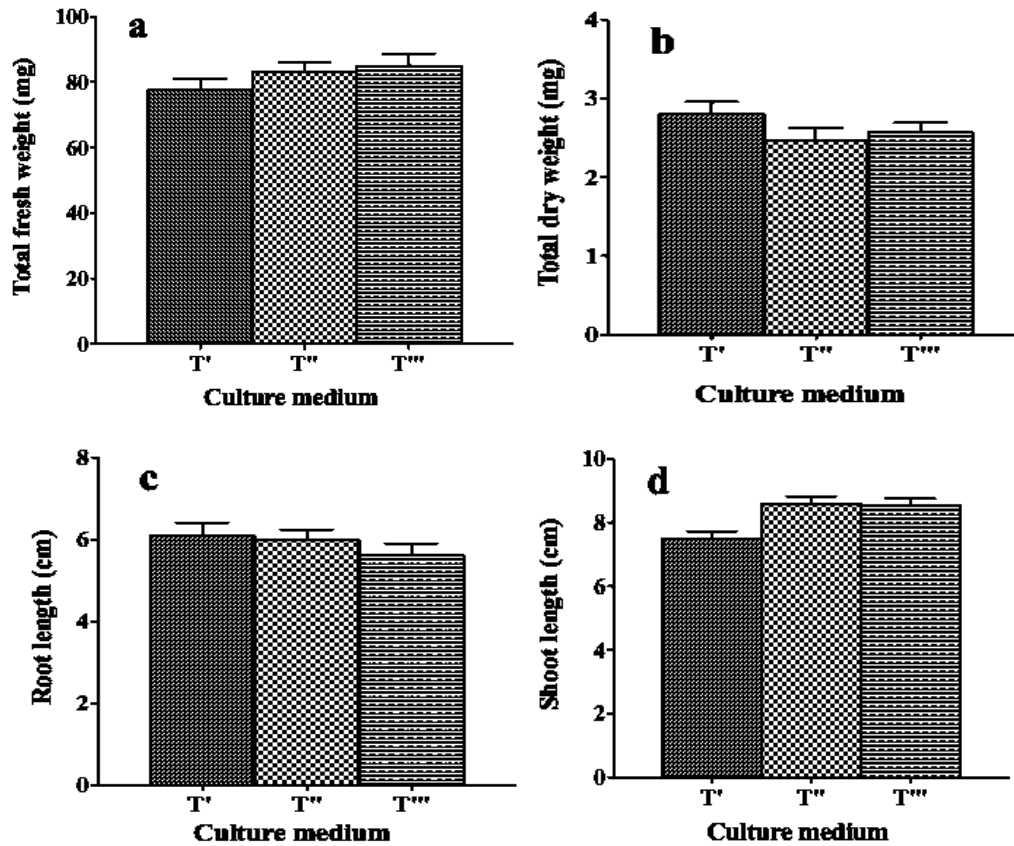


Figure AI-3: Germination analysis of 9 days germinated tomato plants in activated carbon (AC) assisted culture medium. a) Total fresh weight measurement. b) Total dry weight measurement. c) Measure of root length. d) Measure of shoot length. Results are shown average \pm SE of 10 plants to each treatment.

AI.3.2 XRF Measurement

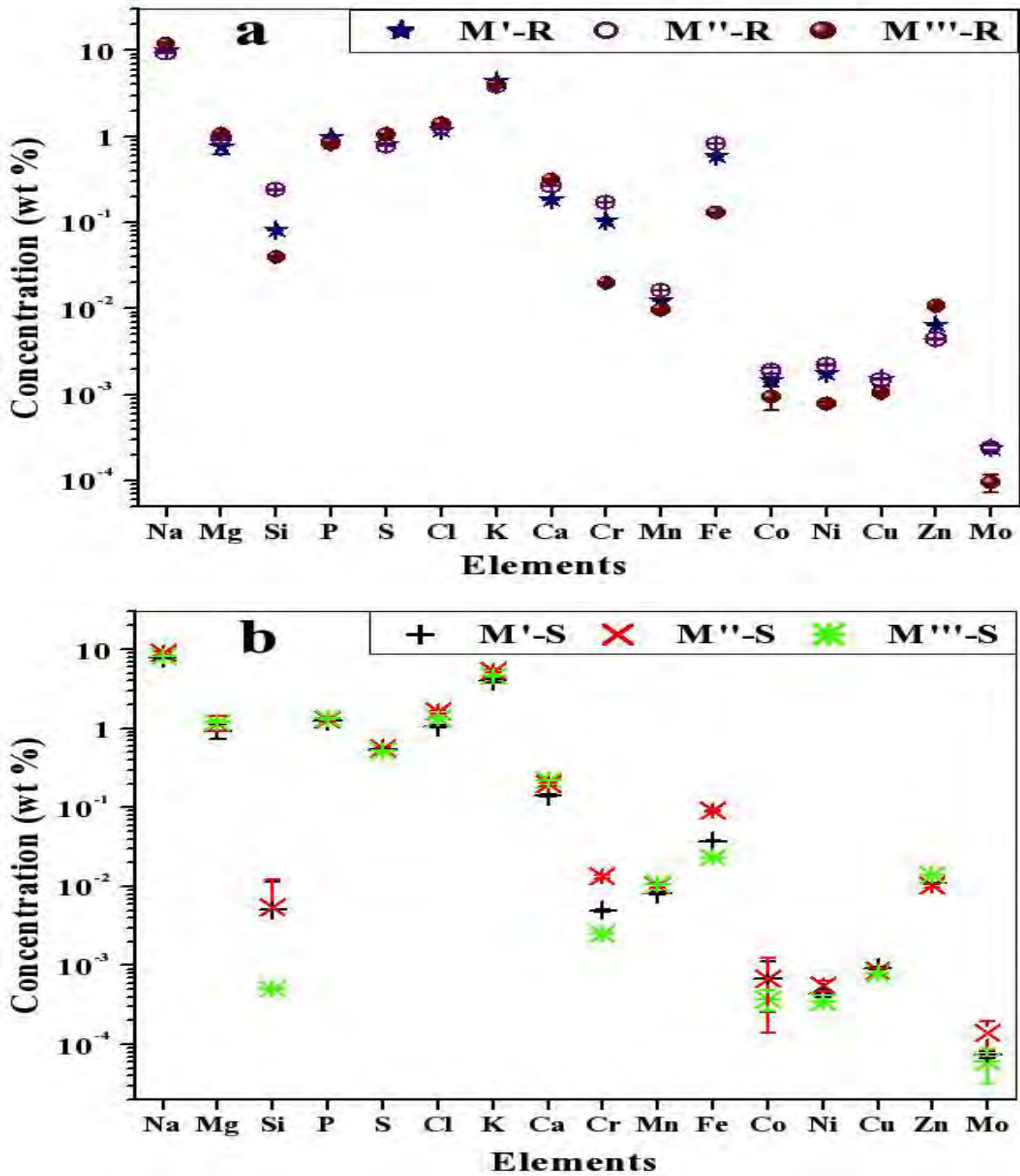


Figure AI-4: XRF results of powder samples of maize plant. a) % Concentration of elements presence in root samples. b) % Concentration of elements in shoot samples. Y axes are plotted to log scale.

AI.3.3 FTIR Analysis

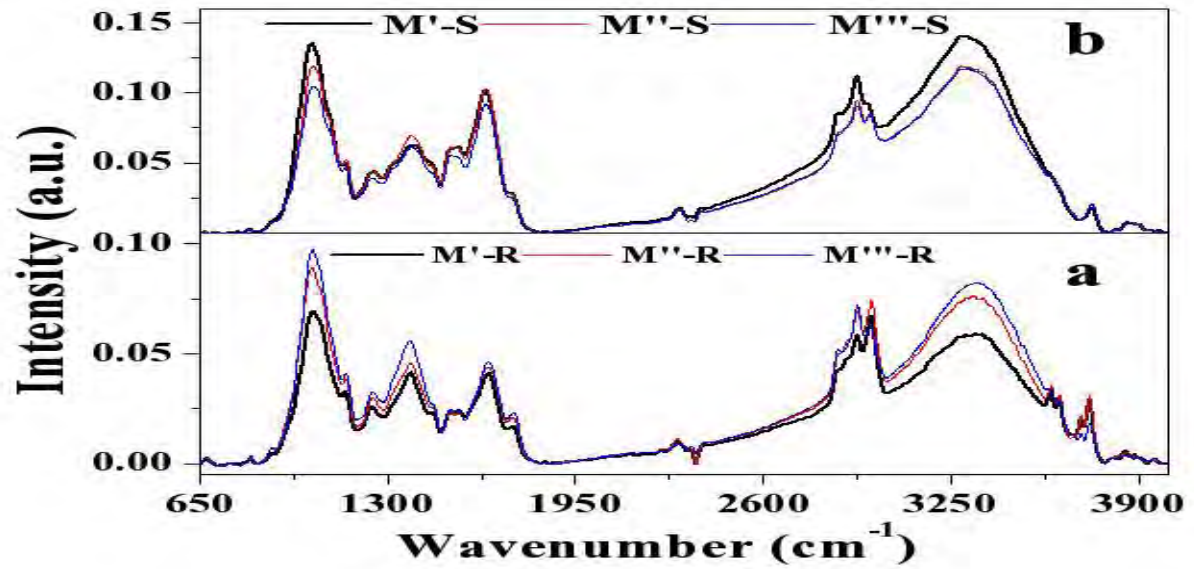


Figure AI-5: FTIR analysis of powder samples of germinated maize plants. a) Root samples. b) Shoot samples.

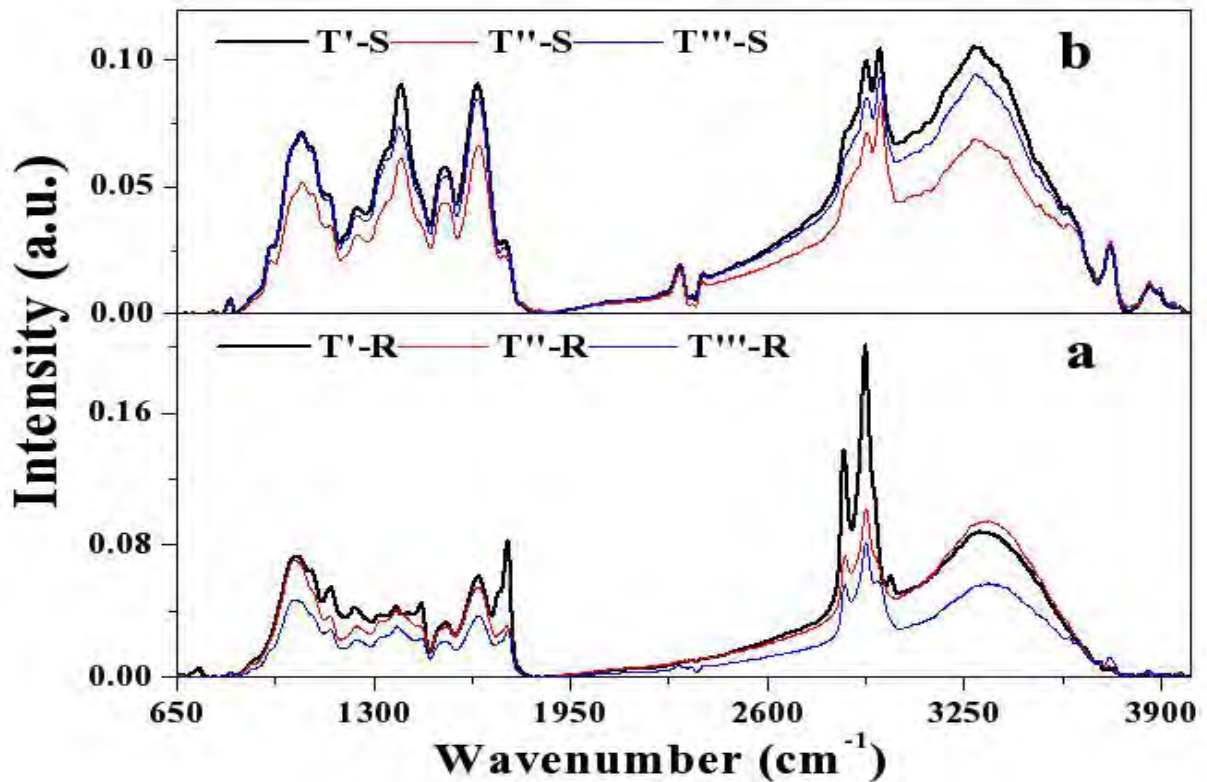


Figure AI-6: FTIR analysis of powder samples of germinated tomato plants. a) Root samples. b) Shoot samples.

AI.4 CONCLUSION

This study showed that AC is promoting the growth of Tomato and Maize plants. The overall effect of allelopathy was rather small: germination increased only by 14% when activated carbon neutralized the adverse effects of either root exudates or decomposing dead roots. We found that the two species of *plants* in their sensitivity to allelochemicals. When activated carbon was added there was a much greater increase of germination in the *Zea Mays* *Var. Saccharata* (Maize) than *Solanum lycopersicum* (Tomato).

APPENDIX II
CHARGE STATE SPECIATION IN IONIC SOLUTIONS
USING ELECTROCHEMICAL IMPEDANCE
SPECTROSCOPY

ANEXO II
DIFERENCIACIÓN DEL ESTADO DE CARGA EN
SOLUCIONES IÓNICAS USANDO ESPECTROSCOPIA DE
IMPEDANCIA ELECTROQUÍMICA

APPENDIX II

Charge State Speciation in Ionic Solutions using Electrochemical Impedance Spectroscopy

AII.1 INTRODUCTION

Iron (Fe) is a metallic element and composes about 5% of the Earth's crust. It is one of the most important elements of life. Soluble iron is available to living organisms, iron deficiencies are widespread, and the factors that influence iron solubility are important to understand ecosystem function. Photosynthesis is particularly dependent on iron availability, in part due to the high iron requirements needed to produce chlorophyll [1]. Iron is essential to animal life and necessary for health of plants [2], human body contains 0.006% iron, majority of which is in the blood. In a healthy adult male total body iron content is 3-5 grams, of which nearly 60% is present in haemoglobin. Every 2 ml of blood contains one mg of elemental iron [3], lack of iron also lowers a person's resistance to infection. Iron is a most important naturally material and also important of its charge states (Fe^{2+} & Fe^{3+}), because each charge state has a different role in redox driven metabolic process. Analysis of charge states of iron is important because, if there is lack or gain of percentage of iron in living cells then how it will affects the structure and growth. In the present work, our aim is to develop an analytical method for determining the charge state speciation of Iron (Fe^{2+} & Fe^{3+}) chloride solution (prepared in distilled water) of different concentrations of iron, by using the “*Electrochemical Impedance Spectroscopy*” (EIS). Analysis of parameters affecting in conduction of Fe^{2+} , Fe^{3+} and mixed composition of (Fe^{2+} & Fe^{3+}) iron chloride solution and how the parameters varies with frequency

Looking for all these aspects we find that the iron is the most important naturally material and also important of its charge states (Fe^{2+} & Fe^{3+}), because each charge state has a different role in redox driven metabolic process. This analysis is also important because if there is lack or gain of % of iron in living cells then how it affects the structure and growth. In the present work our aim is to developing an analytical method for determining the charge state speciation of Iron (Fe^{2+} & Fe^{3+}) Chloride solution (Prepared in Distilled water) of different concentrations of iron, by using the Electrochemical Impedance Spectroscopy (EIS).

We interested to analyse the DC Conductivity of the Fe^{2+} , Fe^{3+} and the mixed composition of (Fe^{2+} & Fe^{3+}) and calculate the behavior of the Iron (Fe^{2+} & Fe^{3+}) Chloride solution with varying frequencies. We also interested to evaluate what factors are mostly affecting the DC conductivity and how the charge transfer taking places with the same concentration of these two compositions of electrolyte solution.

AII.2 METHODOLOGY

Weigh the materials in the stoichiometric ratio and prepare the stock solution of concentration 10^{-2} M in distilled water using magnetic stirrer (approx 30 min.).

Measurent of Cell Geometry

Measure the area and thickness of the sample holder. Run a test of the equipment for normalization of same thickness and frequency range. The measurement must be done by using lower to highr concentration to avoid the higher resistive errors and clean the cell every time during concentration change.

Geometry of the Sample Holder (Cell)

$$D = 30mm = 3cm$$

$$Area(A) = \pi r^2$$

$$\Rightarrow A = 7.065cm^2$$



Figure AII.1: Experimental setup of EIS measurement.

AII.3 RESULTS & DISCUSSION

AII.3.1 Electrochemical Analysis of Iron Chloride Solutions

a) EIS Analysis of Fe²⁺, Fe³⁺ and mixed compositions

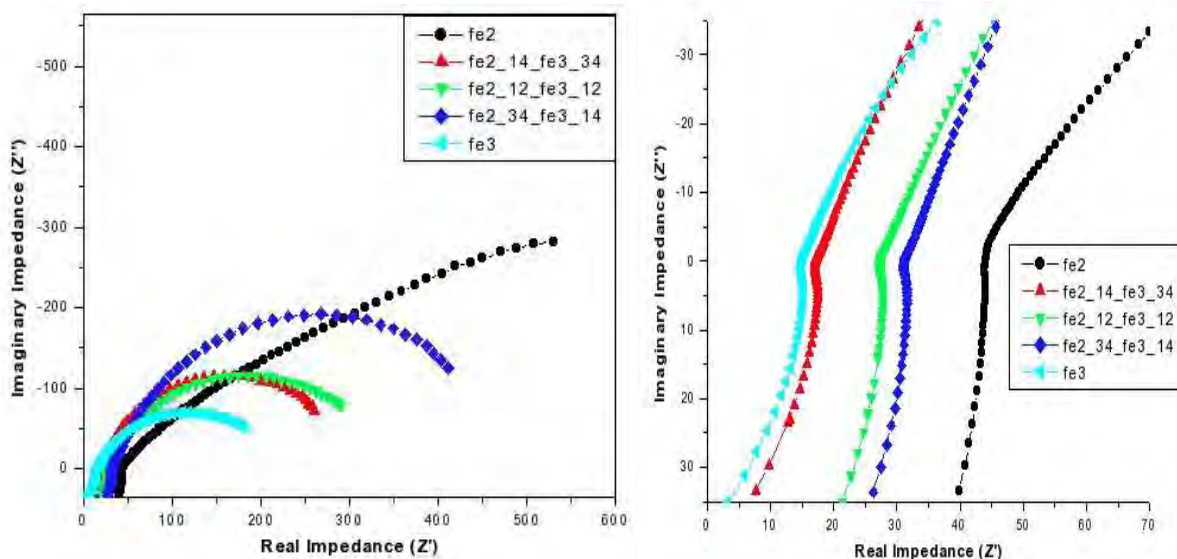


Figure AII.2: EIS measurements (Impedance plots) of chloride solutions of Fe²⁺, Fe³⁺ and their mixed compositions, left figure shows the variation of real and imaginary impedances on full scale frequency (high to low) and right figure shows the variation at lower scale (high frequency).

b) Fe²⁺, Fe³⁺ and (50% Fe²⁺ & 50% Fe³⁺) compositions

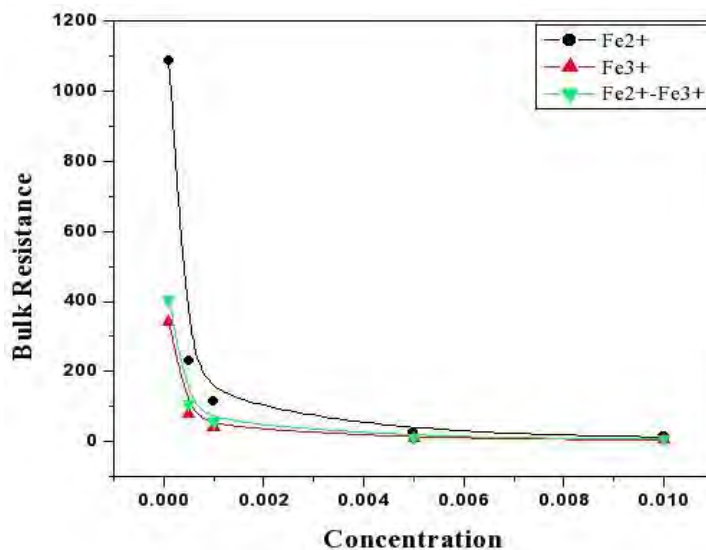


Figure AII.3: Variation of bulk resistance with concentration for solutions of Fe²⁺, Fe³⁺ and their mixed compositions (50-50 %).

TableAII.1: Concentration used and conductivity at that concentration of Iron Chloride solutions.

	Fe2+	Fe2+	Fe3+	Fe3+	Fe2+-Fe3+	Fe2+-Fe3+
Conc.	TDS (mg/L)	Cond. ($\mu\text{S}/\text{cm}$)	TDS (mg/L)	Cond. ($\mu\text{S}/\text{cm}$)	TDS (mg/L)	Cond. ($\mu\text{S}/\text{cm}$)
$1 \cdot 10^{-2}$	1201	2140	3610	6130	2430	4170
$5 \cdot 10^{-3}$	589	1076	1826	3180	1238	2200
$1 \cdot 10^{-3}$	128.7	243	365	679	272	511
$5 \cdot 10^{-4}$	63.4	120.7	189.2	355	140.1	268
$1 \cdot 10^{-4}$	12.8	25.5	42.7	82.5	36	70

c) Temperature & concentration variation of iron chloride solution

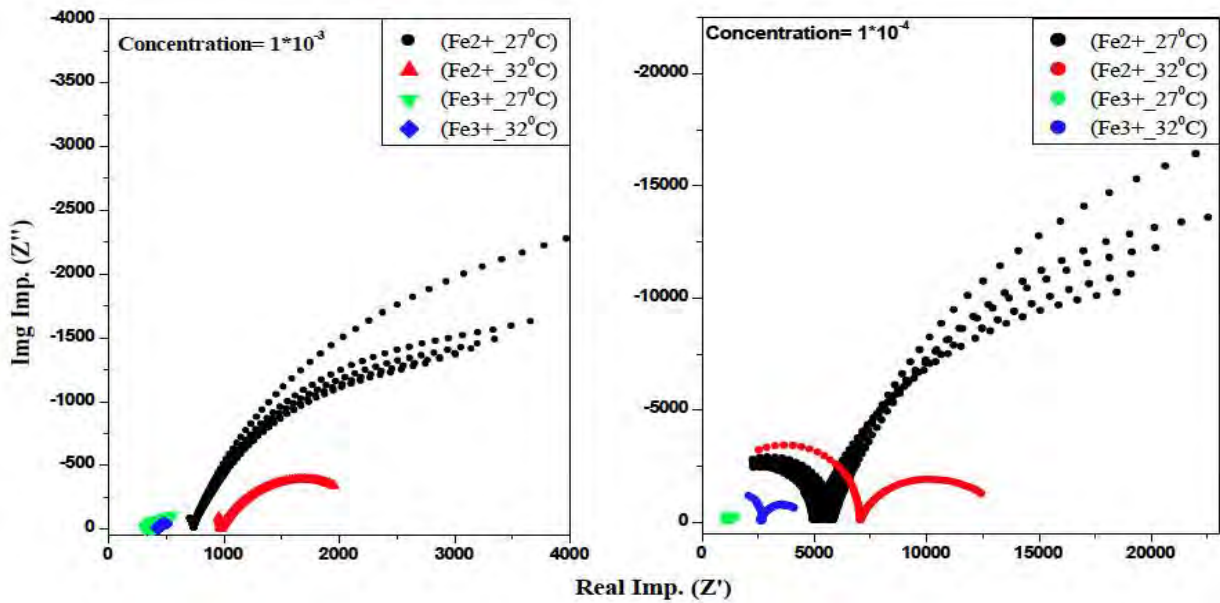


Figure AII.4: Temperature & concentration variation of iron chloride solutions.

d) Conductivity variation of iron chloride solution

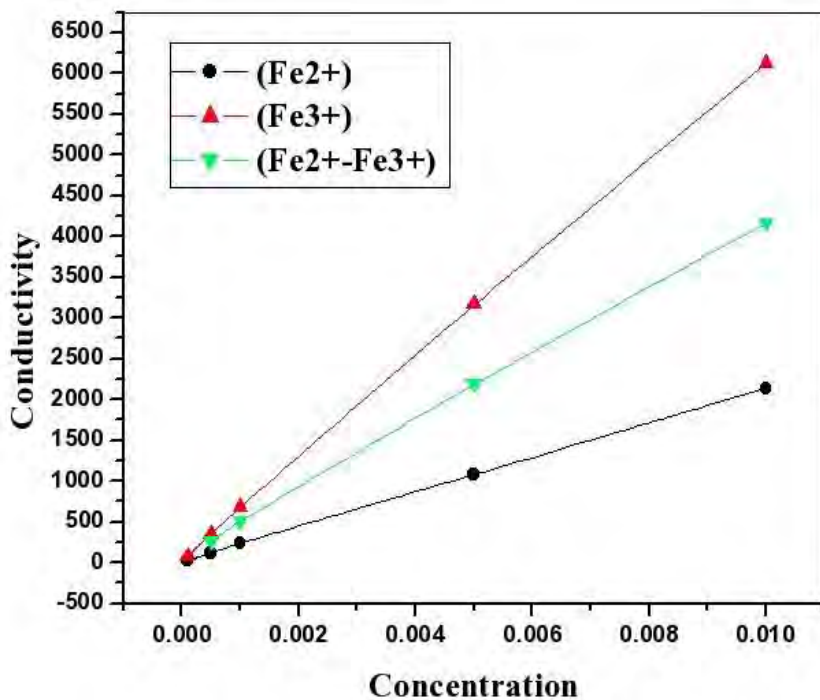


Figure AII.5: Conductivity variation of iron chloride solutions with concentration.

AII.3.2 Electrochemical Analysis of known Concentration of Potassium Chloride and Unknown Biomaterials Solutions

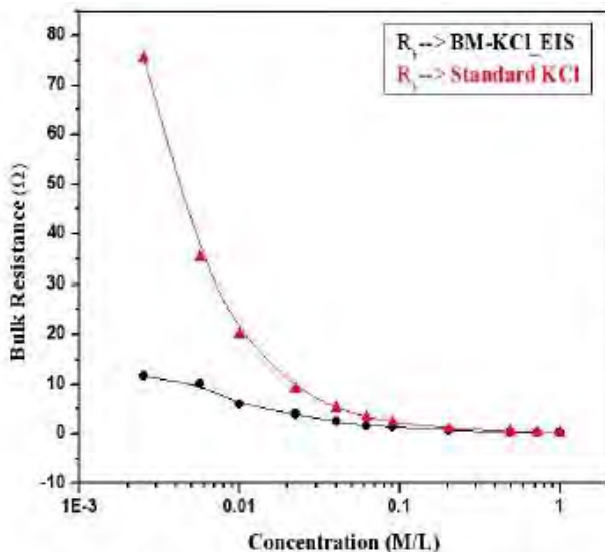


Figure AII.6: Variation in bulk resistance of KCl and KCl+biomaterials solutions with known concentration of KCl and unknown concentration of biomaterials.

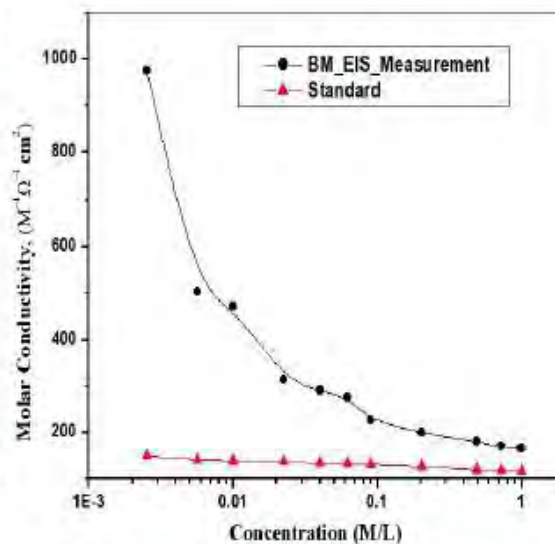


Figure AII.7: Variation in molar conductivity of KCl and KCl+biomaterials solutions with known concentration of KCl and unknown concentration of biomaterials.

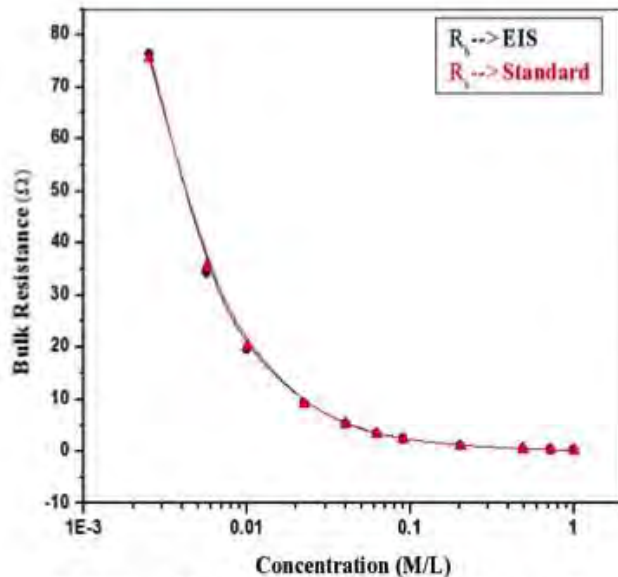


Figure AII.8: Comparative study of bulk resistance with concentration using EIS and DC measurement techniques.

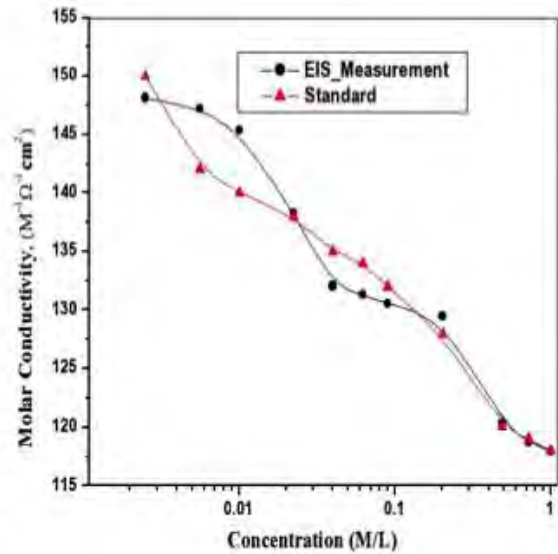


Figure AII.9: Comparative study of molar conductivity with concentration using EIS and DC measurement techniques.

AII.4 CONCLUSION

From the EIS analysis the iron chloride solution prepared of different concentration have different variable parameters. The affecting parameters vary with the concentration change. The Parameters variation also depends on the temperature a small change in Temperature shows a wide change in the variable parameters.

AII.5 REFERENCES

1. Science Highlight, *SSRL*, 2009.
2. K. Nyavor et al., *Appl Microbiol Biotechnol*, 45, 688-691, 1996.
3. Khalid Hassan and Nadeem Ikram, *International Journal of Pathology*, 2(2), 111-116, 2004.

APPENDIX III
DYNAMIC MATRIX ANALYSIS OF BIOLOGICAL SAMPLES
USING PARTICLE INDUCED X-RAY EMISSION (PIXE)
IMAGING

ANEXO III
MATRIZ DINÁMICA ANÁLISIS DE MUESTRAS
BIOLOGICAS USANDO EMISIÓN DE RAYOS X INDUCIDA
POR PARTICULAS (PIXE) IMÁGENES

APPENDIX III

Dynamic Matrix Analysis of Biological Samples using Particle Induced X-Ray Emission (PIXE) Imaging

AIII.1 INTRODUCTION

The Dynamic Analysis method takes this idea one step further, by building a matrix to transform from counts in each channel of the spectrum to contributions to elemental concentration. The images are also quantitative, stored in ppm-charge/flux units.

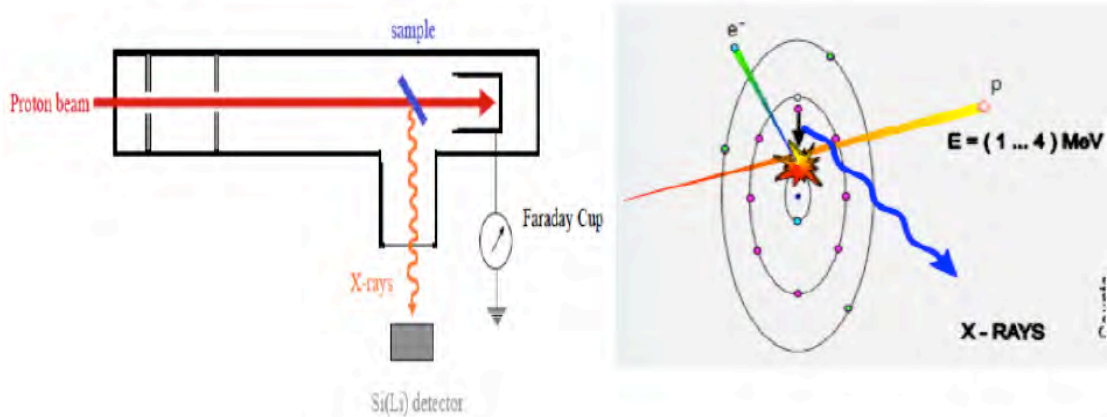


Figure AIII.1: Working methodology of PIXE imaging technique.

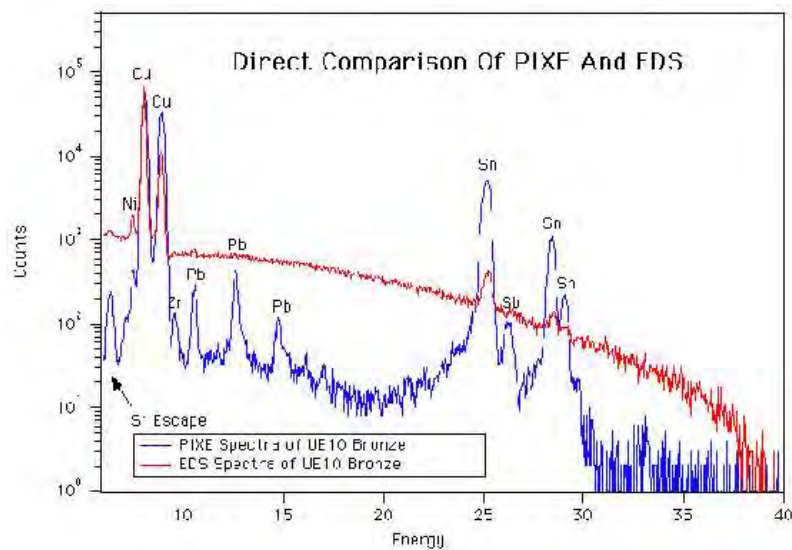


Figure AIII.2: Comparison between PIXE and EDS spectrum.

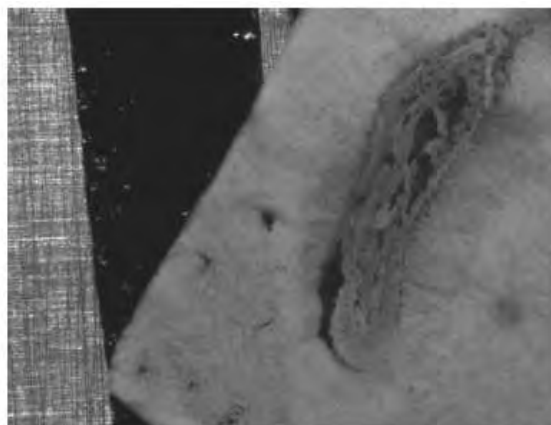
AIII.2 SAMPLE PREPARATION

TableAIII.1: Detail of the PIXE analysed Samples.

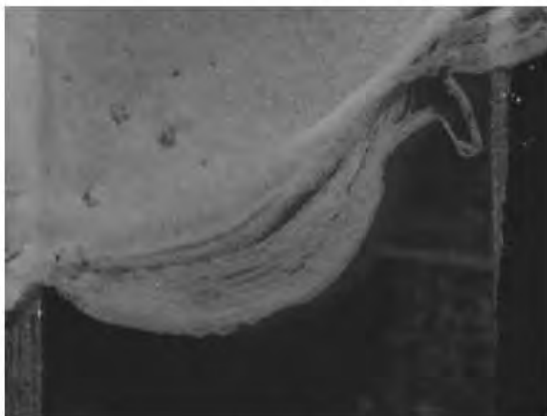
A-5	Agarose + Fe(II)- $1 \cdot 10^{-3}$
A-6	Agarose + Fe(II)- $1 \cdot 10^{-3}$ + CNT (20%)



A6_1_2x



A6_3_2x



A5_1_2x



A6_2_2x

Figure AIII.3: Sample preparation for PIXE measurements.

AIII. RESULTS AND DISCUSSION

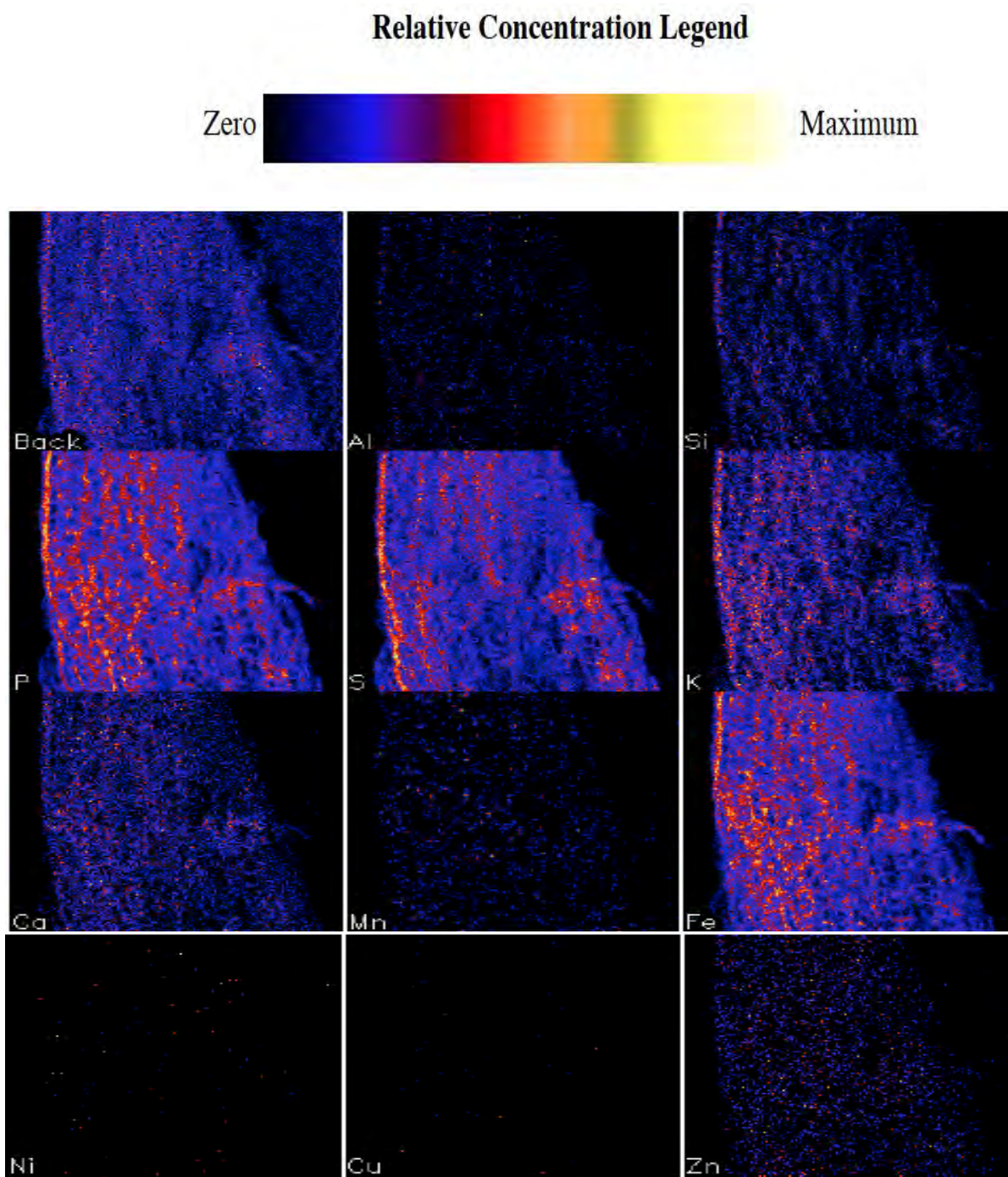


Figure AIII.4: PIXE analysis of longitudinal cross-section of root samples of A5 (A5_1_2x_Root).

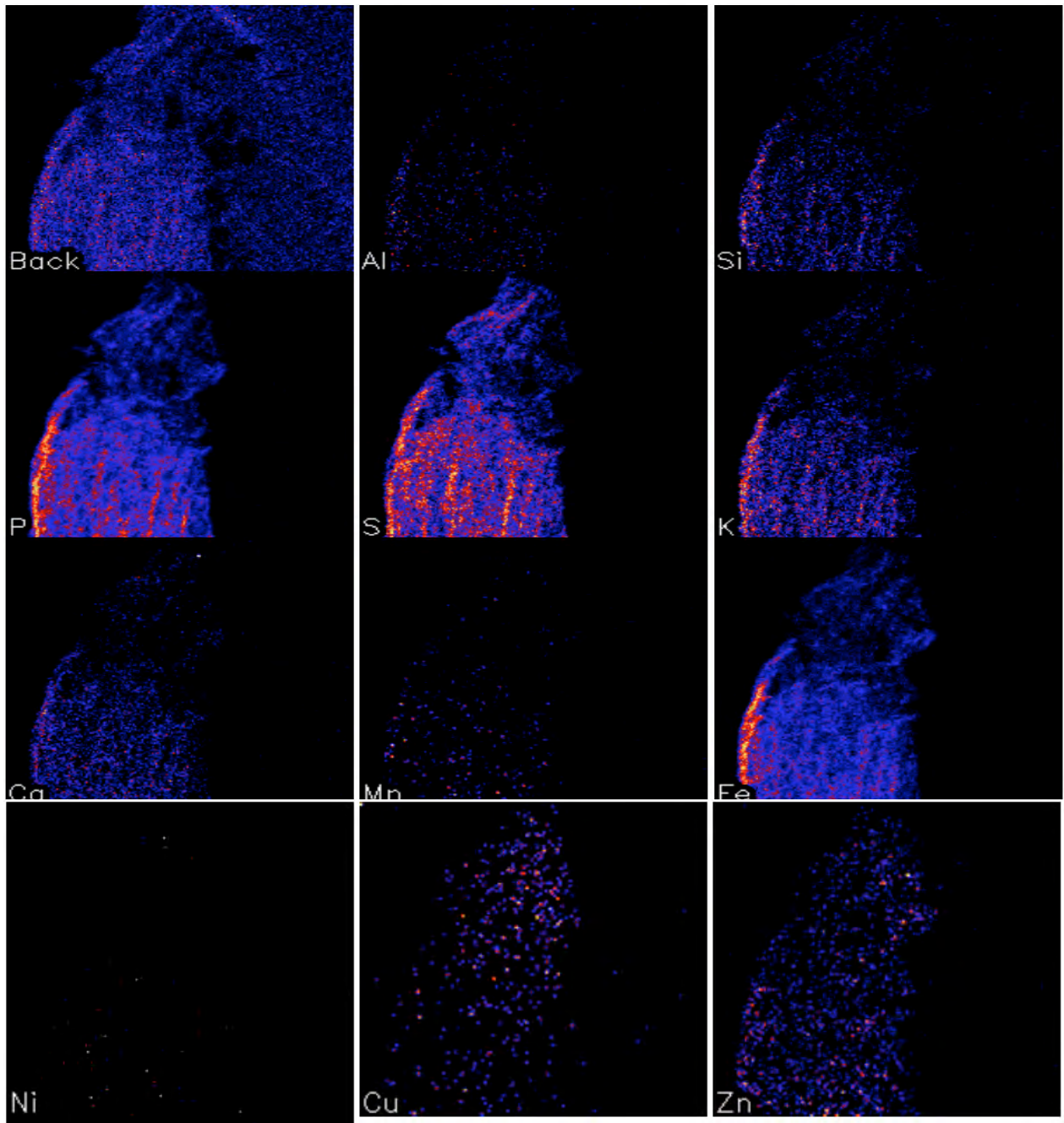


Figure AIII.5: PIXE analysis of longitudinal cross-section of seed samples of A5 (A5_1_2x_SB).

The spectrum corresponds to the total PIXE spectrum for a scan over a melt inclusion trapped in clinopyroxene, and the images to the right are the elemental distribution images projected using Dynamic Analysis

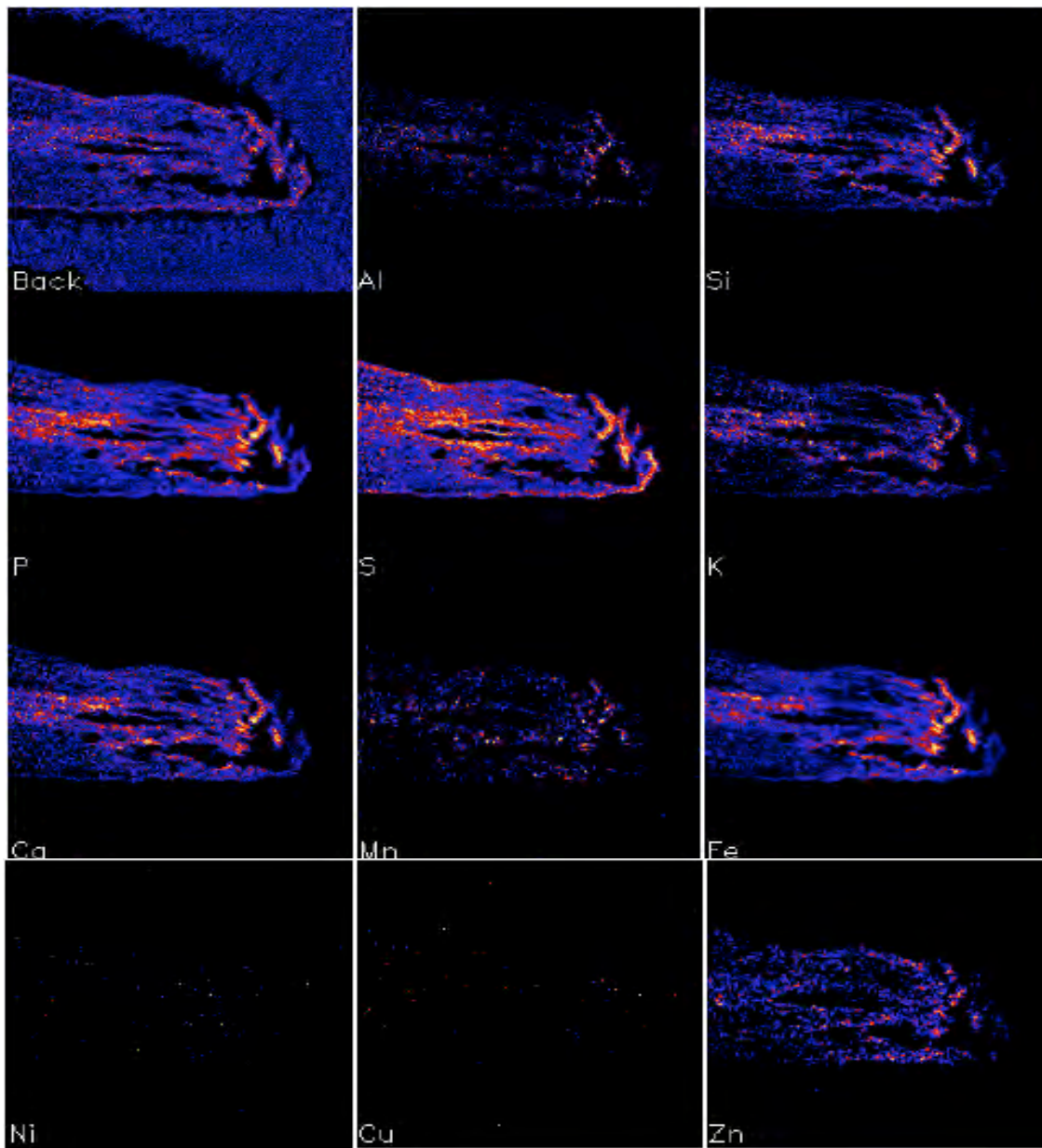


Figure AIII.6: PIXE analysis of longitudinal cross-section of root samples of A6 (A6_1_2x_Root).

Cal: A= 0.0129690, B= -1.30214, Units= keV

Scan: X= 0.100000, Y= 0.100000 mm

X Compress: 2, Y Compress: 2

X Scaled: 1.00000, Y Scaled: 1.00000

X size: 500, Y Size: 500

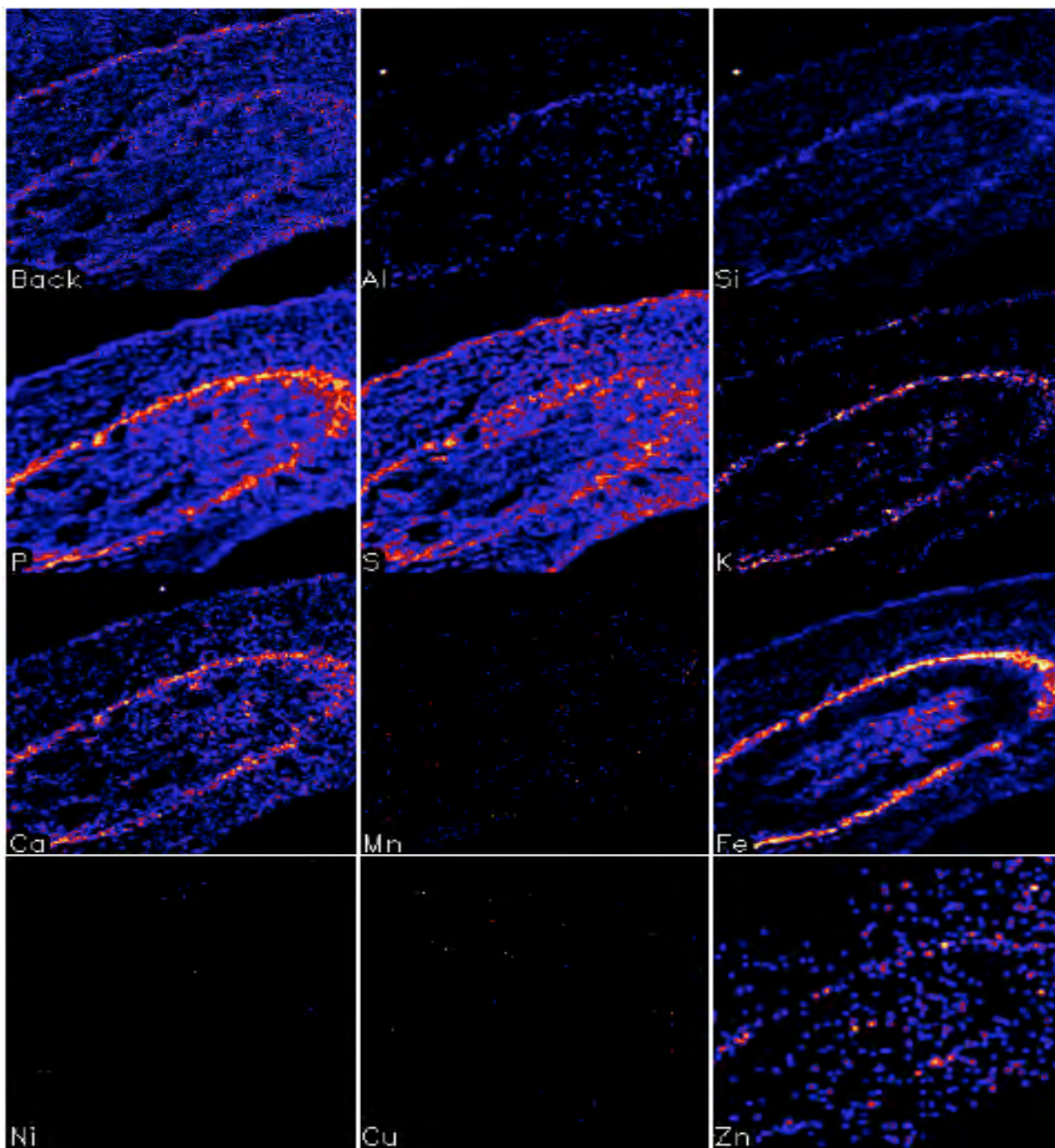


Figure AIII.7: PIXE analysis of transversal cross-section of root samples of A6 (A6_2_ Transversal Root).

Back 1.42 ppm, Al- 5.62%, Si- 5.70%, P- 6.84%, S- 6.07%, K- 0.725%, Ca- 0.872%, Mn- 1.60%, Fe- 5.89%, Ni- 1.67%, Cu- 1.88%, Zn- 0.566%, Sum 0.759%

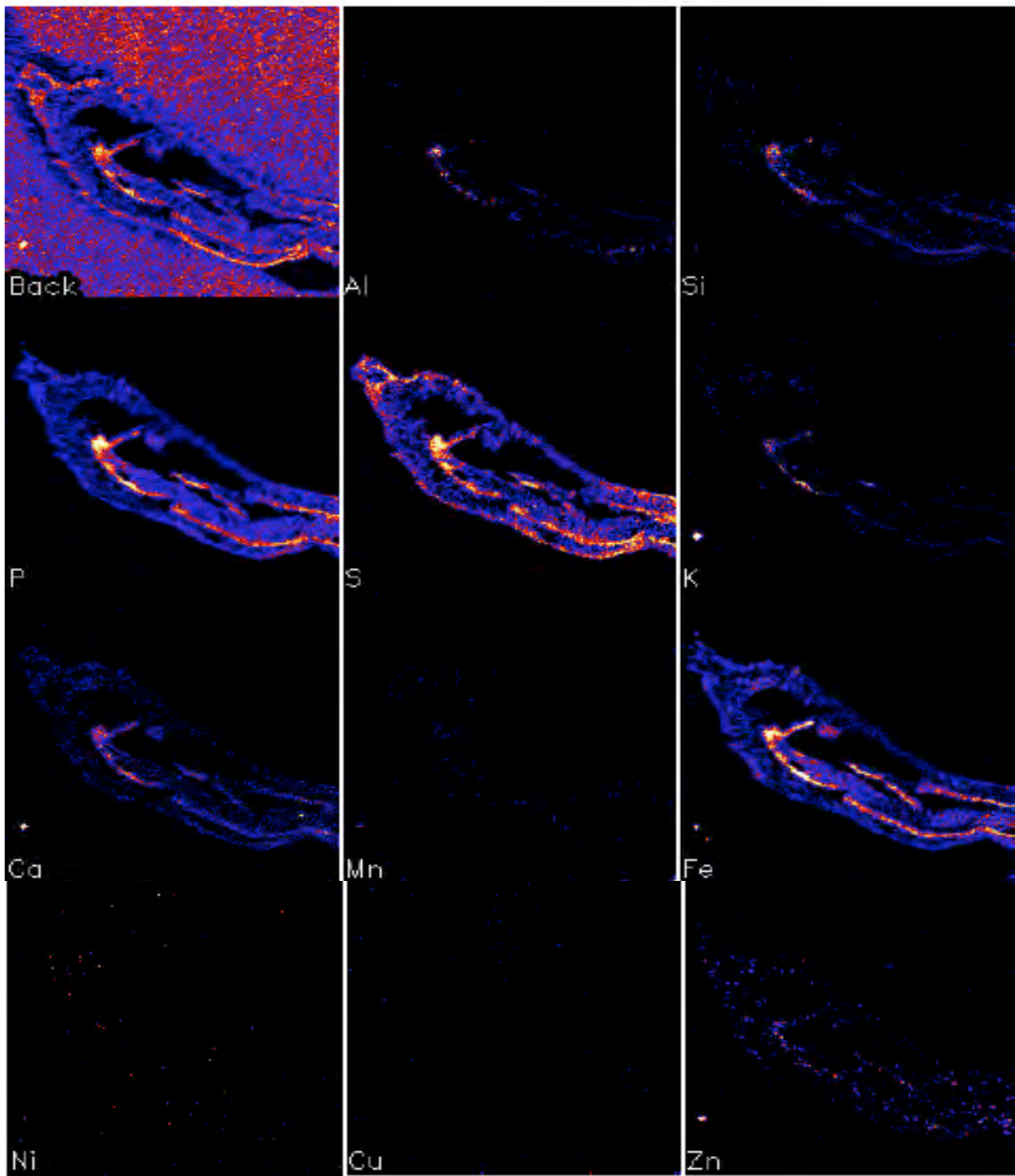


Figure AIII.8: PIXE analysis of longitudinal cross-section of seed samples of A6 (A6_3_SB).

CONFERENCES & PUBLICATIONS

Nanocrystalline Nickel-Cobalt Ferrite ($\text{Ni}_{1/2}\text{Co}_{1/2}\text{Fe}_2\text{O}_4$) for Electromagnetic Interference (EMI) Shielding Applications. D. K. Tiwari, A. K. Thakur, S. E. Borjas-García, L. M. Villaseñor, N. Dasgupta-Schubert. ICANM 2013: International Conference and Exhibition on Advanced & Nano Materials, August 2013, Quebec, Canada.

Interaction of Carbon Nanotubes with Mineral Nutrients for the Promotion of Growth of Tomato Seedlings. D. K. Tiwari, N. Dasgupta-Schubert, L. M. Villaseñor, Dhananjay Tripathi, J. Villegas. International Conference and Exhibition on Advanced & Nano Materials (ICANM), August 2013, Quebec, Canada.

Effect of Manganese Doping on Barium Ferrite and its Dielectric Behavior. D. K. Tiwari, A. K. Thakur. International Multidisciplinary Joint Meeting 2013 (IMJM-13), May 2013, Morelia, Mexico.

Interpretation of Charge State Speciation in Iron-Chloride Solutions using Electrochemical Impedance Spectroscopy (EIS). D. K. Tiwari, L. M. Villaseñor, N. D. Schubert. 16th International Conferences on Photoacoustic and Photothermal Phenomena (16th ICPPP), 2011, Merida, Yucatan, Mexico, 2011.

Interfacing Carbon Nanotubes (CNT) With Plants: Enhancement of Growth, Water and Ionic Nutrient Uptake in Maize (*Zea Mays*) and Implications for Nanoagriculture, D. K. Tiwari, N. D. Schubert, L. M. Villaseñor, J. Villegas, L. Carreto Montoya and S. E. Borjas García, *Applied Nanoscience (Springer)*, DOI 10.1007/s13204-013-0236-7.

Magnetic Properties of Nanocrystalline Nickel-Cobalt Ferrites ($\text{Ni}_{1/2}\text{Co}_{1/2}\text{Fe}_2\text{O}_4$). D. K. Tiwari, L. M. Villaseñor, A. K. Thakur. *Int. J. of Thermophysics (Springer)*, DOI 10.1007/s10765-013-1438-7.

Analysis of Cosmic Rays and their Composition with Reference to Energy Spectrum. Dharendra Kumar Tiwari & Richa Dixit. *The IUP Journal of Physics*, Vol. IV, No. 3, 38-45, July 2011.

Personal Selling Process: Example from the Insurance Sector. Richa Dixit, Harsh Purohit and Dharendra Kumar Tiwari. *Marketing Mastermind, IUP Publications*, 57-58, June 2011.